Electromechanical Transduction in Ionic Liquid–Swollen Nafion^{TM} Membranes

by

Matthew D. Bennett

Dissertation submitted to the Faculty of the
Virginia Polytechnic Institute and State University
in partial fulfillment of the requirements for the degree of

Doctor of Philosophy

in

Mechanical Engineering

Donald J. Leo, Chair
Daniel J. Inman
Harry S. Robertshaw
Timothy E. Long
Richard O. Claus
Garth L. Wilkes
Geoffrey M. Spinks

October 2005
Blacksburg, Virginia

Keywords: Nafion^{TM}, ionic liquid, electroactive polymer, artificial muscle

Electromechanical Transduction in Ionic Liquid–Swollen Nafion™ Membranes

Matthew D. Bennett, Ph.D.
Virginia Polytechnic Institute and State University, 2005
Advisor: Donald J. Leo

Abstract

Traditionally, water has been used as the diluent for ionomeric polymer transducers. The water mobilizes the counterions within the polymer and allows electromechanical transduction to occur. However, these water–swollen devices have limited stability when operated in a non–aqueous environment. In this work, ionic liquids are demonstrated as viable diluents for ionomeric polymer transducers based on Nafion™ membranes. Ionic liquids are molten salts that are highly thermally stable and have an immeasureably low vapor pressure. Therefore, the ionic liquid–swollen transducers exhibit enhanced stability in their performance when operated for long periods of time in air.

Methods for swelling Nafion™ membranes with ionic liquids are presented. Also, techniques for plating the ionic liquid–swollen transducers with metal electrodes are discussed. The performance of the ionic liquid–swollen transducers is compared to that of water–swollen transducers and differences are observed. Apart from the superior stability of the ionic liquid–swollen devices, they are observed to not exhibit the characteristic back–relaxation that is often associated with water–swollen transducers and limits their low frequency response. In order to investigate the physics of transduction in the ionic liquid–swollen membranes, structured experiments are performed using two different ionic liquids: 1-ethyl-3-methylimidazolium trofluoromethanesulfonate (EMI-Tf), which is water miscible, and 1-ethyl-3-methylimidazolium bis(trifluoromethanesulfonyl)imide (EMI-Im), which is hydrophobic. The other experimental parameters are the counterion of the Nafion™ membrane and the swelling level of ionic liquid.

Small–angle X-ray scattering (SAXS) is used to characterize the morphology of the

ionic liquid–swollen Nafion^{TM} membranes. The SAXS testing reveals that the clustered morphology of the Nafion^{TM} membrane is preserved by the EMI-Tf ionic liquid, which is compatible with the hydrophilic cluster phase. By contrast, the hydrophobic EMI-Im ionic liquid is found to disrupt the clustered morphology and lead to partial homogenization of the polymer. This has the effect of inhibiting the ionic conductivity. The SAXS testing also reveals that the mean intercluster spacing increases as the content of ionic liquid and size of the counterions increases. Based on assumptions regarding the swelling mechanism, this is thought to arise from an increase in the mean size of the clusters.

Spectroscopic investigations were also performed using Fourier transform infrared spectroscopy (FTIR) and nuclear magnetic resonance spectroscopy (NMR). These studies show that the ionic liquid interacts with the Nafion^{TM} polymer by displacing the counterions away from the sulfonate exchange sites. The cations of the ionic liquid then associate with the sulfonate sites and the counterions associate with the anions of the ionic liquid. Above a certain critical uptake of ionic liquid, this displacement is complete and additional ionic liquid does not associate with the ions of the polymer. The critical uptake is found to decrease with increasing size of the counterions.

Characterization of the electromechanical transduction behavior reveals that the ionic conductivity and actuation speed increases as the content of ionic liquid and the size of the counterions is increased. The actuation speed is observed to be linearly related to the ionic conductivity, with a slope very close to 1.0. Based on these observations, a model for charge transport in ionic liquid–swollen Nafion^{TM} membranes is presented in which the counterions hop along the anions of the ionic liquid. Only the ionic liquid above the critical uptake is able to participate in this mechanism. Therefore, the critical uptake is a key factor of the model. Experimental results support the general trends relating the actuation speed to the counterion size and uptake of ionic liquid predicted by the model.

Contents

List of Tables

List of Figures

Chapter 1

Introduction

1.1 History of Ionomeric Polymers and Ionomeric Polymer Transducers

Ionomeric polymers are materials that exhibit permselectivity and / or semipermeability due to their molecular structure (125; 25). The unique properties of ion-exchange membranes are caused by the presence of ionic groups that are fixed to the polymer matrix. These ionic groups are for instance, —SO_3^-, —COO^-, etc. in the case of cation exchangers or —NH_3^+, >NH_2^+, —N^+, etc. in the case of anion exchangers (76). Ion-exchange membranes can be either crosslinked or un-crosslinked and are further classified as homogeneous (e.g. containing only the ion-exchanging species) or heterogeneous (an ion-exchange material supported on an inert binder) (76).

The ionic selectivity (permselectivity) of ion-exchange membranes makes them useful in many applications, including water electrolyzers, solid electrolyte fuel cells, chlor-alkali cells, and other electrochemical processors. In the late 1940s it was discovered that ion containing polymers could also be used as electrochemomechanical transducers. The pioneering work in this field was performed by W. Kuhn et al. (73; 74) of the University of Basle (Switzerland) and A. Katchalsky et al. (65; 74) of the Weizmann Institute of Science (Israel). These researchers showed that a polymer made by copolymerizing methacrylic acid with divinyl benzene would swell and dialate upon changes to the pH of the surrounding solution, effectively making a chemomechanical actuator. In 1965 Hamlen et al. extended this idea to demonstrate an electromechanical ionomeric polymer actuator (54). By im-

pregnating a fiber of a copolymer of polyvinly alcohol and polyacrylic acid (supplied by Katchalsky) with platinum, they were able to suspend the fiber in a liquid electrolyte and pass an electric current through the electrolyte to the fiber. The change in pH resulting from the passage of this electric current caused the same swelling and dialation observed by Kuhn and Katchalsky in their early work. In 1973 Yannas and Grodzinsky did a similar experiment using collagen (a natural polymer electrolyte) fibers suspended in a liquid electrolyte (134). Again, mechanical actuation was demonstrated in response to an electrical input. In 1974 and 1975, Grodzinsky and Melcher followed this work by demonstrating that a deformable collagen membrane could produce mechanical motion when activated by an electrical input in a liquid electrolyte (47; 48). More importantly, they also showed that a voltage drop was produced across the membrane when it was acted on by an external mechanical input. Therefore, the polymer electrolyte membrane acted as a sensor. These early works demonstrated the use of a ion–exchange polymers as electromechanical transducers. It would be almost 20 years before this work was continued, using a new polymer called Nafion^{TM}.

DuPont's Nafion^{TM} is one of the most common ion-exchange polymers in use today. Nafion^{TM} was originally developed in the 1960s by DuPont for use as the polymer electrolyte in polymer electrolyte membrane fuel cells (PEMFC). Nafion^{TM} was quickly commercialized as a separator in chlor-alkali cells and has found a myriad of applications since then. Nafion^{TM} polymer is made by a base hydrolysis reaction on a co-polymer of sulfonly fluoride vinly ether and tetrafluoroethylene. The chemical structure of Nafion^{TM} polymer can be seen in Figure 1.1, below. In this formula, m is typically 1 and n varies from 5 to 11. The value of n is related to the degree of sulfonation of the polymer, which is typically reported in the form of equivalent weight (EW) of the membrane. The equivalent weight is defined as the weight of dry polymer per mole of exchange sites and for Nafion is typically in the range 900 to 1500. Lower values of EW are equivalent to higher ion content in the polymer. In Figure 1.1 the polymer is shown in the proton form. However, any cation can be substituted for the proton in this structure by soaking the polymer in an aqueous solution of a salt of that cation. As can be seen in the figure, Nafion^{TM} consists of a Teflon^{TM} backbone polymer with pendant side chains that are terminated in sulfonic acid groups. These acidic sidegroups are hydrophilic and cause the polymer to absorb significant amounts of water (as much as 38% dry weight basis for 1100 EW membrane (22)). This dissolution frees the

cation associated with each pendant acidic group to move within the polymer matrix while the anion maintains a bond to the fluorocarbon backbone. It is this property of Nafion^{TM} membranes which allows them to transmit cations while blocking anions and makes them useful as selective ion exchange membranes in chlor-alkali processes, hydrogen-air fuel cells, and the like.

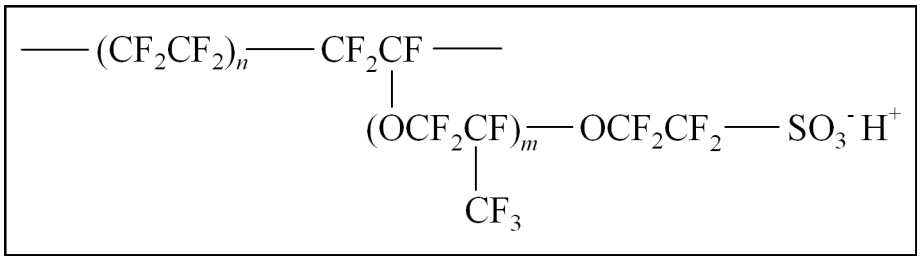

Figure 1.1: The chemical structure of Nafion^{TM} polymer.

More recently, Nafion^{TM} membranes have been used as electromechanical actuators and sensors. In the early 1990s, three groups of researchers published papers that demonstrated the use of Nafion^{TM} membranes as electromechanical transducers. Sadeghipour, Salomon, and Neogi developed an accelerometer using a Nafion^{TM} membrane (113). They demonstrated that the voltage produced by a small cantilever constructed from Nafion^{TM} was proportional to the acceleration. Thus, an electromechanical sensor was produced from an ion-exchange membrane. Almost concurrently with Sadeghipour et al. Oguro et al. and Segalman et al. published results demonstrating the use of Nafion^{TM}-based composites as electromechanical actuators (103; 114). Both groups demonstrated that mechanical deformation is produced in the membrane when an electric field is applied to the material.

Since the early 1990s several other research groups have become involved with ionomeric polymer membranes as actuators. In 1993, Oguro et al. patented the notion of using ionomeric polymer membranes as actuators (102). Oguro et al. have also demonstrated novel applications of ionomeric polymer actuators, using them in active catheters (50), underwater microrobots (49), and as elliptical drive elements in rotary and linear motors (122). Bar-Cohen has focused more on the use of these devices for interplanetary applications, and has demonstrated their ability to operate as low-mass actuators for robotic grippers and dust wipers for camera lenses (6). More recently, Eamex Corporation of Japan has developed toy robotic fish and auto–focus lens actuators using ionomeric polymer actuators (23). Although these represent novel applications for ionomeric polymer actuators,

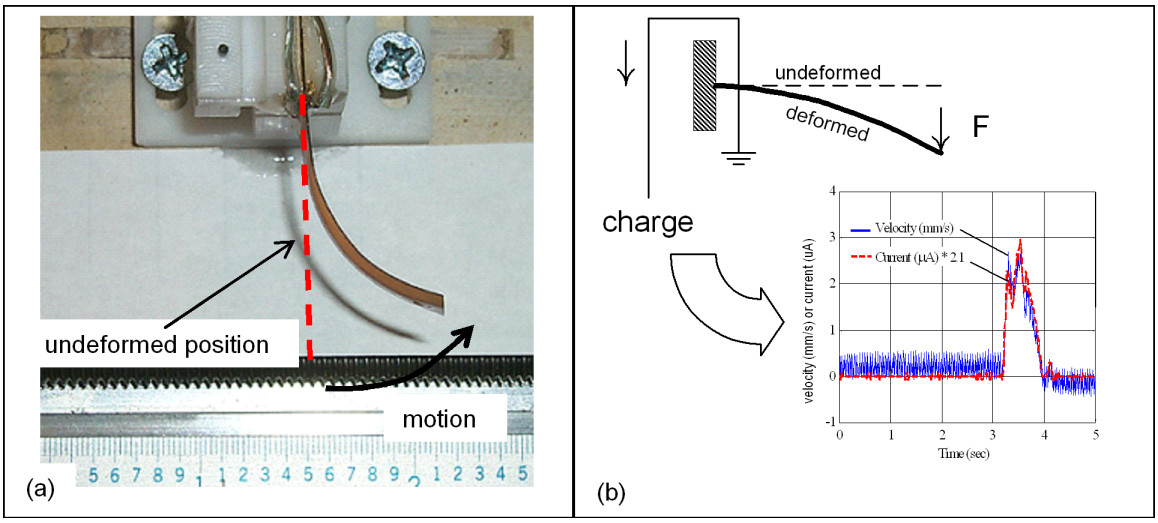

Figure 1.2: An ionomeric polymer membrane as (a) an actuator, (b) a sensor.

the state of the current technology has limited its widespread use.

The principle of electromechanical transduction is shown in Figure 1.2. Figure 1.2a is a picture of a Nafion^{TM} membrane that has been hydrated and coated with a conductive electrode on both sides. Upon application of an electric field, the membrane bends towards the anode due to the motion of the mobile cations and water molecules within the polymer matrix. Work by Mallavarapu and Leo (85) and Kothera and Leo (72) have shown that feedback control may be used effectively to control the motion of these actuators in a free bender configuration. The converse property is exhibited in Figure 1.2b. A cantilever sample of an ion-exchange membrane has deformed by the application of a force to the tip of the sample. It is believed that macroscopic motion of the membrane produces microscopic motion of the mobile cations, resulting in a charge imbalance across the electrodes. Several researchers have demonstrated that the quasi-static displacement of the polymer is correlated with the voltage that is produced by the membrane (116; 95; 66). More recently, Newbury and Leo demonstrated that the current induced in the membrane is proportional to the rate of the mechanical deformation (101; 100).

In their current embodiment, Nafion^{TM}-based transducers consist of a Nafion^{TM} membrane (typically Nafion^{TM}-117, nominal thickness 183 microns) that has been plated on both surfaces with conductive metal electrodes, typically platinum. The Nafion^{TM} polymer membrane is fully saturated with water and when it is subjected to an applied electric field, a transient bending motion towards the anode side can be observed. It has been

suggested that the cations in Nafion^{TM} must play a strong role in the actuation in these membranes. Athough a full physics-based model of transduction in these materials has to–date not been developed, several models have been proposed to explain the actuation in these materials and seek to relate the electromechanical coupling to ion motion (123; 16; 115; 4). Additionally, if the membrane is subjected to an imposed deformation, a charge is developed at the electrodes that can be measured with an external circuit. While the models referenced above do not attempt to describe this sensing behavior, Nemat-Nasser (2002) has developed a model that describes the actuation behavior of Nafion^{TM} membranes using an electrostatics approach (97). This model has been developed further by Farinholt and Leo (2003) (30) and Leo et al. (2005) (79) to describe both the actuation and charge sensing behavior.

1.2 Motivation

Ionomeric polymer transducers based on Nafion^{TM} membranes have been shown to be capable of generating large actuation strains upon the application of low voltages. These materials have the potential to be used in a wide variety of applications, including miniature pumps, control surfaces for small aircraft, flapping wing flying vehicles , adaptive optics, smart valves, and implanted biomedical devices. Additionally, these materials have been found to exhibit high sensitivity to mechanical strain. As sensors, ionomeric polymer transducers exhibit properties that are comparable to piezoelectric ceramic materials (9). However, they have the advantage of being compliant and rugged. For this reason they are potentially useful for many sensing applications, such as in performing meaurements of shear, pressure, vibration, and acceleration.

One of the most difficult obstacles standing in the way of widespread use of ionomeric polymer transducers is their hydration dependence. The use of water as a diluent for these transducers has limited their commercial applications. One possible solution to this problem is to utilize a barrier coating to contain the water within the membrane. Bar-Cohen et al. reported that with the aid of a barrier coating they were able to operate a sample in air for four months (6; 7). However, such a barrier coating will add passive stiffness to the actuator device and reduce the amount of strain that the device can generate (33). Also, the small electrochemical stability window of water as a solvent limits the maximum

operating voltages for these materials and thus limits the amount of strain and stress that the actuators can generate.

A more novel solution is to replace the water with a more stable diluent that will not evaporate when the transducers are used in air. Nemat–Nasser and Zamani have demonstrated Nafion^{TM} transducers solvated with ethylene glycol and glycerol, but the actuation speed is reduced in these materials (98). The current research seeks to overcome the hydration dependence of ionomeric polymer transducers by replacing the water with an ionic liquid.

Ionic liquids are a new class of unique solvents that contain only charged species and have many interesting properties that make them attractive for application to ionomeric polymer transducers. The vapor pressure of ionic liquids is immeasureably low, so they will not evaporate out of the ionomeric polymer transducer when it is operated in air, even at elevated temperatures. Also, ionic liquids are inherently very thermally stable. This means that the ionic liquid-swollen transducers can withstand high temperature processing that would not be possible with their water-swollen counterparts. Ionic liquids also have a larger electrochemical stability window than water, meaning that the transducers can be driven at higher voltages.

1.3 Technical Objectives

The goal of this research is to demonstrate transduction in ionic liquid-swollen Nafion^{TM} membranes. The performance of these new transducers will be compared to the traditional water-swollen materials. This work will also expose the underlying physical mechanisms responsible for the electromechanical transduction behavior. This will be accomplished through experimental characterizations of the morphology and ion associations of the composites. These results will be used to develop a model of ion transport and to explain the observed transduction characteristics. The specific technical objectives for this work are:

- Develop methods to incorporate ionic liquids into Nafion^{TM} membranes that is applicable to different types of ionic liquids and allows for control of the uptake.
- Develop methods to fabricate electromechanical transducers based on ionic liquid-swollen Nafion^{TM} membranes.

- Characterize the morphology of the ionic liquid-swollen Nafion^{TM} membranes.
- Identify the relevant ion associations and arrangements within the Nafion^{TM} / ionic liquid composite membranes.
- Investigate the electromechanical transduction behavior of Nafion^{TM} ionomeric polymer actuators swollen with ionic liquids.
- Develop a physical interpretation of the transport and transduction mechanisms in ionic liquid-swollen Nafion^{TM} membranes.

The remainder of this chapter will be composed of a review of the relevant literature and will be organized as follows. First, a discussion of the morphological studies that have been performed on hydrated Nafion^{TM} membranes will be presented. Second, a review will be made of the previous studies into the ion associations in hydrated Nafion^{TM}. Several studies of Nafion^{TM} swollen with non-aqueous solvents will then be presented. Finally, a discussion will be made of the history and relevant properties of the ionic liquids to be used in this work and previous research on ionic liquid-swollen Nafion^{TM} membranes.

1.4 Morphological Studies of Nafion^{TM}

The generally accepted (although often debated) view of the microstructure of Nafion^{TM} is of a collection of interconnected ionic clusters that contain the sulfonate sites and the absorbed solvent. These clusters are thought to exist as a separated phase within the inert fluorocarbon matrix. This microstructural view of the Nafion^{TM} polymer has been proposed based on the results of small-angle X-ray and neutron scattering studies, atomic force microscopy studies, electron microscopy studies, and mechanical and dielectric relaxation studies. A summary of these studies will now be given in the following sections.

1.4.1 X-Ray and Neutron Scattering Studies

One of the most common techniques used to identify the internal structure of the water and ions in Nafion^{TM} polymer is small-angle X-ray scattering (SAXS). The most comprehensive studies in this area have been performed by Gierke et al. (44; 45). Based on their results, these researchers concluded that the Nafion^{TM} membranes exhibited some sort of geometric

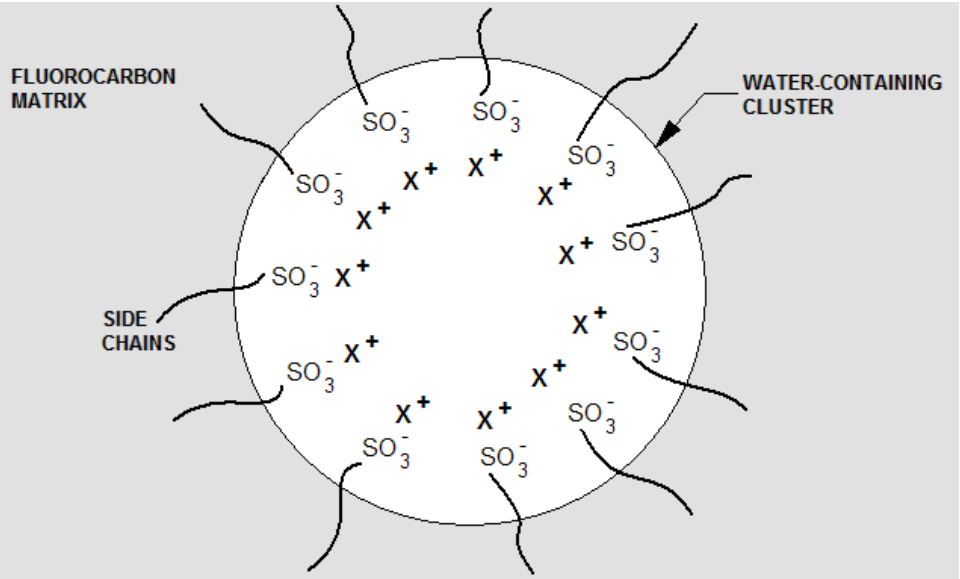

Figure 1.3: A visual representation of the inverted micelle model proposed by Gierke et al. ((44; 45)).

order. This order is explained by the presence of ionic clusters. Gierke et al. explain that the most likely structure for these ionic domains is that of roughly spherical clusters containing the ionic groups and water. These spherical domains were envisioned as being "inverted micelles," embedded in the fluorocarbon matrix and arranged such that the sulfonate groups are arranged at the inner surface of the spherical domain and contained within the water phase. The counterions are situated on a concentric spherical surface within this outer, negatively-charged surface–see Figure 1.3. This arrangement allows the strongly hydrophilic sulfonate sites to be hydrated, while limiting unfavorable interactions between the water and the hydrophobic fluorocarbon backbone polymer. This model of ion clustering in Nafion^{TM} is similar to the "two-phase" model proposed by Marx et al. to explain X-ray scattering in carboxylated hydrocarbon-based ionomers (87).

In addition to proposing a structural model for ionic clustering in Nafion^{TM}, Gierke et al. also have studied the effect of equivalent weight, cation type, and water content on this clustering phenomenon (44; 45). The most important contribution of this work was a model of the inverted micelle cluster that could predict the cluster size based on the mean intercluster spacing, the solvation level of the membrane, and its equivalent weight. This structural model was also used as the basis of several transport models of Nafion^{TM}.

Although several possible explanations exist for the SAXS results oberved by Gierke

et al. the model of roughly spherical clusters was considered the most likely by Gierke et al. and is supported by transmission electron micrographs of Nafion^{TM} membranes that were stained with heavy metal ions (13). Based on the idea that the ionic clusters are spherical in nature and assuming that they are arranged on a paracrystalline grid, the size of the clusters may be determined from the Bragg spacing measured in the SAXS experiments and the fractional weight gain of water during swelling of the polymer. Using this model, Gierke et al. showed that the size of the ionic clusters is linearly proportional to the fractional weight gain of water by the polymer. They also showed that the number of sulfonate sites per cluster is linearly proportional to the fractional weight gain of water. This result is very important because it demonstrates that the growth of the ionic clusters during swelling occurs not simply by an increase in size, but by the reorganization and combination of smaller clusters. Therefore, there are more ionic clusters in a less hydrated sample than in a more hydrated sample.

Hashimoto et al. (55) and Fujimura et al. (34; 35) have also performed a series of SAXS and WAXD studies on Nafion^{TM} membranes and have quantified their results in terms of ionic clustering and crystallinity in the polymer. In this work, the independent experimental parameters were the equivalent weight of the polymer, the water content of the membranes, and the ionic species present in the membranes. These authors also attempt to explain the observed SAXS results with a microstructural model of the morphology of Nafion^{TM}. They contend that the SAXS curves could be explained by one of two likely models: the two–phase model and the core–shell model—see Figure 1.4. The two-phase model is similar to the inverted micelle model proposed by Gierke et al. (44; 45) and the original two-phase model proposed by Marx et al. (87). The core-shell model was originally proposed by Kao et al. (64) and consists of an ion-rich core surrounded by a shell consisting of only fluorocarbon chains. This core-shell structure is envisioned to be immersed in the "intermediate ionic phase" that contains the fluorocarbon chains and some non-clustered ionic sites. The important difference between these two structural models is that in the case of the two-phase model, the geometrical order related to the SAXS results will be associated with the *inter*cluster spacing whereas in the case of the core-shell model, the spacing will be of an *intra*cluster origin. Therefore, the interpretation of the SAXS results is influenced by the model selection. Hashimoto et al. (55) and Fujimura et al. (34; 35) report that both of the models fit their observations rather well, except in predicting the volume change of the

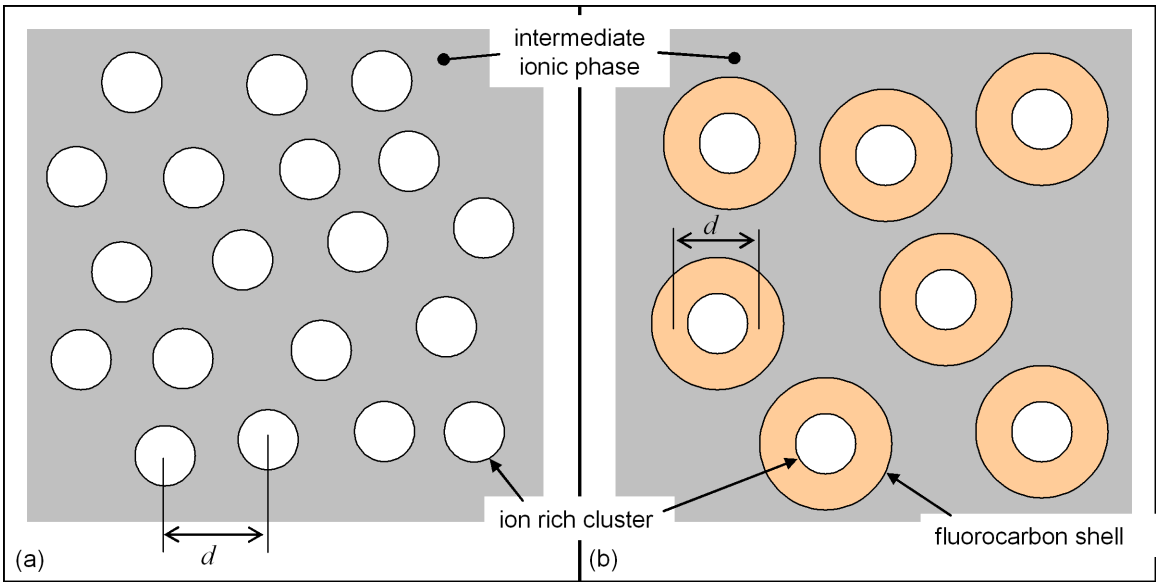

Figure 1.4: (a) The two–phase model and (b) the core–shell model of ion clustering in Nafion™. The dimension reponsible for the observed order within the polymer is labeled as *d*. Adapted from reference (34; 35).

membranes during swelling. In light of this, they report that the core-shell model is more consistent with their measurements. This is in constrast to the work of Gierke et al. (44; 45) in that they favored the two-phase (or "inverted micelle") model to explain their results. An important difference between these two approaches that can explain this discrepancy should now be pointed out, however.

In the work of Gierke et al. (44; 45), the assumption is made that the ionic clusters are spherical in nature and are arranged on a grid. The amount of swelling of the membrane and the intercluster distance (as determined from the SAXS experiments) are then used to determine the average size of the clusters. By using this approach, these researchers were able to make the important conclusion that the clusters do not merely change in size during swelling and de-swelling of the polymer but actually aggregate and dissasociate such that the number of clusters per unit volume of the polymer (given that all of the other relevant parameters remain constant) is a function of the degree of swelling of the polymer. In contrast to this, Hashimoto et al. (55) and Fujimura et al. (34; 35) do not make this assumption and instead they assume that the cluster size is linearly proportional to the Bragg spacing obtained from their SAXS results; no attempt is made to predict the absolute cluster size. They then define two swelling parameters: the microscopic swelling and the macroscopic swelling. The microscopic swelling is defined as the ratio of the Bragg

spacing of the ionic clusters for the hydrated membrane to that of the dry membrane. The macroscopic swelling is defined as the ratio of the swollen volume of the membrane to the dry volume of the membrane. If the actual microstructure of the Nafion^{TM} membrane is described by the two-phase model and the number of clusters remains constant, then the microscopic swelling parameter should be equal to the macroscopic swelling parameter for all swelling values, which is found not to be the case. In fact, this condition is *imposed* by the model of Gierke et al. in their determination of cluster size, where the clusters are assumed to obey the two-phase model and the number of clusters is allowed to change. Therefore, Hashimoto et al. (55) and Fujimura et al. (34; 35) conclude that the two-phase model is unlikely and that the core-shell model is more appropriate. However, it is the opinion of the author that the assumption made by these researchers that the cluster size obeys a linear relationship to the observed Bragg spacing is not valid and that this assumption directly leads to the failure of the two-phase model to accurately describe their observations. Specifically, this assumption seems erronious if one considers that Gierke et al. Hashinoto et al. and Fujimura et al. found that the Bragg spacing is not affected by changing the cation in the polymer even though the degree of swelling of the polymer is strongly a function of the cation type. Furthermore, the two-phase model is supported by other experimental evidence as well, including electron microscopy studies of Nafion^{TM} (13; 109; 107), which will be discussed in mode detail in a later section.

Another study aimed at determining the microstructural morphology of Nafion^{TM} was carried out by Roche et al. (111) in 1981. In this study, small-angle neutron scattering (SANS) as well as SAXS testing was used as an experimental tool. Like Hashimoto et al. (55) and Fujimura et al. (34; 35) and consistent with the results of Gierke et al. (44; 45), these researchers also noted that crystallinity in the Nafion^{TM} polymer could be observed as a peak in the SAXS and SANS curves. This finding was confirmed by WAXD testing. Roche et al. also found that the crystallinity could be eliminated in the polymer by thermal treatment followed by rapid quenching. These researchers also note that a second peak in the SAXS responses is likely due to aggregation of the ions in the polymer into clusters. This clustering peak is observed in both the native (semi-crystalline) and quenched (amorphous) polymers. Although a debate is presented over whether this SAXS maximum is of an interparticle or intraparticle origin, this issue is left as an open question.

More recently, James et al. have performed a series of SAXS tests on Nafion^{TM}

membranes in various states of hydration (62). These tests were supported by a set of atomic force microscopy (AFM) tests performed on the same polymers. In these tests, the equivalent weight of the membrane used was 1100 and only the acid form of the polymer was studied. For the SAXS testing, the polymer was characterized in a controlled humidity environment from 0% to 100% relative humidity (RH). These authors found that the position of the cluster peak did not obey a linear proportionality to the amount of water absorbed by the polymer, as would be expected if the cluster peak were caused by an interparticle ordering. This is consistent with the results of Hashimoto et al. (55) and Fujimura et al. (34; 35). However, they also found that the position of this peak also did not obey a cube root relationship to the volume of sorbed water, which would be expected if the peak were of an intraparticle origin. In fact, neither of these two simple behaviors can succesfully describe the swelling of the Nafion^{TM} membrane. This is consistent with the findings of Gierke et al. and is explained by their model of swelling through cluster agglomeration.

The most interesting aspect of the work of James et al. involves the use of a maximum entropy ("MaxEnt") reconstruction scheme for the interpretation of the SAXS results. In this method, a two-dimensional charge density map of the polymer is generated from the observed X-ray scattering data. Because there are many such charge density maps that will fit a given data set, the method selects the map that corrresponds to the highest entropy for a given goodness-of-fit. This method is described in detail by Elliott and Hanna (26). The advantage of this method is that it does not assume *a priori* a structural model. In this way the MaxEnt technique is superior to other microstructural modeling approaches based on SAXS testing. Of course, a major disadvantage of this method is that it produces a two-dimensional projected interpretation of a three-dimensional charge distribution. However, the method is still useful for making predictions of the microstructure of Nafion^{TM} based on SAXS results as it relates to ionic clustering.

Using this MaxEnt reconstruction, James et al. have been able to quantify the microstructure of Nafion^{TM} membranes in the proton form for various levels of hydration. Based on their results, James et al. conclude that the Nafion^{TM} polymer contains two different types of structures. These two observed structures are attributed to individual ionic clusters with diameter of about 5 nm, and agglomerates of ionic clusters with diameter of about 30 nm. They also found that the number of clusters decreased as the hydration level of the polymer was increased. This finding is consistent with the model of cluster agglom-

eration proposed by Gierke et al. (44; 45). The most important aspect of this work is that the results of the SAXS testing were confirmed by tapping mode AFM testing. The details of this testing will be described in the following section, but it should be mentioned here that both the SAXS results and the AFM results found in James et al. support the notion that the cluster peak oberved in the SAXS data is of an *interparticle* origin and therefore best described by a two-phase model of ionic clustering. Furthermore, these results also support the idea, first proposed by Gierke et al. that the ionic clusters are in a constant state of flux and that the swelling of the polymer by uptake of solvent occurs not simply by an increase in the size of the individual clusters, but by a rearragement and agglomeration of the clusters, with a corresponding decrease in the number of clusters present in a given sample.

1.4.2 Atomic Force Microscopy Studies

Atomic force microscopy (AFM) is a useful tool for probing the morphology of Nafion^{TM} polymers, especially as it relates to ionic clustering in these materials. This is due to the large difference in the mechanical impedance of the hydrophobic fluorocarbon region and the hydrated ionic cluster regions. Also, the adherence of the probe tip to these two regions will also likely be different as a result of the segregation of water in the ionic clusters. A major advantage of AFM over electron microscopy techniques is that it does not require the application of a high vacuum or any pretreatment of the polymer. Therefore, the Nafion^{TM} can be imaged in its hydrated state; further, the water content can be an independent parameter in the testing.

The first reported AFM study of a Nafion^{TM} polymer was performed by Chomakova-Haefke et al. in 1994 (14). In this study, Nafion^{TM} films ca. 0.8 μm thick were cast onto gold-coated cover glasses. These films were then tested in this "dry" state, or were swollen by immersion for 2 h in de-ionozed water. These films were tested in the contact mode and care was taken to ensure that no distortion of the image was introduced either by the scanning angle or through modification of the polymer surface by the probe tip.

The results of these tests revealed a disordered network of folded fibrils in the dry Nafion^{TM} samples. These fibrils had an estimated diameter of 25 to 40 nm and a length of about 1 micron. These fibrils also appeared to contain regions of larger diameter along their length at a periodicity of about 100 nm. Chomakova-Haefke et al. report that the

appearance of the fibrils is similar to a "pearl chain," with the diameter of the pearls being 60 to 80 nm and a spacing between the pearls of 30 to 50 nm. The AFM images of the swollen polymers reveal that the "pearl chain" structure is still evident, although significant alignment of the fibrils seems to be associated with swelling of the polymer. Also, the periodicity of the pearls increased from about 100 nm to 105-135 nm. The authors explain that the observed structure and change due to swelling could be described by the existence of helical structures in the polymer that unwind slightly upon swelling.

A second AFM study of Nafion^{TM} was performed in 1998 by Lehmani et al. (78). In this study, the Nafion^{TM} 117 membrane was used. This membrane has an equivalent weight of 1100 and a nominal thickness of 183 microns. The membranes were pretreated by immersion in concentrated hydrochloric acid followed by boiling in de-ionized water to remove impurities. The samples, so treated, were tested in three states: (1) dried under vacuum at 80°C, (2) dried and imbibed with a single drop of de-ionized water, and (3) dried and imbibed with a single drop of tributylphosphate (TPB). In the case of the solvent-imbibed membranes, the drop of solvent was applied to the sample just before testing and the AFM apparatus was placed in an enclosure with several petri dishes of solvent positioned around it. This was in an effort to prevent dehydration of the membrane during testing.

This work is different from the study of Chomakova-Haefke et al. in that the AFM testing was performed in the tapping mode. Height images were obtained for the three samples over dimensions of 1 X 1 μm and 50 X 50 nm. In the images of the dry sample, the authors note the presence of spherical domains having an average diameter of 45 nm. For smaller scan areas the average diameter of these spherical domains was found to be 11 nm. This nodular structure was preserved in the water-solvated sample. For the sample solvated with TPB, the nodular structure seemed to disappear and all of the calculated parameters increased substantially. This could correspond to the large degree of swelling of the Nafion^{TM} polymer in TBP (40).

There are several problems with the two above described studies of the microstructure of Nafion^{TM} membranes by AFM techniques. In both of these studies the samples were either "dry" or solvent-soaked, with no intermediate solvation levels considered. In the first study, the "dry" samples were not really dry at all, but were simply allowed to equilibrate with their environment. The hydrated samples were soaked with water prior to testing, but no mention was given as to how the hydration level of the samples were controlled

during the test. In the second report, the same problem is apparent. Most importantly, no effort was made in either experiment to *measure* the hydration level of the polymer, before, after, or during the testing. A more serious problem is the manner in which the tests were carried out. In both studies, the AFM was used to measure the height of the samples above the reference plane. For instance, although the 11-45 nm spherical domains observed by Lehmani et al. *could* correspond to the ionic clusters (or cluster agglomerates) in the polymer, no evidence to support this conclusion is given. Because the AFM imaging was performed in a height mode, these structures could simply be caused by imperfections on the surface of the membrane. Conversely, AFM phase imaging of the Nafion^{TM} polymer will be able to distinguish between the softer ionic domains and the stiffer fluorocarbon matrix, particularly in the presence of a solvent, and will not be corrupted by the presence of surface features.

In 2000, two groups of researchers performed more controlled and informative AFM studies of the morphology of Nafion^{TM} membranes (62; 63; 91). In these studies, the polymer was imaged using tapping mode AFM, but both the height and phase images were recorded. McLean et al. (91) have reported that their AFM testing of Nafion^{TM} 117 membranes in the potassium ion form revealed the presence of ionic domains in the polymer. These ionic domains, which are clearly visible in tapping mode phase images, are on the order of 4-10 nm in diameter. The smaller of these ionic domains are likely individual ionic clusters while the larger observed inclusions are most probably agglomerates of two or more ionic clusters. These images were obtained on membranes that had been allowed to equilibrate with the ambient humidity in the environment. When the membrane was soaked in room temperature de-ionized water, the size of the ionic clusters and cluster agglomerates increased to ca. 7-15 nm in diameter. These results are consistent with and in support of the model of Gierke et al. of inverted micellar ionic clusters in Nafion^{TM}.

A similar study performed by James et al. (62; 63) has also revealed the existence of ionic domains of diameter ca. 5-30 nm in Nafion^{TM} 115 membranes. The larger of these features were attributed to agglomerates of ionic clusters. Like the study of McLean et al., James et al. found that the most useful information could be gained from the phase images and that the features observed in the phase images did not always correspond to the features observed in the height images. They explain that, “features at the same height can have a different phase signal and vice versa, indicating minimal topographic

coupling." These membranes were imaged under various ambient humidity conditions from 9 to 34% RH (+/- 2%) and it was found that the phase image contrast increased with the relative humidity as the hydrophilic ionic clusters absorbed more water and became softer relative to the hydrophobic matrix. Using a cluster-counting algorithm, the authors found that the number of clusters decreased and that the average cluster area increased in the sample conditioned at 34% RH relative to the sample conditioned at 9% RH. Again, this is consistent with and in support of the results of Gierke et al. and their model of cluster formation.

1.4.3 Electron Microscopy Studies

Electron microscopy investigations of the microstructure of Nafion^{TM} membranes have been carried out by a number of researchers and are in good agreement with the results obtained using SAXS and AFM methods. The disadvantage of using electron microscopy to perform this characterization is that the hydration level of the membrane cannot be controlled in these experiments due to the high vacuum that must be applied inside of the microscope. This method is useful as a validation tool for the other tests, however.

The first characterization of Nafion^{TM} membranes by electron microscopy was performed in 1977 by Ceynowa (13). In this work, Nafion^{TM} 125 membranes were used. These membranes were prepared by first exchanging the mobile cations in the polymer for lead ions followed by washing and embedding in epoxy. Thin (60-80 nm) sections were then microtomed and imaged using transmission electron microscopy (TEM). The lead ions were exchanged into the polymer to increase the electron density of the clusters and improve the contrast between the clusters and the fluorocarbon matrix. Using this method, Ceynowa was able to obeserve the presence of 3-6 nm diameter particles uniformly distributed in the polymer. Gierke et al. report the observation of similar 3-10 nm particles in TEM images of stained, ultramicrotomed sections (44). These particles are associated with the ionic clusters. Further evidence of this fact is provided by imaging of the polymer in the proton cation form. In this case no particles are observed due to the low electron density of the clusters.

A similar experiment was performed in 1992 by Rieberer and Norian on Nafion^{TM} samples that were prepared by casting from solution and exchanged into the cesium ion form (109). These researchers also oberved small uniformely arranged particles in the polymer

of 1-5 nm in diameter and with an average size of 3 nm. Similar results were obtained from samples that were prepared by exchanging a sample of Nafion^{TM} 117 membrane into the potassium ion form followed by dehydration, embedding in epoxy, and ultramicrotoming.

In 1997, Porat et al. performed TEM on cast Nafion^{TM} films in the proton form (107). In this work, TEM images of cast Nafion^{TM} films clearly reveal the presence of homogeneously distributed 5 nm diameter particles in the polymer. It is surprising that the ionic clusters would appear so clearly in the acid form of the polymer, but the authors contend that the contrast of their images is significantly enhanced through the use of an energy filter that effectively removes inelastically scattered electrons from the image.

More recently, Winey and co–workers have shown that scanning transmission electron microscopy (STEM) can be effectively used to directly image ionic clusters in poly(ethylene-co-methacrylic acid) and poly(styrene-*ran*-methacrylic acid) (77; 131; 68). The ionic aggregates within these materials were found to be nearly sperical with a narrow size distribution.

1.5 Investigations of Ion Associations in Nafion^{TM}

In addition to studies of the microstructural morphology of Nafion^{TM} films, an understanding of the ion associations that are present in the polymer is neccesitated by the goal of understanding the mechanisms of ion transport. For example, incomplete hydration of the cations or the fixed anionic sites will result in contact cation / anion pairs and significantly reduce the ionic conductivity of the polymer. Ion transport mechanisms may be influenced by the solvent and also by the mobile cation. For example, in the hydrated acid form, proton transport in Nafion^{TM} may occur by the Grotthus mechanism (ion hopping among adjacent water molecules), or by the vehicle mechanism (bulk diffusion of H_3O^+ ions) (110). In the presence of an ionic liquid the situation becomes much more complex. It is currently unknown to what degree the ions of the ionic liquid associate with the fixed anions and bound cations of the Nafion^{TM} polymer. The concept of ion solvation may need to be reformulated in the ionic liquid. Of course, one of the most pressing questions is: to what degree does the ionic liquid participate in the electromechanical transduction? In order to better understand these devices, an understanding of the ion associations is essential.

1.5.1 Nuclear Magnetic Resonance Studies

A useful tool for understanding the degree of ion pairing in an electrolyte is Nuclear Magnetic Resonance (NMR). In 1978, Komoroski and Mauritz performed a sodium-23 NMR study on Nafion^{TM} polymers at various hydration levels (70). Care was taken during the preparation of these polymers to ensure that no excess electrolyte was present in the polymer (SO_3:Na ratio = 1:1). The water content of the samples was varied from 1% (dry weight basis) up to greater than 30%. These researchers report that the line width and chemical shift of the ^{23}Na NMR response in Nafion^{TM} increases significantly as the amount of water present in the polymer is reduced. This response broadening is associated with increased binding of the sodium cations to the fixed sulfonate sites. The most significant changes in the line width are observed for low hydration levels corresponding to 3-4 water molecules per sodium ion. The authors suggest that this indicates that 3-4 water molecules probably exist in the first hydration sphere of sodium in the ionic clusters of Nafion^{TM}. Komoroski and Mauritz also performed sodium-23 NMR on a model salt of the sodium-exchanged Nafion^{TM} polymer, sodium trifluoromethanesulfonate (CF_3SO_3Na). They report that for an aqueous 2.6 M solution of this salt, which corresponds to a water to sodium ratio about that of water–saturated Nafion^{TM} (30°C, about 35% water by dry weight), the linewidth of the ^{23}Na NMR response is about an order of magnitude larger than that of Nafion^{TM}. This is evidence that the mobility of an unbound sodium ion in the Nafion^{TM} polymer is significantly reduced as compared to the corresponding aqueous solution of the model salt. It may be reasonable to conclude that the confinement of the anions and cations to discrete ionic clusters may increase their mutual proximity and give rise to a larger number of the cations being in some state of association with the anions than would exist in solution. However, within the solubility limit of the model salt, the direction and magnitude of the NMR shift is the same for the model salt and for Nafion^{TM}, indicating that the mechanism causing the shift is the same, i.e. cation / anion electrostatic attraction.

In a later paper, Komoroski and Mauritz (1982) have quantitatively interpreted these results using a two-state model of ion association where the ions are assumed to be either bound or unbound (71). This model assumes that the observed chemical shift of the ^{23}Na NMR responses are proportional to the weighted averages of those values for the strictly bound and unbound states. For the unbound state, the chemical shift was determined from

the model salt. Because measurements cannot be made on the bound state, the chemical shift of the bound state was estimated to be 50% larger than the value measured at 1 wt.% water uptake. Using this method, the authors determined that at 30 wt.% water, only 0.4% of the sodium ions were in the bound state. This value increased to 7% at 5 wt.% water and to 66% at 1 wt.% water. Komoroski and Mauritz proceed to propose a four-state model of ion binding in Nafion^{TM} and to determine the probability of these four states using an energetics approach, but this result cannot be directly compared to the NMR results. The four states that they propose are: completely dissociated hydrated ion pairs, ion pairs at the contact of undisturbed hydration shells, outer sphere complexed, and inner sphere complexes. The outer sphere complex of this conceptualization is similar to an idea of ion pairing proposed by Falk in which several water molecules may be shared by a cation and a sulfonate site (see Figure 1 of ref (28)).

Komoroski and Mauritz have also performed NMR investigations on Nafion^{TM} polymers exchanged into the lithium and cesium ion forms and swollen with water (71). Very similar findings resulted from these studies. That is, the ^{7}Li and ^{133}Cs line widths and chemical shifts increase substantially as the water content of the polymers is reduced. This is indicative of the formation of contact ion pairs as the polymers are dehydrated. Of interest is the fact that the line widths did not undergo large changes at high water contents but changed rather dramatically as the swelling level was reduced below a specific value. For the ^{23}Na study this swelling level was found to be approximately 3-4 water molecules per sulfonate site. However, for the ^{133}Cs investigation, the line width was found to not increase substantially until the water content of the polymer had been reduced to less than 1 water molecule per exchange site. This indicates that less water is required to mobilize the cesium ions as compared to the smaller sodium ions.

1.5.2 Infrared Spectroscopy Studies

Fourier transform infrared spectroscopy (FTIR) has also been used to characterize Nafion^{TM} membranes. In 1979, Lowry and Mauritz performed an exhaustive FTIR study of 1100 EW Nafion^{TM} films in various cation forms and with various water contents (83). The 1060 cm^{-1} band of the FTIR spectrum of Nafion^{TM} was identified as the stretching vibration of the sulfonate groups. An earlier FTIR study of Nafion^{TM} by Heitner-Wirguin (1978) echoed this conclusion (57). Lowry and Mauritz report that this SO_3^- stretching band increases in

width and shifts to higher frequencies as the water content of the membrane is decreased. This is similar to the observed behaviour of the ^{23}Na NMR response observed by Komoroski and Mauritz (70). This increase in frequency is interpreted as being caused by polarization of the S—O bond by the cations. As water is removed from the membranes, the separation distance between the cations and exchange sites is reduced. As the cation moves closer to the exchange sites, its polarizing effect on the S—O dipole is increased. This increased polarization leads to an upward shift in the SO_3 stretching vibrational frequency. The shift in frequency is only observed at low water contents, indicating that it is caused by short-range interactions; this corresponds to the observations of Komoroski and Mauritz (70). Also in concert with the findings of Komoroski and Mauritz, the water content at which the shift begins decreases with increasing size of the counterions. The magnitude of the shift from the dry state to the fully water–swollen state is also a function the size of the cation. In the dry or semi-dry state this effect is the largest for smaller cations and smallest for larger cations. This is due to the larger electric field of the smaller cations when in contact with the sulfonate exchange sites. In the fully hydrated state no discernable difference between the different cation forms of Nafion^{TM} is evident as sufficient shielding water is present.

This formulation leads to the conclusion that the frequency shift at low water contents corresponds to the formation of contact ion pairs. This result supports the work of Komoroski and Maurtiz in that it demonstrates that as water is removed from the membrane ion contact pairs form and as water is added to the membrane the ion dissociation equilibrium shifts towards more of the cations existing in the unbound state. In 1982 a similar FTIR study of Nafion^{TM} in various cation forms and for various water contents was performed by Falk (29) and the results and conclusions of that study were identical to those of Lowry and Mauritz. Other infrared investigations have also been performed on Nafion^{TM}, including one by Kujawski et al. in 1992 (75) and another by Cable et al. in 1995 (12). The findings of those studies were in excellent agreement with the work of Lowry and Mauritz in terms of the effect of counterion size and of water content on the symmetric stretching frequency of the sulfonate group.

1.6 Studies of Nafion^{TM} with Non-Aqueous Solvents

Several investigations of Nafion^{TM} membranes swollen with other solvents than water have also been undertaken. An early study of this type was undertaken in 1976 by Lopez et al. (81). In this study the rates of ion exchange of Nafion^{TM} membranes in water, acetonitrile, and propylene cabonate were determined. This exchange rate is basically a smeared measurement of the selectivity coefficient and the diffusion coefficient. The rate of exchange from proton form to sodium or cesium form was found to be much lower in the aprotic solvents than in water, indicating a decrease in the selectivity coefficient, the diffusion coefficient, or both. Lopez et al. also found that the equilibrium solvent content of the membranes was affected by the method of pretreatment. In 1977, Lopez et al. continued this work by measuring the diffusion and selectivity coefficients of Nafion^{TM} membranes swollen with water, methanol, acetonitrile, and propylene carbonate (82); the diffusion coefficients were measured using a radiotracer method. In this study the diffusion coefficients of sodium and cesium ions Nafion^{TM} swollen with protic solvents were found to be two to four orders of magnitude larger than in the aprotic solvents. The authors attribute this difference to ineffective solvation of the exchange sites by the aprotic solvents. Water and methanol can stabilize the exchange sites through hydrogen bonding, but the aprotic solvents can only coordinate with the sulfonate sites through ion–dipole interactions. Also, the partial positive charge on the acetonitrile and propylene carbonate molecule is delocalized, further weakening this interaction. For this reason, a larger number of contact ion pairs are likely present in the membranes solvated with aprotic solvents, this reducing the number of free cations and the diffusion coefficient of these ions. A very interesting finding of this study is that the differences in the diffusion coefficients do not seem to be related to the ability of the solvent to swell the membrane. For example, the volume increase upon swelling of the membranes in water and acetonitrile are very similar (16% and 15%, respectively) although the diffusion coefficient for sodium ions is three orders of magnitude larger in water as compared to acetonitrile (1.1-1.3$(10)^{-6}$ and 3.8-5.0$(10)^{-9}$ cm^2/s, respectively). In methanol, the volume increase upon swelling was 90%, although the sodium diffusion coefficient in this solvent was almost identical to that of water (1.2$(10)^{-6}$ cm^2/s). These authors also report that when the same experiments were performed on a second batch of membranes swollen with water, the measured diffusion coefficients were about half of those measured in the

initial experiments. This indicates that some variation in the composition of the membrane from batch to batch likely exists.

Aldebert et al. have performed a similar study on Nafion^{TM} membranes swollen with water, ethanol, *n*–methylformamide, and propylene carbonate (3). In this study, the diffusion coefficient was determined by monitoring the conductivity of the membranes during swelling. The diffusion coefficient for lithium ion in these membranes was found to be strongly dependent on the solvent, with the largest diffusion coefficient measured for water and ethanol. The lithium diffusion coefficient for *n*–methylformamide was found to be about an order of magnitude smaller than that of water and the diffusion coefficient for propylene carbonate was about two orders of magnitude smaller than water. Again, this likely indicates that the less protic solvents are incapable of effectively solvating the exchange sites. These authors also note that there does not appear to be any correlation between the degree of swelling and the diffusion coefficients. They do note that the diffusion coefficient is decreased as the size of the ion is increased, however. The authors explain that this indicates a steric dependence of the diffusion coefficient, but it is more likely caused by the decrease in the ion hydrophilicity with increasing size.

In 1993, Gebel et al. performed a comprehensive study of the swelling properties of Nafion^{TM} in a wide variety of solvents (40), although the transport properties were not measured. These authors concluded that the swelling of the membrane was driven by a balance of the solvation of the charges and the elastic deformation of the polymer. The fact that the swelling is driven by the solvation of the charges was confirmed by the observation of a strong dependence of the swelling on the identity of the counterion. Although it is very difficult in Nafion^{TM} to correlate the solvent properties to their ability to swell the membrane, a relationship between the donor number of the solvent and the volume change on swelling was observed. Gebel et al. also report that the swelling is anisotropic and that this anisotropy varies from one membrane to the next, providing further evidence of presence of some batch to batch variation in the composition.

In 2001, Doyle et al. performed an exhaustive investigation of the relationship between the ionic conductivity of Nafion^{TM}–117 membranes swollen with various solvents and solvent mixtures and the solvent properties (21). Their conclusion was that the most important factors controlling the ionic conductivity are the solvent viscosity, molar volume, and donor properties. A range of ionic conductivities of over five orders of magnitude was

observed for the solvents studied. Although a correlation between the solvent uptake by the membrane and the ionic conductivity was observed, the authors note that a one-to-one relationship does not exist and that several of the solvents do not seem to fit this trend at all. Also, the conductivity is found to depend only weakly on the solvent uptake at high degrees of swelling. No direct correlation between the solvent properties and the ionic conductivity could be found, although trends to exist, such as the tendancy for ionic conductivity to increase with decreasing solvent viscosity and molecular weight and increasing donor number. These authors also note that hydrogen–bonding solvents seem to perform especially well. An empirical fit to the measured conductivity data was produced by a scaling function containing the solvent density, viscosity, and molecular weight, as well as the weight uptake of the solvent by the polymer. Furthermore, a second empirical function containing the donor number, dielectric constant, and solubility parameter was developed to predict the weight uptake of a particular solvent by the membrane. These authors provide as a general conclusion that the dissociation of the cations is the fundamental limiting factor in determining the ionic conductivity of a particular Nafion^{TM} / solvent system.

Further evidence of this is provided by Doyle et al. (20). In this work, the ionic conductivity of Nafion^{TM} membranes swollen in several organic solvents are measured, sometimes with the addition of complexing agents designed to improve ion dissociation. For example, the ionic conductivity of Nafion^{TM} membranes swollen in 1:1 mixtures of ethylene carbonate:dimethyl carbonate can be increased by about an order of magnitude upon addition to the swelling bath of small amount of crown ethers. It is thought that the crown ethers act as complexing agents, improving the cation / anion dissociation and therefore leading to higher ionic conductivities. However, this effect is only apparent when the ionic conductivity of the starting Nafion^{TM} / solvent system is quite low ($<10^{-4}$ S/cm). No improvement is observed for samples swollen in solvents in which more complete dissociation is already acheived.

1.7 Ion Transport Models of Nafion^{TM}

In order to explain the unusual properties of Nafion^{TM} membranes, models of ion transport based on the microstructure of the polymer have been proposed. The most well-known of these ion transport models is the cluster–network model proposed by Gierke in 1977

(43). This model consists of a homogeneously distributed arrangement of ionic clusters interconnected by short, narrow channels as described by Gierke and Hsu (46). Through their formulation, Gierke and Hsu are able to estimate the size of the ionic clusters based on SAXS data and swelling measurements of the polymer. This model also predicts that not only the size of the clusters but the number of sulfonate sites per cluster changes with changes to the water content, indicating that the clusters may undergo a rearrangement during swelling. Gierke and Hsu have also used their model to predict the diameter of the interconnecting channels based on measurements of the diffusion coefficient of water in Nafion^{TM} and the calculated size of the clusters based on SAXS and swelling experiments. This calculated channel diameter is used to explain the performance of Nafion^{TM} membranes in chlor–alkali cells.

Chlor–alkali cells generate caustic (sodium hydroxide) by the electrochemical reaction of water and brine (sodium chloride). Water is fed into one side of the cell and concentrated brine is fed into the other; the two half–cells are separated by a Nafion^{TM} membrane. Water is reduced at the cathode to hydroxyl ions that combine with sodium ions transporting across the Nafion^{TM} membrane to produce caustic. Chlorine gas is liberated in the anode compartment. The current efficiency of a chlor–alkali cell is defined as $CE = 1/(1 - J_{OH}/J_{Na})$ where CE is the current efficiency, J_{OH} is the ion flux of hydroxyl ion and J_{Na} is the ion flux of sodium ion. Therefore, high current efficiencies are acheived when the majority of the current passed through the membrane is carried by the sodium ions. Indeed, the purpose of the Nafion^{TM} membrane is to separate the two solutions and prevent transport of hydroxyl ions into the anode compartment. One would expect the Nafion^{TM} to fulfill this role only if the internal concentration of electrolyte is significantly less than the concentration of exchange sites. In an operating cell this is often not the case, however. Mauritz and Fu have shown that the internal concentration of a Nafion^{TM} membrane of 1100 EW may be greater than 4 M when equilibrated in 15 M NaOH (typical of an operating cell) (88). By constrast, the concentration of exchange sites in Nafion^{TM} is between 5 M and 15 M (46). Under these conditions as much as 90% of the current through the membrane may be carried by the sodium ions. This is explained by Gierke and Hsu's cluster–network model as exclusion of the hydroxyl ions from the narrow channels interconnecting the ionic clusters. Therefore, even though a large concentration of hydroxyl ions may be present within the membrane, the motion of these ions is highly restricted in

relation to the sodium ions. The cluster–network model explains this limited anion mobility by pointing out that the transport of an anion from one cluster to an adjacent cluster is hindered by the fact that the anions are excluded from the interconnecting channels, which are regions of high negative charge density. In the model, Gierke and Hsu calculate the surface charge density of the channels based on the calculated channel diameter. This surface charge density is then used to calculate the potential distribution within the channel. Ultimately an expression for the current efficiency is derived as a function of the potential distribution within the channels and the ratio of the hydroxyl ion mobility to the sodium ion mobility. The only unknown quantitiy is the mobility ratio, which is fixed by fitting of the model to experimental data obtained with a 1400 EW membrane. Using this same value for the mobility ratio, the model is able to accurately predict the current efficiency of membranes of 1100, 1200, 1500, and 1600 equivalent weight. By contrast, no value of the mobility ratio will allow the model to accurately predict the current efficiency over the range of equivalent weights if the effect of electrostatic anion exclusion from the channels is not considered, which corresponds to the clasical view of ionomer membranes with homogeneously distributed fixed charges. Therefore, the model matches well with experimental results by predicting that the ion mobility within Nafion^{TM} membranes is strongly influenced by the clustered morphology of the polymer.

In 1983, Hsu and Gierke extended this concept to an elastic model of cluster formation (60). They showed that by considering the energy change associated with the hydration of an initially dry cluster, a model could be formulated that predicted the hydrated size of the cluster with good correlation to experiment. Using this model these authors concluded that the cluster diameters observed in Nafion^{TM} are controlled by a balance between interactions at the surface of the cluster and the energy of elastic deformation. This model was also used to calculate the size of the channels interconnecting the clusters. Based on their calculations, Gierke and Hsu predicted that the channel diameters are about 1.4 nm, which is in good agreement with the values calculated from water transport experiments of 1.2-1.3 nm (43; 46). This elastic energy formulation also suggests that the channels are stable at room temperature but are likely to be in a constant state of flux, with channels continuously forming and collapsing.

Hsu et al. have also shown that percolation theory can be used to succefully predict the conductivity of Nafion^{TM} membranes as a function of the volume fraction of the aque-

ous phase (59). In this work it was shown that the conductivity (σ) of Nafion^{TM} obeys a power law dependence on the excess (above a threshold limit) volume fraction of conductive (aqueous) phase (eqn. 1.1); this relation is accurate above and near the threshold limit. The power (n) is a universal constant that applies to any percolative system and is independent of the system's mechanical, chemical, or thermodynamical properties. The limiting threshold volume fraction (c_0) of the conducting phase depends on the dimensionality and manner in which the conductive phase is dispersed and is typically around 0.15 for 3D continuous random systems. This model also contains a scaling factor (σ_0) that depends on the details of the conduction mechanism and can only be predicted from microscopic transport models. The authors report that a salient feature of their model is that the dimensional and topological information of cluster connectivity are contained in the $(c-c_0)^n$ factor while the details of ion transport are contained in the σ_0 factor, which can be computed empirically. In order to evalute the model, the conductivity of Nafion^{TM} samples with various volume fractions of conductive phase were measured. The volume fraction of aqueous phase was controlled by changing the equivalent weight of the polymer and the concentration of the equilibrating electrolyte. Hsu et al. found that the measured conductivity increased dramatically at a conductive phase volume fraction of about 0.10, which is less than the ideal limiting value of 0.15. The authors suggest that this discrepany indicates that the ion clusters are not randomly dispersed in the polymer but are rather arranged in a conductive network with connecting channels between them. This model has also been presented in Gierke and Hsu (46) and Hsu and Gierke (60).

$$\sigma = \sigma_0(c - c_0)^n \tag{1.1}$$

In 1985, Wódzki et al. extended this notion of using a percolation model to explain ion conduction in Nafion^{TM} by allowing the scaling factor, which they relate to the conductivity of the internal solution, to vary as a function of the membrane equivalent weight and the concentration of equilibrating electrolyte; in the previous work this factor was held constant. By fitting their model to measured data, Wódzki et al. found that the critical volume fraction of conductive phase was 0.10, which is in agreement with the findings of Hsu (59). Also, they report that the existence of connecting channels between the clusters may be a reasonable explanation for the discrepancy between their calculated critical volume fraction and the theoretical critical volume fraction of 0.15.

1.8 Ionic Liquids

Ionic liquids are salts that exist in their liquid state at low temperatures. Typically, ionic liquids consist of organic cations and organic or inorganic anions. They are non-flammable, have a high thermal and electrochemical stability, and have no measureable vapor pressure. The first reported ionic liquid was discovered in 1914 by Walden (129) This compound, ethylammonium nitrate, melts at 12-14°C. Since that discovery, a number of other ionic liquids have been investigated. These fall into several groups. In 1951, Hurley and Weir reported on *N*-ethylpyridinium bromide–aluminum chloride melt (61) and in 1982 Wilkes et al. reported on diakylimidazolium chloroaluminate melts (130). While these chloroaluminate melts have high conductivities and wide electrochemical stability windows, they are easily and irreversibly hydrolyzed and are therefore very water instable. In 1978 Ford and Hart characterized the ionic liquid triethyl-*N*-hexylammonium triethyl-*N*-hexylboride, which is water stable (actually water immiscible) but highly viscous (32).

More recently, a new class of fluid and water-stable ionic liquids has been discovered based on nitrogen-containing cyclic cations and organic fluorine-containing anions. A useful review of much of the relevant literature on this class of ionic liquids has been performed by Hagiwara and Ito (52). In 1992 Cooper and Sullivan characterized several of these compunds and reported on one that had properties making it attractive as an electrolyte (15). 1-ethyl-3-methylimidazolium trifluoromethanesulfonate, they found, has a viscosity at 25°C of 42.7 cP, a melting temperature of -10°C, an ionic conductivity at 25°C of 9.3 mS/cm, an electrochemical stability window of greater than 4 V, and a weight loss at 350°C of less than 0.03% per minute. The preparation of this compound was described by Fuller and Carlin in 1998 and they reported that the purity of their salt was greater than 99.95% and that the electrochemical stability window of this salt was 4.2 V (37). In 1996, Bonhôte et al. conducted an excellent study of the properties of 34 ionic liquids based on dialkyimidazolium cations and fluorine-containing organic anions (10). The best performing of these compounds studied were based on the trifluoromethanesulfonate ("triflate"), bis(trifluoromethanesulfonyl)imide ("imide"), or trifluoroacetate ("acetate") anions. These compounds were found to have viscosities of between 34 and 45 cP and ionic conductivities of 8.4-9.6 mS/cm (at 20°C). While the imide compounds were water-immiscible (saturation water content at 20°C 1.4-3.0% by mass), the triflate and acetate compounds were found to

be water-soluble. Also, the 1-ethyl-3-methylimidazolium triflate and imide compounds were found to be thermally stable to temperatures of greater than 400°C under air or nitrogen, while the acetate compound began to degrade at 150°C under air and nitrogen.

In 1998, Koch et al. were awarded a US patent on hydrophobic ionic liquids (69). In this patent the authors examine the oxidative stability and ionic conductivity of a number of ionic liquids based on substituted imidazolium or pyridinium cations. The van der Waals volumes of a number of cations and anions are also presented (as calculated using Hyperchem^{TM} software). Koch et al. report that increasing the size of the cations and anions in the ionic liquid serves to reduce the water reactivity or solubility of the ionic liquid. They also report that an increase in the sizes of the ions will lead to a decrease in the ionic conductivity. While this idea serves to explain many of their results, it is an oversimplifications. For example, the two salts 1-ethyl-3-methylimidazolium trifluoromethanesulfonate and 1-ethyl-3-methylimidazolium bis(trifluoromethanesulfonyl)imide have very similar ionic conductivities (8.6 and 8.8 mS/cm @ 20°C, respectively) and similar viscosities (45 and 34 cP @ 20°C, respectively) (10) although the calculated van der Waals volumes of the anions are 80 Å^3 and 143 Å^3, respectively (69). Xu et al. have also performed a detailed study of the properties of several ionic liquids and make the important discovery that ionic liquids obey the Walden Rule (133). That is, the specific conductivity of an ionic liquid is inversely proportional to its viscosity. Bonhôte et al. claim that the viscosity of the ionic liquid can be lowered by delocalizing the charge on the anion, which decreases hydrogen bonding, but that as the alkyl chains are lengthened this effect is negated by increased van der Waals forces (10). A similar argument is made by Xu et al. (133). They report that the attractive force between the ions arise from the Coulombic cohesive energy, which decreases with increasing ion size, and from the van der Waals energy, which will increase with increasing ion size. Xu et al. report that there will exist a minimum in the ion–ion interactions at a specific molar volume (the cube root of the molar volume is proportional to the sum of the ionic radii). Futhermore, they utilize the glass transition temperature of many different ionic liquids as a probe for the ion–ion interactions and show that a broad minimum in the glass transition temperature does occur at a molar volume of 250 cm^3/mol, which corresponds to an interionic separation of about 0.6 nm. This comparison was made for ionic liquids with weakly polarizable species and Xu et al. report that the minimum in the glass transition temperature should be observed at a lower molar volume for polarizable

species. A correlation between the glass transition temperature of an ionic liquid and the ion–ion interactions has also been suggested by Sun et al. (119).

More recently, Hagiwara et al. have reported on the properties of 1-ethyl-3-methylimidazolium fluorohydrogenate ionic liquid (51). This ionic liquid was prepared by the reaction of 1-ethyl-3-methylimidazolium chloride with anhydrous hydrogen fluoride. The authors characterized this ionic liquid by infrared and Raman spectroscopy and report that the anion in this ionic liquid likely exists in multiple states of the general form $F(HF)_n^-$ (n=2-4). The electrochemical stability window of this ionic liquid was measured to be about 3 V. Furthermore, this ionic liquid has the excellent properties of a melting point of -90°C and an ionic conductivity of 120 mS/cm. In a subsequent paper, Hagiwara et al. further studied this ionic liquid as well as other fluorohydrogenate salts with di-substituted imidazolium cations (53). The stoichiometry of these salts was determined to be RMImF·2.3HF, where R is an alkyl group of between 1 and 6 carbons, M is the methyl group, and Im represents the imidazole ring. The anions in these ionic liquids are believed to exist as $(HF)_2F^-$ and $(HF)_3F^-$. The authors report that the vapor pressure of these salts is below 1 Pa, which was the limit of their apparatus. These ionic liquids were characterized by infrared spectroscopy and the authors note that no change in the weight or the IR spectra were observed after exposure of the salts to air for several days. Also, a strong dependence of the properties on the length of the cation alkyl chain was found. As the chain lenght was increased, the viscosity of the salts increased and the conductivity decreased; the electrochemical stability window was about 3 V for all of these ionic liquids. Hagiwara et al. report that these salts obey the Walden rule. The activation energies for viscosity and conductivity were also measured and were found to have similar values and trends with increasing cation alkyl chain length, leading the authors to conclude that the high conductivity of these salts is explained by their low viscosity and not to a special ion transport mechanism such as ion hopping. In fact, the salts with short cation side chains displayed remarkable properties. Dimethylimidazolium fluorohydrogenate ionic liquid was found to have a viscosity (at 25°C) of 5.1 cP and an ionic conductivity of 110 mS/cm while 1-ethyl-3-methylimidazolium fluorohydrogenate was found to have a viscosity of 4.9 cP and an ionic conductivity of 100 mS/cm. This represents an improvement in these properties of an order of magnitude as compared to the corresponding salts with triflate or imide anions.

Very little study has been thus far undertaken to determine the toxicity of ionic

liquids in mammals, which is clearly an obstacle to widespread use of these materials. The only known investigation was carried out by Pernak et al. (2001) in which the LD_{50} of 3-hexyloxymethyl-1-methylimidazolium tetrafluoroborate was found to be 1400 mg/kg in male and 1370 mg/kg in female Wistar rats (105). The LD_{50} metric is defined as the amount of a substance per body weight that is lethal to half of the test subjects within 14 days of dose administration. The LD_{50} metric is intended to gauge oral or dermal toxicity and is used to separate compounds into several classes: highly toxic ($LD_{50} < 5$ mg/kg), very toxic ($LD_{50} < 50$ mg/kg), toxic ($LD_{50} < 500$ mg/kg), and slightly toxic ($LD_{50} < 5000$ mg/kg). On this scale, the ionic liquid characterized by Pernak et al. is only slighty toxic; by comparison, the LD_{50} for nicotine is 50 mg/kg.

1.9 Ionic Liquid / Polymer Composites

Previous efforts to incorporate ionic liquids into polymer membranes are manifest. In 1997, Fuller et al. incorporated 1-ethyl-3-methylimidazolium trifluoromethanesulfonate (EMI-Tf) and 1-ethyl-3-methylimidazolium tetrafluoroborate (EMI-BF4) ionic liquids into poly(vinylidene fluoride)-hexafluoropropylene (PVdF(HFP)) copolymer and were able to acheive films with room temperature conductivities of 5.6-5.8 mS/cm at an IL:polymer ratio of 2:1 (36). Sutto et al. have reported on the preparation of PVdF(HFP) gels containing various amounts of the ionic liquids EMI-BF4, 1,2-dimethyl-3-*n*-propylimidazolium tetrafluoroborate (dMPI-BF4), 1,2-dimethyl-3-*n*-butylimidazolium tetrafluoroborate (dMBI-BF4), and 1,2-dimethyl-3-*n*-butylimidazolium hexafluorophosphate (dMBI-PF6) (121). They found that for a gel containing 85% (wt.) of ionic liquid (EMI-Tf), the room temperature conductivity was 5.5 mS/cm; ionic liquid contents above 15% did not produce stable solids. In 2002, Tsuda et al. reported on the preparation of a polymer / ionic liquid composite consisting of poly-2-hydroxyethyl methacrylate and 1-ethyl-3-methylimidazolium fluorohydrogenate (126). These authors report that for a molar fraction of 0.60 ionic liquid, the room temperature conductivity of this composite is 23 mS/cm. They also report that the electrochemical stability window of this gel is 3.5 V, improved slightly over the neat ionic liquid (3.2 V).

More relevant to the current work are some of the investigations that have been performed on ionic liquid / Nafion^{TM} composites. In 1999, Fuller and Carlin reported on

the performance of Nafion^{TM} polymer membranes impregnated with EMI-Tf and EMI-BF4 ionic liquids (38). The experimental protocol in this study did not include any provisions to control the amount of water present in the Nafion^{TM} membrane or to control the amount of ionic liquid introduced into the membrane. Instead, the ionic liquid was simply applied to one surface of the membrane and the conductivity was then measured as a function of temperature at 22°C and 125°C. Nevertheless, an ionic conductivity of 0.25 mS/cm was measured for the ionic liquid / Nafion^{TM} composite at 22°C.

A more comprehensive study was performed by Doyle et al. in 2000 in which 1-butyl-3-methylimidazolium trifluoromethanesulfonate (BMI-Tf) and 1-butyl-3-methylimidazolium tetrafluoroborate (BMI-BF4) ionic liquids were incorporated into Nafion^{TM}-117 membranes in the hyrogen and lithium counterion form (19). In this study, the triflate ionic liquid was preferred over the tetrafluoroborate because of an increased high–temperature stability observed in the former. This may have been due to the low purity of the BMI-BF4 ionic liquid, however (85%). Doyle et al. incorporated the ionic liquid into the Nafion^{TM} membranes by soaking first drying the membranes at 120°C under vacuum for 48 hours and then soaking the dried membrane in an excess of the ionic liquid. They showed that the amount of ionic liquid imbibed into the membrane could be increased by heating the ionic liquid during the soak, with a solvent uptake of up to 54% (wt.) at 100°C (2 hour soak). For a proton–form Nafion^{TM}-117 membrane (1100 EW) treated in this way with the BMI-Tf ionic liquid, a room–temperature ionic conductivity of about 0.1 mS/cm was acheived. The conductivity was shown to be higher for membranes with lower equivalent weights and higher temperatures. Thermal gravimmetric analysis (TGA) was also performed on these samples and they were shown to be stable up to 350°C, which corresponds to the decomposition of the neat ionic liquid.

Bennett and Leo have also shown that ionic liquids based on the 1-ethyl-3-methylimidazolium cation and the bromide or triflate anion can be used with electromechanical transducers (8). They do not provide measurements of ionic conductivity in these materials, but the stability of the ionic liquid–swollen transducers is shown to be improved over water–based materials when operated in air. Repeated cycling of a platinum– and gold–plated Nafion^{TM}-117 membrane swollen with water by a 1.5 V (peak), 2 Hz sine wave in air revealed that the strain generated by that device decreased nearly to zero after about 2000 cycles. The authors report that this decrease is due to dehydration

of the device when operated in air. By contrast, the same actuator swollen with EMI-Tf ionic liquid operated for over 250,000 cycles with only a 25% decrease in the free strain generated.

Ionic liquids have also been used as electrolytes in conducting polymer actuators. In 2002, Lu et al. showed that polypyrrole and polyaniline actuators and electrochromic devices that were operated in BMI-BF4 ionic liquid had comparable performance to the devices operated in the traditional propylene carbonate electrolytes, but with much enhanced stability over the traditional devices (84). Interestingly, they also showed that the direction of the actuation was reversed when these actuators were operated in the ionic liquids. Mazurkiewicz et al. have also reported that the stability (as indicated by cyclic voltammetry) of polypyrrole films was improved when BMI-PF6 ionic liquid was used as the electrolyte in the place of tetrabutylammonium hexafluorophosphate dissolved in propylene carbonate (90). Stability of these films was demonstrated up to 1000 cycles. Ding et al. have also utilized ionic liquids as electrolytes for polypyrrole actuators and have also observed improved stability in these materials (18). The strain generation of these actuators in the 1-ethyl-3-methylimidazolium bis(trifluoromethanesulfonyl)imide (EMI-Im) and BMI-PF6 ionic liquids was almost identical to the strain generation of the polypyrrole actuators operated in TBA-PF6 / PC electrolytes. Furthermore, the actuation strain in the ionic liquids of greater than 1% peak-to-peak was shown to be stable to 6000 cycles at an applied potential of between +5 V and -5 V and an actuation frequency of 1 Hz. By contrast, the performance of the actuators operated in the organic electrolyte degraded rapidly under this cycling, decreasing from an initial value of greater than 1% peak-to-peak to 0.3% after 3600 cycles. As with Lu et al., Ding et al. also found that the direction of the actuation in the ionic liquid electrolytes was reversed from the propylene carbonate electrolyte. This is due to a cation–driven actuation mechanism in the ionic liquids as compared to an actuation mechanism driven by anion motion in the TBA-PF6 / PC electrolyte.

In the previous works, the conducting polymer actuators were operated in a liquid electrolyte. Bimorph acutators have also been demonstrated in which the electrolyte is supported on a membrane between two conducting polymer films. Zhou et al. have shown that an ionic liquid may be trapped by soaking it into a porous poly(vinylidene fluoride) membrane and subsequently adding methyl methacrylate monomer (140). Polymerization and cross-linking of the poly(methyl methacrylate) is then initiated and the final solid

electrolyte may be used as a separator for a bimorph conducting polymer actuator. It was found that the ionic conductivity of this polymer / ionic liquid composite within the PVdF film was 0.28 mS/cm, as compared to 3.5 mS/cm when the process was performed outside of the confines of the PVdF membrane. The authors showed that a polypyrrole actuator made using this technique generated +/- 2% strain under an applied voltage of +/- 2.0V and that the actuator could be operated for 3600 cycles without degredation. Vidal et al. have also used an ionic liquid as the electrolyte for a bimorph conducting polymer actuator (128). In this work, an actuator was fabricated in which poly(3,4-ethylenedioxythiophene) (PEDOT) was coated onto each side of a polybutadiene / poly(ethylene oxide) (PBN/PEO) polymer network. The method utilized generated PEDOT layers that penetrated into the PBN/PEO network gradually, with the concentration of the PEDOT being higher near the surfaces. Following this preparation, the composite polymer film was soaked in a 50/50 solution of dichloromethane and EMI-Im for 24 hours, followed by evaporation of the dichloromethane. The authors report that this resulted in a loading of EMI-Im ionic liquid on the order of 10% (wt.). Vidal et al. also reported that actuation in these devices was generated by the motion of cations. They also report that the current drawn by the device when driven by a +/- 2 V sqaure wave potential is stable for over 10,000 cycles in air (1 Hz), indicating no loss of conductivity of the electrolyte. Further, the actuator was operated at +/- 2V for 6 hours each day for one month with no observed degredation of the actuation ability. The authors report that at higher frequencies larger actuation voltages can be used and that operation at potentials up to 5 V at frequencies of 10 Hz can produce stable responses for 7 million cycles.

1.10 Summary

Even though Nafion^{TM} membranes have been in use since the early 1960's, the fundamental principles of their operation are still not well understood. Numerous studies have attempted to uncover the underlying mechanisms of ion transport through an investigation of the microstructure of the polymer and the ion associations within it. The most useful interpretations consider that the ions in the Nafion^{TM} cation–exchange polymer aggregate into clusters ca. 4-5 nm in diameter. Within this framework a thin layer of negative charge exists at the surface of the clusters and also within the pores that interconnect the clusters.

Exclusion of the anions from this layer is used to explain the unique anion–blocking properties of Nafion^{TM} membranes. The remarkable ability of Nafion^{TM} membranes to transmit cations is thought to result from this interconnected conductive network of clusters. Percolation theory has been used to determine the critical volume fraction of conductive phase for ion transport to occur. This volume fraction is experimentally found to be lower than the limit predicted by theory, confirming a high degree of connectivity in this network. Experiment has also been used to probe the ion associations in Nafion^{TM} and show that at high hydration levels the cations in the membrane are largely dissociated, which further explains its high cation conductivity in its water–swollen state. Studies of the properties of Nafion^{TM} membranes swollen with non–aqueous solvents reveal that the ability of the solvent to effectively shield the cations and the anionic exchange sites is of critical importance.

Recently, a new class of non-aqueous solvents has been studied for use as electrolytes in a variety of applications. These ionic liquids have several advantages that make them attractive for use in Nafion^{TM} polymer transducers. They are non-volatile, non-flammable, have a large electrochemical stability window and a high thermal stability. Ionic liquids also have a high inherent ionic conductivity and therefore are useful as highly–stable electrolytes. Ionic liquids have been incorporated into polymer membrane films for use as solid–state electrolytes and into conducting polymer actuators and have shown improved performance over conventional organic solvents.

Electromechanical transducers based on Nafion^{TM} membranes have been extensively studied since the early 1990's. Although models of this transduction are still debated, it has been well accepted that the fundamental process responsible is transport or reorientation of the ions within the material. One of the key problems facing ionomeric polymer transducers today is their reliance on water as a solvent for continued performance. Not only does the water quickly evaporate when the transducers are operated in air, but the electrochemical stability window of water is small and therefore limits the maximum voltage that can be applied to a hydrated Nafion^{TM} transducer.

1.11 Research Plan

The goal of the current work is to demonstrate improved performance of Nafion^{TM} polymer transducers by swelling them with an ionic liquid in the place of water. Additionally, the

fundamental mechanism responsible for transduction in these ionic liquid / Nafion^{TM} composite transducers will be identified through an investigation of the polymer microstructure, the ion associations within the polymer, and the observation of the macroscopic transduction behavior. Deliverables of this work will be a method for fabricating Nafion^{TM} transducers with improved performance over current water–based materials and an understanding of the transduction behavior in ionic liquid–swollen Nafion^{TM} membranes.

The model of the physical interpretation of transduction in ionic liquid–swollen Nafion^{TM} transducers will be based on characterizations of the properties of these materials. In order to develop this model, several experimental methods will be utilized. Small-angle X-ray scattering (SAXS) will be used to make determinations of the morphology of the ionic liquid / Nafion^{TM} composites and to investigate the effect that the ionic liquids have on that morphology. Infrared spectroscopy will be used to investiagte the ion associations within the polymer by analyzing the stretching vibration of the sulfonate exchange site. Nuclear magnetic resonance spectroscopy will be used to make determinations of the mobility of the counterions within the polymer. Metal plated and ionic liquid–swollen Nafion^{TM} membranes will also be characterized for their transduction performance, in terms of their actuation and sensing capabilities. Several experimental parameters will be varied for each test. These include the structure of the ionic liquid used, the uptake of ionic liquid within the membrane, and the identity of the counterion in the membrane.

Based on the experimental observations, theories describing the effect of the ionic liquids on the morphology of the membranes and the ion associations within the membranes will be presented. These theories will be coupled with the observed electromechanical transduction behavior in order to propose a model for the charge transport mechanism in the membranes. Ultimately, this work will lead to an understanding of the key properties of the ionic liquid and the polymer that lead to desireable transducer performance.

1.12 Contributions

The purpose of this research has been to investigate the mechanisms of transduction in ionic liquid–swollen Nafion^{TM} membranes. This was accomplished through the development of improved fabrication methods for these materials. Morphological characterizations of the ionic liquid–swollen polymer was also performed. Further, the ion associations within the

membranes were studied. The electromechanical transduction properties of ionic liquid–swollen Nafion^{TM} membranes were also characterized. The results of these investigations were used to develop a model that is capable of explaining the observed behavior. In summary, the contributions of this research are:

- Methods were developed for controllably incorporating ionic liquids into Nafion^{TM} membranes,
- Methods were developed for electroding Nafion^{TM} membranes imbibed with ionic liquids,
- The morphology of the ionic liquid–swollen Nafion^{TM} membranes was investigated using small–angle X-ray scattering (SAXS),
- The ion associations within the ionic liquid–swollen Nafion^{TM} membranes were elucidated by Fourier transform infrared spectroscopy (FTIR) and nuclear magnetic resonance spectroscopy (NMR) studies,
- The electromechanical transduction behavior of the composite membranes was investigated,
- An understanding was developed of the fundamental mechanisms responsible for electromechanical transduction in ionic liquid–swollen Nafion^{TM} membranes, and
- The use of ionic liquids in electromechanical transducers based on Nafion^{TM} membranes was shown to overcome many of the limitations created by the use of water.

The remainder of this dissertation will be organized as follows. Chapter 2 will present the results of an initial investigation performed on ionic liquid–swollen transducers and will highlight the differences that have been observed between these new materials and traditional water–swollen transducers. Chapter 3 will present the results of a structured investigation into the morphology of the ionic liquid / Nafion^{TM} polymer composites. Chapter 4 will present the results of an investigation into the ion associations within the polymer using infrared spectroscopy and nuclear magnetic resonance spectroscopy. A structured investigation of electromechanical transduction in ionic liquid–swollen Nafion^{TM} membranes will be presented in Chapter 5. Chapter 6 will formulate the model of the transduction

mechanisms based on the morphological, spectroscopic, and transduction results. Chapter 7 will summarize the findings and present the conclusions of this research.

Chapter 2

Initial Demonstration of Transduction in Ionic Liquid–Swollen Nafion^{TM} Membranes

This chapter will present some of the initial work that was performed with ionic liquid-swollen Nafion^{TM} transducers. Bennett and Leo in 2004 demonstrated the first use of ionic liquids as diluents for ionomeric polymer transducers (8). Ionic liquids have the potential to overcome many of the obstacles to development of the traditional water–swollen ionomeric transducers. This chapter will describe some of the obstacles that were encountered in the early stages of this work and the methods that were developed to overcome those obstacles. Discussion will be given of the methods used for incorporating ionic liquids into Nafion^{TM} membranes, of the issues that arise when these membranes are plated with metal electrodes, and of the performance of these electroded and ionic liquid–swollen membranes as electromechanical transducers. Improved stability over water–based materials when operated as actuators will be demonstrated.

2.1 Incorporation of Ionic Liquids into Nafion^{TM} Membranes

In order to utilize an ionic liquid as a diluent for an ionomeric polymer membrane–based transducer, a viable method for incorporating the ionic liquid into the transducer must be developed. This method should not only allow for the incorporation of large amounts of the ionic liquid into the membrane, but should also allow for some degree of control over the amount of ionic liquid that is incorporated.

In order to prepare Nafion^{TM} membranes for swelling with an ionic liquid, they were dried in an oven at 110°C under vacuum. Initially, the Nafion^{TM} membranes were swollen with ionic liquid by soaking the dry membrane in neat ionic liquid under elevated temperature for an extended period of time. Figure 2.1 shows the time-dependent uptake of five ionic liquids into dry, proton form membranes. The uptake reported is the volume of ionic liquid within the swollen membrane as a percentage of the dry volume of the membrane. These volumes are calculated from the measured weights of the membrane in the dry and swollen forms. These weights are used with the density of the dry membrane and the density of the ionic liquid to determine the volumetric uptake of ionic liquid from

$$V = \frac{(w_s - w)\rho}{w\rho_i}, \tag{2.1}$$

where V is the fractional volumetric uptake of ionic liquid, w is the dry weight of the polymer, ρ is the density of the dry polymer, w_s is the swollen weight of the polymer, and ρ_i is the density of the ionic liquid. The volumetric uptake of ionic liquid is typically expressed as a percentage.

Where available, the densities of the ionic liquids were obtained from the literature. For those ionic liquid densities that were not reported in the literature, the density was estimated from weight and volume measurements. For this testing, the empty weight of a 1 cc syringe was measured. A small amount of ionic liquid was then drawn into the syringe and the weight was measured again. The volume of ionic liquid was determined using the scale on the syringe. The mass of ionic liquid was determined by taking the difference between the full and empty weight of the syringe. The density of the ionic liquid was then computed as the ratio of the measured weight to the measured volume. The densities of several of the ionic liquids studied in this work are presented in Table 2.2.

The dry density of the polymer was determined in a similar manner from weight and volume measurements of dry samples. To dry the samples, they were baked at 100°C

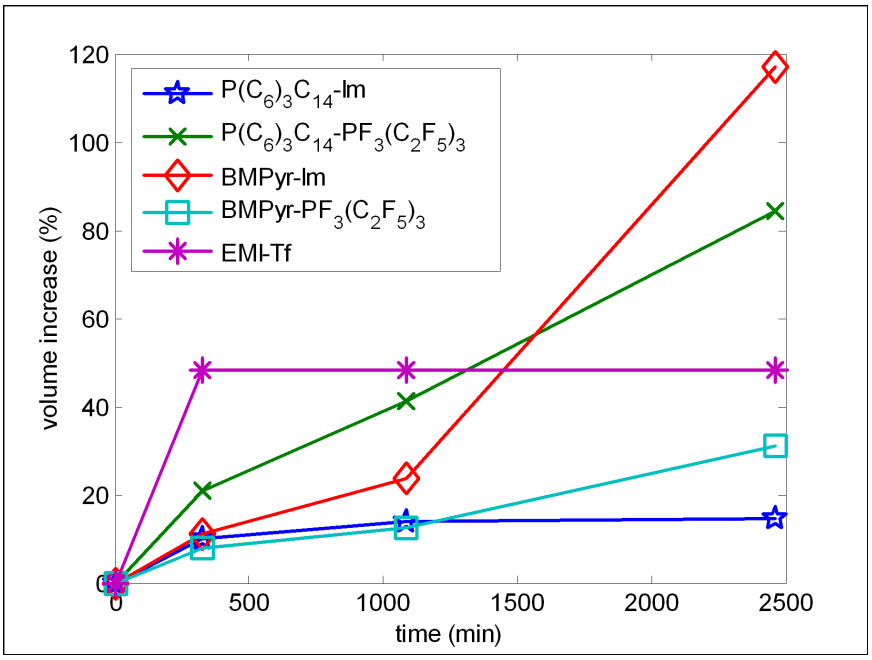

Figure 2.1: The time history of the uptake of five ionic liquids by an initially dry metal–plated Nafion^{TM} membrane at 100°C.

Table 2.1: Abbreviations for seven of the ionic liquids studied in the course of this research.

full name	abbreviation
trihexyl(tetradecyl)phosphonium bis(trifluoromethylsulfonyl)imide	$P(C_6)_3C_{14}$-Im
trihexyl(tetradecyl)phosphonium tris(pentafluoroethyl)trifluorophosphate	$P(C_6)_3C_{14}$-$PF_3(C_2F_5)_3$
1-butyl-1-methyl-pyrrolidinium bis(trifluoromethylsulfonyl)imide	BMPyr-Im
1-butyl-1-methyl-pyrrolidinium tris(pentafluoroethyl)trifluorophosphate	BMPyr-$PF_3(C_2F_5)_3$
1-ethyl-3-methyl-imidazolium trifluoromethanesulfonate	EMI-Tf
1-ethyl-3-methyl-imidazolium bis(trifluoromethanesulfonyl)imide	EMI-Im
1-ethyl-3-methyl-imidazolium bromide	EMI-Br

under vacuum for 12 hours. Although it is recognized that this process does not result in complete removal of all water from the membrane, the samples are considered to be as dry as is possible using the available equipment. The length and width of the samples were measured using a steel scale and the thickness was measured with a Mitutoyo digital caliper. The geometry of each sample was then used to compute its volume. The weight of the samples were measured with an electronic analytical balance and the density was computed as the ratio of the weight to the volume. The density measurements used in this research were obtained by averaging the measured densities of several samples.

The identifiers used in Figure 2.1 and in most of this dissertation are abbreviations

Table 2.2: Degree of swelling of ionic liquid for five metal plated Nafion^{TM} membranes in the proton form. The dry membranes were soaked in the ionic liquids at 100°C for 41 hours. Also presented are the densities of the ionic liquids.

diluent	uptake (% of dry volume)	density (g/cm^3)
$P(C_6)_3C_{14}$-Im	84.4	1.08
$P(C_6)_3C_{14}$-$PF_3(C_2F_5)_3$	117.2	1.17
BMPyr-Im	18.2	1.40
BMPyr-$PF_3(C_2F_5)_3$	31.0	1.60
EMI-Tf	48.2	1.39$^{(a)}$

$^{(a)}$ from reference (10)

for the ionic liquids. This will facilitate the discussion, as the full names are quite long. For the full names and abbreviations of the ionic liquids that were initially examined, see Table 2.1. The cation of the ionic liquid comes first in the name and the anion follows. Although these abbreviations may seem confusing, effort has been made to use the abbreviations that are most commonly found in the literature, although discrepancies do exist. For example, the bis(trifluoromethanesulfonyl)imide anion is sometimes abbreviated as "Im," sometimes as "$(Tf)_2N$," and sometimes as "TFSI." In this dissertation, this anion will be reffered to as "Im."

As can be seen from Figure 2.1, the rates of diffusion and equilibrium contents of these ionic liquids in the Nafion^{TM} polymer are highly varied. The EMI-Tf ionic liquid diffuses into the membrane very quickly and reached equilibrium after less than 5.5 hours (equilibrium was likely reached before this point, actually). By contrast, the other ionic liquids diffused into the membrane much more slowly. Besides the EMI-Tf ionic liquid, only the $P(C_6)_3C_{14}$-Im ionic liquid reaches equilibrium during the 41 hour, 100°C soak. Also of interest is the fact that the rate of diffusion seems to increase dramatically for the two $BMPyr^+$ ionic liquids after about 20 hours. This could indicate that these ionic liquids induce a more profound change to the morphology of the Nafion^{TM} polymer than the others.

2.2 Electroding of Ionic Liquid / Nafion^{TM} Composites

An ionomeric polymer transducer is composed of four main parts–see Figure 2.2. As can be seen, the transducer is comprised of an ionomeric polymer membrane (typically Nafion^{TM}) that is swollen with a diluent (typically water) and plated on both surfaces with two sets of

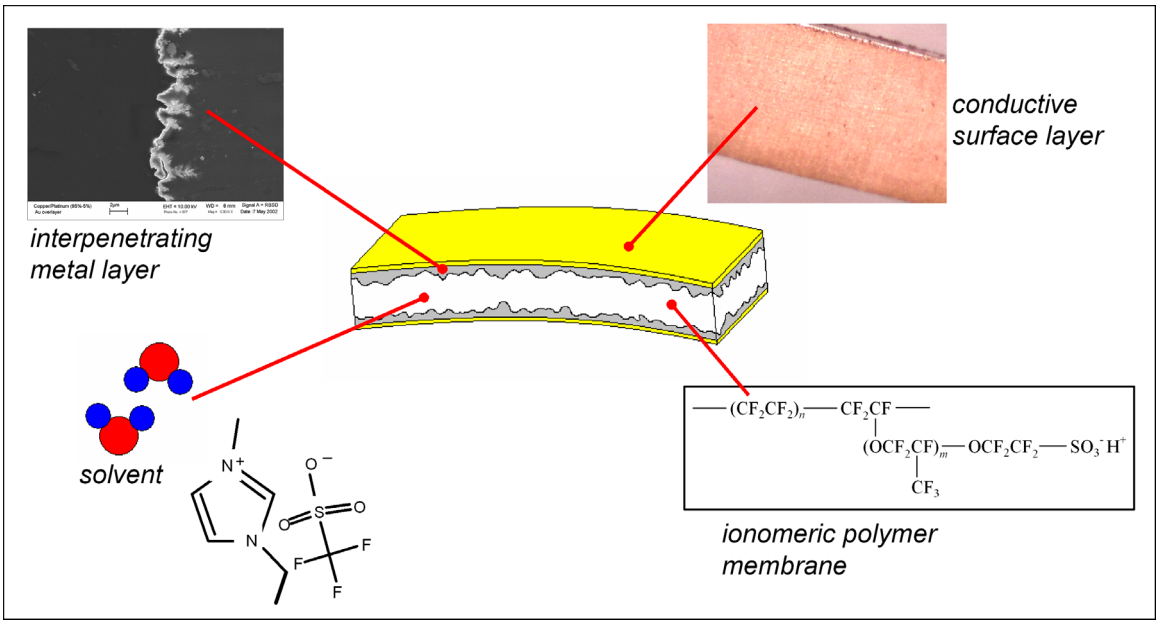

Figure 2.2: Schematic of an ionomeric polymer membrane transducer.

electrodes. The first set of electrodes penetrates into the surface of the polymer membrane. This penetration creates a very high polymer / metal interfacial area and gives rise to a large accumulation of electrical charge when an electric field is applied across the membrane thickness (2; 1). The interpenetrating electrode is not very conductive along the length of the transducer, though. For this reason, a second electrode is applied to the surface of the interpenetrating layer to improve the surface conductivity.

Typically, the interpenetrating electrode of a Nafion^{TM} transducer is composed of platinum. Variations on the electroless plating of Nafion^{TM} membranes with platinum have been reported by a number of researchers (94; 92; 93; 108). The interpenetrating platinum electrode is typically deposited using an "exchange / reduction" process. In this process the membrane is soaked in a solution of the platinum salt tetraammineplatinum chloride ($Pt(NH_3)_4Cl_2$). Bennett and Leo have also shown that copper metal may be used as the electrode, but that its use is severaly hindered by its low oxidative stability (9). Once the membrane is fully exchanged into the tetraammineplatinum ion form it is soaked in a solution of sodium borohydride ($NaBH_4$), which acts as a reducing agent. The sodium borohydride reduces the metal ions to their neutral state at and just below the surfaces of the membrane. This process results in metal electrodes that penetrate into the membrane to a depth of 10-20 microns and form continuous layers at the surface. The exchange

/ reduction process is typically repeated 5-6 times to increase the metal loading in the electrode layers and improve the polymer / metal interfacial area. Following the exchane / reduction process, a second electrode layer is deposited in order to improve the surface conductivity. In this work the surface electrode is gold and is applied by electroplating. The thickness of the electroplated gold layer is approximately 1 micron.

Typically, the membranes are electroded in their water–swollen state in an aqueous process and are used in their water–swollen state. However, the goal of the current research is to eliminate the dependence of ionomeric polymer transducers on water as a solvent. Therefore, in this work, these electroded membranes are dehydrated by baking in a vacuum oven and are then imbibed with an appropriate ionic liquid. However, it has been found that the swelling that takes place during the ionic liquid incorporation is very damaging to the metal electrodes. The cause of this damage has been identified as the large amount of strain that the electrode must undergo between the as–plated water–swollen state and the ionic liquid–swollen state. DuPont reports that a Nafion^{TM} membrane will increase in size in the planar direction by 15% between its room humidity–equilibrated state (50% RH, 23°C, 5% water by dry weight) and its fully water–swollen state (boiled for 1 hour, 38% water by dry weight) (22). This means that the metal electrodes will undergo a compressive strain of *greater* than 15% during the drying process after the metal deposition and will then undergo a tensile strain during the incorporation of the ionic liquid, the magnitude of which will depend on the amount of ionic liquid absorbed. This large cyclic strain from the water–swollen state to the ionic liquid–swollen state is very damaging for the electrodes and can cause cracking of the gold surface electrode on the membranes—see Figure 2.3. This cracking leads to an increase in the the surface resistance of the electrodes from about 1 Ω/cm to more than 1 MΩ/cm.

In order to overcome this problem, the electroding technique was modified. In this new technique the electrode is deposited as before using an exchange / reduction approach, but ethanol is added to the aqueous metal salt and sodium borohydride solutions. The gold electroplating solution is also diluted with ethanol. Gebel et al. have reported that Nafion^{TM} membranes swell by 45% in pure ethanol and by 14% in water at room temperature from their dry state (40). Therefore, by using a rule of mixtures as a approximation, a Nafion^{TM} membrane equilibrated in 25% ethanol and 75% water should swell by 21.75% from its dry state. The actual swelling will likely be larger than this, as Gebel et al. performed

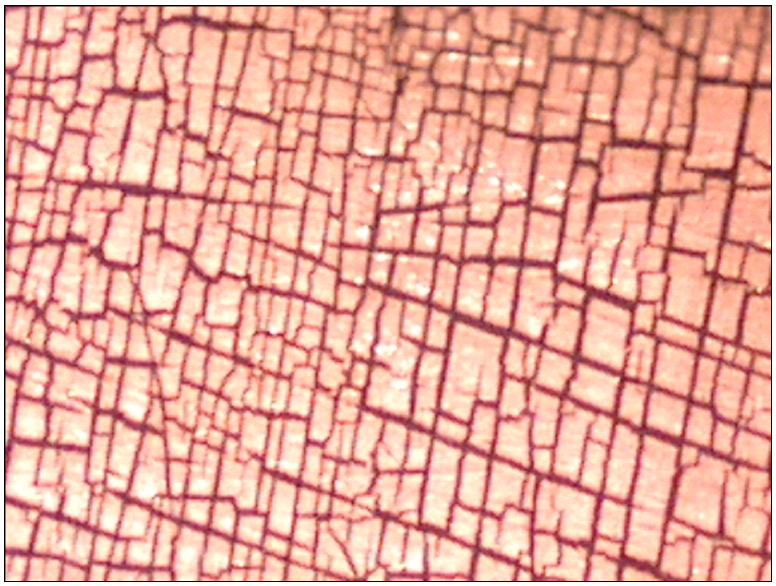

Figure 2.3: Photograph of a highly swollen metal–plated Nafion^{TM} membrane showing cracking of the surface electrode.

the incorporation by soaking at room temperature; during the plating the membranes are swollen by boiling in solvent. This increased swelling during the plating process will result in an increased size of the as–plated metal electrode as compared to the size of the electrode plated without utilizing ethanol. Therefore, once the membrane is dehydrated and re–swollen with ionic liquid the electrode will actually be smaller than its original size. The idea is that the net decrease in the size of the electrode layer from the as–plated state to the ionic liquid–swollen state will reduce the tendancy for the electrodes to crack and suffer a dramatic loss of conductivity. This technique has been proven to be sucessful in depositing interpenetrating platinum electrodes and electroplated gold layers and has been shown to overcome the problem of cracking of the electrode when the membranes are swollen with ionic liquid.

For the transducers studied in the early stages of this work, the electrode deposition process was as follows. A Nafion^{TM}-117 membrane (nominal thickness 183 μm) was first sanded on both sides in a 90° cross–hatching pattern using 600-grit sandpaper. The membrane was then boiled in 1.0 M H_2SO_4 in a solution of 3:1 deionized water:ethanol (by volume) for one hour to ensure that it is in the proton form. It was then boiled for one hour in 3:1 water:ethanol (by volume) to fully swell the membrane and remove any excess acid. The plating process began by soaking the membrane in a 3:1 water:ethanol solution of

tetraammineplatinum chloride ($Pt(NH_3)_4Cl_2$). The solution was prepared to a concentration of 0.001 M and then an additional quantity of $Pt(NH_3)_4Cl_2$ salt was added, in a ratio equivalent to one $Pt(NH_3)_4^{2+}$ ion to two sulfonate exchange sites. The number of sulfonates in the membrane was determined from the equivalent weight (1100) and the dry weight of the membrane. The proton–form membrane was soaked in the $Pt(NH_3)_4Cl_2$ solution overnight (about 12 hours), with vigorous stirring. The membrane was then removed from the solution, rised thoroughly with 3:1 DI water:ethanol, and soaked in a 3:1 water:ethanol solution of 0.1 % (by weight) sodium borohydride ($NaBH_4$) for 8 hours, without stirring or agitation. The sodium borohydride reduced the absorbed $Pt(NH_3)_4^{2+}$ ions in the membrane to metallic platinum, at the surface of the membrane and also within the polymer, to a depth of about 10-20 microns. Following the reduction process, the membrane was boiled in 1.0 M H_2SO_4 for one hour to exchange it back into the proton form. A measured amount of $Pt(NH_3)_4Cl_2$ salt was then added to the tetraammineplatinum chloride solution and the exchange reduction process was repeated. In order to increase the loading of platinum metal within the surfaces of the membrane, the plating process was repeated a total of five times.

Following the deposition of platinum onto the membrane, the membrane was again boiled in 1.0 M H_2SO_4 and a layer of gold was applied by electroplating. A commercially–available gold plating solution was used (24K Pure Gold Plating Solution, Gold Plating Services, Inc.). This solution was mixed in a ratio of three parts gold plating solution to one part ethanol prior to use. The deposition of gold onto the platinum–plated membrane was carried out at a temperature of 65°C under a DC current of 3.23 mA/cm^2 of membrane area using platinized titanium anodes immersed in the solution and positioned on each side of the membrane. The total deposition time was 5 minutes. Following the gold plating, the membrane was boiled in 1.0 M H_2SO_4 in a solution of three parts deionized water to one part ethanol.

2.3 Initial Transduction Results

Using the processes described for metal electrode deposition and ionic liquid incorporation, ionomeric polymer transducers based on Nafion^{TM} membranes have been fabricated. These transducers were characterized and compared to similar water–based materials in terms of environmental stability and actuation performance.

2.3.1 Characterization Methods

In order to evaluate the performance of electromechanical transducers based on ionic liquid / Nafion^{TM} composites, a number of properties and performance metrics of these devices were measured. One of the metrics that was used to compare the transducer materials employing different solvents is the free strain generated by the transducers when driven by a small voltage. Because Nafion^{TM} membranes bend when stimulated by an applied voltage, they are tested in a cantilevered configuration. One end is fixed in a spring-loaded clamp fitted with gold foil electrodes that contact the conductive metal surfaces of the sample and the deflection of the free end is measured with a laser vibrometer–see Figure 2.4. In order to obtain the frequency response between the generated strain and the applied voltage, a random voltage signal was used to drive the polymer and the driving voltage and tip displacement were measured by a Tektronics Fourier analyzer. The tip displacement was then converted into strain using

$$\frac{\epsilon}{V} = \frac{\frac{\delta}{V}t}{L_f^2}, \tag{2.2}$$

where $\frac{\delta}{V}$ is the frequency response between tip displacement (zero-to-peak) and input voltage, t is the thickness of the sample, and L_f is the free length of the sample. This equation assumes that the actuator deforms with a constant curvature. This assumption can be verified qualitatively by observing the deformed shape of an ionomeric polymer actuator under application of a voltage—see Figure 1.2. Also, several researchers have measured the deformed shape of ionomeric polymer actuators and have confirmed that the shape most closely resembles constant curvature (99; 5).

In addition to characterizing the frequency response between strain output and voltage input, the step response of the samples was also measured. As with the frequency domain testing, the experimental setup shown in Figure 2.4 was used. In this case, a DSpace digital signal processor was used both to generate the input signal to the polymer and to record the output of the laser vibrometer, which was used to measure the tip displacement of the actuator strip. For this testing, a step was used as the input signal to the polymer actuators. As before, equation 2.2 was used to determine the generated strain at the outer surface of the actuator, with the exception that the deflection (δ) and the strain (ϵ) were not normalized by the applied voltage (V).

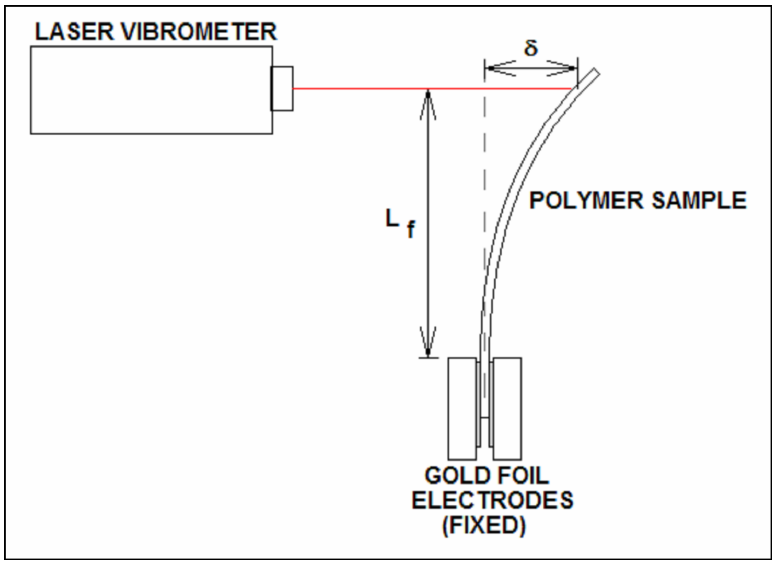

Figure 2.4: A schematic of the experimental setup used to measure the free strain generated by the transducer as an actuator.

2.3.2 Characterization of Environmental Stability

Traditionally, the diluent of choice for ionomeric polymer transducers has been water. Transducers swollen with water are able to generate large actuation strains at low applied voltages and are able to operate at high frequencies. Furthermore, water is inexpensive, non–flammable, and non–toxic. The use of water in these devices does limit their operation in several key ways, however. First, water is volatile and will quickly evaporate out of the membranes if they are operated in a non-aqueous environment. Second, the electrochemical stability window of water is relatively small and the actuation voltages that can be used for these transducers are limited by this low stability. Third, transducers that are swollen with water typically exhibit a characteristic back–relaxation when driven by a step voltage input. That is, upon application of a step voltage input to the water–swollen actuator, the membrane will quickly bend towards the anode side, followed by a slower bending motion back towards the cathode side. The magnitude of this second bending motion, which is called the back–relaxation, is often larger than the initial bending towards the anode side. This back–relaxation is a problem for applications involving the use of Nafion^{TM} membranes as acutators, especially at low frequencies.

In order to overcome the problems associated with water–swollen Nafion^{TM} membrane transducers, the use of ionic liquids to replace the water is explored in this work. In

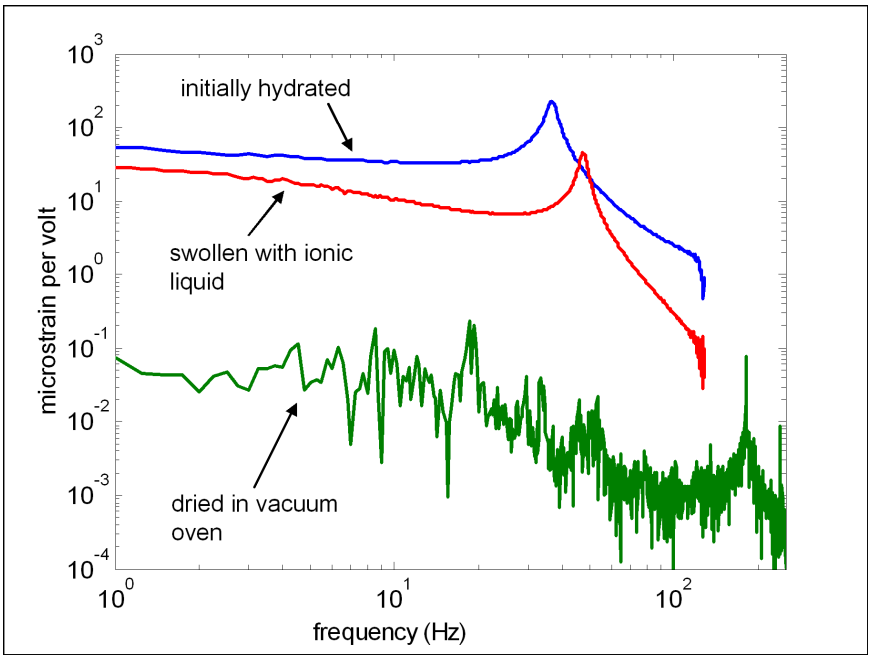

Figure 2.5: Free strain frequency response for a plated Nafion^{TM}-117 membrane in the water–swollen, dry, and ionic liquid–swollen forms. The ionic liquid used was EMI-Br.

order to demonstrate the importance of the diluent, an experiment has been performed in which a Nafion^{TM} transducer was characterized after drying in a vacuum oven–see Figure 2.5. For this test the free strain frequency response was measured using the equipment and method described in the previous section. As can be seen from Figure 2.5, the free strain generated by the dry sample is about four orders of magnitude less than the free strain generated by the water–swollen sample. Note that the small amount of strain generated by this sample is likely due to residual water inside the polymer—*complete* dehydration of the polymer is difficult to achieve and the polymer likely absorbed some moisture from the air during the testing. Also shown in this figure is the free strain response of the sample after incorporation of 1-ethyl-3-methylimidazolium bromide (EMI-Br) ionic liquid. As can be seen, the free strain generated by the ionic liquid sample is recovered to about half of the strain originally generated by the hydrated sample.

The long–term stability of transducers incorporated with ionic liquids and operated in air has also been demonstrated. This was first done again using the EMI-Br ionic liquid–see Figure 2.6. In this test, two samples were tested on each of three consecutive days. One of the samples was initially in the water–swollen form and the other sample was swollen

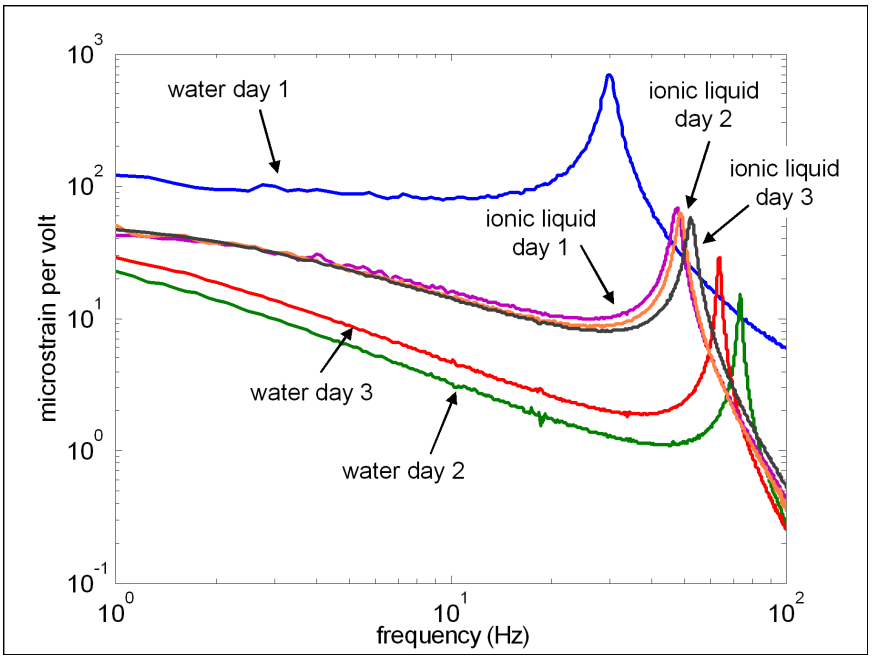

Figure 2.6: Free strain responses of two samples (water- and ionic liquid-solvated) over three consecutive days. The ionic liquid used was EMI-Br.

with the EMI-Br ionic liquid. Between the tests the samples were stored on a clean surface in the lab, exposed to the ambient environment. As can be seen from the figure, a dramatic difference in the responses from day one to day two is evident in the water–swollen sample. This is due to the evaporative loss of the water between the two tests. Further change in the response of the water–swollen sample is witnessed from day two to day three. This change is likely due to changes in the relative humidity of the testing environment. Also, it should be noted that although this sample had lost most of the water by the second day of testing, it was not completely dry. Rather, the water content inside the sample becomes equilibrated with the humidity of the surrounding air, hence there is still a quantifiable amount of water inside the polymer and some electromechanical effect is still evident. By contrast, the sample that was dried in the vacuum oven is much drier and generates almost an unmeasurably small amount of strain (see Figure 2.5).

The sample that was swollen with ionic liquid did not display the same changes in its free strain response, however. As can be seen from Figure 2.6, its response at 1 Hz changes by less than 10% over the course of three days, whereas the strain response of the water–swollen sample drops by 96% (at 1 Hz) after drying under standard room conditions for one day. Thus, although there is some loss of strain caused by using ionic liquids to

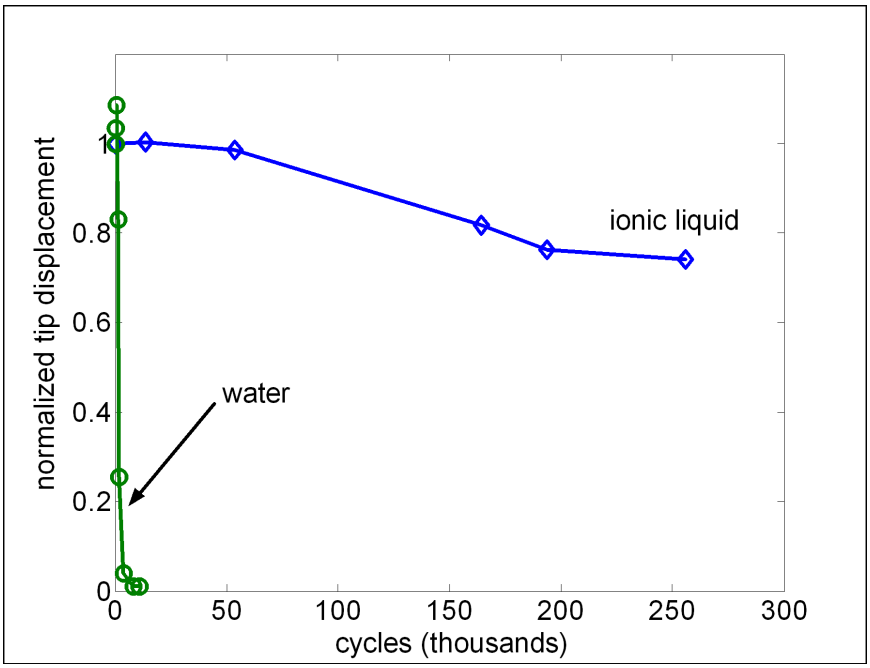

Figure 2.7: Time history of the tip displacement of a Nafion^{TM} actuator sample in the water and ionic liquid (EMI-Tf) forms. The input was a 1.5 V (peak), 2 Hz sine wave and the displacement has been normalized by the initial value.

replace water in ionomeric polymer transducers, the advantage of long–term stability in air is demonstrated.

The improved stability of the ionic liquid–swollen actuators as compared to water–swollen actuators has also been demonstrated by continuously driving these actuators in air–see Figure 2.7. For this testing, 1-ethyl-3-methylimidazolium trifluoromethanesulfonate (EMI-Tf) ionic liquid used was used. In this test, stability was quantified by cycling the actuators (one swollen with the ionic liquid and the other swollen with water) continuosly with a 1.5 V (peak), 2 Hz sine voltage input and monitoring the change in their free tip displacement. The time–dependent peak displacement of the actuators was normalized by the measured displacement at the beginning of the test. As can be seen in Figure 2.7, the strain response of the sample in the ionic liquid form is far more stable than the water sample when these actuators are operated in an air environment. Although the strain generated by the ionic liquid–swollen actuator did decrease eventually, it retained over 80% of its performance after more than 100,000 actuation cycles and more than 70% of its performance after 250,000 actuation cycles (note that the x–axis in the figure is logarithmic scale). By contrast, the water–swollen transducer retained only 4% of its initial deformation

Table 2.3: Viscosity of five ionic liquids studied in this research.

diluent	viscosity (cP @ 25°C)
$P(C_6)_3C_{14}$-Im	322[†]
$P(C_6)_3C_{14}$-$PF_3(C_2F_5)_3$	348[†]
BMPyr-Im	76[†]
BMPyr-$PF_3(C_2F_5)_3$	224[†]
EMI-Tf	45[(a)]

[(a)] from reference (10)

[†] measured at Penn State

after 3600 actuation cycles.

The initial results demonstrate the improved stability of ionic liquids as solvents for Nafion^{TM} polymer membrane transducers as compared to water. Next, a discussion will be presented to compare the transduction performance of the devices employing the ionic liquids to the traditional water–swollen materials.

2.3.3 Comparison to Water–Based Transducers

In order to determine the influence of an ionic liquid on the transduction behavior of Nafion^{TM} ionomer actuators, an initial investigation was performed. The transducers that were characterized in this study were fabricated using the interpenetrating platinum and electroplated gold electrodes that deposited using the water / ethanol process described in Section 2.2. The swelling of the membranes with ionic liquid was performed by heating the dry, plated membranes in the neat ionic liquid. For this testing, five different ionic liquids were used. The samples were swollen with the ionic liquids using the process described in Section 2.1. The volumetric uptake of each ionic liquid is presented in Table 2.2. The viscosities of these ionic liquids are presented in Table 2.3. These viscosities were kindly measured by Dr. Ralph Colby of the Pennsylvania State University and the densities were obtained using the process described in Section 2.1, except where indicated. The transducers were also tested in their water–swollen state as a baseline for comparison.

The free strain generated by benders swollen with three of these ionic liquids and water is shown in Figure 2.8. In this figure the solid lines represent frequency responses measured using a Fourier analyzer with a random input to the polymer while the discrete data points represent single frequency measurements performed in the time domain. The degree of swelling in the $P(C_6)_3C_{14}^+$ ionic liquids was very large and caused significant crack-

ing to the electrodes, resulting in a loss of conductivity. Therefore, transducer responses with these samples were not obtained. From the viscosity data (Table 2.3) and Figure 2.8 it is clear that the higher viscosity of the ionic liquids as compared to water (0.91 cP (135)) limits the mobility of the ions within the polymer membrane. This is manifested as a rolloff in the strain response at higher frequencies. This is especially evident for the sample swollen with the BMPyr-$PF_3(C_2F_5)_3$ ionic liquid and the sample swollen with the BMPyr-Im ionic liquid. For the BMPyr-$PF_3(C_2F_5)_3$–swollen sample the slow response can be explained by the high viscosity of the ionic liquid (224 cP). For the BMPyr-Im–swollen sample, the slow actuation speed can be explained by the small loading of ionic liquid (18.2% by volume).

Even in the least viscous ionic liquid (EMI-Tf) the limited mobility of the ions is observed, although this effect is less evident than in the other two samples. From these results it seems that the EMI-Tf ionic liquid possesses an appropriate combination of low viscosity and intermediate uptake in the membrane that will lead to desirable transduction in Nafion^{TM} actuators. Furthermore, this ionic liquid has an electrochemical stability window of 4.1 V and has also been shown to be thermally stable up to 400°C (10). For the proton–exchanged transducers, the sample solvated with the EMI-Tf ionic liquid actually generated larger induced strains (per unit volt input) than the water–swollen sample.

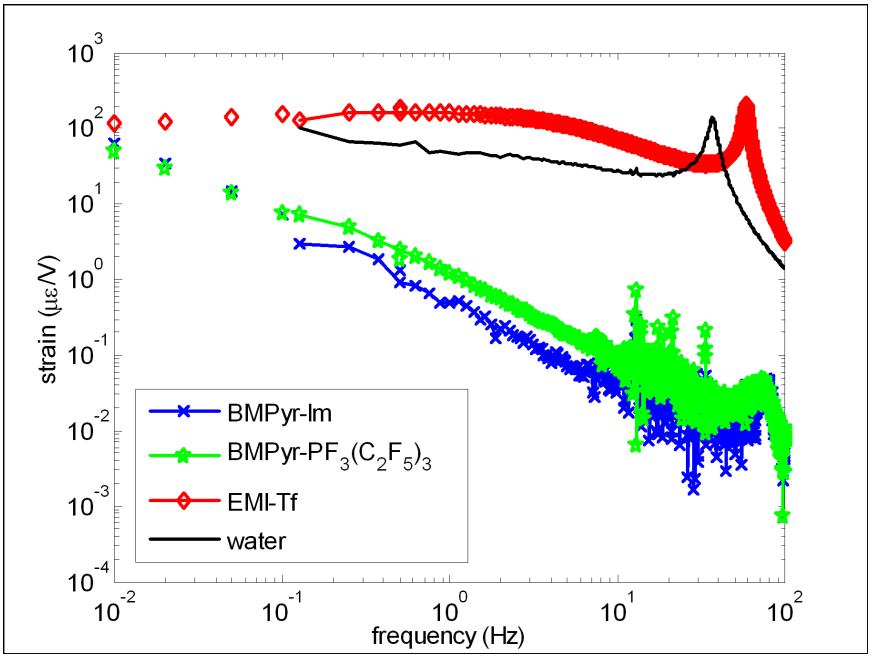

Figure 2.8: Free strain frequency response for Nafion^{TM} bender actuators in the proton form swollen with three ionic liquids and water.

This testing has also been performed for transducers in the lithium counterion form swollen with water and with the EMI-Tf ionic liquid. In order to convert the membranes into the lithium counterion form they were soaked in 0.5 M LiCl overnight after the metal plating process. Following the exchange, the samples were rinsed, dried, and swollen with ionic liquid using the standard process. In this case the generated strain per unit volt is almost an order of magnitude higher for the water–swollen sample than the ionic liquid–swollen sample—see Figure 2.9. The response of the lithium form water–swollen actuator is also about an order of magnitude larger than that of the proton form water–swollen sample. However, the response of the EMI-Tf–swollen actuators is very similar for the membranes in both the lithium and proton forms. This is illustrated in Figure 2.9b. This large difference in the response of the water–swollen actuators likely indicates that the fundamental ion transport mechanism is altered for the water–swollen transducers when the cation is changed from proton to lithium.

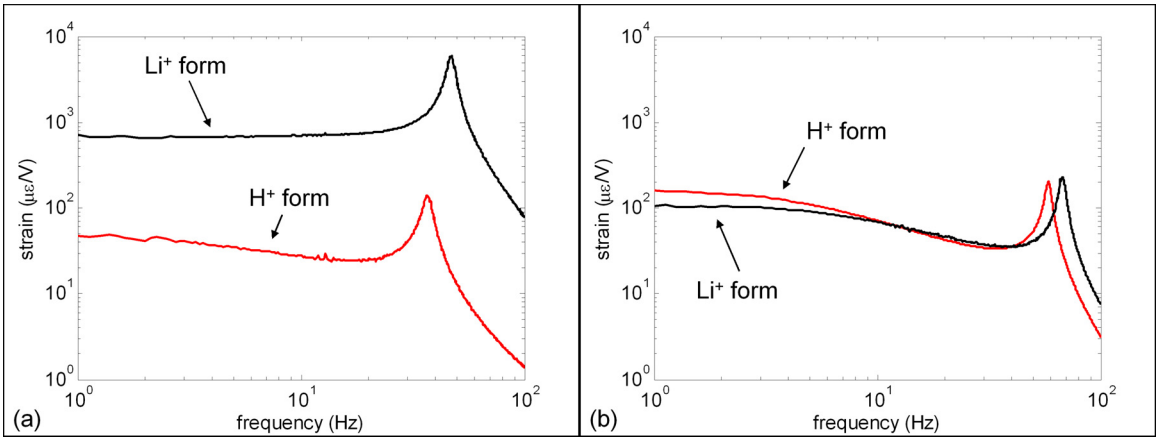

Figure 2.9: Comparison between the free strain frequency response for Nafion^{TM} actuators in the lithium and proton counterion forms and swollen with (a) water, (b) EMI-Tf ionic liquid.

Ren and Gottesfeld have postulated that hydrogen ion transport in proton–exchanged Nafion^{TM} membranes likely occurs by a combination of the Grothus mechanism and the vehicle mechanism (110). In the Grothus mechanism, protons hop from one water molecule to the next, with no net movement of the water molecules–see Figure 2.10. In the vehicle mechanism, hydrated protons (hydronium ions) physically transport through the membrane–see Figure 2.11. The Grothus mechanism requires the water molecules to be highly oriented by hydrogen bonding and its contribution likely decreases with increasing temperature.

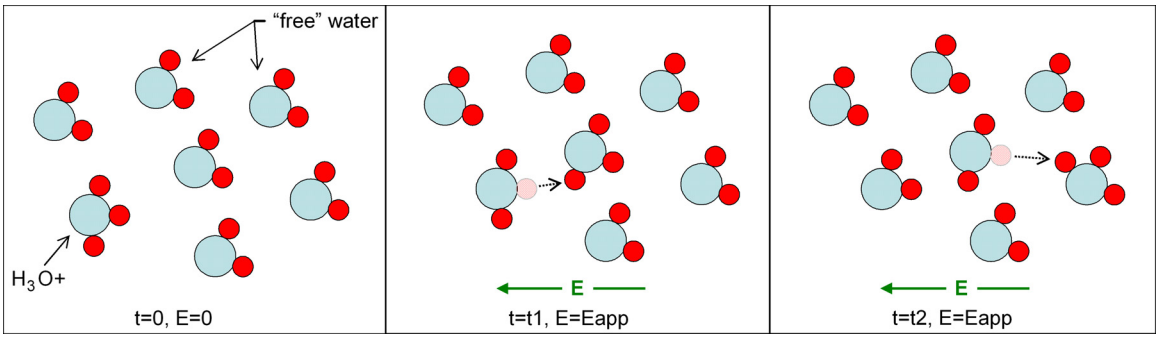

Figure 2.10: Illustration of the Grothus mechanism for proton transport.

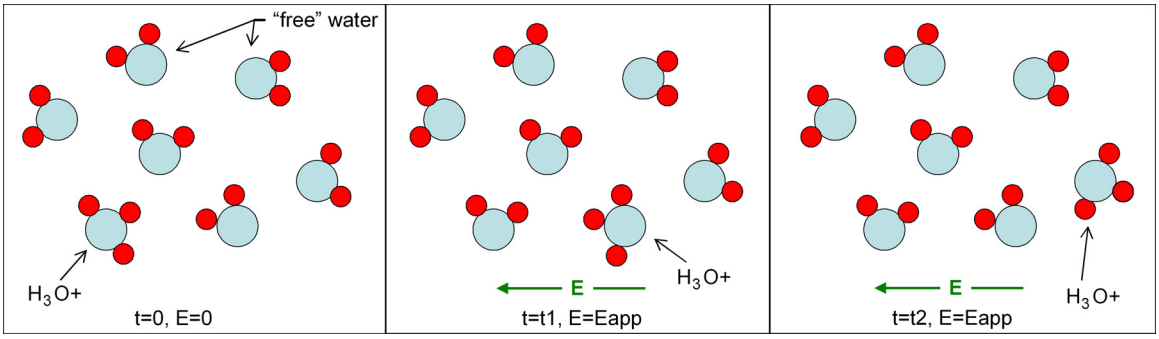

Figure 2.11: Illustration of the vehicle mechanism for proton transport.

However, ion transport within the water–swollen lithium–exchanged membrane likely occurs exclusively by the vehicle mechanism. This change in the transport mechanism between the proton– and lithium–exchanged actuators is the most reasonable explanation for the large difference that is observed in their response. By contrast, the actuation responses of the proton– and lithium–exchanged membranes swollen with EMI-Tf ionic liquid are very similar. This could indicate that ion transport in these two membranes occurs by the same mechanism, even though the cation has been changed.

The time–domain response of the proton form samples to a step voltage input was also measured–see Figure 2.12. As can be seen in this figure, the samples swollen with the $BMPyr^+$ ionic liquids exhibit a very slow response to a step input. By contrast, the water–swollen sample has a very small rise time in response to a step, which is characteristic of the high ionic conductivity of water–swollen Nafion^{TM}. The samples swollen with EMI-Tf ionic liquid have a slightly longer rise time, but still reach their peak within 500 ms. The samples swollen with the $BMPyr^+$ ionic liquids have very long rise times and are still deforming after 250 s. This is consistent with the steep rolloff observed in the frequency response for these samples.

Most interesting is that the ionic liquid samples do not exhibit the characteristic back–relaxation that the water sample does, for the time period studied. This back relaxation is problematic for applications where DC positioning with ionomeric polymer transducers is required. The step response was also measured for the EMI-Tf–swollen actuator and water–swollen actuator in the lithium ion form—see Figure 2.13. As can be seen, the step responses are dramatically different for the water–swollen actuators in the two counterion forms. The peak strain generated by the lithium form actuator is almost an order of magnitude greater than that generated by the proton form actuator. By contrast, the responses of the proton– and lithium ion–exchanged samples swollen with EMI-Tf ionic liquid are very similar. These results are in concert with the observed differences in the free strain frequency responses. This could indicate that the mechanism of charge transport is different for the water–swollen sample in the proton form as compared to the lithium form. By the same argument, the charge transport mechanism for the EMI-Tf–swollen actuators would be assumed to be unchanged between the two counterion forms of the membrane.

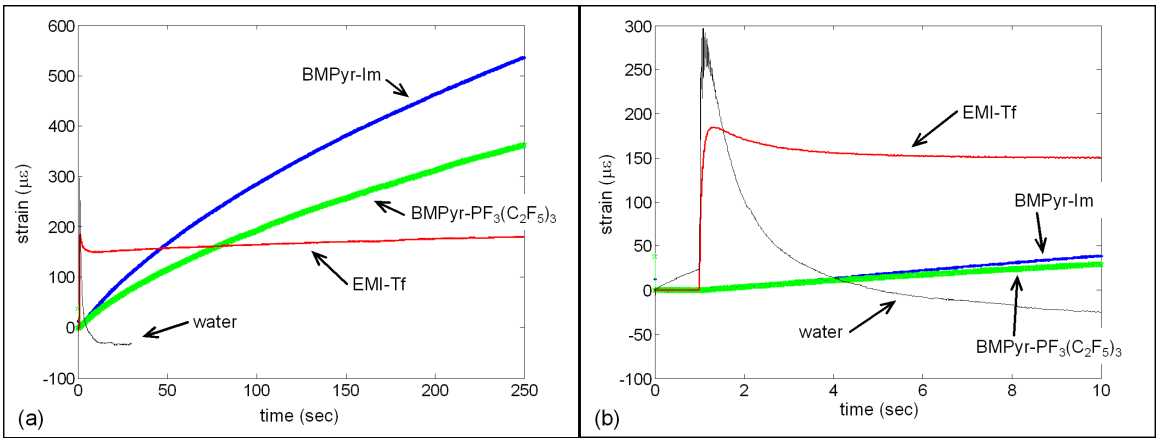

Figure 2.12: (a) Time response of three ionic liquid–swollen actuators and a water–swollen actuator in the proton form to a 1 V step input. (b) The first ten seconds of the response.

2.4 Summary

The initial results presented in this chapter demonstrate the potential for using ionic liquids as swelling agents for ionomeric polymer (Nafion^{TM}) transducers. The ionic liquid–swollen materials are shown to be more environmentally stable than their water–swollen counterparts. Also, techniques have been developed to incorporate ionic liquids into Nafion^{TM}

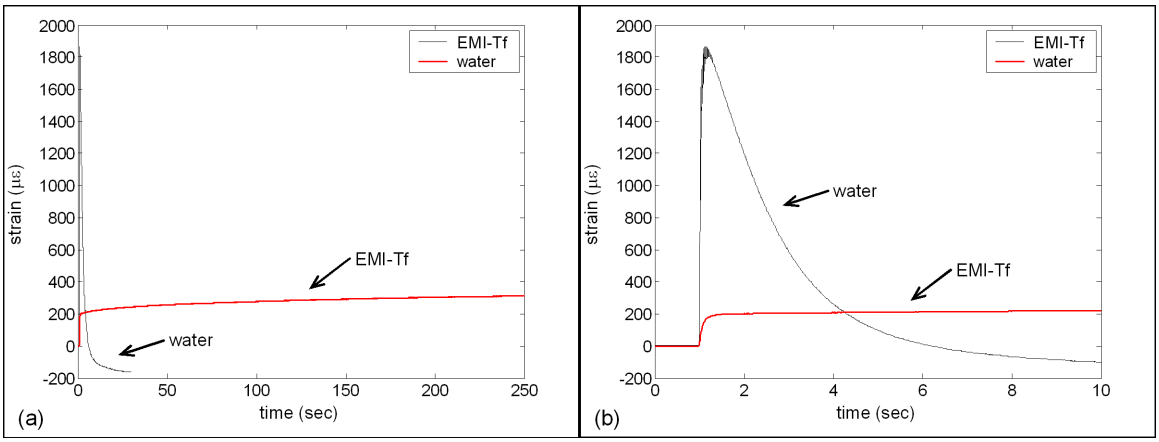

Figure 2.13: (a) Time response of an EMI-Tf–swollen actuator and a water–swollen actuator in the lithium form to a 1 V step input. (b) The first ten seconds of the response.

membranes and to deposit metal electrodes on those membranes. A new electroding process has been developed for these transducers that overcomes the problems of electrode damage during incorporation of the ionic liquid. The ionic liquid–swollen materials are found to have a slower speed of response than the water samples. One reason for this slow speed is the increased viscosity of the ionic liquids as compared to water.

Long–term cycling of the ionic liquid–swollen actuators revealed that they have the potential to overcome the stability problems associated with using water–swollen devices in air. Comparisons between the behavior of the ionic liquid–swollen materials and tranditional water–swollen actuators reveal that different ion transport mechanisms may be at work in the ionic liquid–swollen polymers. Also, unlike the water–swollen materials, the ionic liquid–swollen actuators do not exhibit a back–relaxation when actuated at very low frequencies. This is an advantage for these materials in terms of position control applications. The results presented thus far demonstrate the potential of this research and motivate further study of these materials as electromechanical transducers.

Chapter 3

Morphological Characterization

3.1 Motivation

In order to develop a physical interpretation of the mechanisms of transduction in Nafion^{TM} / ionic liquid composites, an understanding of the morphology of these membranes is required. Investigation of the morphology of the ionic liquid–swollen membranes is important because it has been suggested by many authors that the morphology of the Nafion^{TM} polymer is at least partially responsible for its unique ion transport properties (46; 60; 89; 137; 138; 136). Numerous previous studies have attempted to elucidate the morphology of Nafion^{TM} membranes, primarily in the dry and water-swollen state. Although the specific morphology of the Nafion^{TM} polymer is still a source of debate (89), all of the proposed models include the notion of separation of the polymer into at least two phases: a hydrophobic phase that contains the fluorocarbon backbone polymer and a hydrophilic phase that contains the sulfonate exchange sites, counterions, and diluent. The most common model of the morphology of Nafion^{TM} is that initially proposed by Gierke in which the sulfonate exchange sites are envisioned to reside on the surface of roughly sperical domains that contain the counterions and solvent (43). These "clusters," as they are called, are thought to be embedded within a matrix phase of inert, Teflon^{TM}-like fluorocarbon polymer. This model is used to explain the unique ion transport properties of Nafion^{TM} (60; 46). It should be noted that although the term "ionic clusters" is conventionally used in the perfluorosulfonate ionomer literature, these features are also sometimes referred to as "aggregates" or "multiplets" when discussing other types of ionomers (24; 89).

Because ion transport can only occur in the hydrophilic phase of the polymer, the

geometry and arrangement of this phase in relation to the hydropbobic regions is of critical importance. In order to understand the morphology of the Nafion^{TM} membranes when swollen with an ionic liquid, a structured investigation was performed.

3.2 Sample Preparation

The SAXS testing is intended to determine the effect of the ionic liquid present within the polymer on the morphology of the composite. For this testing several experimental parameters were varied, including counterion type, identity of the ionic liquid, and uptake of the ionic liquid.

The polymer used was commercially-available Nafion^{TM}-117. This membrane has a nominal equivalent weight of 1100 and a nominal thickness of 183 μm. The Nafion^{TM} membrane is in the proton counterion form as-recieved. It was initially treated by boiling in 1.0 M sulfuric acid for one hour in order to ensure complete proton exchange. The membrane was then boiled in de-ionized water for one hour to remove any loosely bound protons and co-ions. Following this treatment the membrane was cut into strips and the strips were soaked in 0.5 M aqueous solutions of the chloride salt of the cation to be exchanged into the membrane. For the SAXS testing five counterion forms of the membrane were studied: lithium (Li), potassium (K), cesium (Cs), tetraethylammonium (TEA), and 1-ethyl-3-methylimidazolium (EMI). The structures of the TEA and EMI cations are shown in Figure 3.1. Lithium chloride, potassium chloride, cesium chloride, and tetraethylammonium chloride were obtained from Alfa Aesar. Sodium chloride was obtained from Mallinckrodt and 1-ethyl-3-methylimidazolium chloride was obtained from Sigma Aldrich. All salts were used as-recieved and solutions were prepared from Type III DI water (resistivity 18.2 MΩ-cm).

In order to ensure a full exchange into the desired counterion form, the hydrated and proton-exchanged Nafion^{TM} strips were soaked in the salt solutions for several days, with periodic agitation. The strips were then removed from the salt solutions, rinsed with DI water, and soaked in DI water for several hours in order to ensure complete removal of any excess salt from the membrane. The strips were then placed between sheets of cellulose filter paper and dried in a oven at 110°C overnight a under vacuum ($\sim$70 torr). The weights of the dry Nafion^{TM} strips were measured using a Mettler-Toledo analytical balance and

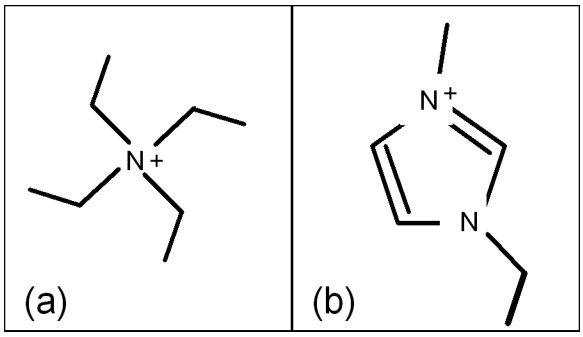

Figure 3.1: Chemical structure of the (a) tetraethylammonium ion, (b) 1-ethyl-3-methylimidazolium ion.

they were swollen with ionic liquid.

As with all of the testing, the two ionic liquids used for the SAXS experiment were 1-ethyl-3-methylimidazolium trifluoromethanesulfonate (abbreviated "EMI-Tf") and 1-ethyl-3-methylimidazolium bis(trifluoromethanesulfonyl)imide (abbreviated "EMI-Im"). The properties of these ionic liquids are presented in Table 3.1 and the chemical structures of the ionic liquids are presented in Figure 3.2. As can be seen, the two ionic liquids are very similar in terms of their viscosity, melting point, conductivity, and electrochemical stability window. However, the EMI-Im ionic liquid is hydrophobic whereas the EMI-Tf ionic liquid is water miscible. The results presented in this dissertation will show that this difference in hydrophobicity will greatly affect the way that the ionic liquid interacts with the membrane and the corresponding ion transport properties of the composite.

The process described in Section 2.1 for swelling Nafion^{TM} membranes with ionic liquid involved soaking the dried membranes in the neat ionic liquid at elevated temperature for extended periods of time. Although the heating treatment has been shown to be effective at incorporating ionic liquids into Nafion^{TM} membranes, the process is very slow and is the uptake is inherently difficult to control. Also, the diffusion of the ionic liquids into the membrane is found to vary significantly as their structure is changed. For example, the diffusion of the EMI-Im ionic liquid into the membrane is very slow. Testing has revealed that Nafion^{TM} will increase in volume by only 11% when swollen in neat EMI-Im ionic liquid at 150°C for over 20 hours.

In order to overcome this limitation, the ionic liquids were mixed with methanol to facilitate diffusion into the Nafion^{TM} membranes. Gebel et al. have reported that Nafion^{TM} membranes swell by 51% in pure methanol at room temperature (40). Also, the ionic

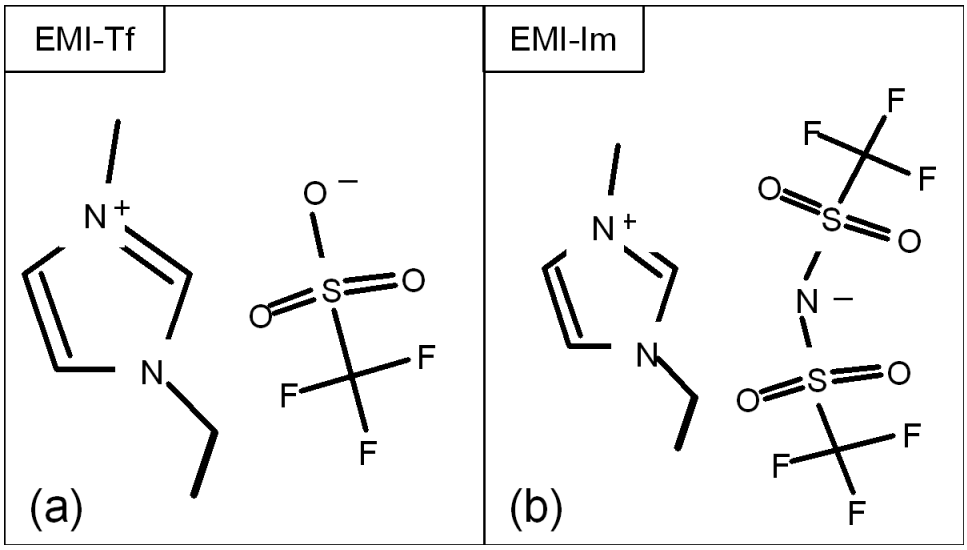

Figure 3.2: Chemical structure of the (a) 1-ethyl-3-methylimidazolium trifluoromethanesulfonate (EMI-Tf) ionic liquid, (b) 1-ethyl-3-methylimidazolium bis(trifluoromethanesulfonyl)imide (EMI-Im) ionic liquid.

Table 3.1: Relevant properties of the two ionic liquids used for the SAXS testing.

ionic liquid	viscosity (cP @ 25°C)	density (g/cm^3)	melting point (°C)	conductivity (mS/cm @ 25°C)	sat. water content (mass % @ 20°C)	stability window (V)
EMI-Tf	45 (10) 43 (15)	1.390 (10) 1.383 (15)	-9 (10) -10 (15)	8.6 (10) 9.3 (15)	soluble (10)	4.1 (10)
EMI-Im	34 (10)	1.520 (10)	-3 (10)	8.8 (10)	1.4 (10)	4.3 (10)

liquids used in the course of this research are miscible with methanol. After drying, the strips were soaked in a 1:1 (by volume) mixture of ionic liquid and methanol for three hours at either 25°C or 70°C. By increasing the temperature of the soak, the content of ionic liquid within the membrane was increased. After soaking in the ionic liquid / methanol mixture, the membranes were placed between two cellulose filter papers and baked at 80°C under vacuum for 3 hours to remove the methanol. The weights of the ionic liquid-swollen membranes were then measured.

For the purposes of this work, the uptake of ionic liquid within the membrane reported is the volume of ionic liquid as a percentage of the dry volume of the membrane. This volumetric uptake was determined from the dry and swollen weights and the density of the dry membrane and the ionic liquid using equation 2.1. The densities of the ionic liquids were obtained from the literature and are listed in Table 3.1. The densities of the dry membranes were obtained using the process described in Section 2.1 on dried bare Nafion^{TM}

Table 3.2: Measured dry density of Nafion^{TM} polymer in five cation forms. All values are in g/cm^3

cation	density
Li	1.97
K	2.11
Cs	2.14
EMI	1.81
TEA	1.72

membranes that had been exchanged into the appropriate counterion form. The calculated dry densities of the Nafion^{TM} membrane in the five counterion forms are listed in Table 3.2.

For the SAXS study, 20 ionic liquid–swollen Nafion^{TM} samples were tested. Four samples in each counterion form were prepared, with two swollen in each ionic liquid, one at room temperature and one at 70°C. In addition to the swelling time and temperature, the uptake of ionic liquid is found to be dependent on the identity of the counterion within the polymer. This can be attributed to the use of methanol as a swelling agent to facilitate the diffusion of the ionic liquids into the polymer. The smaller cations such as lithium and sodium have a higher charge density and therefore a higher affinity for the relatively polar methanol. This results in more ionic liquid being drawn into the membranes exchanged with the smaller ions as compared to those exchanged with the larger ions (TEA, EMI). Although this influence is undesireable, the use of methanol to swell the membranes is necessary due to the very low uptake of the neat EMI-Im ionic liquid in Nafion^{TM} membranes, even at elevated temperatures.

3.3 Testing Protocol

Small-angle X-ray and neutron scattering is a common method for investigating the morphology of ionomers (125). For the current work, transmission small-angle X-ray scattering (SAXS) was used to investigate the morphology of the Nafion^{TM} / ionic liquid composites. In this testing, an X-ray beam is passed through a sample of material and measured on a screen on the far side–see Figure 3.3. The incident beam is collimated with a series of pinholes before it strikes the sample. The testing is performed under a high vacuum and due to the interaction of the X-rays with electrons in the sample, the beam is scattered. If the electron density within the sample fluctuates with some geometric regularity, then the

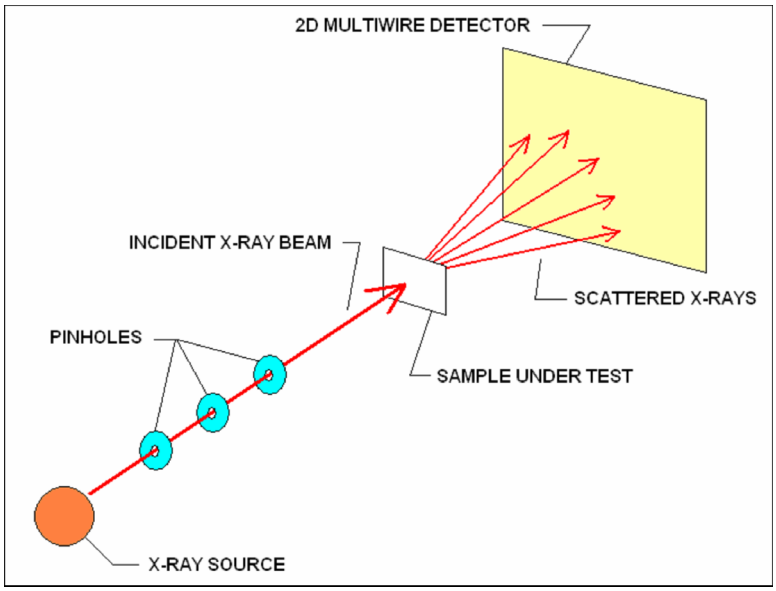

Figure 3.3: Schematic of the SAXS setup used for the morphological characterization.

beam will be scattered more intensely at specific angles, which are related to the spacing of the electron density fluctuations. In this way SAXS can be used to characterize morphology and order within a material. This order can be related crystallinity, phase separation, microscopic inclusions, etc. In the case of the Nafion^{TM} polymer, the order is related to the presence of aggregated domains that contain the sulfonate exchange sites and counterions.

The majority of the SAXS testing was performed at the Army Research Laboratory, Multifunctional Materials Branch, with the assistance of Dr. Rick Beyer. The X-ray generator was of the rotating drum type and it was excited at 40 kV, with a driving current of 60 mA. The wavelength of the resulting X-rays was 1.542 Å. The ionic liquid-swollen Nafion^{TM} strips that were used for the SAXS testing were approximately 1 cm X 5 cm and were mounted to a sample holder using double-sided tape. The sample holder is designed such that only the Nafion^{TM} film was in the path of the X-ray beam. In the SAXS setup at the Army Research Lab, the X-ray beam is collimated with a series of pinholes before striking the sample–see Figure 3.3. The X-rays are scattered by the sample and a pattern is generated on the detector screen. The samples were illuminated for 40 minutes each in order to collect a sufficient number of X-rays on the screen. If the sample contains some morphological regularity, then the generated pattern will exhibit fringes. The location of these fringes is related to the geometric spacing of the order.

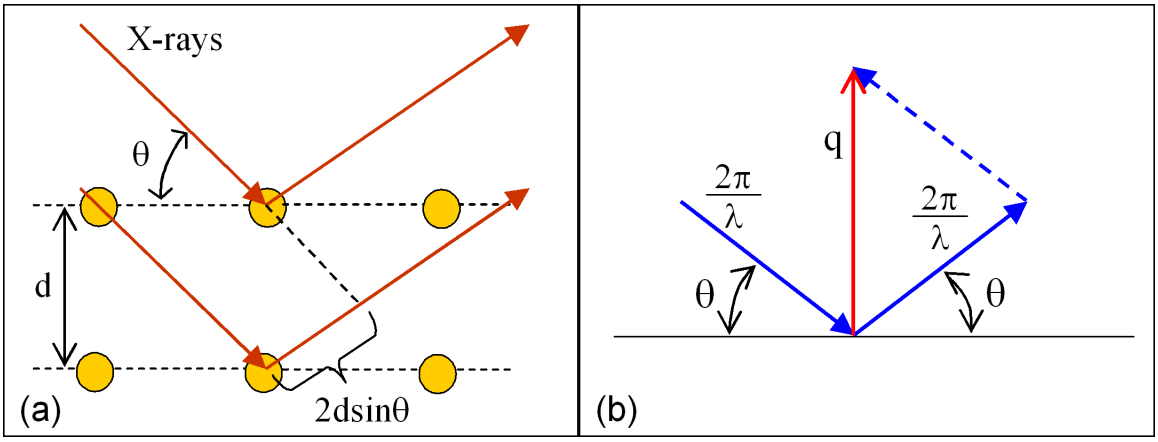

Figure 3.4: (a) Representation of X-ray scattering by electron density fluctuations within a material. (b) Illustration of the scattering vector.

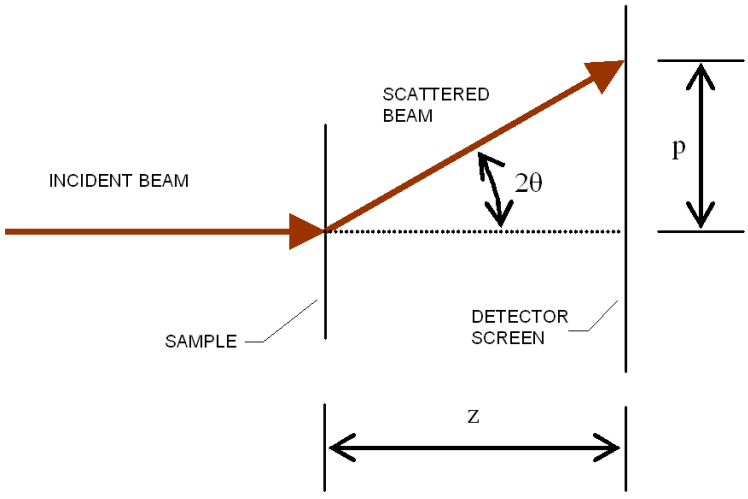

Figure 3.5: The X-rays are scattered through an angle of 2θ in relation to the incident beam.

A schematic representation of X-rays scattering by an ordered material is shown in Figure 3.4. As can be seen, the presence of the two regions of high electron density causes the incident X-ray beam to be scattered by an angle of θ in relation to the plane of the inclusions. By reorienting this representation, we can see that the X-rays are actually scattered through an angle of 2θ in relation to the incident beam–see Figure 3.5. If we assume that the electron density fluctuations occur within the material at a geometric interval of d, then this interval is related to half of the scattering angle by Bragg's law

$$n\lambda = 2dsin\theta, \tag{3.1}$$

where λ is the wavelength of the incident X-rays, θ is the scattering angle, and n is an integer value related to the periodicity of the fringe pattern. Similarly, the length of the scattering vector, q is given by

$$q = \frac{4\pi}{\lambda} sin\theta. \tag{3.2}$$

The mean intercluster spacing is therefore related to the length of the scattering vector by

$$d = \frac{2\pi}{q}, \tag{3.3}$$

where n is assumed to be 1, corresponding to the primary scattering harmonic.

The scattering of X-rays by a material will generate a characteristic pattern of measurement events on the detector screen. Shown in Figure 3.6 is a typical SAXS result for an ionic liquid-swollen Nafion^{TM} membrane. Visible in the center of the image is the lead beamstop, which protects the detector screen from damage caused by the high intensity of non-scattered X-rays. As can be seen, the X-ray scattering occurs over a wide range of angles. However, a faint halo is visible about midway between the center of the image and the edge. This halo is associated with the so-called "ionomer peak" of the Nafion^{TM} SAXS result, which will appear in the processed data. In order to convert this image into a curve of scattered intensity versus q (or d), the beam center is first determined using a silver behenate crystal. The data is then scaled to abolute intensity by correcting for noise and background X-rays using a glassy carbon calibrant. The radial positions of the scattered X-rays are then used to determine the lattice spacing based on the geometry of the test.

If a scattered X-ray strikes the detector at a distance p from the center (see Figure 3.5), then the scattering angle is related to p and z (sample-to-detector distance) by:

$$tan(2\theta) = \frac{p}{z}. \tag{3.4}$$

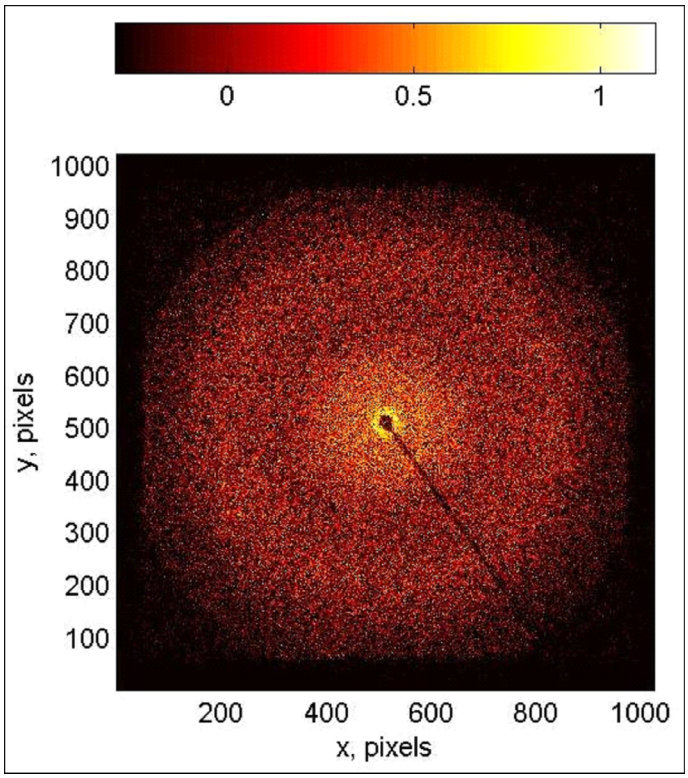

Figure 3.6: Measured scattering pattern for an ionic liquid-swollen Nafion^{TM} membrane. The units are number of measured X-ray strikes.

If we make the small-angle approximation that $\theta \approx sin\theta \approx tan\theta$, then using equations 3.2 and 3.4 we can find a relationship between the position of the scattered X-rays on the detector screen and the length of the scattering vector:

$$q = \frac{2\pi p}{\lambda z}. \tag{3.5}$$

Similarly, using equation 3.3 we can derive an expression relating d to the measured signal:

$$d = \frac{\lambda z}{p}. \tag{3.6}$$

Once the measured image is converted to q and d coordinates, the data is integrated radially and converted to a single curve. This is possible because the samples are considered to be isotropic in the plane perpendicular to the incident X-ray beam.

3.4 Results

Prior to the sturctured investigation performed on the EMI-Tf– and EMI-Im–swollen membranes, an initial round of SAXS testing was performed with the assistance of Dr. Garth Wilkes and Dr. Pankaj Gupta at Virginia Tech. This initial testing involved the use of a slit scattering system, which is fundamentally similar to the pinhole system depicted in Figure 3.3, except that the X-ray radiation is not collimated by the series of pinholes prior to striking the sample. This testing validated the use of SAXS for performing characterizations of the morphology of ionic liquid–swollen Nafion^{TM} membranes. The results are presented in Appendix A.

In order to interpret the SAXS results, an assumption of the basic structure of the polymer must be made. For the current study, the Nafion^{TM} polymer was assumed to consist of two regions, the hydrophobic backbone phase and the hydrophilic ionic phase. This assumption is consistent with the previous literature. The SAXS results for the Nafion^{TM} membranes swollen with the EMI-Tf ionic liquid at room temperature are shown in Figure 3.7. The absolute amplitude of the curves is arbitrary and they have been shifted vertically for clarity. Several interesting features can be observed in the figure. First, the curves exhibit a rounded peak or shoulder at q values of around 0.2 Å^{-1}, which corresponds to a d value of 31 Å (3.1 nm). This peak is associated with the presence of the ionic clusters and the d value corresponding to this peak can be considered as an estimation of the mean spacing between the cluster centers. Second, the curves exhibit an even more broadened

peak at q values of about 0.05 $Å^{-1}$ (d=12.6 nm). This peak is associated with crystallinity in the Teflon^{TM}-like matrix phase (89; 34; 86). Third, some of the curves exhibit a sharp upturn at very small q values. This upturn has been previously observed in water-swollen Nafion^{TM} membranes (89; 41; 27). Although its origin remains unknown, several researchers have postulated that this feature is related to large-scale inhomogeneities in the distribution of the clusters (62; 27; 89). This upturn can be thought of as arising from the aggregation of the clusters into larger cluster agglomerates ("clusters of clusters").

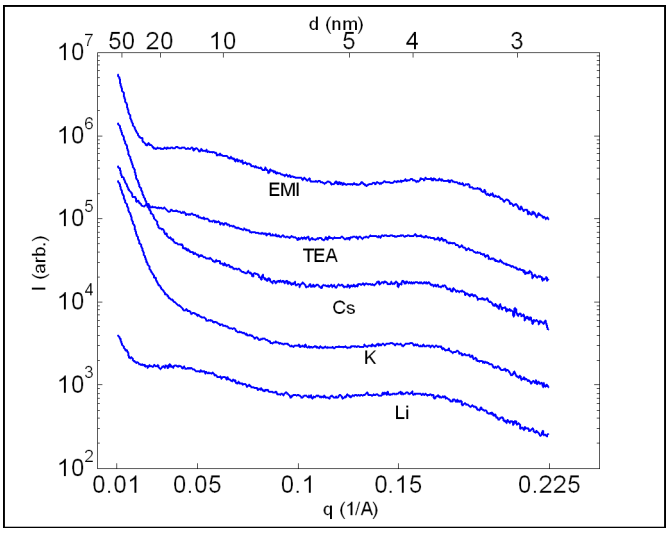

Figure 3.7: SAXS results for Nafion^{TM} membranes in five counterion forms swollen with EMI-Tf ionic liquid at room temperature.

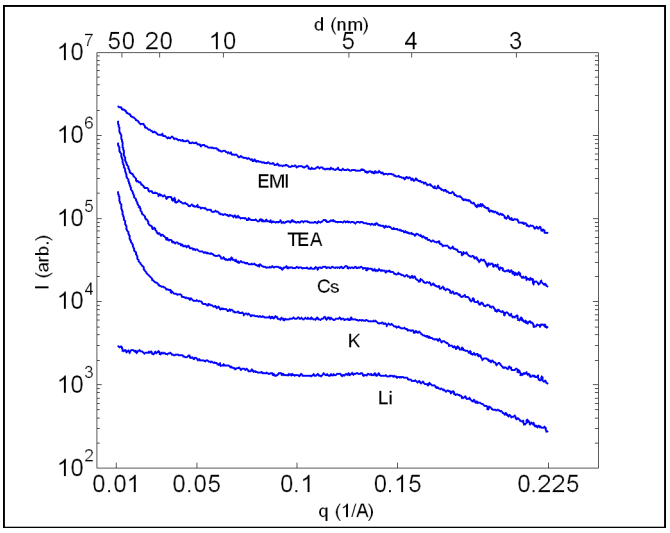

Figure 3.8: SAXS results for Nafion^{TM} membranes in five counterion forms swollen with EMI-Tf ionic liquid at 70°C.

In general, the shape of the curves shown in Figure 3.7 is similar to that expected for a water-swollen Nafion^{TM} membrane. The ionomer peak (associated with the mean intercluster spacing), the semi-crystalline Teflon^{TM} peak, and the small-angle upturn are all present. SAXS was also performed on the membranes that were swollen with EMI-Tf at 70°C—see Figure 3.8. These samples contain more ionic liquid than those swollen at room temperature. As can be seen, the ionomer peak and low-angle upturn are present, but the feature thought to be associated with the crystalline portion of the polymer has diminished somewhat. Also, the ionomer peak has decreased in magnitude and shifted to lower q values (higher d). It seems that by increasing the content of ionic liquid within the membrane, the crystallinity has been disrupted and the mean distance between the ionic domains has increased—see Figure 3.9.

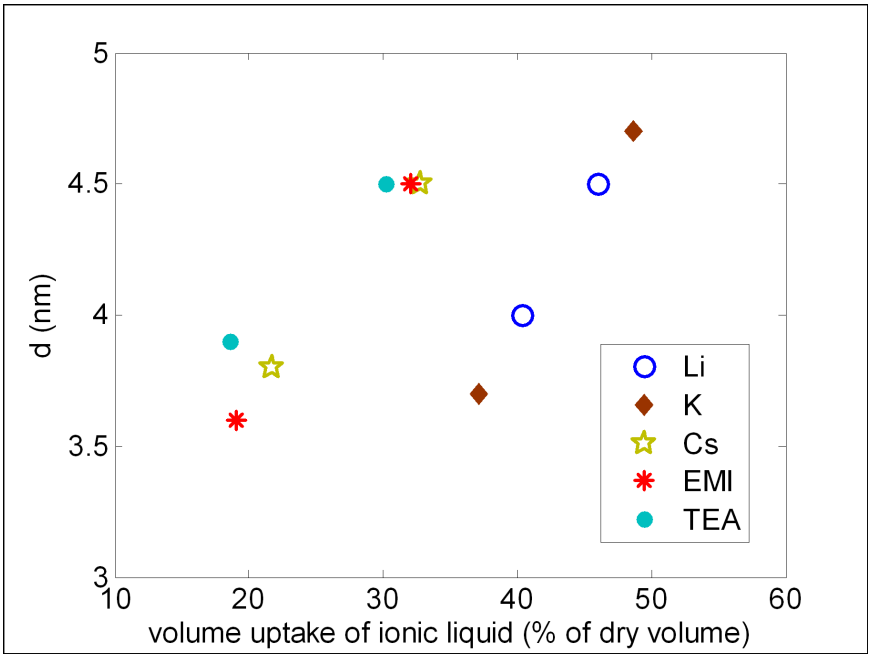

Figure 3.9: Mean intercluster spacing vs. uptake for EMI-Tf–swollen Nafion^{TM} membranes in five counterion forms.

Shown in Figure 3.9 is the d value obtained from Figures 3.7 and 3.8 plotted versus the uptake of EMI-Tf ionic liquid within the membrane. Although the exact d value is difficult to obtain from Figures 3.7 and 3.8, the results clearly indicate that the mean intercluster spacing increases as the amount of ionic liquid within the membrane is increased. Additionally, the relationship between the lattice spacing and the uptake of ionic liquid is found to also depend on the size of the counterion within the membrane. The mean

intercluster spacing is smaller for the membranes exchanged with the smaller counterions and increases with increasing counterion size, for a given swelling level of ionic liquid.

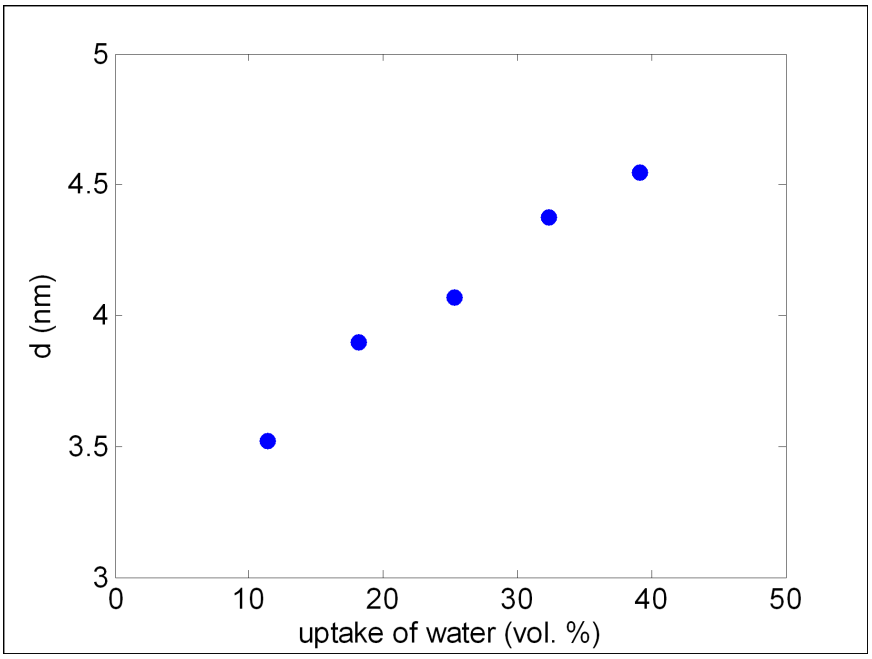

Figure 3.10: Mean intercluster spacing vs. uptake for water–swollen 1200 EW Nafion^{TM} membrane in the lithium counterion form. From reference (46).

Gierke et al. and Gierke and Hsu have performed an extensive SAXS study and analysis of water–swollen Nafion^{TM} membranes (45; 46). The results obtained with the EMI-Tf ionic liquid exhibit good agreement with those of Gierke and co–workers. For instance, the increase in the mean intercluster spacing with increasing uptake of diluent is observed in both systems—see Figure 3.10. Also, their SAXS results for water–swollen Nafion^{TM} demonstrate the same dependence on the size of the counterion—see Figure 3.11. As can be seen from the figure, the Bragg spacing for the H^+, Li^+, and Na^+ ions all seems to follow the same linear trend with water uptake. However, the K^+, Rb^+, and Cs^+ ions depart from this trend. Unfortunately, apart from the H^+ and Li^+ ions, only a single data point is available for each of the counterion forms of the membrane. It is interesting to note that the increase in the Bragg spacing for the K^+, Rb^+, and Cs^+ ions follows the trend of increasing ionic radius, though. This is the same trend that is observed for the Nafion^{TM} membranes swollen with the EMI-Tf ionic liquid.

Making determinations of ion size is not an easy task. A common method is to estimate ion size by making measurements of the distance between the cations and anions

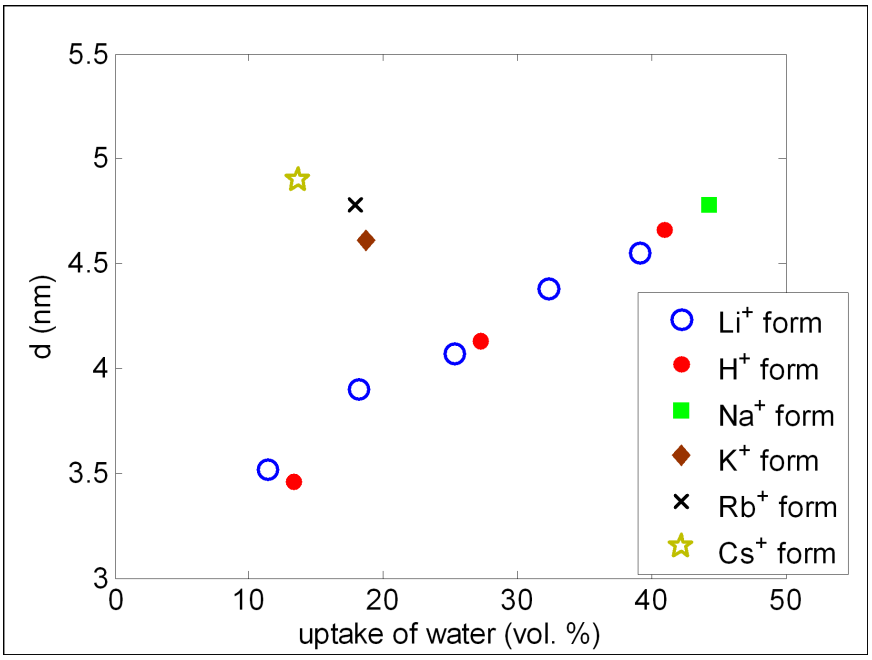

Figure 3.11: Mean intercluster spacing vs. uptake for water–swollen 1200 EW Nafion^{TM} membrane in the six different counterion forms. From reference (46).

in crystals using X-ray crystallography. By making assumptions about the size of some common ions (e.g. F^- and O^{2-}), the sizes of a large number of ions can be determined using this method. In 1927, Pauling estimated the size of a number of ions based on crystallography measurements and an inverse relationship between size and nuclear charge. In 1976, Shannon included additional effects to update those estimations. The ionic radii published by Shannon remain the most commonly accepted to date.

Although the sizes of the alkali metal ions have been known for some time, analytical measurements of the sizes of the complex TEA and EMI ions are not available. However, researchers have estimated the sizes of these ions based on computational simulations of the shape of the ions. Koch et al. have used Hyperchem^{TM} to estimate the van der Waals volume of the EMI ion (69) and Sun et al. have used Insight^{TM} to estimate the van der Waals volume of the TEA ion (120). The van der Waals volume of an ion is defined as the volume of an ion if it were just touching its neighbors but with no overlap. This is equivalent to the effective ionic radii published by Shannon.

The volumes and radii presented in Table 3.3 are related by assuming that the ions are spherical and that $V = 4/3\pi r^3$, where V is volume and r is radius. As can be seen from the table, the lithium ion is the smallest of the group that were studied, followed by

Table 3.3: Estimated sizes for the cations exchanged into the Nafion™ membranes that were studied by SAXS.

ion	radius (Å)	volume (Å^3)
Li	0.59[a]	0.86†
	0.60[b]	0.90†
K	1.37[a]	10.77†
	1.33[b]	9.85†
Cs	1.67[a]	19.51†
	1.69[b]	20.22†
EMI	3.04†	118.0[c]
TEA	3.20†	136.9[d]

[a] from reference (118).
[b] from reference (104).
[c] van der Waals volume determined using Hyperchem software, from reference (69).
[d] van der Walls volume determined using Insight software, from reference (120).
† calculated from $V = 4/3\pi r^3$.

potassium, cesium, EMI, and finally TEA. The increase in the size of the ions corresponds to a decrease in electronegativity. As the size of the ions increases and electronegativity decreases, the mean intercluster spacing observed in the ionic liquid–swollen Nafion™ membranes increases.

Although the specific reasons for the observed dependence of the mean intercluster spacing on the size of the counterions are unknown, several possibilities exist. In addition to their important SAXS investigations of water–swollen Nafion™ membranes, Gierke and Hsu also developed a model for the clustering phenomenon in Nafion™ membranes that is able to predict the size of the clusters and number of exchange sites per cluster based on the observed lattice spacing (d) and uptake of water (46). It is important to note that SAXS is able to reveal information about the geometric regularity of scatterers (in this case, ionic clusters), but in order to make determinations regarding the *size* of the clusters, assumptions must be made as to their shape and distribution. Although Gierke and Hsu's model is interesting, its validity is debatable, especially when considering the results for the ionic liquid–swollen materials. One important contribution of the model was its introduction of the notion of rearragement of the clusters on swelling of the polymer. Gierke and Hsu suggested that the polymer swells upon introduction of diluent not only by an increase in the size of the clusters but also by a rearragement of the clusters, so

that the number of clusters actually decreases on swelling. Further evidence for this idea is provided by James et al. based on maximum entropy reconstructions of SAXS results for water–swollen Nafion^{TM} (62). Those authors found that as the water content within a Nafion^{TM} membrane was increased, the spacing between the clusters was increased and the number density of the clusters was decreased.

Based on this idea of cluster aggregation, theories can be formed to explain the effect of counterion size on the observed mean intercluster spacing. The SAXS testing measures the spacing between the clusters and conclusions regarding the size of the clusters cannot be drawn directly from the SAXS results. However, if we assume that the ionic liquid swells the clusters and not the fluorocarbon matrix, then there are only two reasonable explanations for the increased lattice spacing in the Cs–, EMI– and TEA–exchanged membranes. Either the clusters themselves are larger or the number density of the clusters is smaller. This is represented schematically using the simplified model of spherical clusters embedded in an incompressible fluorocarbon matrix in Figure 3.12. If we consider the baseline case in the top portion of this figure to be the Nafion^{TM} membrane exchanged with a smaller ion such as lithium, then it is clear that either of the proposed conditions will result in an increase in the mean intercluster spacing *and* an increase in the average size of the clusters. For case (b), the cluster size will increase because the number density of clusters has decreased, leading to an increase in the number of sulfonate exchange sites per cluster. The assumption that the EMI-Tf ionic liquid swells only the clusters is reasonable considering the fact that the ionic liquid is water miscible and the fluorocarbon matrix phase of the Nafion^{TM} polymer is highly hydrophobic.

Conclusions can be drawn concerning the relative contribution of the two effects presented in Figure 3.12 based on the measured density of the dry polymer in the various cation forms. If the increase of the lattice spacing due to the presence of the larger cations was due to an increase in the average size of the clusters (as in case (a) of Figure 3.12), then one would expect the mass density of the polymer to decrease. However, if the increased lattice spacing were due to a decrease in the number density of the clusters, then one would expect the mass density to remain unchanged or possibly to increase. In fact, a very interesting trend is observed in the variation of the density of the dry polymer with the size of the counterion—see Table 3.2. For the alkali metal ions, the density increases with increasing ion size. This trend of increasing density with increasing cation size among the

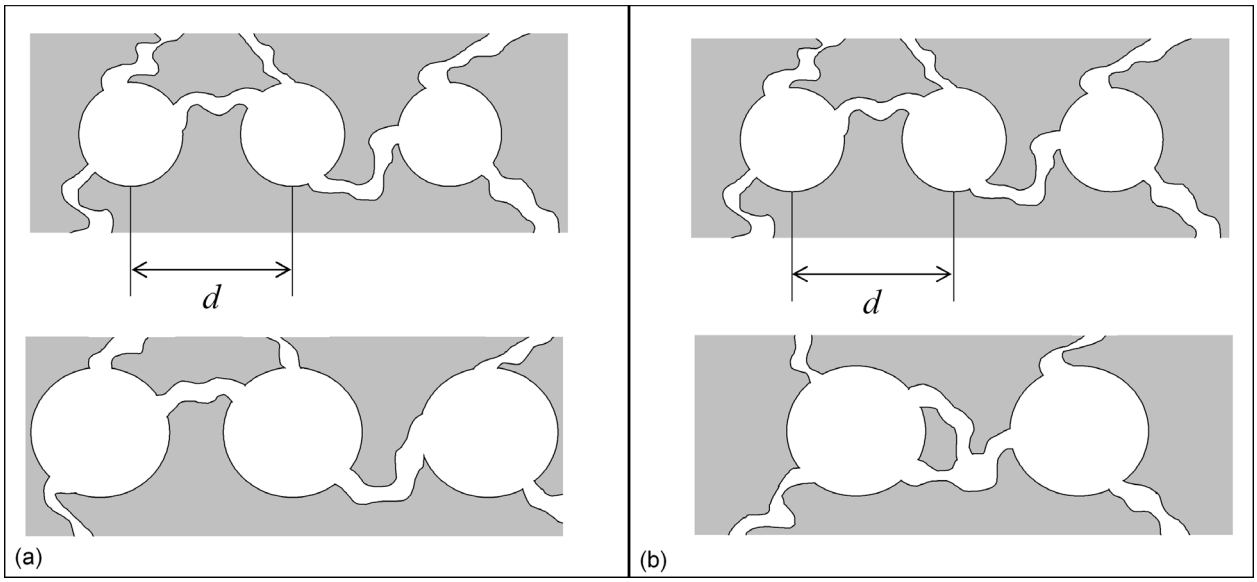

Figure 3.12: (a) Increase in the measured intercluster spacing due to increased cluster size as compared to a baseline (top). (b) Increase in the measured intercluster spacing due to a decrease in the number density of the clusters as compared to a baseline (top).

alkali metal ions has also been observed by Gierke and Hsu (46). However, for the much larger complex ions, the density of the polymer decreases with increasing ion size. This result would suggest that as the size of the cations within the polymer is increased, the number density of the clusters decreases, possibly with an associated increase in the size of the clusters, until a critical size for the cations is reached. Beyond this critical size, the diameter of the clusters will increase with increasing cation size, with little associated change in the number density of the clusters.

Although this representation of the morphology of the Nafion^{TM} polymer is able to explain the observed trends in the SAXS results, it does not take into account several important factors. First of all, the polymer is assumed to exhibit the classical phase separated ionic cluster morphology that has come to be associated with Nafion^{TM}. Second, the effect of the cation size on the strength of the electrostatic forces within the clusters are neglected. Third, the fluorocarbon matrix phase is assumed to be incompressible. Finally, the ionic liquid is assumed to reside exclusively within the clusters on swelling. However, the proposed explanation for the behavior of the polymer is consistent with the experimental results and represents one reasonable theory for the effect of cation size on the morphology of Nafion^{TM} membranes.

This idea only explains the effect of cation size on the lattice spacing that has been observed in the SAXS results, irrespective of the presence of a diluent. It does not seek to explain what happens to the clusters when the polymer is swollen with an ionic liquid. However, from Figure 3.9 it is clear that the mean intercluster spacing increases with increasing content of ionic liquid, for all of the cations studied. Although *definitive* conclusions can be made from the available data, the clusters most likely increase in size and decrease in number density upon absorption of ionic liquid. Based on the claims presented here, which are formulated from observed trends in the measured data, the size of the ionic clusters within the Nafion^{TM} polymer increases with increasing size of the counterions and with increasing uptake of ionic liquid.

In addition to the SAXS experiments that were carried out on the membranes swollen with the 1-ethyl-3-methylimidazolium trifluoromethanesulfonate (EMI-Tf) ionic liquid, investigations were also performed on a set of membranes swollen with the 1-ethyl-3-methylimidazolium bis(trifluoromethanesulfonyl)imide (EMI-Im) ionic liquid. Some of the relevant properties of these two ionic liquids are presented in Table 3.1. As can be seen, the melting point, viscosity, conductivity, and electrochemical stability window of the two ionic liquids are very similar. However, the EMI-Im ionic liquid is hydrophobic whereas the EMI-Tf ionic liquid is water miscible. The difference in hydrophobicity must arise from the difference in the chemical structures of the anions of the two ionic liquids, considering that the cations are the same. The most likely explanation for the increased hydrophobicity of the EMI-Im ionic liquid is the highly fluorinated nature of the bis(trifluoromethanesulfonyl)imide anion—see Figure 3.2. The charge on this ion may also be more delocalized and is probably less accesible to water than the charge on the trifluoromethanesulfonate anion.

The more hydrophobic nature of the EMI-Im ionic liquid leads to some interesting differences in the SAXS results for those membranes as compared to the EMI-Tf ionic liquid–swollen samples—see Figures 3.13. As can be seen, the ionomer peak at a q value of about 0.2 Å^{-1} (d=3.1 nm) that is associated with the presence of the ionic clusters in the membrane is highly attenuated as compared to the results for the EMI-Tf samples. The SAXS results for the EMI-Im–swollen membranes also do not exhibit the sharp upturn at low scattering angles that was observed in the EMI-Tf–swollen samples. As the content of ionic liquid within the membrane is increased, the height of the ionomer peak decreases

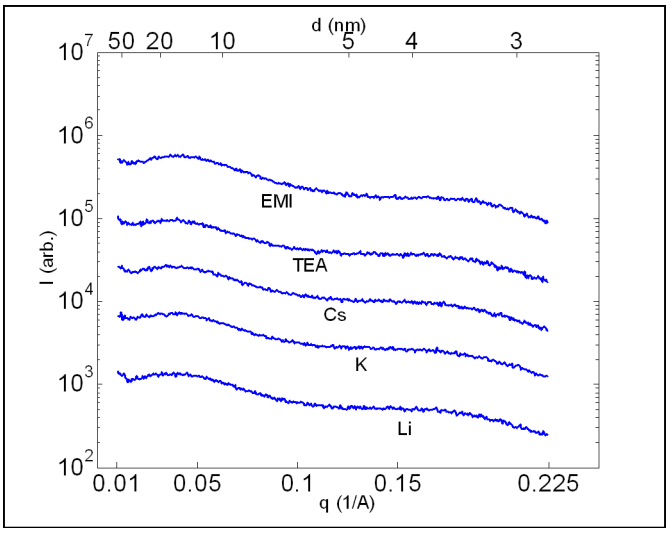

Figure 3.13: SAXS results for Nafion^{TM} membranes in five counterion forms swollen with EMI-Im ionic liquid at room temperature.

further, to the point that it is almost non–existent in the samples that were swollen at 70°C—see Figure 3.14. In addition to the reduction in the height of the ionomer peak, the peak associated with the semi–crystallinity of the fluorocarbon matrix (at about q=0.05 Å^{-1}, d=12.6 nm) is highly diminished for the more swollen membranes. These more highly swollen samples also do not exhibit the low–angle upturn.

The most reasonable explanation for the diminution of the of the prominent features of the SAXS image in the membranes swollen with the EMI-Im ionic liquid is a profound change in the morphology of these membranes on swelling. Whereas the SAXS testing of the EMI-Tf–swollen Nafion^{TM} membranes revealed evidence for a structure very similar to that observed for water–swollen membranes, the SAXS results for the EMI-Im–swollen samples do not. The very weak ionomer peak in the SAXS curves for the less–swollen membranes suggests that the quasi–phase separated morphology of the polymer is broken up. It seems that the EMI-Im ionic liquid may disrupt ionic clustering in the Nafion^{TM} membranes. Further support for this idea is provided by the fact that the ionomer peak is almost non–existent in the highly swollen membranes. If the SAXS results are indicative of an interruption in the clustered morphology of the polymer, then it is reasonable to conclude that the EMI-Im ionic liquid is absorbed into the fluorocarbon matrix phase. This is rational considering that the EMI-Im ionic liquid is hydrophobic and should be miscible with the hydrophobic Teflon^{TM}–like phase of the Nafion^{TM} polymer. In fact, the

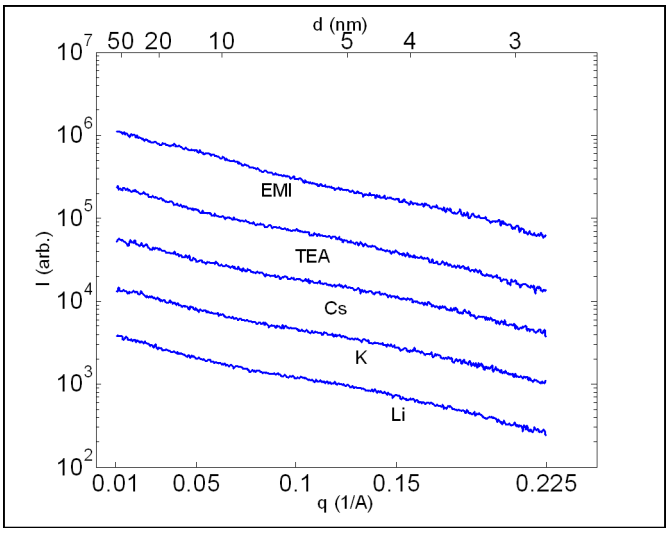

Figure 3.14: SAXS results for Nafion^{TM} membranes in five counterion forms swollen with EMI-Im ionic liquid at 70°C.

ionic liquid is most likely absorbed to some extent into both the matrix phase and the cluster phase. If it were integrated into both phases, the presence of the ionic liquid within the membrane would decrease the electron density contrast between the matrix and the clusters. One would expect this decrease in electron density contrast to reduce the intensity of the ionomer peak in the SAXS measurements. That expectation is consistent with the experimental observations. In addition to decreasing the electron density contrast between the two phases, the EMI-Im ionic liquid also likely interrupts the physical boundary between the two phases, thus increasing the homogeneity of the polymer.

If a diluent is absorbed at least partially into the matrix of the polymer, then one would expect the size of the clusters to increase at a lower rate than if the diluent were absorbed exclusively by the clusters. Although the SAXS testing does not directly measure the size of the clusters, two mechanisms responsible for an increase in the observed inter-cluster spacing when the polymer is swollen have been proposed—see Figure 3.12. Both of these proposed mechanisms are associated with an increase in the size of the clusters. Therefore, the mean intercluster spacing measured by the SAXS testing should be directly related to the mean size of the clusters. If the clusters are smaller, then the intercluster spacing would be expected to be smaller. If the position of the ionomer peak is extracted from Figures 3.13 and 3.14 and plotted against the volumetric uptake of ionic liquid, then the plot in Figure 3.15 is obtained. As can be seen from the figure, the mean intercluster

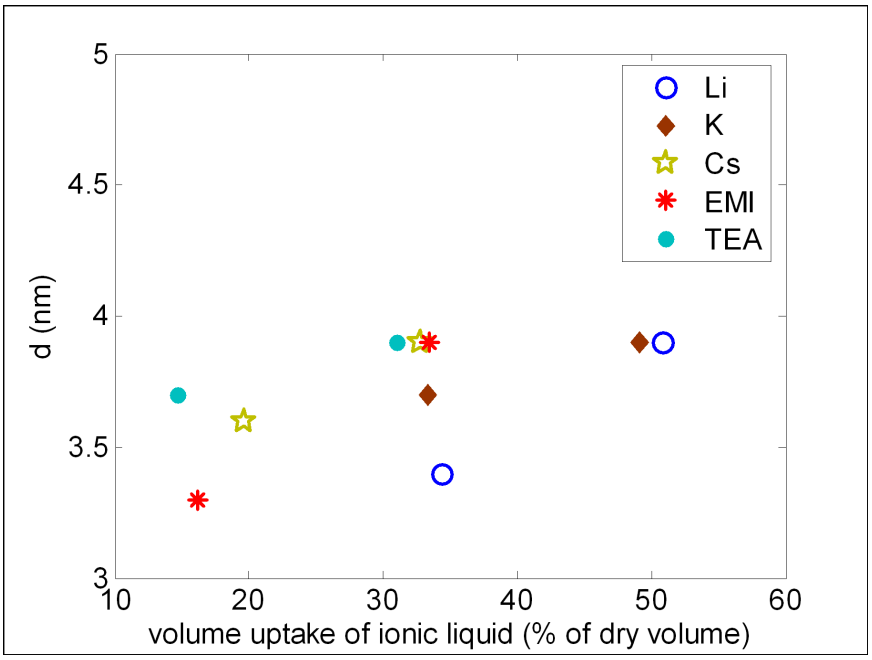

Figure 3.15: Mean intercluster spacing vs. uptake for EMI-Im–swollen Nafion^{TM} membranes in five counterion forms.

spacing observed in the membranes swollen with the EMI-Im ionic liquid is indeed smaller than that observed in the EMI-Tf–swollen membranes, especially at the higher swelling levels. Combined with the very small ionomer peak, this result suggests that the EMI-Im ionic liquid is in fact absorbed into the matrix phase of the Nafion^{TM} polymer. These samples also exhibit a dependence of the cluster spacing on the cation, with the mean intercluster spacing increasing with increasing size of the counterion.

Further evidence for the incorporation of the EMI-Im ionic liquid into the fluorocarbon phase of the polymer is provided by the absence of the low–angle upturn in the data and the disappearance of the crystalline peak when the content of ionic liquid within the membrane is increased. The low–angle upturn has been observed by several researchers in SAXS results for water–swollen Nafion^{TM} membranes (89; 41; 27) and has been attributed to the presence of large–scale inhomogeneities in the distribution of the clusters (62; 27; 89). Therefore, the absence of the low–angle upturn in the SAXS results for the EMI-Im–swollen membranes supports the idea that the presence of the EMI-Im ionic liquid has disrupted the clustered morphology of the polymer and perhaps eliminated the clusters altogether. Additionally, the SAXS results for the more highly swollen samples do not exhibit the expected crystalline peak. This indicates that the crystallites in the Teflon^{TM}–like matrix

have been disrupted, most likely by the introduction of ionic liquid into that phase.

3.5 Summary and Conclusions

Small-angle X-ray scattering has been used to probe the morphology of Nafion^{TM} membranes swollen with two ionic liquids at two different swelling levels. The results are interpreted by assuming that the polymer exhibits the classical "clustering" that has been commonly observed for ionomers such as Nafion^{TM}. Similarities and differences are evident in the observed trends. The results for the lower swelling level reveal two peaks, one associated with the presence of crystallites in the Teflon^{TM}–like matrix phase of the polymer and one associated with the presence of ionic clusters embedded within this matrix. Also, the results for both of the ionic liquids exhibit an increase in the measured spacing between the clusters with increasing size of the counterions of the membrane and with increasing content of ionic liquid. As the content of ionic liquid within the membranes is increased, the mean intercluster spacing increases dramatically for the EMI-Tf ionic liquid while the increase is much more modest for the EMI-Im ionic liquid. Also, the intensities of the ionomer peak and the crystalline peak are greatly diminished for the membranes that were more highly swollen with the EMI-Im ionic liquid.

Two mechanisms are proposed to explain the increase in the mean intercluster spacing with increasing cation size and uptake of ionic liquid. These mechanisms are bulk swelling of the clusters, resulting in an increase in their mean diameter, and rearragement of the clusters, so that their number density has decreased. Density measurements suggest that the latter mechanism (reorganization) is responsible for the larger observed intercluster spacing in the membranes exchanged with larger cations as compared to those exchanged with smaller cations, for a given range of cation sizes. These same density measurements suggest that for the largest cations, the larger observed cluster spacing is due to increased cluster diameter, as compared to the membranes exchanged with the smaller cations. During swelling of the polymer with an ionic liquid, the observed increase in the mean intercluster spacing is likely caused by a combination of these mechanisms.

The SAXS results suggest that the clustered morphology of the polymer is at least partially disrupted by the presence of the EMI-Im ionic liquid. Evidence for this includes the smaller intercluster spacing and the smaller ionomer peak observed for these samples

as compared to the membranes swollen with the EMI-Tf ionic liquid. Further evidence is provided by the lack of a small–angle upturn in the SAXS data and the dissappearance of the crystalline peak for the more highly swollen membranes. The most reasonable explanation is that the EMI-Im ionic liquid is absorbed at least partially into the fluorocarbon matrix phase of the polymer. This may have the effect of "smearing" the two phases, and at the very least will reduce the size of the clusters as compared to the EMI-Tf ionic liquid, for a given swelling level.

The SAXS results reveal that the membranes swollen with the EMI-Tf ionic liquid exhibit a morphology that is more similar to water–swollen membranes than the samples swollen with the EMI-Im ionic liquid. Also, the mean intercluster spacing is found to increase with increasing cation size and loading of ionic liquid. Based on the proposed models of cluster reorganization, this increase in the mean intercluster spacing should be associated with an increase in the mean diameter of the clusters.

Chapter 4

Spectroscopic Investigation of Ion Associations

4.1 Motivation

Developing a model of electromechanical transduction in ionic liquid–swollen Nafion^{TM} membranes requires an understanding of the relevant ion associations within the membranes. Initial transduction experiments reveal that the actuators will bend towards the anode when an electric field is applied. This type of motion is similar to that observed in water–swollen Nafion^{TM} actuators and indicates that the bending motion is caused by the movement of cations within the membrane towards the cathode. For the water–swollen membranes, it is easy to understand that the macroscopic actuation motion is generated by microscopic motion of the cations. Only two ions exist in those membranes, the sulfonate exchange sites and the cations associated with them. The sulfonate exchange sites are covalently bonded to the Nafion^{TM} polymer and therefore cannot move in response to an electric field. However, when a diluent is added to the polymer, sufficient charge separation is generated between the cations and the sulfonate exchange sites to allow the solvated cations to move about within the polymer. However, if the water is replaced by an ionic liquid then the situation becomes more complex. In addition to the sulfonate exchange site and associated cation, there are two additional ions present within the membrane. The role that these ions play in the actuation is unclear.

In order to develop an understanding of what role the ionic liquid plays in the

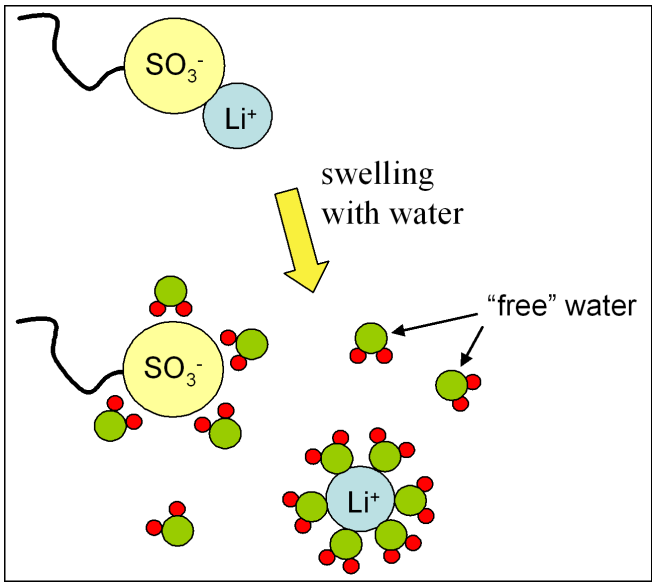

Figure 4.1: Schematic of separation between a cation / anion pair due to swelling of a Nafion™ membrane with water.

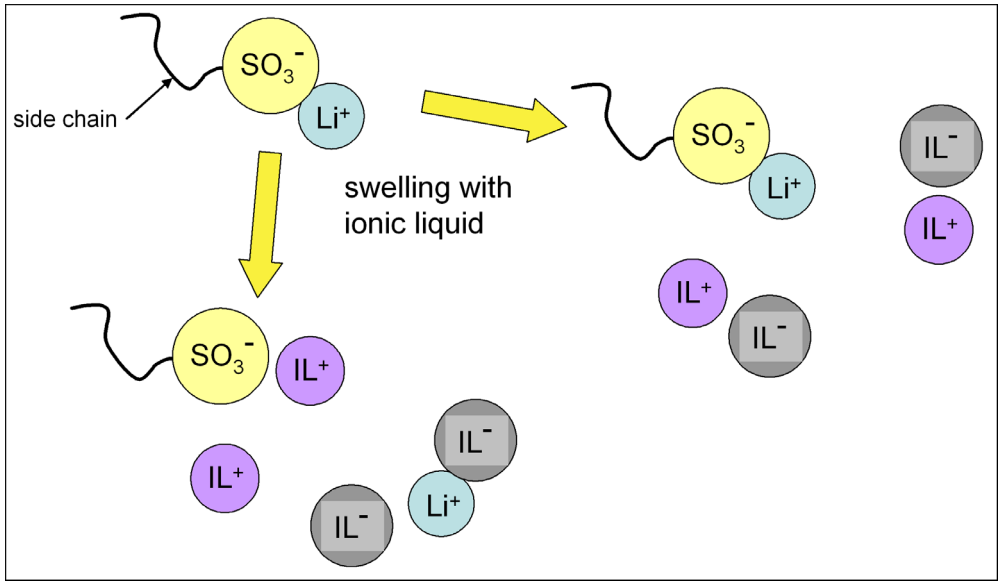

Figure 4.2: Two possiblities for the arrangement of ions within an ionic liquid–swollen Nafion™ membrane.

transduction, a picture of the arrangement of the various ions within the ionic liquid–swollen membranes must be developed. When a Nafion^{TM} membrane is swollen with water, the expected arrangment of the ions is shown in Figure 4.1. As a polar protic solvent, water is able to associate well with both the cations and the sulfonate exchange sites and generate effective separation beween them (28). However, when an ionic liquid is used as the diluent, then the association of the ionic liquid with the ions in the Nafion^{TM} membrane is harder to predict. Two possibilities are shown in Figure 4.2.

Spectroscopic investigations of chemical species can be used to gain insight into the structure of those species by examining the way that the various atoms and bonds within a molecule interact with applied electromagnetic radiation. In order to elucidate the principal associations between the ions within the ionic liquid–swollen membranes, a structured investigation was undertaked using Fourier transform infrared spectroscopy (FTIR) and nuclear magnetic resonance spectroscopy (NMR). These techniques were used to study the effect of the ionic liquid on the local environment of the sulfonate exchange site and the counterion of the membrane in order to provide supporting evidence for a model of the arrangement of the ions.

4.2 Sample Preparation

For the structured experiment to investigate the ion associations, two ionic liquids were used, 1-ethyl-3-methylimidazolium trifluoromethanesulfonate (EMI-Tf) and 1-ethyl-3-methylimidazolium bis(trifluoromethanesulfonyl)imide (EMI-Im). The properties of these ionic liquids are presented in Table 3.1. The swelling level of the ionic liquids within the membrane was varied, and six different cation forms of the Nafion^{TM} membrane were used (Li^+, Na^+, K^+, Cs^+, EMI^+, and TEA^+). As before, the Nafion^{TM}-117 membrane was used for this set of tests. The membranes were pretreated by boiling for one hour in 1.0 M sulfuric acid followed by boiling for one hour in DI water. The membranes were then soaked for several days in 0.5 M solutions of the chloride salts of the six ions listed above. Following this the membranes were soaked for several hours in DI water and were then dried by baking overnight at 110°C under a vacuum of approximately 70 torr. After drying, the dry weights of the membranes were recorded and they were swollen with ionic liquid.

One of the experimental parameters that was varied in the spectroscopic study was

the content of ionic liquid within the membrane. In order to vary this parameter, the temperature *and* soak time of the membranes in the ionic liquid / methanol mixture was controlled. For this testing, the ionic liquids were mixed with methanol in a ratio of two parts ionic liquid to one part methanol (by volume). Most of the incorporation processes were carried out a room temperature. The soak times in the ionic liquid / methanol solution varied from 30 seconds to 180 minutes. Five different swelling levels were targeted: 5%, 10%, 20%, 30%, and 40% (by volume). For the highest uptake of ionic liquid, the membranes were soaked in the ionic liquid / methanol solution for 180 minutes at 65°C. Because the rate of diffusion of the ionic liquid into the membranes is lower for the membranes exchanged with the larger cations and for the EMI-Im ionic liquid as compared to the EMI-Tf ionic liquid, the soak times were adjusted accordingly in order to acheive the targeted uptake. Due to these differences in the diffusion rates, the targets for the swelling were not acheived for all of the samples even with the adjustments to the swelling process. However, for both of the ionic liquids in all of the cation forms, the swelling levels was varied over a range, allowing conclusions regarding the effect of the uptake on the properties of the membranes to be made.

After the membrane samples were soaked in the ionic liquid / methanol solution they were dried again under 100°C and 70 torr vacuum, this time for 4 hours. The purpose of this second drying process was to remove the methanol from the membranes. After the methanol was removed the membranes were weighed again and the content of ionic liquid within the membranes was computed from equation 2.1 using the measured dry density of the membranes (Table 3.2) and the reported densities of the ionic liquids (Table 3.1). This second drying process also served to distribute the ionic liquid more homogeneously throughout the membranes. Because the diffusion of the ionic liquid / methanol solution was not allowed to proceed to equilibrium, the solution was likely not well distributed throughout the volume of the membrane, especially for the membranes that were soaked for very short times. By holding the membranes at an elevated temperature for several hours, the ionic liquid had an opportunity to diffuse into the less swollen areas of the membranes, thus ensuring a more even distribution. Although no testing was performed to verify this, nothing in the experimental results suggests that the distribution of ionic liquid within the samples was inhomogeneous. This description is, of course, referring to the macroscopic distribution of ionic liquid within the thickness, length, and width of the membrane, and not

the microscopic distribution of the ionic liquid within the ionic clusters or the fluorocarbon matrix, which was discussed in Chapter 3.

The membrane samples prepared in this way were tested using two experimental methods: FTIR and NMR spectroscopy. Due to the limitations of the NMR testing, only the membranes that were exchanged with the lithium, sodium, and cesium ions could be tested using that technique. This is because the NMR method is designed to investigate only a single nucleus. Therefore, the utility of the technique is in question when the cation of interest contains many nuclei, such as in the case of TEA^+ and EMI^+. The NMR testing was not performed on the potassium–exchanged membranes due to the low NMR sensitivity of potassium. Also, a large quantity of sample was required for the NMR testing in order to improve the signal–to–noise ratio (SNR) of the test. By contrast, all of the samples were tested using FTIR and that testing required only a small piece of membrane. Therefore, for the lithium–, sodium–, and cesium–exchanged samples, the original size of the Nafion^{TM} membrane used was 5 cm X 10 cm. Those membranes were pretreated, exchanged, and swollen with ionic liquid using the process described above. A strip approximately 1 cm X 5 cm was then cut from the sample and set aside to be tested using FTIR. The remainder of the sample was cut into strips about 0.5 cm X 5 cm. These strips were then stacked on top of each other and the stack was inserted into a 10 mm NMR tube. The tube was then back–filled with dry nitrogen gas and capped. The strips that were set aside for the FTIR testing were stored in liquid–tight polypropylene bags that were back–filled with nitrogen and sealed. For the cationic forms of the membrane that could not be tested by NMR (K^+, EMI^+, and TEA^+), smaller pieces of Nafion^{TM} membrane were used. In this case the original membranes were about 1 cm X 5 cm and were pretreated, exchanged, and swollen with ionic liquid using the process described above. After swelling with ionic liquid, the samples were stored in liquid–tight polypropylene bags that were back–filled with nitrogen to prevent the introduction of water into the samples.

4.3 Fourier Transform Infrared Spectroscopy

4.3.1 Testing Protocol

Fourier transform infrared spectroscopy (FTIR) involves the illumination of a sample of material with broadband infrared radiation and observing which parts of that signal are

absorbed and which parts are reflected or transmitted. A brief introduction to the method will be provided in this section (39; 127; 56). A common method of obtaining the FTIR spectrum for a sample is to pass broadband infrared radiation through the sample and to measure the spectral intensity of the radiation on the far side. This is called transmission spectroscopy. However, transmission spectroscopy is inappropriate for the current work due to the high absorption of infrared radiation by the Nafion^{TM} polymer and the relatively thick films that were used. This problem is compounded by the high absorption of infrared (IR) radiation by the ionic liquids used. In order to overcome this problem, the ionic liquid–swollen Nafion^{TM} membranes were tested by using a technique called attenuated total reflectance (ATR). In this type of FTIR experiment, the sample is placed on a crystal (called an internal reflection element, or IRE) into which the IR beam is projected. Common IRE crytal material are germanium or zinc selenide; for the current study, the crystal used was thallium bromoiodide. The crystal is beveled at each end and the sample is pressed tightly against one surface of the crystal using a C-clamp pressure plate assembly. The beam of infrared light enters the crystal at one end and is reflected inside the crystal many times before exiting at the opposite end. At each internal reflection, the beam penetrates a short distance into the polymer membrane—see Figure 4.3. The distance that the beam penetrates into the membrane is dependent on the ratio of the refractive indices of the polymer and the crystal, but is typically very small ($\sim$1 micron). Because the penetration distance is so small, the sample must be held in intimate contact with the surface of the crystal. This intimate contact is ensured by clamping the sample and the crystal together in the C-clamp pressure plate.

In order to perform the ATR testing, a background scan is first conducted without a sample present. The purpose of this test is to determine the effect of the system components (crystal, sample holder, air in the test chamber) on the signal measured by the detector. The background scan was used as a baseline for the testing of the samples. For this background scan, broadband IR radiation is shined through the IRE crystal in the sample holder, but without a sample present. The signal measured by the detector is then converted to a spectrum of background emissivity through a Fourier transform. The Fourier transform allows the user to consider the broadband signal as a summation of individual signals that each contain only a single frequency. In this way, the emissivity can be plotted over the spectrum of frequencies of interest. For interpreting ATR results, wavenumber is typically

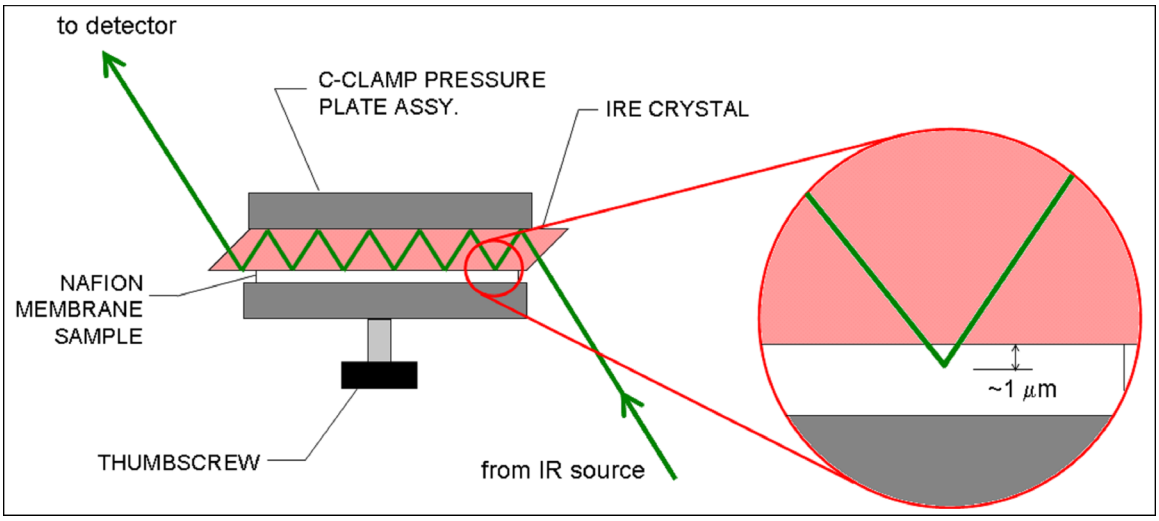

Figure 4.3: Schematic of the ATR test setup.

used in place of frequency, however. The wavenumber of a wave is related to its wavelength by:

$$\tilde{\nu} = \frac{1}{\lambda}, \tag{4.1}$$

where $\tilde{\nu}$ is wavenumber and λ is wavelength (typically in cm). Wavelength is related to frequency by the well–known equation

$$\lambda = \frac{c}{\nu}, \tag{4.2}$$

where ν is frequency (in Hz) and c is the speed of light (299,792,458 m/s). It is easy to show that

$$\tilde{\nu} = \frac{\nu}{c}. \tag{4.3}$$

Therefore, wavenumber is proportional to frequency.

After the background emissivity spectrum is collected, a membrane is loaded into the sample holder and the emissivity of the sample is measured. Again, a Fourier transform is used to convert the measured signal into the frequency (wavenumber) domain. The transmittance of the sample can then be obtained by taking the ratio of the sample emissivity to the background emissivity. For ATR testing, the data is typically converted to absorbance; the absorbance of the sample is the logarithm of the inverse of the transmittance,

$$A = \log_{10}(1/T), \tag{4.4}$$

where A is absorbance and T is transmittance.

For the current work, a background scan was taken only at the beginning of a round of testing, during the setup of the equipment. Also, the presence of water in the sample chamber presents an obstacle to obtaining good quality results because water strongly absorbs IR energy. In order to elminate water, the sample chamber is continuously purged with dry air. Also, the samples were stored in baggies filled with dry nitrogen until testing. In order to reduce the effect of water on the data, the chamber was allowed to purge for about 30 minutes before collecting the background scans. Unfortunately, the sample chamber had to be opened each time a new sample was introduced. For this reason, the chamber was allowed to purge for five minutes after each sample was mounted before a scan was collected. The IRE crystal was cleaned when necessary using methyl–ethyl ketone (MEK). For the collected data, 64 consecutive scans were collected for each sample. These scans were averaged in order to reduce the effects of noise on the measured signal. ATR spectra were also obtained for the neat ionic liquids by applying a small drop of the ionic liquid directly to the crystal. The crystal was cleaned after this testing with MEK and then a spectrum was collected for the bare crystal with no sample present to ensure that all ionic liquid and contaminants had been removed.

4.3.2 Results

Fourier transform infrared spectroscopy is a useful tool for performing characterizations of polymers because using it, one is able to identify key features of the polymer structure and is often able to draw conclusions about changes to this structure due to processing. This is possible because the frequencies at which energy is absorbed by a polymer can be correlated to the atoms present in the polymer and the type and structure of the bonding that those atoms experience. This can be best understood by making an analogy to a mechanical system. Although classical mechanics is certainly not sufficient to describe the complexities of infrared spectroscopy, it is sufficient to provide qualitative information. For the single degree of freedom system shown in Figure 4.4a, the resonant frequency in Hz is

$$\nu = (1/2\pi)\sqrt{\frac{k}{m}}, \tag{4.5}$$

where m is the mass and k is the stiffness of the spring. However, molecular vibration involves the motion of many atoms moving simultaneously, without a fixed reference point. Consider the representation of a diatomic molecule shown in Figure 4.4b as two point masses

(atoms) connected by a massless spring (a chemical bond). If the the stiffness of the spring connecting the two masses is k, then the resonant frequency for the system (in Hz) is

$$\nu = (1/2\pi)\sqrt{\frac{k}{\mu}}. \tag{4.6}$$

In this case, μ is the reduced mass and is related to the masses of the two atoms (m_1 and m_2) by

$$\mu = \frac{m_1 m_2}{m_1 + m_2}. \tag{4.7}$$

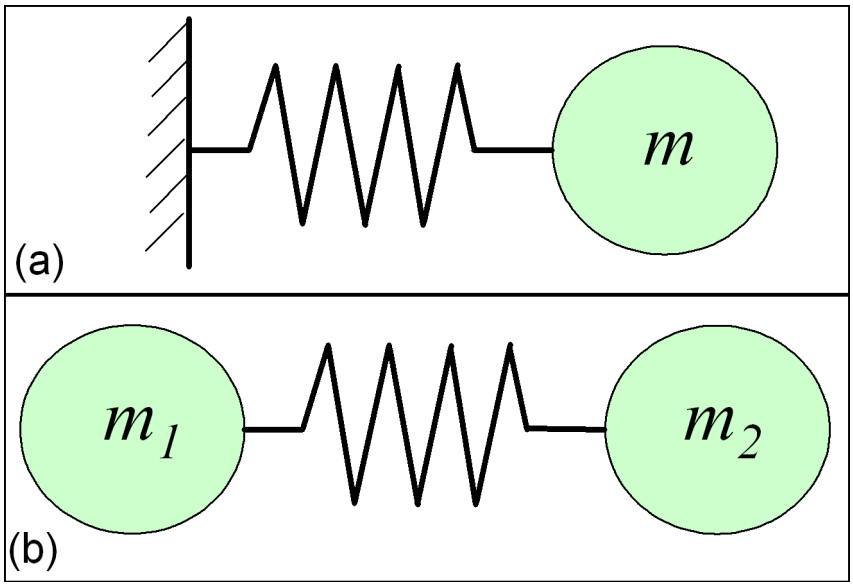

Figure 4.4: (a) Single degree of freedom spring–mass system. (b) Mechanical analog of a diatomic molecule.

It is clear from equation 4.6 that the stretching resonant frequency of a molecule is dependent on the stiffness of the bond and the masses of the two atoms. For example, the resonant frequency of a C–H bond is approximately $8.72(10)^{13}$ Hz, or 2907 cm^{-1} (see equation 4.3). This resonance can be computed from the mass of the carbon and hydrogen atoms ($19.944(10)^{-27}$ kg and $1.674(10)^{-27}$ kg respectively (132)) and the stiffness of the C–H single bond (463 N/m (39)). Therefore, this analogy tells us that the C–H bond will absorb infrared radiation strongly at 2907 cm^{-1}. By changing the mass of the atoms involved in the bond, the frequency at which the bond will absorb will be changed. For example, a C–F bond will absorb at lower frequencies than a C–H bond due to the much larger mass of the fluorine atom as compared to the hydrogen atom. For atoms bonded to hydrogen, changing the mass of the atom will have very little effect on the resonant frequency, because the

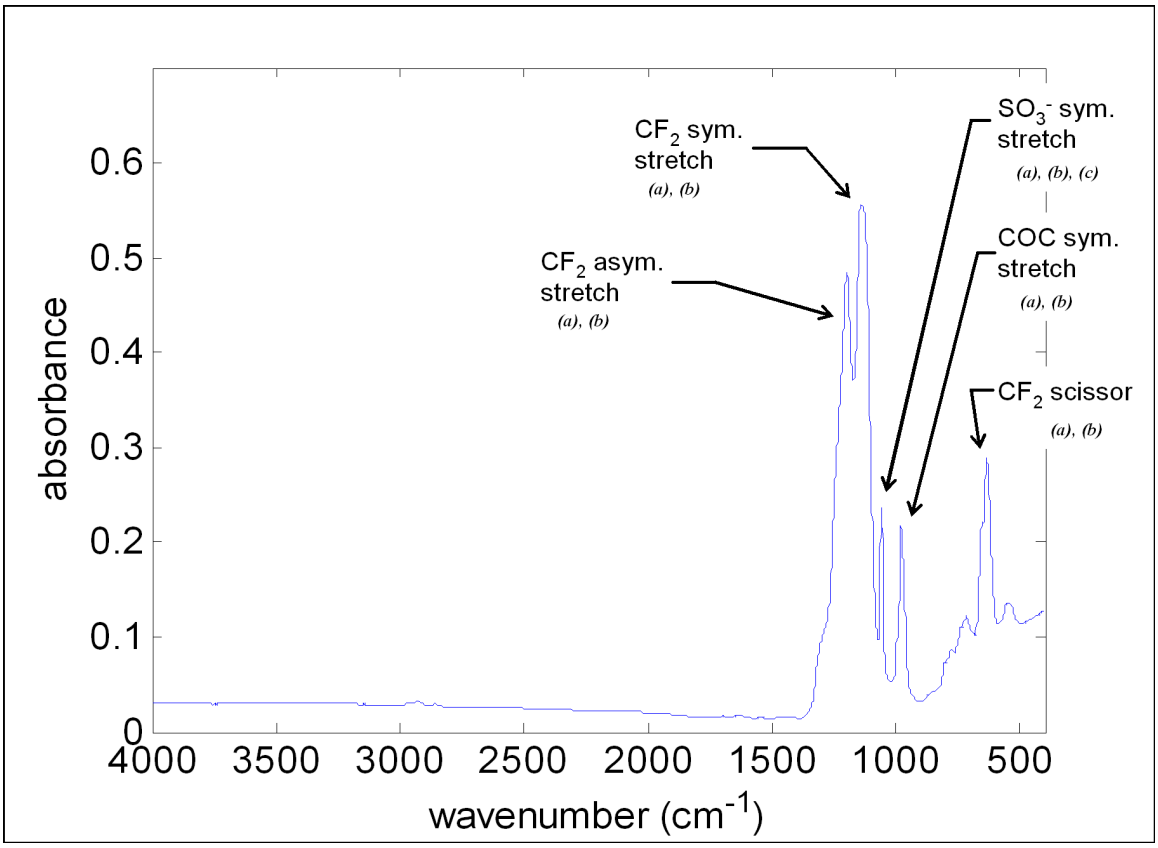

Figure 4.5: Infrared spectrum for a dry, potassium–form Nafion^{TM}-117 membrane. *(a)* peak assignment from reference (29). *(b)* peak assignment from reference (57). *(c)* peak assignment from reference (83).

reduced mass (equation 4.7) is dominated by the less massive atom (hydrogen). Changing the stiffness of the bond will have a much greater effect on the absorption frequency of the molecule. Whereas the single C–H bond has a stiffness of about 463 N/m, double bonds have stiffnesses of about 1100 N/m and triple bonds have stiffnesses of about 1600 N/m (39). The stiffness is also affected by the electronegativity of the bonded atoms. For example, an O–H bond will typically absorb at higher frequencies than a N–H or C–H bond due to the increased electronegativity of the oxygen atom (39). The resonant frequency of the O–H bond is higher because of the increased polarization of the bond. This is in spite of the increased mass of the oxygen atom as compared to nitrogen or carbon.

Several researchers have performed FTIR studies of Nafion^{TM} membranes. Shown in Figure 4.5 is the IR spectrum of a dry, potassium–exchanged Nafion^{TM}-117 membrane collected using ATR. The origins of the major peaks are identified. As can be seen, most of the peaks in the Nafion^{TM} polymer arise from vibrations of the fluorocarbon backbone.

Figure 4.6 provides a graphical description of the meaning of symmetrical stretching, asymmetrical stretching, and scissor mode vibration. As can be seen from Figure 4.5, the peak at about 1060 cm^{-1} has often been assigned to symmetrical stretching of the SO_3^- group. Several important studies have been made of the effects that the counterion and the content of water have on the position of this peak—see Table 4.1. Considering the first column of this table, it is clear that the symmetric stretch of the sulfonate group increases in frequency for decreasing size of the counterion, for the dry membranes. This was first observed by Lowry and Mauritz in 1980 (83). They explain that in the dry membranes the smaller cations generate a larger electrostatic field, which results in an increased polarization of the S–O dipole. This increased polarization causes the SO_3^- symmetric stretch to occur at a higher frequency. The dependence of the sulfonate stretch on the size of the cation has been confirmed by numerous researchers since Lowry and Mauritz, including Falk (1982, (29)), Kujawski et al. (1992, (75)), and Cable et al. (1995, (12)). All of these authors have supported the original claim that the size dependence arises from an increased polarization of the S–O dipole due to the increased electrostatic field of the smaller cations.

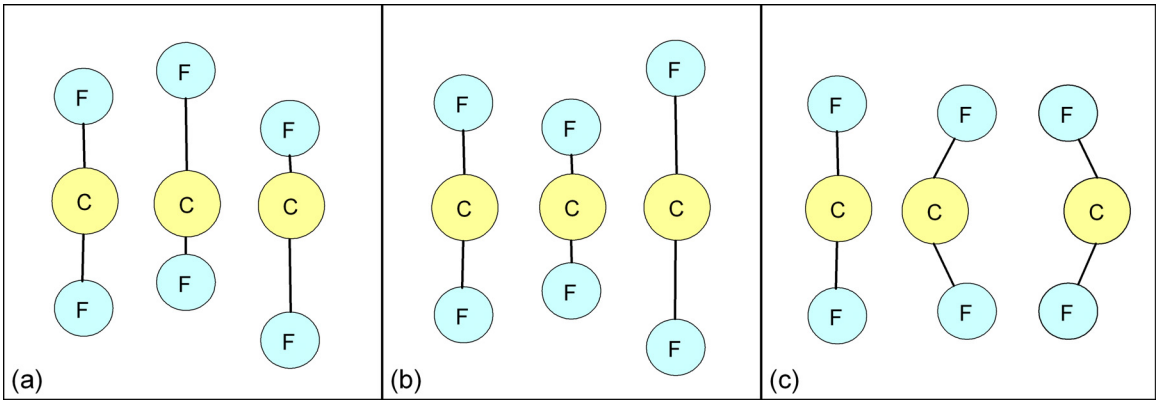

Figure 4.6: Vibrational modes for a CF_2 group: (a) asymmetric stretching, (b) symmetric stretching, (c) bending (scissor) mode.

For the dry membranes, the data that is available from the literature suggests that the sulfonate stretching frequency exhibits a linear dependence on the cation size—see Figure 4.7. For this plot, the sizes of the ions were taken from Shannon (118) and are listed in Table 3.3; the reported size of the ruthenium ion is 1.52 nm. The results of the current study also support this trend—see Figure 4.8. As can be seen, with the exception of the large EMI^+ and TEA^+ ions, the sulfonate stretching frequency decreases linearly with increasing size of the cation, for the dry membranes. The departure of the EMI^+

Table 4.1: Symmetric stretching of the SO_3^- group for different ions. All values in cm^{-1}.

	peak position	
cation	dry	water–swollen
Li^+	$1073^{(a)}$	$1058^{(a)}$
	$1071^{(b)}$	$1057.5^{(b)}$
	$1070.4^{(c)}$	$1057.9^{(c)}$
Na^+	$1064^{(a)}$	$1058^{(a)}$
	$1065^{(b)}$	$1059^{(b)}$
	$1063.7^{(c)}$	$1057.9^{(c)}$
	$1062.5^{(d)}$	$1058^{(d)}$
K^+	$1059^{(a)}$	$1058^{(a)}$
	$1060^{(b)}$	$1058.5^{(b)}$
	$1059.8^{(c)}$	$1057.9^{(c)}$
Rb^+	$1057^{(a)}$	$1057^{(a)}$
	$1057^{(b)}$	$1057.5^{(b)}$
Cs^+	$1055^{(b)}$	$1056^{(b)}$
	$1054^{(c)}$	$1055^{(c)}$
TBA^+	$1048^{(d)}$	$1048^{(d)}$

$^{(a)}$ from reference (83)
$^{(b)}$ from reference (29)
$^{(c)}$ from reference (75)
$^{(d)}$ from reference (12)

and TEA^+ ions from this trend suggests that the sizes of these ions are overestimated. This is reasonable considering that the sizes of the alkali metal ions were obtained directly from crystallography measurements whereas the sizes for the EMI^+ and TEA^+ ions were determined from volume estimations of the ions and by assuming the ions to be spherical. The volume estimations themselves were obtained from computer simulations and not from direct measurements. Both of these factors could lead to errors in the estimation of the sizes for these ions, especially the assumption that the ions are spherical. However, the vibrational frequency is seen to decrease with increasing cation size for all of the data.

A dramatic change is observed in the Nafion^{TM} membranes when they are swollen with water, however—see Table 4.1. As can be seen, the frequency of the symmetric sulfonate stretch in the water–swollen membranes is not dependent on the size of the counterion and occurs at about 1058 cm^{-1} over a wide range of sizes. It should be noted that the deviation from this trend for the very large cesium and tetrabutylammonium (TBA^+) ions is most likley due to the small uptake of water in the membranes exchanged with those relatively hydrophobic ions. Cable et al. have reported that the maximum water content

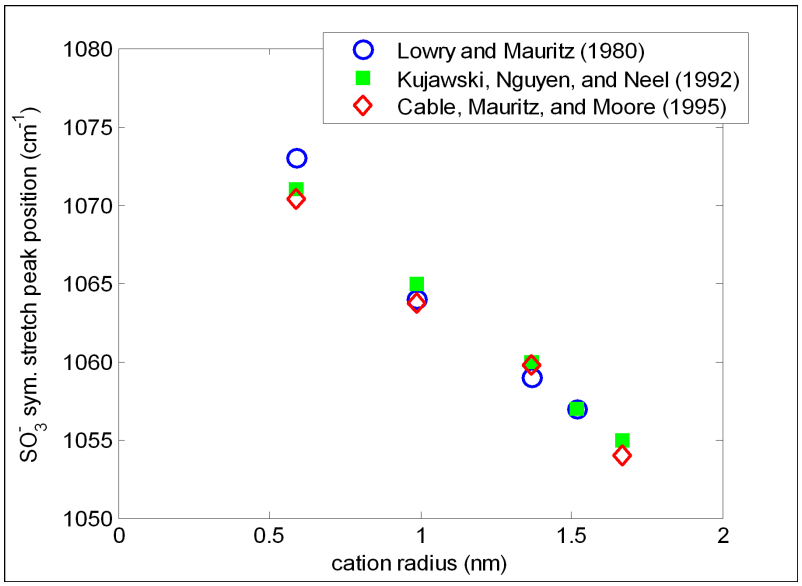

Figure 4.7: Symmetric sulfonate stretching frequency versus cation size for dry Nafion^{TM} membranes exchanged with a number of alkali metal ions. The size of the cations are obtained from (118).

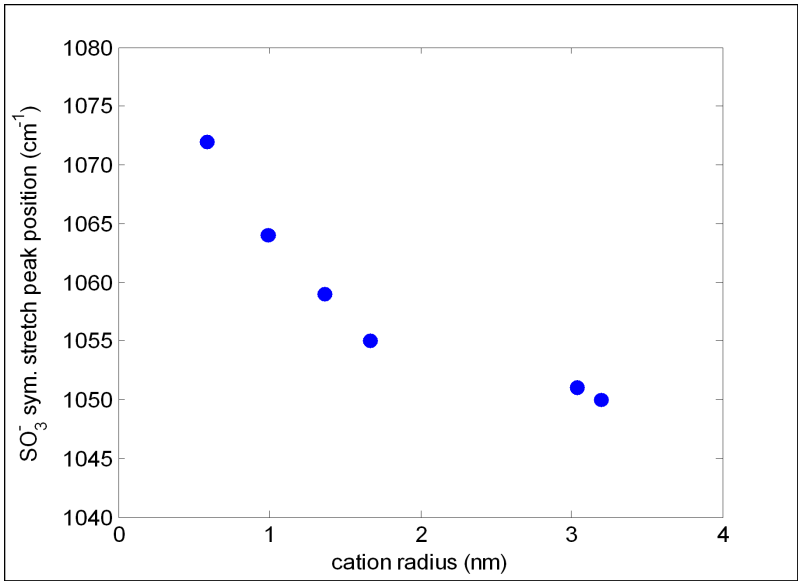

Figure 4.8: Results of the current study showing the symmetric stretching SO_3^- frequency versus cation size for dry Nafion^{TM} membranes. The cation size was obtained from (118) for the alkali metal ions, calculated from volume cited in (69) for the EMI^+ ion, and calculated from volume cited in (120) for the TEA^+ ion.

of the TBA–form membranes is about 1% (12). The reason that the vibrational frequency of the sulfonate is insensitive to the cation size in the swollen membranes is that the water effectively shields the cation from the sulfonate exchange site. Therefore, the exchange site is not affected by the electrostatic field of the cation. This is depicted graphically in Figure 4.1. In general, swelling of the membrane with water leads to a decrease in the symmetric stretching sulfonate frequency, corresponding to a decrease in the polarization of the S–O dipole. However, for the larger rubidium and cesium ions, the frequency actually increases upon hydration. This indicates that water more strongly polarizes the S–O dipole than the very large alkali metal ions. This effect would likely also be manifested in the TBA–exchanged membrane, if the water content were increased.

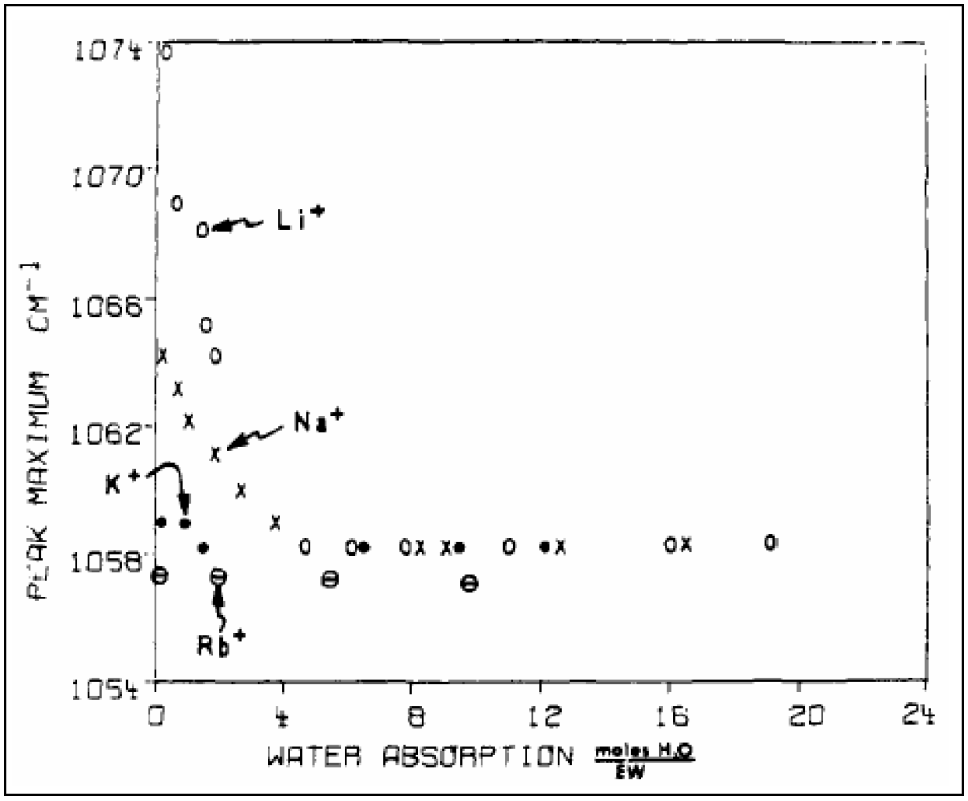

Figure 4.9: Symmetric stretching SO_3^- vibration for a Nafion^{TM} membrane in various cation forms and swollen with various contents of water. Reprinted with permission from reference (83). Copyright 1980 American Chemical Society.

Lowry and Mauritz have also measured the symmetric stretching frequency of the sulfonate group at a number of intermediate water contents, for several alkali metal ion forms of a Nafion^{TM} membrane. As can be seen in Figure 4.9, the SO_3^- peak shifts towards lower frequency as the water content of the membrane is increased, until it reaches about 3-4

water molecules per sulfonate for Li^+ and Na^+ or about 2 water molecules per sulfonate for K^+. Above this critical uptake of water, the vibrational frequency of the sulfonate group does not change. This indicates that the anions and cations are fully solvated and that additional water will not further shield the sulfonate exchange sites from the electrostatic field of the cations. This shift occurs at lower water content for the larger ions because they are less tightly bound to the exchange site and therefore fewer water molecules are required to separate them from the exchange sites.

A similar investigation has been performed in the current work. First, the spectra of the neat ionic liquids were measured—see Figure 4.10. These spectra clearly show peaks around 3200 cm^{-1} that are associated with the vibration of the CH groups on the imidazole ring. Also evident are the peaks at around 1600 cm^{-1} that are associated with the C=C group on the imidazole ring and the peaks at 1150 cm^{-1} that are associated with the CF_3 groups on the anions. Most importantly, both of the ionic liquids exhibit a peak that is associated with the vibration of the sulfonate groups in the anions. For the EMI-Tf ionic liquid this peak occurs at 1031 cm^{-1} and for the EMI-Im ionic liquid it occurs at 1056 cm^{-1}.

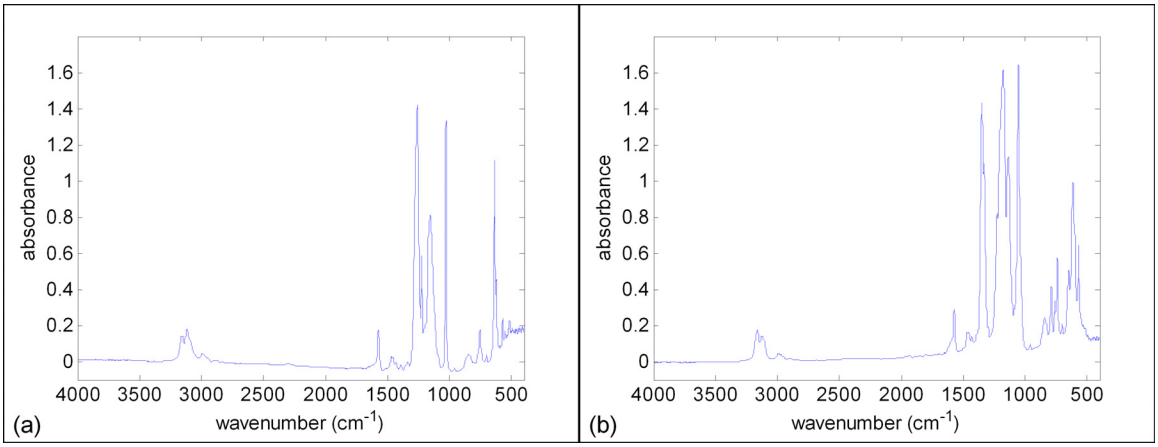

Figure 4.10: IR spectra of the neat (a) EMI-Tf and (b) EMI-Im ionic liquids.

In order to investigate the interactions between the ionic liquids and the Nafion^{TM} membrane, infrared spectra were collected for membranes that were exchanged with several different cations and swollen with various loadings of ionic liquid. This study focused on the peak at around 1060 cm^{-1} that is associated with the symmetric stretching vibration of the SO_3^- group of the polymer. As shown in Figure 4.11, this peak shifts to lower

wavenumbers as the content of ionic liquid within the membrane is increased. This result is for sodium ion exchanged membranes that were swollen with EMI-Tf ionic liquid. The peak on the right side of this figure corresponds to the symmetric stretching vibration of the sulfonate in the ionic liquid whereas the peak on the left corresponds to the sulfonate in the Nafion^{TM} membrane. As can be seen, the ionic liquid peak is absent in the spectrum of the dry membrane. For presentation purposes, the magnitude of these spectra were normalized using the magnitude of the peak at 982 cm^{-1}. This peak has most commonly been attributed to the symmetric stretch of the COC ether linkages in the sidechain (29; 57), but may also be associated with the backbone fluorocarbon chain (124; 80). The peak at 982 cm^{-1} was found to be unaffected by the introduction of ionic liquid into the membrane and was therefore used as a reference to scale the magnitudes of the spectra. The spectra have also been shifted vertically for clarity.

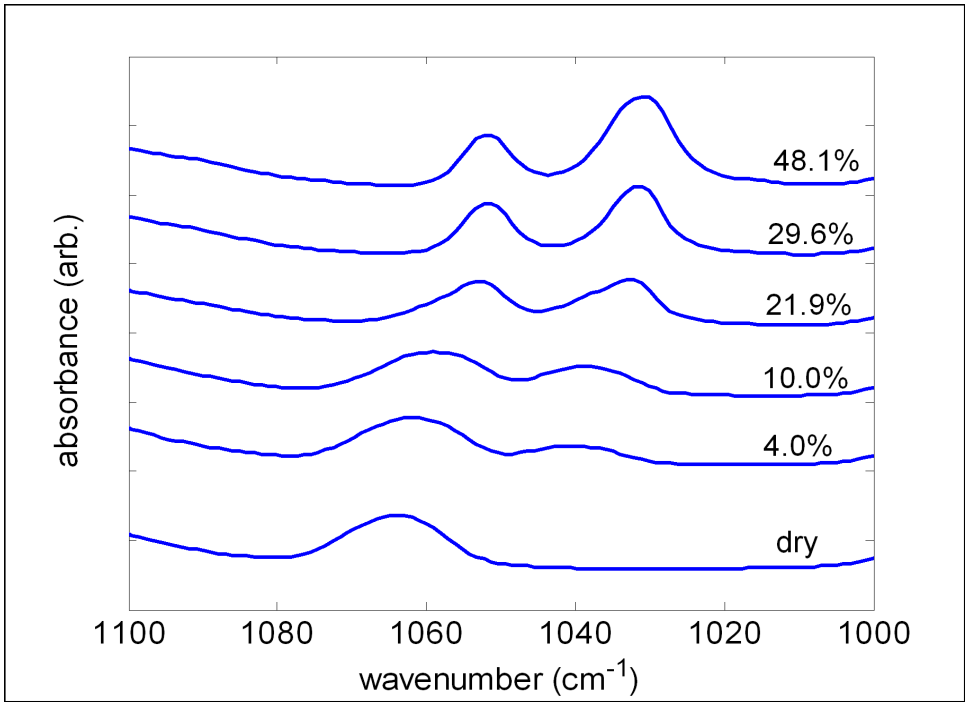

Figure 4.11: A portion of the IR spectrum for Nafion^{TM} membranes exchanged into the sodium ion form and swollen to the indicated levels with EMI-Tf ionic liquid. All loadings are reported as a percentage of the dry membrane volume.

From the measured IR spectra, the position of the sulfonate symmetric stretching peak was determined and plotted versus uptake of ionic liquid for the six cation forms of the membrane that were studied. This data is shown in Figure 4.12. As can be seen, for

most of the cations, the frequency decreases with increasing content of ionic liquid until a critical loading of ionic liquid above which the frequency remains constant. The shape of the curves are very similar to those observed by Lowry and Mauritz (see Figure 4.9). Above the critical loading of ionic liquid, the sulfonate symmetric stretching peak occurs at 1052 cm^{-1}. This is lower than the frequency of 1058 cm^{-1} that has been observed in water–swollen Nafion^{TM} membranes. Also, for the EMI^+ and TEA^+ ions, the frequency actually increases with increased loading of ionic liquid, more so for the TEA^+ ion. The smallest shift in frequency is observed for the EMI^+ ion.

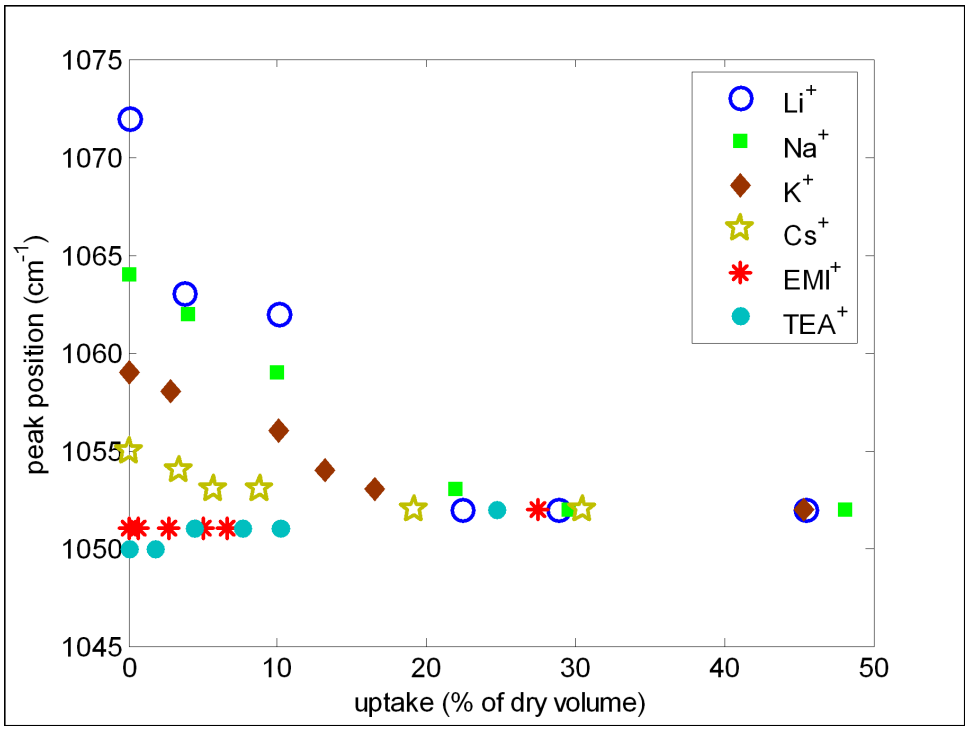

Figure 4.12: Position of the symmetric stretching peak of the sulfonate group in the Nafion^{TM} polymer for various loadings of EMI-Tf ionic liquid. The counterion form of the Nafion^{TM} membranes is indicated in the legend.

The reason for the shift in the symmetric stretching frequency of the sulfonate group upon introduction of ionic liquid into the membrane is the displacement of the counterion of the membrane away from the sulfonate site. This is accompanied by an association of the EMI^+ cation of the ionic liquid to the exchange site. Therefore, the cation of the ionic liquid replaces the counterion of the membrane in associating with the sulfonate group and displaces the counterion away from the exchange site. This situation is depicted in the left side of Figure 4.2. For the smaller lithium, sodium, and potassium ions this exchange

results in an increase in the size of the ion associated with the sulfonate. Due to the larger size of the EMI^+ ion, the electrostatic field in the vicinity of the exchange site is smaller, which leads to decreased polarization of the S–O dipole. This in turn leads to a decrease in the symmetric stretching vibrational frequency of the SO_3^- group. Because the TEA^+ ion is larger than the EMI^+ ion, the displacement of a TEA^+ ion away from a sulfonate site to be replaced by an EMI^+ ion actually results in an increase in the local electrostatic field created by the cation and an increase in the polarization of the S–O dipole. This is why the frequency of the SO_3^- group was observed to increase when the TEA–exchanged membranes were swollen with the EMI-Tf ionic liquid. It is also clear that the ionic liquid has a less polarizing effect on the sulfonate group than water, in that the observed vibration saturates to 1058 cm^{-1} for water–swollen membranes and to 1052 cm^{-1} for the membranes swollen with EMI-Tf. This is reasonable considering the large size of the EMI^+ cation and the fact that for the water–swollen membranes there are 2-4 water molecules associated with each sulfonate group (see Figure 4.9) and for the ionic liquid–swollen membranes, probably less than one EMI^+ ion per sulfonate group (see Figure 4.12). It is uncertain why the frequency is observed to increase for the EMI–exchanged membranes upon swelling with ionic liquid, but the increase is only 1 cm^{-1}, which is about the resolution of the wavenumber vector. Therefore, this discrepancy can likely be attributed to experimental uncertainty.

It is interesting to note that the symmetric stretching frequency of the sulfonate group does not change at high loadings of ionic liquid within the polymer. Also, the loading at which the peak position becomes constant decreases as the size of the counterion is increased. Similar behavior was observed by Lowry and Maurtiz for Nafion^{TM} membranes swollen with water (83). In order to illustrate this effect more clearly, the FTIR data was plotted versus the uptake of ionic liquid expressed in terms of the number of moles of ionic liquid per mole of exchange sites in the polymer—see Figure 4.13. This molar uptake was determined from

$$f = \frac{V}{\rho}\left(\frac{1100\text{g}}{\text{mole}}\right)\left(\frac{1.39\text{g}}{\text{cm}^3}\right)\left(\frac{\text{mole}}{260.23\text{g}}\right), \tag{4.8}$$

where f is the molar loading of ionic liquid, V is the uptake of ionic liquid in the polymer as a fraction of the dry volume, 1100 is the equivalent weight of the Nafion^{TM} membrane in grams (of dry polymer) per mole of exchange sites, ρ is the dry density of the membrane, 1.39 g/cm^3 is the density of the EMI-Tf ionic liquid, and 260.23 g/mole is the molecular weight of the EMI-Tf ionic liquid.

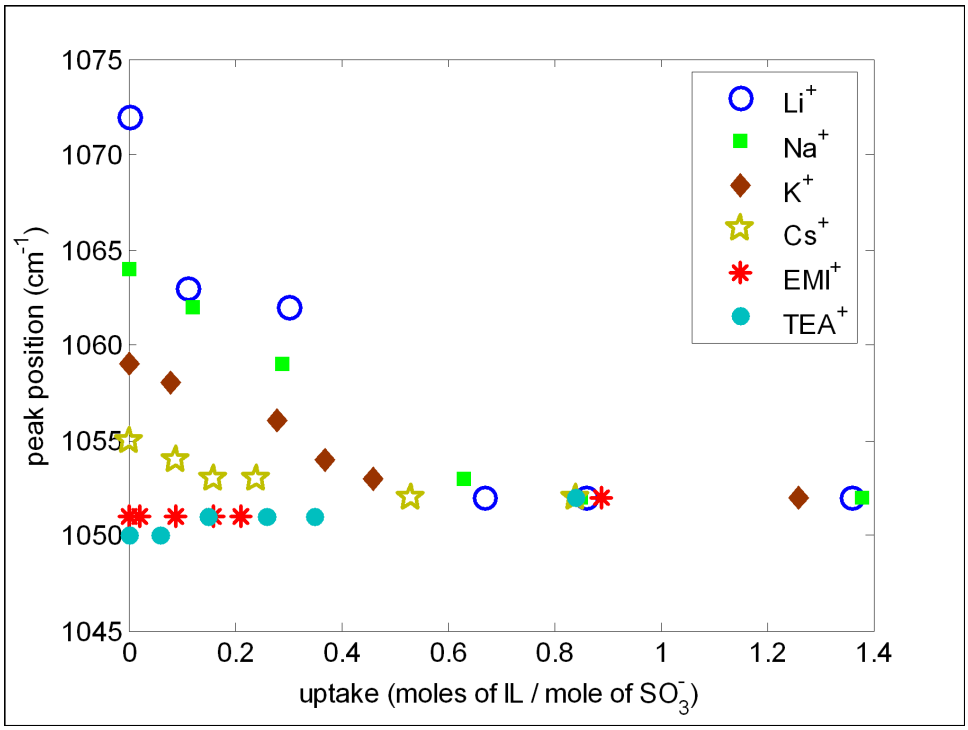

Figure 4.13: Position of the symmetric stretching peak of the sulfonate group in the Nafion™ polymer versus the loading of EMI-Tf ionic liquid, expressed as a molar ratio.

In order to estimate the critical uptake from the data presented in Figure 4.13, the symmetric sulfonate stretching frequency was assumed to exhibit a linear dependence on the molar loading of ionic liquid below the critical uptake. Based on this assumption, straight lines were fit to the first four data points for the lithium, sodium, and potassium form membranes. Because the data for the cesium–exchanged membranes only covers a range of 3 cm^{-1}, the first five data points were used in order to obtain a good fit for the cesium form samples. The slope (m) and y–intercept (b) obtained from these linear fits were then used to determine the critical uptake of ionic liquid from

$$f_{c,IR} = \frac{(1052 - b)}{m}, \tag{4.9}$$

where $f_{c,IR}$ is the critical uptake of EMI-Tf ionic liquid determined from the FTIR results and 1052 cm^{-1} is the saturation value of the symmetric sulfonate stretching peak above the critical uptake. Using this method, the critical uptake for the alkali metal ions was determined and is presented in Table 4.2. This method was also used to determine the critical uptake for the TEA form membranes. Because insufficient data was available, the critical uptake for the EMI form membranes could not be determined using this method.

Table 4.2: Critical uptake of EMI-Tf ionic liquid for Nafion^{TM} membranes in six different counterion forms as determined by FTIR.

cation	critical uptake (mol IL/mol SO_3^-)
Li^+	0.66
Na^+	0.69
K^+	0.56
Cs^+	0.48
EMI^+	0.45
TEA^+	0.44

However, from Figure 4.13, it was estimated to be 0.45 mol/mol. The critical uptake as it is defined in this document is the minimum loading of ionic liquid that is required to displace all of the counterions away from the sulfonate exchange sites. The observed trend of decreasing critical uptake with increasing size of the counterions is due to a decrease in the electrostatic binding energy between the counterions and the exchange sites as the size of the counterions is increased. Therefore, less ionic liquid is required to displace the larger counterions from the sulfonate sites. This trend was also observed by Lowry and Mauritz for water–swollen Nafion^{TM} membranes—see Figure 4.9.

The fact that the critical uptake occurs at a molar loading of ionic liquid that is below 1.0 for all of the counterion forms of the membrane could indicate that each EMI^+ ion can effectively shield the exchange sites from more than one counterion and would also seem to indicate that each EMI^+ ion is associated with more than one exchange site. This is perhaps surprising but may signify that the association of the counterion with the anion of the ionic liquid is more entropically favorable than its association with the exchange site of the Nafion^{TM} membrane. Alternatively, this could indicate that not all of the exchange sites are interacting with an ionic liquid cation. Some of the sulfonates may still be tightly bound to a counterion in the highly swollen membranes. It is possible that a portion of the exchange sites are inaccesible to the ionic liquid. However, this situation seems unlikely for the reason that if a significant portion of the exchange sites were inaccesible to the ionic liquid (31-56% based on the observed range of critical uptake of 0.44-0.69 mol/mol), then the position of the symmetric sulfonate stretching peak at high uptake levels would be related to the size of the counterion. This is found to not be the case, as the peak in all of the counterion forms of the membrane was located at 1052 cm^{-1}.

It is clear that the counterions do in fact associate with the anion of the ionic

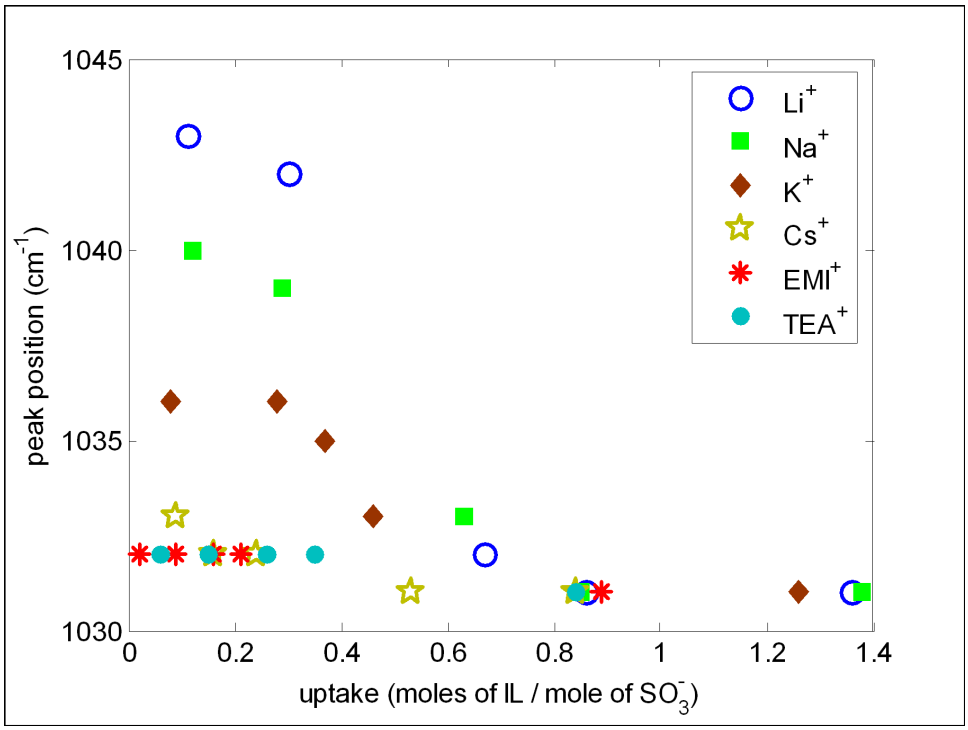

Figure 4.14: Symmetric stretching of the sulfonate peak in the trifluoromethanesulfonate anion of the EMI-Tf ionic liquid for a range of loadings in Nafion^{TM} membranes exchanged with various counterions.

liquid (as shown in Figure 4.2) by observing the change in the position of the sulfonate peak of the ionic liquid with increased loading. This is shown in Figure 4.14. As can be seen, the peak shifts to lower frequencies upon introduction of the ionic liquid into the membrane, much the same way that the peak associated with the symmetric stretching of the sulfonate in the Nafion^{TM} polymer shifted to lower frequencies. This can be explained as follows. When a small amount of ionic liquid is introduced into the membrane, the EMI^+ ions displace the counterions from the sulfonate exchange sites. This displacement causes the peak associated with the sulfonate exchange site to shift down in frequency slightly [1]. The shift in the sulfonate peak of the Nafion^{TM} polymer is slight at low loadings of ionic liquid because only a small portion of the sulfonate / counterion pairs are disrupted. However, each time a counterion (or more than one counterion) is displaced by an EMI^+ ion, the counterion(s) associates with the anion of the ionic liquid. At low loadings of ionic

[1]This is actually the superposition of two peaks, one associated with the sulfonate / counterion pairs (at 1064 cm^{-1}, for sodium) and one associated with the sulfonate / EMI^+ ion pairs (at 1052 cm^{-1}). As more ionic liquid is absorbed into the membrane, the magnitude of the first peak decreases and the magnitude of the second peak increases. This has the effect of shifting the observed composite peak towards 1052 cm^{-1}.

liquid, all of the EMI^+ ions are associated with the exchange sites. This means that all of the trifluoromethanesulfonate ("triflate") anions of the ionic liquid are associated with the counterions of the Nafion^{TM} polymer. For the smaller counterions (Li^+, Na^+, and K^+), the close proximity of the counterion to the triflate anion polarizes the S–O dipole of the anion. This results in an increase in the symmetric stretching frequency of the sulfonate as compared to the observed frequency for the neat ionic liquid of 1031 cm^{-1}. As can be seen from Figure 4.14, the vibrational frequency is related to the size of the counterion, with higher frequencies observed for the smaller counterions. This is because the polarization of the S—O dipole is increased by decreasing the size of the proximate cation.

As more ionic liquid is added to the membrane, the frequency of the triflate SO_3^- moves closer to the 1031 cm^{-1} value. As with the data shown in Figure 4.13, the symmetric sulfonate stretching frequency of the triflate anion saturates at the critical uptake of ionic liquid. This indicates that once a sufficient quantity of ionic liquid is introduced into the membrane to interact with all of the available exchange sites, the additional ionic liquid that is absorbed exists within the polymer in its native state. This is analagous to the idea of "free water" inside a water–swollen membrane. That is, water not involved in the hydration of the cations or the exchange sites but that exists in the membrane as liquid water. The critical uptake exhibited in Figure 4.14 matches well with the critical uptake determined from Figure 4.13 of about 0.66 mol/mol for the lithium–exchanged membranes, 0.69 mol/mol for the sodium–exchanged membranes, 0.56 mol/mol for the potassium–exchanged membranes, and 0.48 mol/mol for the cesium–exchanged membranes, 0.45 mol/mol for the EMI–exchanged membranes, and 0.44 mol/mol for the TEA–exchanged membranes. The relationship between critical uptake and counterion size indicates that the larger cations are more easily displaced from the sulfonate exchange sites, thus leading to a lower critical uptake.

The reason that the critical uptake is less than 1.0 mole of EMI-Tf ionic liquid per mole of exchange sites is unclear. It is interesting to note that for the TEA–exchanged membranes, the position of the sulfonate peak of the ionic liquid moves to higher wavenumbers as the content of ionic liquid within the membrane is reduced—see Figure 4.14. This is contrary to the expectation, as a smaller cation (EMI^+) is being replaced by a larger one (TEA^+). This should lead to a reduction in the polarization of the S–O dipole and a reduction in the SO_3^- vibrational frequency. This could be another indication that each ion

pair of the ionic liquid is associated with more than one counterion / exchange site pair of the Nafion^{TM} membrane. If more than one counterion is associated with each triflate anion, then the resulting increased polarization of the S–O dipole would lead to a higher than expected symmetric stretching frequency.

Although there is strong evidence for the claim that the ions of the ionic liquid do not associate with the ions of the Nafion^{TM} polymer in a 1:1 ratio, discrepancies do exist. Several factors could be responsible for the unusual observed behavior or, if considered more fully, could lead to alternate explanations of the data. First, peak shifts of 1-2 cm^{-1} while probably statistically significant could also be subject to experimental uncertainty. Second, the relative importance of the size of the assocating ions and the number of associating ions in affecting the polarization of the S–O dipole is unknown. Third, the effect that changes to its local environment have on the polarization of the EMI^{+} cation are unknown. This study only considered the polarization of the sulfonate anions. And finally, while the infrared spectroscopy study has elucidated the nature of the ion associations within the ionic liquid–swollen Nafion^{TM} membranes, conclusions cannot be drawn directly from this data concerning the arrangement of the ions. That is, the physical positioning of the ions in relation to each other is unknown.

In addition to the testing for the membranes swollen with the EMI-Tf ionic liquid, investigations were also performed using the EMI-Im ionic liquid. Unfortunately, the no reliable conclusions could be drawn from the data as the EMI-Im ionic liquid exhibited a peak in the IR spectrum at 1056 cm^{-1} that obscures the symmetric stretching peak of the sulfonate in the Nafion^{TM} polymer in the region around 1052-1065 cm^{-1}. A portion of the IR spectrum for sodium–exchanged membranes swollen with the EMI-Im ionic liquid is shown in Figure 4.15. As can be seen, the peak from the ionic liquid and the peak from the Nafion^{TM} membrane cannot be distinguished.

In summary, infrared spectroscopy is a useful tool for probing the ion associations in Nafion^{TM} membranes. For the current study, attenuated total reflectance (ATR) infrared spectroscopy was used to monitor the symmetric sulfonate stretching of the SO_3^- groups in both the Nafion^{TM} polymer and in the triflate anion of the EMI-Tf ionic liquid were observed over a range of loadings of ionic liquid and for membranes exchanged into different counterion forms. The observations match trends that have been reported in the literature. For the dry membranes, the vibrational frequency of the SO_3^- group of the polymer is found

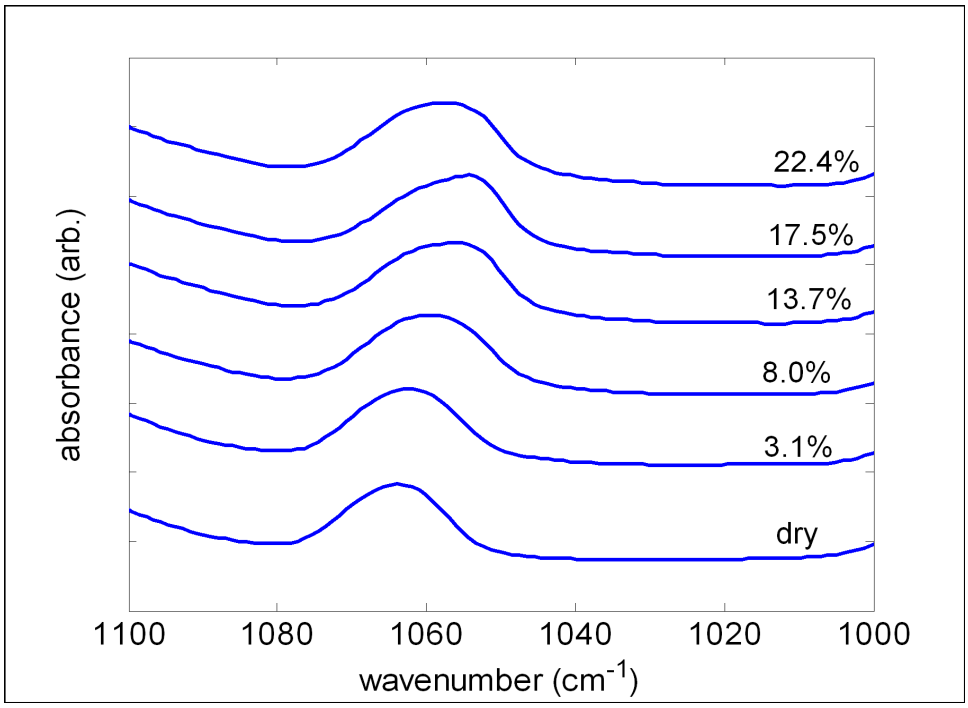

Figure 4.15: A portion of the IR spectrum for Nafion^{TM} membranes exchanged into the sodium ion form and swollen to the indicated levels with EMI-Im ionic liquid. All loadings are reported as a percentage of the dry membrane volume.

to increase with decreasing size of the counterion. This is due to increased polarization of the S—O dipole by smaller cations. Also, both frequencies are found to shift upon introduction of ionic liquid into the polymer. This shift is observed to be smallest for the membranes exchanged with the EMI^+ ion. These results reveal that the EMI^+ ion of the EMI-Tf ionic liquid displaces the counterion of the polymer from the sulfonate exchange site. The counterion of the polymer then associates with the triflate anion of the ionic liquid. In effect, upon introduction of the ionic liquid into the membrane, the two cations exchange roles. This is depicted on the left side Figure 4.2.

At high loadings of ionic liquid, the symmetric sulfonate stretching frequencies are not a function of the loading of ionic liquid or of the size of the counterion. The critical uptake at which the frequencies becomes constant is the minimum amount of ionic liquid required to displace all of the counterions from the sulfonate exchange sites in the polymer and is a function of the counterion size. As the size of the counterion is increased, the critical uptake is decreased. This is because the electrostatic energy binding the counterions to the exchange sites decreases as the size of the counterions is increased. The FTIR results reveal

that above the critical uptake, additional ionic liquid that is introduced into the membrane does not associate with the exchange sites or the counterions of the polymer.

For all of the counterion forms of the polymer, the critical uptake of EMI-Tf ionic liquid was found to be less than 1.0 mole of ionic liquid per mole of exchange sites. This supports the notion that the ions of the ionic liquid do not associate with the ions within the polymer in a ratio of 1:1 and that in fact, each EMI^+ ion may be associated with more than one sulfonate exchange site and each triflate anion may be associated with more than one counterion.

4.4 Nuclear Magnetic Resonance Spectroscopy

Nuclear magnetic resonance spectroscopy (NMR) is a useful tool for probing the local electronic environment of individual nuclei. Alkali metal NMR can be used to make determinations about the immediate chemical environment of alkali metal ions in aqueous and non-aqueous solvents (106). Komoroski and Mauritz have performed alkali metal NMR studies on Nafion^{TM} membranes over a range of hydration levels and have identified distinct trends in the results (71; 70). They attribute these trends to the increasing mobility of the counterions of the Nafion^{TM} membrane with increasing water content. NMR spectroscopy was used in the current study to investigate the local electronic environment and mobility of the alkali metal ions $^7Li^+$, $^{23}Na^+$, and $^{133}Cs^+$ in Nafion^{TM} membranes swollen to various levels with EMI-Tf and EMI-Im ionic liquid. This data was used to gain insight into the effect of the ionic liquids on the mobility of the counterions and to draw conclusions about the relative importance of the counterions and the ions of the ionic liquid in the electromechanical transduction mechanisms.

4.4.1 Testing Protocol

NMR spectroscopy is an investigation of the relaxation processes that occur within a specific nucleus when excited by electromagnetic radiation. It differs from infrared spectroscopy in that it is performing measurements of relaxation instead of absorption or transmission and in that it is a probe of the local environment of nuclei, not chemical bonds. Because of the nature of the NMR technique, it is more difficult to make analogies to classical mechanics. However, an attempt will be made here to introduce the reader to the basic concepts

(67; 11; 17; 42; 58).

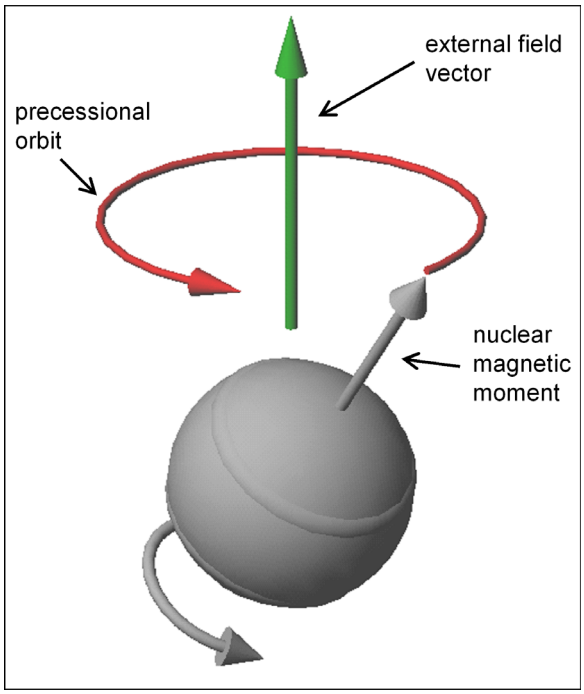

Figure 4.16: Illustration of the precessional motion of a nucleus in a magnetic field.

Protons, neutrons, and electrons can be imagined as spinning on their axes. In some atoms, the spins of the particles cancel each other out and the nucleus has no net spin. However, in atoms where the number of neutrons plus the number of protons is odd, or where the number of protons and the number of neutrons is odd, the nucleus posseses a net spin. The net spin of a nucleus can be found by

$$I = \frac{p+n}{2}, \tag{4.10}$$

where I is the net spin, p is the number of unpaired protons in the nucleus, and n is the number of unpaired neutrons in the nucleus. The spin can be thought of as the angular momentum of the spinning nucleus. In the presence of a magnetic field the spin of a nucleus is quantized and the number of possible spin states can be found from

$$(2I+1). \tag{4.11}$$

For the current discussion, nuclei with spin-1/2 will be considered. From equation 4.11 it is clear that a spin-1/2 nucleus will have two spin states. If the direction of the magnetic field is chosen to be in the $+z$ direction, then these two spin states are up and

down. That is, the spin vector can either be aligned with the magnetic field vector (as shown in Figure 4.16), or against it. Although the magnetic field is attempting to align the nucleus completely with the field vector, this does not correspond to either of the stable spin states for the nucleus. Instead, the nucleus rotates on its own axis and precesses about the axis of the magnetic field vector—see Figure 4.16. The nucleus is acted on by a magnetic moment that is proportional to its spin and its gyromagnetic ratio

$$\mu = \gamma I, \tag{4.12}$$

the gyromagnetic ratio (γ) being an isotope–specific constant of proportionality. The z-component of the spin (I_z) is

$$I_z = \frac{m_z h}{2\pi}, \tag{4.13}$$

where m_z is the quantum number describing the two spin states (for spin-1/2 nuclei, m_z=$\pm$1/2), and h is Planck's constant (h=6.626(10)$^{-34}$ J·s). The interaction energy between the nucleus and the external magnetic field is then

$$E = \mu_z B_0, \tag{4.14}$$

where B_0 is the magnitude of the applied static magnetic field and μ_z is the z-component of the magnetic moment

$$\mu_z = \gamma I_z, \tag{4.15}$$

$$\mu_z = \frac{\gamma m_z h}{2\pi} \tag{4.16}$$

Because the spin is quantized into two states (m_z=$\pm$1/2), the energy of the two states can be found from equations 4.14 and 4.16 as

$$E_{1/2} = \frac{1/2\gamma h B_0}{2\pi}, \tag{4.17}$$

$$E_{-1/2} = \frac{-1/2\gamma h B_0}{2\pi}. \tag{4.18}$$

The energy difference between the two states is then

$$E_{1/2} - E_{-1/2} = \Delta E = \frac{\gamma h B_0}{2\pi}. \tag{4.19}$$

This energy can be related to a frequency by considering that the energy of a photon of electromagnetic radiation is related to Planck's constant by

$$E = h\nu, \tag{4.20}$$

where ν is the frequency of the photon in Hertz. Therefore, because the nuclei of interest can only exist in two spin states, they can only absorb energy at a frequency equal to

$$\nu = \frac{\gamma B_0}{2\pi}. \tag{4.21}$$

This frequency is called the Larmor frequency and it is the frequency at which the spin vector of the nuclei are precessing about the axis of the magnetic field vector. As can be seen from equation 4.21, the Larmor frequency is only a function of the gyromagnetic ratio and the strength of the static magnetic field *at the nucleus*.

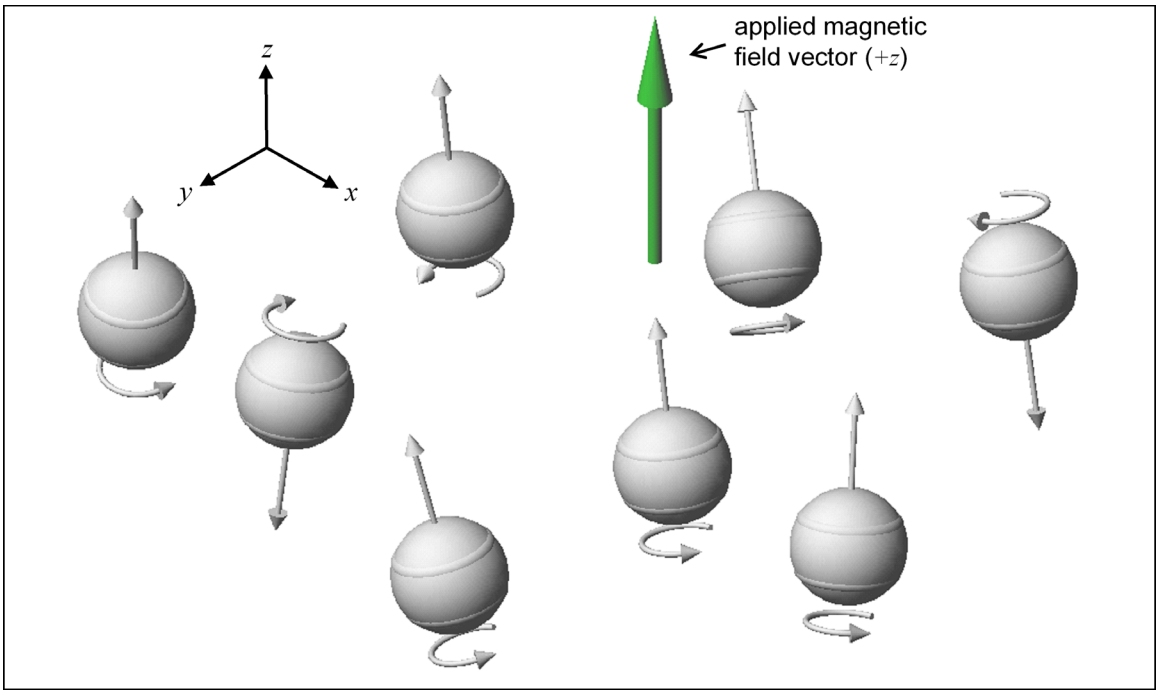

Figure 4.17: The application of a static magnetic field generates a net magnetization within a material.

In the absence of an external magnetic field, the spins of the nuclei in a sample average such that the sample contains no net magnetization. However, when a static field is applied, the spins can assume one of two states, up (aligned with the field) or down (aligned against the field). Because the up spin state is of slightly lower energy, there is a small surplus of nuclei with up spin. This small excess gives rise to a net magnetization in the sample in the $+z$ direction—see Figure 4.17. Although the individual spin vectors of the nuclei possess x- and y-components of their spin, there is no net magnetization of the sample in the x-y plane. This is because there is a large number of nuclei in the sample and each one is precessing with a different phase relative to the external coordinate system. The

method of NMR spectroscopy is to induce some net arrangement to the nuclei of a sample and then observe the mechanisms by which that order decays. The first step is to induce a net z magnetization into the sample using a static magnetic field.

In addition to the static magnet that applies a field in the z-direction, NMR spectrometers also contain an electromagnetic coil that induces a transverse magnetization to the sample. This induced transverse magnetization is generated by the B_1 field. The B_1 field signal is composed of the convolution of sine wave at the Larmor frequency and a pulse. The interaction of the B_1 field with the B_0 field effectively induces a torque on the net magnetization of the sample. The purpose of the B_1 field is to rotate the net magnetization of the sample 90° into the x-y plane. The pulse duration τ required to rotate the magnetization through an angle of β is

$$\beta = \gamma B_1 \tau. \tag{4.22}$$

The rotation of the magnetization occurs by two mechanisms. First, because the B_1 pulse is at the Larmor frequency of the nuclei of interest in the sample, it can cause the spin of some of the nuclei to flip from one state to another until the z-component of the magnetization vector goes to zero. Second, the pulse causes the phases of the precessing nuclei to become correlated. That is, the nuclei are all precessing with the same phase with respect to the exteral coordinate system. Therefore, the sample contains a net magnetization in the x-y plane that is rotating around the z axis at the Larmor frequency. After the pulse is removed from the sample, the relaxation of the nuclei within the sample back to their equilibrium state is observed by the spectrometer.

The B_1 coil that is used to create the *rf* pulse is also used to measure the relaxation of the sample magnetization (in the x-y plane) after the pulse is removed. This relaxation is typically thought of as consisting of two parts. The spin–lattice relaxation time (T_1) is related to the lifetime of a nucleus that has been excited to its higher energy spin state by the *rf* field. This relaxation time is associated with a rate constant, R_1 ($=1/T_1$) and is related to the transfer of energy from the nucleus to the sample around it. In solids where mobilities are low, the transfer of energy from the excited nucleus to the sample can be small and T_1 relaxation times can be very long (67). Macroscopically, the spin–lattice relaxation is associated with the return of the longitudinal magnetization (in the $+z$ direction) to its equilibrium value. The spin–spin relaxation time T_2 is associated with the relaxation of

the phase correlation of the nuclei. This dephasing of the sample leads to a decrease of the transverse magnetization. One mechanism by which this dephasing occurs is related to the interactions between neighboring nuclei that have the same precessional frequency but different quantum states. In this situation, the two nuclei can swap spin states. This transfer of energy will not affect T_1 because the net population of nuclei in the higher and lower energy states has not changed but the average lifetime of a nucleus in the higher energy state will be decreased. In a real sample, both T_1 and T_2 relaxation processes occur simultaneously. However, T_2 is always less than or equal to T_1. That is, relaxation of the transverse magnetization always occurs more rapidly than relaxation of the longitudinal magnetization.

Immediately after the pulse is removed from the sample, there exists a net magnetization in the x-y plane. The spectrometer then monitors the decay of that magnetization in the time domain. The measured time domain signal is called a free induction decay (FID). Typically, NMR data is presented as a Fourier transform of the FID. The typical format for data presentation is a spectrum of signal amplitude versus frequency. The frequency in this case is called the "chemical shift". The chemical shift is given the symbol δ and is represented as parts–per–million (ppm). The reason for referring to the resonant frequency of a nucleus in this way is that the frequency is dependent on the magnitude of the static magnetic field generated by the spectrometer. Therefore, by reporting the chemical shift of a nucleus, or the change in frequency relative to an accepted standard, comparison of results between different groups is possible. The chemical shift of a nucleus is related to a reference frequency by

$$\delta = \frac{(\nu - \nu_{ref}) * 10^6}{\nu_{ref}}, \tag{4.23}$$

where ν is the measured frequency and ν_{ref} is the frequency of the reference standard. The chemical shift of a particular nucleus is related to its local chemical environment. As shown in equation 4.21, the precessional frequency of a nucleus is related to the field strength at the nucleus, which is related to the strength of the applied static field. The strength of the magnetic field at the nucleus is also related to the local environment of the nucleus. For instance, the circulation of electrons around a nucleus will generate a small magnetic field that opposes the external field. This will shield the nucleus from the external field and decrease its precessional frequency. Therefore, in general, if the electron density near a nucleus is larger, the precessional frequency of the nucleus will be lower. In some molecules,

such as benzene, the particular structure of the molecule actually enhances the effect of the external field. This is called desheilding.

In addition to the chemical shift, an NMR spectrum can also reveal important information related to the relaxation processes that are occuring within a sample. In samples that exhibit solution–like behavior, mobilities can be high and T_1 processes can dominate the relaxation. However, as mentioned before, T_2 cannot be less than T_1. Therefore, when T_1 relaxation is fast, T_2 tracks T_1 (this is called the motional narrowing limit). From standard NMR aquisition processes utilizing a 90° pulse, T_2 is related to the width of the pulse by

$$\Delta\nu = \frac{1}{\pi T_2}, \tag{4.24}$$

where $\Delta\nu$ is the width of the peak at half of its height (in Hz). Therefore, increased peak width in the NMR spectrum is indicative of faster relaxation processes in the sample.

For the current study, alkali metal NMR was performed on samples of Nafion^{TM}-117 membranes that were exchanged into the lithium, sodium or cesium counterion form and swollen to various levels with EMI-Tf and EMI-Im ionic liquid. The purpose of these experiments was to evaluate the mobility of the Li^+, Na^+, and Cs^+ ions within the membranes as a function of the uptake of ionic liquid and relate this mobility to the properties of the ionic liquid. The membrane samples were prepared using the procedure described in Section 4.2, whereby a 5 cm X 10 cm sample was pretreated, ion exchanged, dried, and swollen with ionic liquid. The samples were then cut into strips approximately 0.5 cm X 5 cm. The strips were stacked on top of each other and the stack was inserted into a 10 mm NMR tube, which was backfilled with dry nitrogen and capped. For the ^{7}Li and ^{133}Cs work, glass tubes were used. For the ^{23}Na work, Teflon^{TM} tubes were used to prevent signal interference from the sodium present in the glass. The samples were then characterized using the Varian Unity 400 spectrometer in the NMR laboratory at Virginia Tech. The field strength of the spectrometer is 9.39 T and the relevant parameters of the testing used for each isotope are listed in Table 4.3. The acquisition time is the length of time that data is recorded after each pulse. The relaxation delay is a dwell after the completion of data collection and prior to the start of the next pulse.

The NMR acquisition involved 200-500 collected scans were for each sample. The large number of scans helps to improve the signal-to-noise ratio. The program NUTS (Acorn NMR Inc.) was used to process the data. The signal-to-noise ratio was also improved by

Table 4.3: Properties of the three nuclei studied.

isotope	spin	Larmor frequency (MHz)	90° pulse width (μs)	number of scans	acquisition time (s)	relaxation delay (s)
^{7}Li	3/2	155.429	23	200	0.2	1.0
^{23}Na	3/2	105.795	20	500	0.5	0.1
^{133}Cs	7/2	52.462	35	200	0.5	0.2

multiplying the FID by a decaying exponential function prior to the Fourier transform. This has the effect of decreasing the amplitude of the FID at long times, when the sample magnetization has decayed substantially and the measured signal consists primarily of noise. This also decreases the apparent relaxation time of the sample and so broadens the observed peak in the NMR spectrum. The data was corrected by substracting the additional peak width that was introduced by the exponential function from the measured peak width. The frequency width associated with the exponential function varied from 50 Hz to 500 Hz, with larger values being used for the data exhibiting larger $\Delta\nu$. After the FID was modified in this way, it was Fourier transformed and a plot of NMR amplitude versus chemical shift was generated. The chemical shift was plotted relative to the measured chemical shift of a 0.1 M aqueous solution of the chloride salt of the nucleus of interest. From the NMR spectrum, the chemical shift and peak width at half height (PWHH) were obtained for the particular sample. These were then plotted versus the uptake of ionic liquid for both the EMI-Tf and EMI-Im ionic liquids.

4.4.2 Results

The motivation for this study was derived from similar studies that have been performed by Komorosi and Mauritz on water–swollen Nafion^{TM} polymer exchanged into alkali metal forms (70; 71). They have found that as the water content of the polymer is increased, $\Delta\nu$ decreases significantly and the chemical shift (δ) moves closer to zero (relative to a 0.1 M aqueous chloride salt solution). The change in the chemical shift for varying water content is shown in Figure 4.18. As can be seen, the chemical shift of the samples at high water content is very close to that of the sodium nuclei in 0.1 M NaCl solution. This indicates that at high water contents, the local chemical environment of the sodium ions in the Nafion^{TM} polymer is very similar to that of the ions in dilute solution. That is, the local chemical environment of the sodium ions is dominated by the effects of the water in

the ion's hydration shell. This water has a dramatic shielding effect on the chemical shift of the sodium ion. As the water is removed, the sodium ion is less shielded and its chemical shift moves upfield (becomes more negative). Although this loss of water is accompanied by the formation of contact pairs of Na^+ and SO_3^- ions, Komoroski and Maurtiz report that the sulfonate groups of Nafion^{TM} are poor electron donors (70). Therefore, the proximate sulfonates are not able to effectively shield the sodium ions and make up for the deshielding effect of dehydration. The NMR work of Komoroski and Mauritz coupled with the infrared spectroscopy studies of Lowry and Mauritz provides strong evidence for the formation of contact ion pairs in dry Nafion^{TM} and the separation of those ion pairs on swelling of the polymer with water.

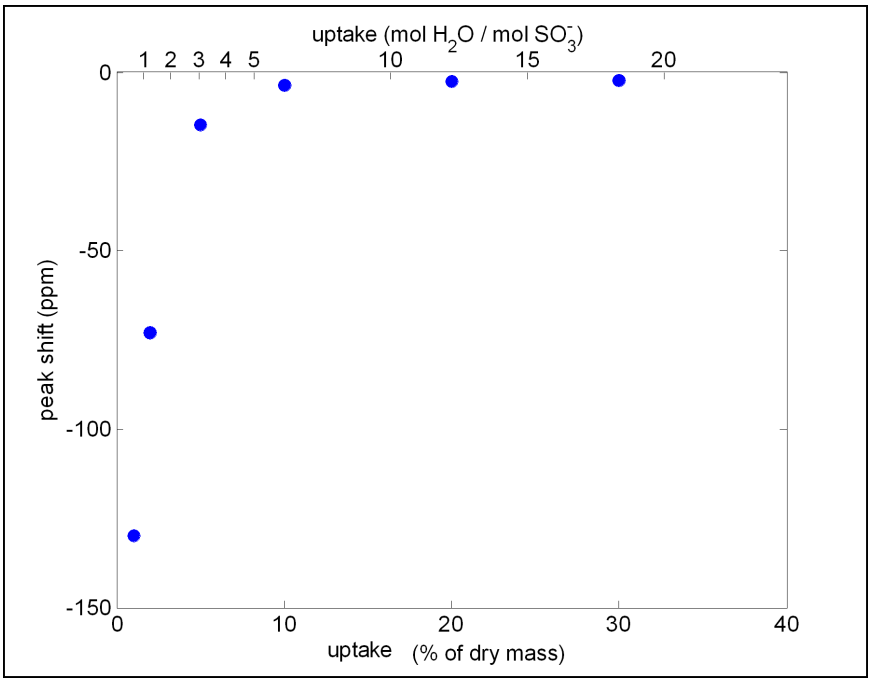

Figure 4.18: ^{23}Na chemical shift of Na–exchanged Nafion^{TM} membrane at different water contents. Chemical shifts are relative to 0.1 M NaCl. The data is from reference (70).

Komoroski and Mauritz have also measured the peak width of the sodium NMR line as a function of water content—see Figure 4.19. As indicated in equation 4.24, the peak width is related to the speed at which the transverse magnetization of the sample relaxes. There are numerous mechanisms by which magnetization in a sample can relax, including spin–rotation coupling, dipole–dipole coupling, sheilding anisotropy, and scalar coupling (67). However, for nuclei that possess spins greater than 1/2, relaxation by nuclear

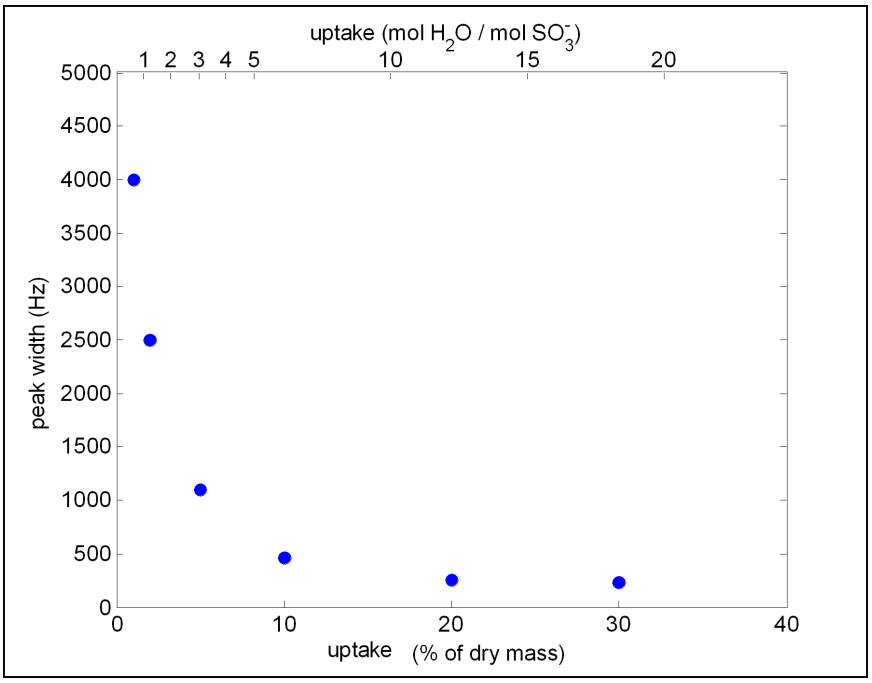

Figure 4.19: ^{23}Na peak width at half height of Na–exchanged Nafion^{TM} membrane at different water contents. The data is from reference (70).

quadrupolar coupling is often several orders of magnitude faster than any other mechanism (67). Nuclei with spin greater than 1/2 will couple with an electric field gradient in the vicinity of the nucleus; this coupling is very effective at transferring energy away from the nucleus. The property that describes the strength of this coupling for a given isotope is the nuclear electric quadrupole moment, Q. This property has units of length squared and its common dimension is 10^{-28} m^2, also called the *barn*. The Q values of the three nuclei studied in this work are listed in Table 4.4. Kidd describes the ^{7}Li and ^{133}Cs nuclei as "low-Q" whereas the ^{23}Na nucleus is thought of as "medium-Q" (67). For medium-Q nuclei, relaxation in any real sample is dominated by quadrupolar coupling, but the spectral lines are still narrow enough to be observed. Low-Q nuclei produce more narrow lines and for moderate or low electric field gradients, relaxation mechanisms other that quadrupolar coupling may be present. High-Q nuclei produce peaks that are often too broad to be observed, even in highly symmetric environments.

The broadening observed in sodium–exchanged Nafion^{TM} upon dehydration is due to the increased rate of relaxation of the magnetization in the sample, caused by quadrupolar coupling of the sodium nuclei to local electric field gradients within the polymer. The strength of this relaxation mechanism is related to the electric quadrupole moment of the

Table 4.4: Nuclear electric quadrupole moment for the three nuclei studied. From reference (67).

isotope	Q (10^{-28} m^2)
^{7}Li	-0.03
^{23}Na	0.15
^{133}Cs	-0.003

nucleus, the electric field gradient in the vicinity of the nucleus, and the mobility of the molecule. In a Nafion^{TM} membrane, the electric field gradient at the sodium nucleus increases as the sodium ions move closer to the sulfonate exchange sites. However, Komoroski and Mauritz reported on the NMR spectra of a model salt of the sodium form of Nafion^{TM}, sodium trifluoromethanesulfonate (CF_3SO_3Na). For an aqueous 4.5 M solution of this salt, the peak width was found to be 33 Hz (70). This concentration corresponds to a water to sulfonate ratio of approximately 8; for the Nafion^{TM} polymer at this ratio the peak width was observed to be about 400 Hz. This could indicate that the electronic environment of the model salt solution is more symmetric than that of the membrane, which is probably true. However, this also indicates that the sodium ions in the salt solution are far more mobile than the sodium ions in the polymer and that the relaxation by quadrupolar coupling is strongly influenced by this mobility.

As can be seen from Figure 4.19, the measured NMR peak width saturates at a swelling level of about 3-4 water molecules per exchange site. This is in good agreement with the FTIR measurements of Lowry and Mauritz, in which the position of the symmetric sulfonate stretching peak was found to saturate at a swelling level of about 3-4 water molecules per sulfonate for sodium form membranes (see Figure 4.9). This indicates that 3-4 water molecules per sulfonate are required to displace the sodium counterions from the exchange sites and that above this uptake, additional water exists within the membrane in an unbound "free" state.

In NMR spectroscopy, the parameter describing the mobility of the molecules under study is called the rotational correlation time and is related to the speed at which molecules freely tumble within a sample of material. This is the speed of the molecular rotation, whereas the discussion up to this point has been focused on the speed of nuclear rotation. The relaxation of the magnetization in Nafion^{TM} membranes exchanged with alkali metal ions occurs by quadupolar coupling with local electric field gradients. How-

ever, this quadrupolar coupling mechanism is related not only to the magnitude of the field gradient and the electric quadrupolar moment (Q), but also to the rotational correlation time (67; 31). That is, as the rotational correlation time is increased, the strength of the quadrupolar coupling of the nuclei to the local electric field is increased and the relaxation time is decreased. Because the relaxation time is inversely related to the peak width, this is analagous to saying that as the rotational speed of the molecules decreases, the width of the observed peak increases. *Therefore, the peak width is related to the mobility of the molecules.* Common factors affecting the rotational speed of the molecules within a sample are temperature, viscosity, and molecular size. That is, molecules rotate more slowly as the temperature is decreased and as the viscosity and molecular size is increased. The damping effect of increasing molecular size can be thought of as a viscous force. Komoroski and Mauritz have in fact observed that the ^{23}Na peak width of Nafion^{TM} swollen with 5% water (by weight) decreased by almost half (from 1100 Hz to 600 Hz) when the temperature was increased from 30°C to 90°C. This is due to a decrease in the rotational correlation time (increased mobility of the ions) with increasing temperature.

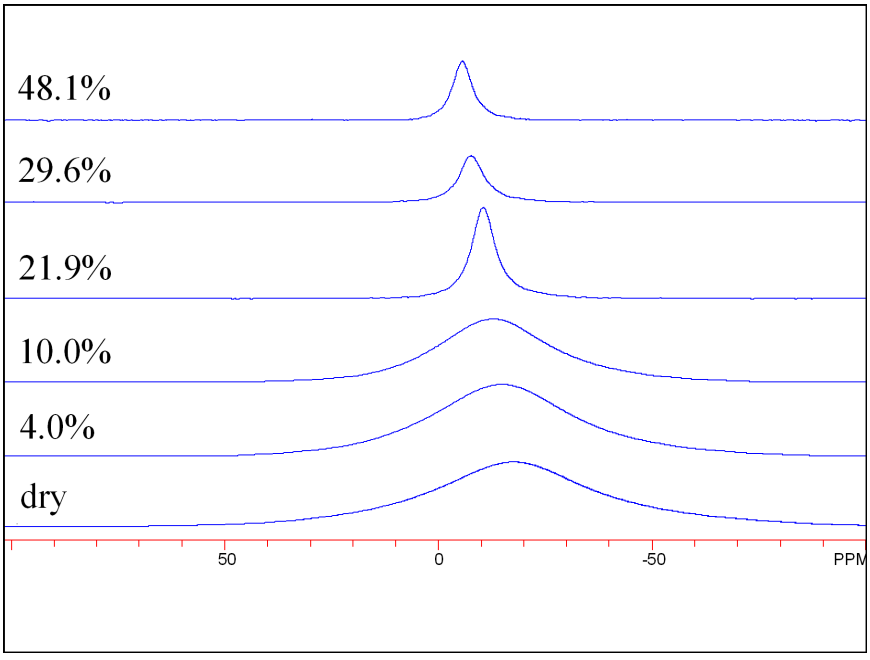

Figure 4.20: ^{23}Na NMR spectra for Nafion^{TM} membranes in the sodium form and swollen to the indicated level with EMI-Tf ionic liquid. All uptake values are as a percentage of the dry volume.

In the current work, nuclear magnetic resonance spectroscopy investigations have

been carried out on Nafion^{TM} membranes exchanged into the lithium, sodium, and cesium forms and swollen with EMI-Tf or EMI-Im ionic liquid. The spectra obtained for a series of sodium–exchanged membranes swollen to various extents with EMI-Tf are shown in Figure 4.20. As can be seen, the spectra exhibit a single peak that decreases in width and shifts downfield as the content of ionic liquid within the membrane is increased. This experiment was also performed for membranes swollen with the EMI-Im ionic liquid and the measured peak widths versus uptake for both ionic liquids are shown in Figure 4.21. The molar loading of both ionic liquids were determined using equation 4.8; for the EMI-Im ionic liquid, its properties (ρ=1.52 g/cm^3, MW=331.25 g/mole) were used in place of the properties of the EMI-Tf ionic liquid. As can be seen from Figure 4.21, the shape of the curve for the EMI-Tf ionic liquid is very similar to the data measured by Komoroski and Mauritz (see Figure 4.19). The magnitude of the peak width at low uptake of ionic liquid is also in good agreement with their results. The peak width for the dry membrane is measured to be about 4000 Hz; this decreases to 525 Hz for the highly swollen membranes. By the argument presented above, this decrease in the peak width is indicative of an increase in the mobility of the sodium ions as the content of ionic liquid within the membrane is increased.

The increased mobility of the counterions is due to their displacement from the exchange sites by the EMI$^+$ cations of the EMI-Tf ionic liquid. As the content of ionic liquid within the membrane is increased, more and more of the counterions are displaced from the exchange sites and associated with the trifluoromethanesulfonate anions of the EMI-Tf ionic liquid. The mobility of the counterions is expected to increase by this exchange because the triflate anions are relatively more mobile than the fixed sulfonate exchange sites, which are bound to the polymer backbone. As with the FTIR results, the NMR data also exhibits a critical uptake of ionic liquid above which the observed behavior changes. As can be seen from Figure 4.21, above the critical uptake, the mobility of the counterions saturates. This indicates that all of the counterions have been displaced from the exchange sites and that additional absorbed ionic liquid above the critical uptake does not associate with the counterions or the exchange sites. The same method used to determine the critical uptake from the FTIR was used to determine the critical uptake from the NMR results. That is, a straight line was fit to the first four data points in Figure 4.21. The slope (m) and y–intercept (b) obtained from this linear fit were then used to determine the critical uptake

from

$$f_{c,NMR} = \frac{(\Delta\nu_s - b)}{m}, \tag{4.25}$$

where $f_{c,NMR}$ is the critical uptake determined from the NMR results and $\Delta\nu_s$ is the saturation peak width above the critical uptake. Using this method, the critical uptake for EMI-Tf ionic liquid in a sodium–exchanged membrane was determined from the ^{23}Na NMR study to be 0.65 mol/mol. This is in good agreement with the value of 0.69 mol/mol that was determined from the FTIR analysis.

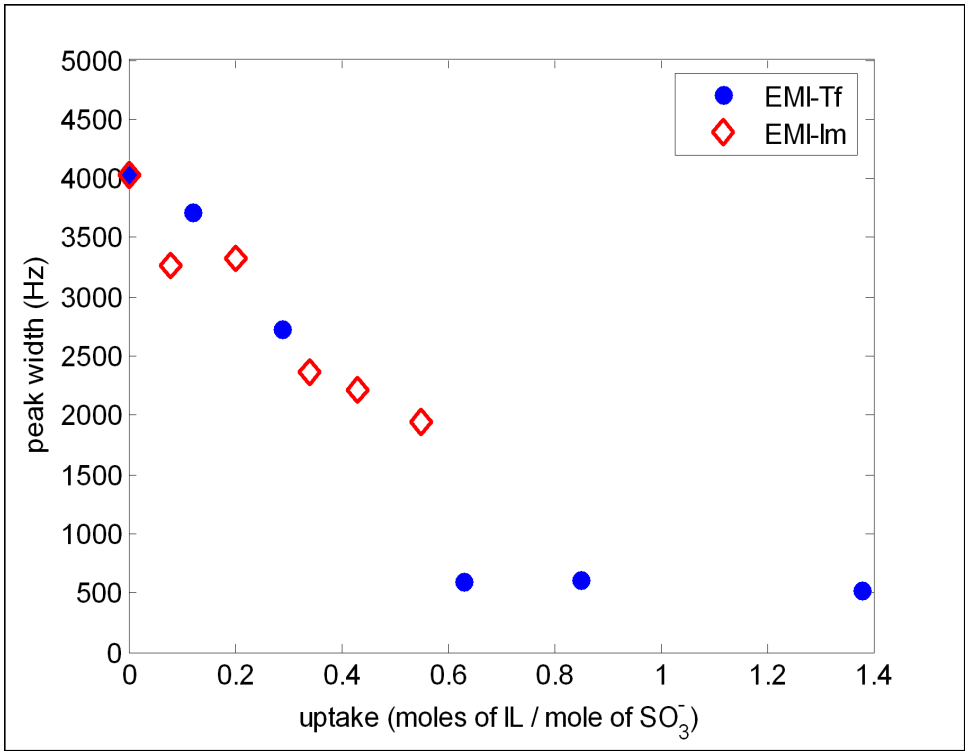

Figure 4.21: ^{23}Na NMR peak width at half height for sodium–exchanged Nafion^{TM} membranes swollen to various levels with EMI-Tf and EMI-Im ionic liquid.

In comparison to the results of Komoroski and Mauritz, the peak width above the critical uptake is larger for the membranes swollen with EMI-Tf ionic liquid (525 Hz) than for those swollen with water (230 Hz) (70). This indicates that the sodium ions in a water–swollen membrane are more mobile than in an ionic liquid–swollen membrane. Although several factors could be used to explain this difference, the most obvious is the higher viscosity of the EMI-Tf ionic liquid (45 cP) as compared to water (1 cP). Although the uptake values for the EMI-Im ionic liquid do not cover the same range as the EMI-Tf ionic

liquid, it is apparent from the data that the mobility of the sodium ions in the EMI-Im–swollen membranes is inferior to that in the EMI-Tf–swollen membranes. Considering that the viscosity of the EMI-Im ionic liquid is actually *lower* than that of the EMI-Tf ionic liquid, this is most likely due to the disruption of the clustered morphology by the EMI-Im ionic liquid, which was discussed in Chapter 3. This disruption causes a partial mixing of the conductive and non–conductive phases of the polymer, which hinders the ion mobility. Also, the critical uptake is not observed for the membranes swollen with EMI-Im ionic liquid, likely due to the limited range of swelling for that ionic liquid.

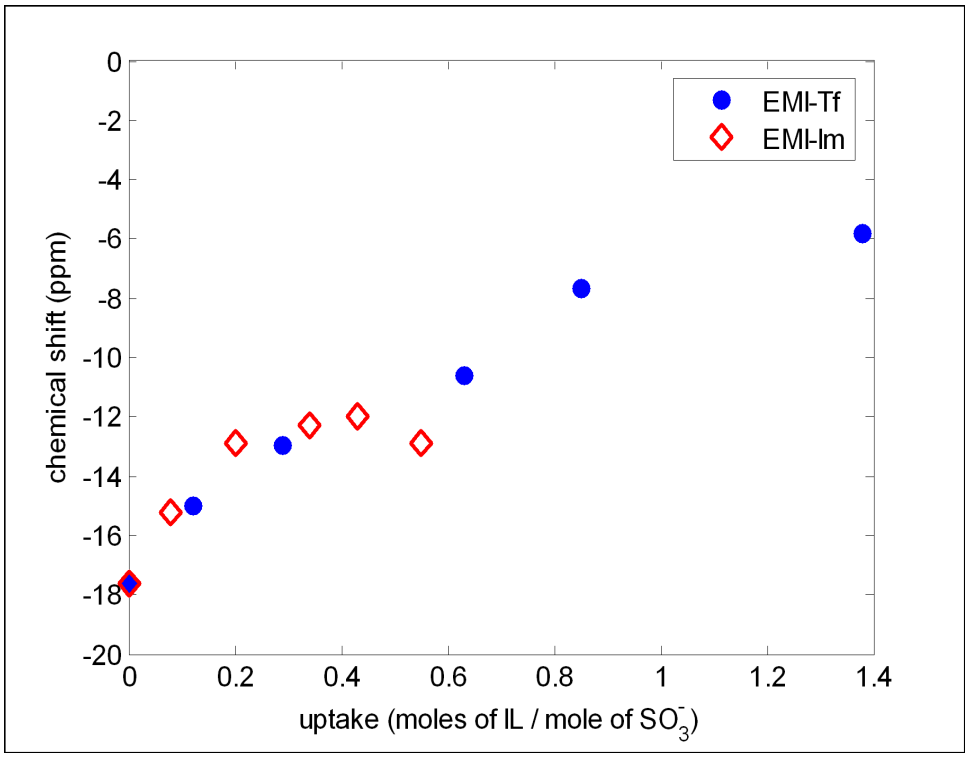

Figure 4.22: ^{23}Na NMR peak width at half height for sodium–exchanged Nafion^{TM} membranes swollen to various levels with EMI-Tf and EMI-Im ionic liquid.

In addition to the peak width, the ^{23}Na chemical shift of the membranes swollen with ionic liquid was also measured—see Figure 4.22. As can be seen, the chemical shift does move closer to zero (with respect to 0.1 M NaCl) as the content of ionic liquid within the membrane is increased. However, the range of the chemical shift is distinctly different from that observed by Komoroski and Mauritz, even for the dry polymer. Whereas they observed a chemical shift of about -130 ppm at low swelling levels, the current study measured that

value to be closer to -18 ppm. In general, a downfield shift is indicative of increased sheilding of a nucleus. For the water–swollen polymer, this can be explained as shielding of the ion by water entering its hydration shell. The origin of this shift in the ionic liquid–swollen materials is unclear. It has been claimed that the counterions are displaced from the sulfonate sites by the ionic liquid and associated with the anions of the ionic liquid. However, the $CF_3SO_3^-$ anions of the EMI-Tf ionic liquid should have no more shielding effect on the sodium nuclei than the sulfonate sites of the polymer. In general, the measurement of the peak width will be of more importance for the current study. The peak width can be related to the mobility of the counterions whereas the chemical shift is affected by too many unknown parameters to be useful in forming conclusions regarding ion motion within ionic liquid–swollen Nafion^{TM} membranes.

In addition to sodium, NMR investigations were also performed on lithium– and cesium–exchanged membranes. The spectra for the lithium exchanged membranes swollen with EMI-Tf ionic liquid are shown in Figure 4.23. Peak widths versus uptake for both the EMI-Tf and EMI-Im ionic liquids are shown in Figure 4.24. As can be seen, the peak widths for both ionic liquids decrease with increasing content of ionic liquid up to the critical uptake, at which point the peak widths become relatively constant. The source of the small increase in the peak width at low swelling is unknown, but could be due to mishandling of the samples, resulting in uptake of water by the dryer polymers. Because of this feature, the method of fitting a straight line to the first four data points in order to determine the critical uptake could not be used for this data. However, it is evident from Figure 4.23 that the critical uptake of EMI-Tf ionic liquid exhibited in the ^{7}Li NMR data is in good agreement with the value of 0.66 mol/mol that was determined from the FTIR investigation. From Figure 4.23, the critical uptake is approximately 0.5 mol/mol for the membranes swollen with EMI-Im ionic liquid. The reason that the critical uptake is lower for the EMI-Im ionic liquid is unknown, but could be related to the larger size of the bis(trifluoromethanesulfonyl)imide anion as compared to the trifluoromethanesulfonate anion.

It is interesting to note that for the lithium–exchanged membranes, the NMR peak widths are not in agreement with published results. In addition to their NMR investigations of sodium–exchanged Nafion^{TM}, Komoroski and Mauritz also performed ^{7}Li and ^{133}Cs NMR studies on Nafion^{TM} (71). For their results with the ^{7}Li NMR, the peak width was found

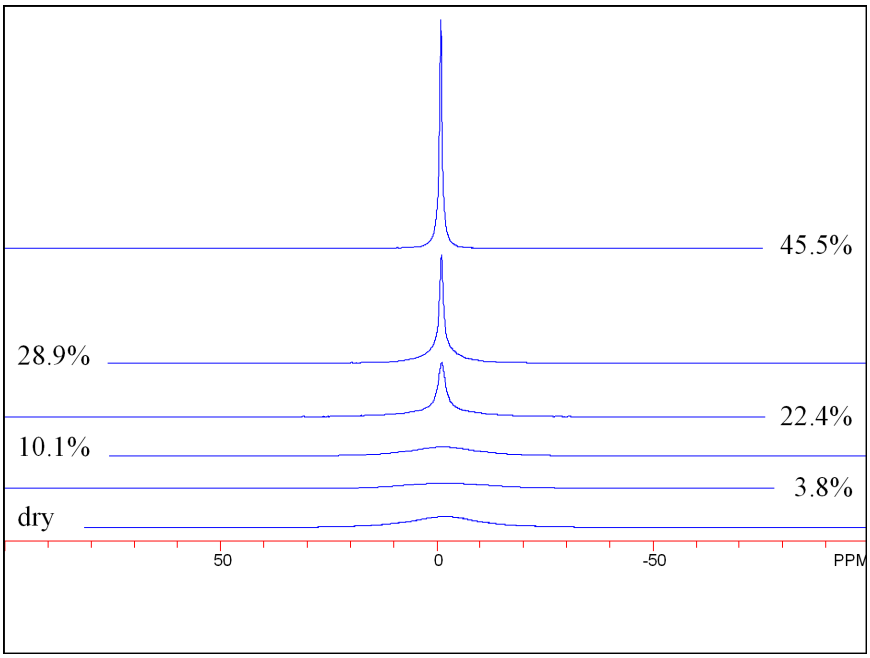

Figure 4.23: ^{7}Li NMR spectra for Nafion^{TM} membranes in the lithium form and swollen with EMI-Tf ionic liquid. All uptake values are as a percentage of the dry volume.

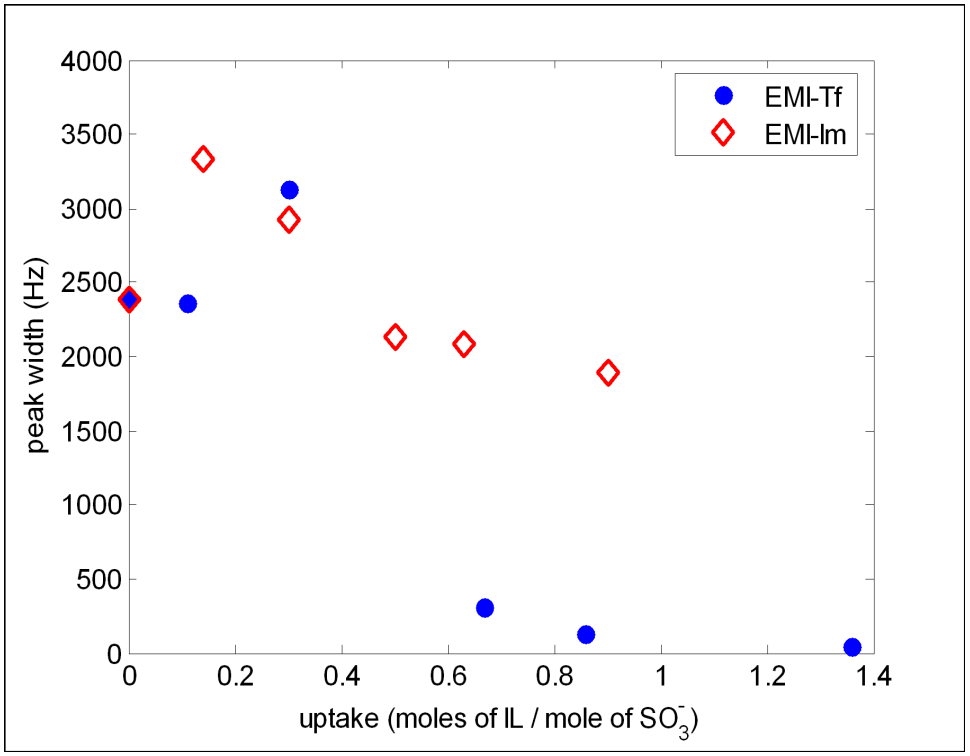

Figure 4.24: ^{7}Li NMR peak width at half height for lithium–exchanged Nafion^{TM} membranes swollen to various levels with EMI-Tf and EMI-Im ionic liquid.

to vary from about 100 Hz at a water content of about 2% (by weight) to around 10 Hz at a water content of about 24%. For the EMI-Tf–swollen membranes, the peak width varies from about 2400 Hz (dry) to about 45 Hz. The discrepancy at high swelling levels is expected, but for the relatively dry polymers, the data should be more comparable. One explanation is the fact that Komoroski and Mauritz performed their experiments on Nafion^{TM} polymer that was in the powdered form whereas the current study was performed on stacks of Nafion^{TM} membranes. The membrane forms of the polymer would be expected to exhibit more anisotropy as compared to the powdered form, which would lead to increased peak widths. For the sodium–form membranes, the closer agreement between the current work and the literature is probably related to the higher electric quadrupole moment of ^{23}Na as compared to ^{7}Li and ^{133}Cs. Therefore, the anisotropy effects are not observable in the ^{23}Na NMR study. The difference between the properties of the powdered Nafion^{TM} and the film could also be responsible for the discrepancies in the measured chemical shift as compared to the literature.

As with the ^{23}Na data, the ^{7}Li NMR results reveal that the samples swollen with the EMI-Tf ionic liquid exhibit a much narrower peak than the samples swollen with the EMI-Im ionic liquid. This indicates that the lithium ions are relatively more mobile in the membranes swollen with EMI-Tf ionic liquid than in those swollen with EMI-Im ionic liquid. Again, this is most likely due to the disrupting effect that the EMI-Im ionic liquid has on the clustered morphology of the Nafion^{TM} polymer.

Further evidence for the increased mobility of the counterions within a Nafion^{TM} membrane when swollen with an ionic liquid is provided by the ^{133}Cs NMR results. The spectra for cesium–exchanged Nafion^{TM} swollen with EMI-Tf ionic liquid are shown in Figure 4.25. As can be seen, the ^{133}Cs NMR results do not exhibit a single, Lorentzian peak. Rather, the observed spectrum seems to be made up of the superposition of two peaks, one broad downfield peak and a more narrow upfield peak. This characteristic shape was also observed for the Nafion^{TM} membranes swollen with EMI-Im ionic liquid. No mention of this irregular shape is given in the previous work by Komoroski and Mauritz (71). It is believed that the upfield peak is related to the mobility of the cesium ions within the polymer, although the origin of the downfield peak is unknown. In order to separate the observed data into two peaks, the line fitting subroutine of the program NUTS was used. This subroutine includes an optimization routine that will fit a spectrum with any number

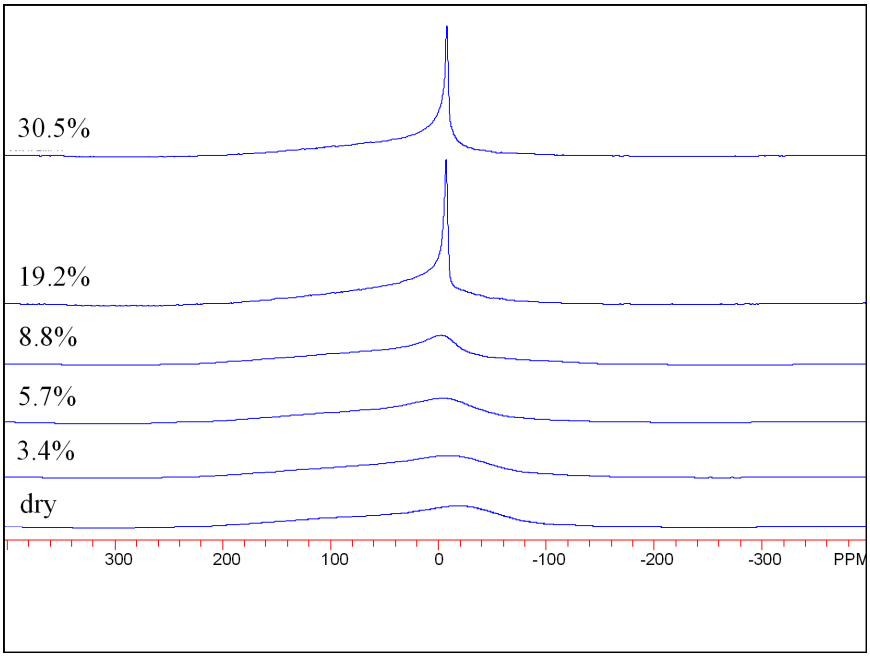

Figure 4.25: ^{133}Cs NMR spectra for Nafion^{TM} membranes in the lithium form and swollen with EMI-Tf ionic liquid. All uptake values are as a percentage of the dry volume.

of peaks (in this case, two) by varying the height, width, and position of those peaks. After using this optimization function to obtain the best fit of two peaks to the data, the width of the upfield fitted peak was obtained. This peak width is plotted versus uptake for the two ionic liquids in Figure 4.26.

The critical uptake is also observed in the ^{133}Cs NMR results, for the EMI-Tf ionic liquid. As before, the critical uptake was determined by fitting a straight line to the first four data points in Figure 4.26. By this method, the critical uptake for cesium–exchanged Nafion^{TM} swollen with EMI-Tf ionic liquid was determined to be 0.46 mol/mol. This matches well with the value of 0.48 mol/mol determined from FTIR results. The range of swelling was insufficient to observe a saturation in the NMR peak width for the EMI-Im ionic liquid. However, the peak width for the samples swollen with EMI-Im ionic liquid is larger than that for the samples swollen with EMI-Tf ionic liquid, for equivalent levels of swelling. This indicates that the cesium ions are more mobile in the EMI-Tf–swollen membranes than in the EMI-Im–swollen membranes and is consistent with the ^{23}Na and ^{7}Li NMR results.

It is also interesting to note that Komoroski and Mauritz observed the ^{133}Cs NMR

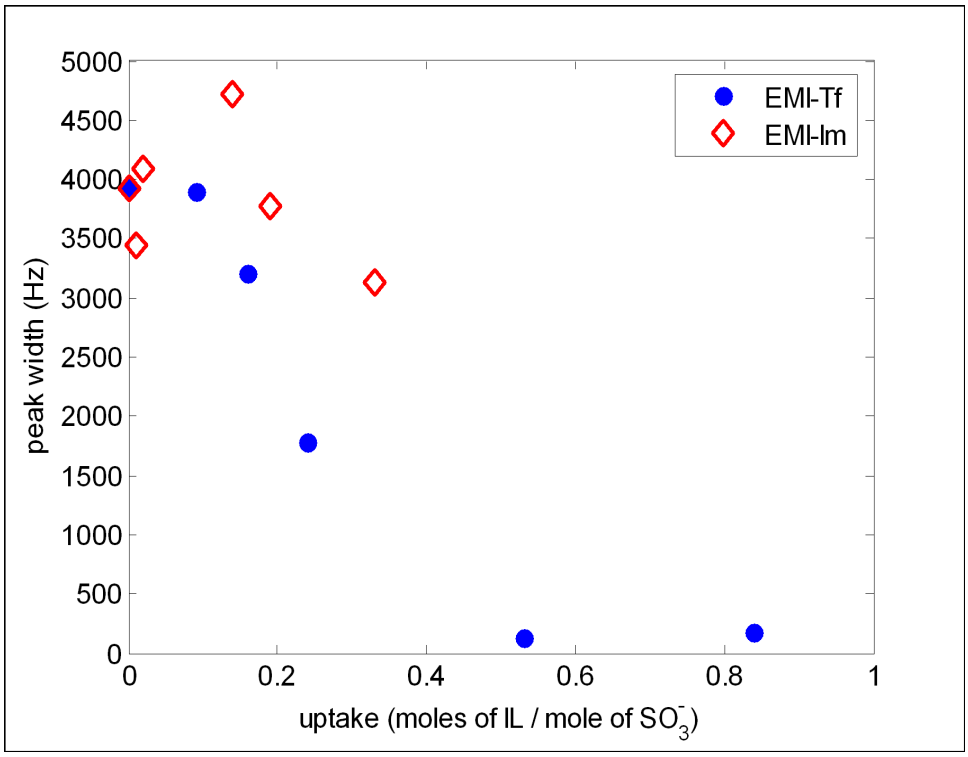

Figure 4.26: Width of the upfield fitted peak for ^{133}Cs NMR on cesium–exchanged Nafion^{TM} swollen with various levels of EMI-Tf and EMI-Im ionic liquid.

peak width of cesium–exchanged and water–swollen Nafion^{TM} to saturate at a swelling level of less than 1 water molecule per sulfonate site (71). This is significantly less than the 3-4 water molecules per exchange site that was observed for sodium–exchanged membranes in their NMR studies or by Lowry and Mauritz in an FTIR investigation. This decrease in the critical uptake with increasing counterion size for water–swollen membranes is in agreement with the observed trend for the ionic liquid–swollen membranes. This supports the notion that the critical uptake is dependent on the counterion size due to its effect on the electrostatic binding energy between the counterions and the sulfonate exchange sites.

4.5 Summary and Conclusions

Fourier transform infrared spectroscopy (FTIR) and nuclear magnetic resonance spectroscopy (NMR) have been used to gain an understanding of the ion associations within Nafion^{TM} membranes swollen with ionic liquids. These studies were performed on Nafion^{TM} polymer in different counterion forms and swollen over a range of uptakes with two different

Table 4.5: Critical loading of EMI-Tf ionic liquid in Nafion^{TM} membranes in various counterion forms as determined by FTIR and NMR spectroscopy.

cation	radius (nm)	critical uptake (moles/mole of SO_3^-) FTIR	NMR
Li^+	0.59[a]	0.66	—
Na^+	0.99[a]	0.69	0.65
K^+	1.37[a]	0.56	—
Cs^+	1.67[a]	0.48	0.46
EMI^+	3.04[b]	0.45	—
TEA^+	3.20[c]	0.44	—

[a] from reference (118)
[b] from the volume cited in (69)
[b] from the volume cited in (120)

ionic liquids.

FTIR was used to monitor the symmetric stretching frequency of the SO_3^- group of the Nafion^{TM} membrane and of the EMI-Tf ionic liquid. This study was performed for membranes in six counterion forms and swollen over a range with EMI-Tf ionic liquid. The FTIR investigation revealed that the counterion of the membrane is displaced from the sulfonate exchange site when the polymer is swollen with EMI-Tf ionic liquid. This displacement is associated with a change in the polarization of the S—O dipoles that can be observed by monitoring the symmetric stretching frequency of the sulfonate groups. The magnitude of this change is greater for the smaller counterions such as lithium and sodium and less for the larger counterions. The change in frequency on swelling is the lowest for the membranes exchanged with the EMI^+ ion. Above a critical loading of ionic liquid within the membrane, the stretching frequency does not change. This indicates that the association of the ionic liquid with the ionic groups of the polymer saturates at this loading and any additional ionic liquid is not involved in the association. The critical loading is then the minimum amount of ionic liquid that is required to dissociate all of the counterions from the exchange sites. The critical loading is found to decrease with increasing size of the counterions—see Table 4.5. This indicates that the larger counterions are more easily separated from the sulfonate exchange sites by the ionic liquid. This is because the electrostatic binding energy between the counterions and the sulfonate exchange sites is decreased by increasing the size of the counterions. A similar trend has been observed by Lowry and Mauritz (83) and Komoroski and Mauritz (71) for water–swollen membranes.

NMR testing was also performed, in this case on lithium–, sodium–, and cesium–form membranes swollen with both ionic liquids. The NMR results reveal that the mobility of the counterions increases as the content of ionic liquid within the membrane is increased. This is manifested as a decrease in the width of the measured peak in the NMR spectrum. The mobility of the counterions is increased by the introduction of the ionic liquid because the ionic liquid displaces the counterions from the exchange sites. Once displaced, the counterions associate with the anions of the ionic liquid. The increased mobility of the counterions due to this exchange is expected, considering that the sulfonate exchange sites are bound to the polymer, whereas the ionic liquid anions are not. Therefore, the exchange sites are relatively more fixed than the ionic liquid anions.

The critical uptake of ionic liquid was also observed in the NMR results, as the peak width was found to become relatively constant at high loadings of ionic liquid. This critical loading determined from the NMR testing also exhibited a dependence on the counterion size and was found to be in good agreement with the critical loading determined from the FTIR testing—see Table 4.5. The NMR results demonstrate that the mobility of the counterions is much higher for the membranes swollen with EMI-Tf ionic liquid than for the membranes swollen with EMI-Im ionic liquid. This is true for all of the counterions studied and is surprising considering that the viscosity of the EMI-Im ionic liquid is actually *lower* than that of the EMI-Tf ionic liquid. This can be attributed to the disruption of the clustered morphology of Nafion^{TM} by the introduction of the EMI-Im ionic liquid into the polymer, as described in Chapter 3.

Taken together, the FTIR and NMR results indicate that the counterions of the polymer are the primary charge carriers in Nafion^{TM} membranes swollen with ionic liquid. The counterions are released from the sulfonate exchange sites by the ionic liquid in a process whereby they are replaced with the EMI^{+} ions. Both the FTIR and NMR results demonstrate that the arrangement of the ions reaches a uniform state above a critical loading of ionic liquid. The loading at which this transition occurs is related to the size of the counterions, with the transition occuring at lower loadings of ionic liquid for larger counterions. It is interesting to note that although the critical loading of ionic liquid is related to the size of the counterions, it was found to be below 1.0 moles of ionic liquid per mole of exchange sites for all of the cases studied. The specific reasons for this are unknown, but the result suggests that each ionic liquid molecule can effectively displace more than

one counterion. In this case the ionic liquid would not associate with the membrane and the counterions in a 1:1 ratio. Another possibility is that some of the sulfonate / counterion contact pairs present in the dry membrane are inaccesible to the ionic liquid. However, in light of the available data, the former explanation seems more likely.

Chapter 5

Structured Investigation of Transduction

5.1 Motivation

The goal of this research is to reveal the underlying mechanisms responsible for transduction in ionic liquid–swollen Nafion^{TM} membranes. In order to accomplish this, the morphology of the membranes has been studied by small angle X-ray scattering (SAXS). The relevant ion associations within the polymer have also been investigated by infrared spectroscopy (FTIR) and nuclear magnetic resonance spectroscopy (NMR). Those investigations were carried out over a range of experimental parameters, including the counterion of the Nafion^{TM} membrane, the structure of the ionic liquid, and the uptake of ionic liquid within the membrane. The SAXS results revealed that the classical clustered morphology of the Nafion^{TM} membrane is preserved by the EMI-Tf ionic liquid and disrupted by the EMI-Im ionic liquid. The results presented in Chapter 4 for the FTIR and NMR testing illustrated that the counterions of the polymer are the primary charge carriers in an ionic liquid–swollen Nafion^{TM} membrane. These results revealed that the mobility of the counterions was increased by increasing the uptake of ionic liquid and by increasing the size of the counterion.

In this chapter, the results of a structured investigation of electromechanical transduction in ionic liquid–swollen Nafion^{TM} membranes will be presented. By characterizing the transduction behavior of the membranes over a range of conditions, these results can be

combined with the SAXS, FTIR, and NMR results in order to gain insight into the mechanisms of charge motion and electromechanical transduction in ionic liquid–swollen Nafion^{TM} membranes. Through this understanding, the hope is that this research will eventually lead to the development of new polymers and ionic liquids that are engineered specifically to tailor these interactions and achieve improved transduction performance.

5.2 Sample Preparation

The ionic liquid–swollen Nafion^{TM} actuators were prepared by plating with interpenetrating platinum electrodes using an exchange / reduction process similar to that described in Section 2.2. As noted in Chapter 2, a problem that plagued the early work involved the cracking of the electroplated gold electrodes when the membranes were swollen with ionic liquid. Initially, this problem was overcome by the addition of ethanol to the solutions used to plate the membrane. This increased the size of the as–plated membranes and reduced the tendancy for the electrodes to crack. However, this process was found to be limited in that the electrodes continued to crack for membranes swollen with a high uptake of ionic liquid. In order to overcome this problem, a new process was developed in which the gold layer was added to the actuators *after* they were swollen with ionic liquid. The platinum layer was deposited prior to the inroduction of the ionic liquid, using the exchange / reduction method described in Section 2.2, with the exception that the use of ethanol as a co–solvent in the plating solutions was ommited from the process.

The electrodes fabricated by the exchange / reduction process have been found to exhibit variations from one batch to another, resulting in differences in the observed transduction behavior. However, previous results revealed that within one sheet of material, the consistency of the electrodes is quite good (9). For this reason, all of the transducers studied in the course of this work were plated at the same time, as one large sheet. Following the plating of this large membrane by platinum, it was boiled in sulfuric acid and then in deionized water to convert it back to the proton form. The membrane was then cut into five equally–sized pieces and each one was soaked in a 0.5 M solution of the chloride salt of the counterion which was to be exchanged into the membrane. The membranes were allowed to soak in these solutions for several days, with intermittent agitation, in order to ensure complete exchange. The ion exchange is possible even after the membrane has

been plated because of the highly porous nature of the platinum electrode. Following the exchange of the protons for one of the five selected counterions, the membranes were cut into strips 5 mm wide and 35 mm long. The strips were rinsed and soaked in DI water for 3 hours to remove any excess electrolyte. The plated and exchanged samples were then dried overnight (∼12 hours) at 110°C and under a vacuum of 70 torr. The dry weight of each of the membranes was then recorded and they were swollen with an ionic liquid.

The swelling process was carried out using a mixture of ionic liquid and methanol, in a ratio of one part ionic liquid to two parts methanol (by volume). The dry membranes were soaked in the mixture for 3.5 hours at three different temperatures. For the lowest uptake, the soak was performed at room temperature (∼25°C). A set of samples was also swollen to an intermediate uptake by soaking in the ionic liquid / methanol mixture at 65°C. In order to achieve a high uptake of ionic liquid within the polymer, a group of samples were also swollen at 90°C. At this higher temperature the methanol evaporated very quickly, even though the jars were tightly sealed. For this reason, the maximum uptake of EMI-Tf by the polymer was much higher than the maximum uptake of EMI-Im. This is because the Nafion^{TM} membranes will easily absorb neat EMMI-Tf, especially at high temperature, but will not easily absorb EMI-Im, even at high temperature. Therefore, after the methanol had evaporated, very little EMI-Im ionic liquid was incorporated into the polymer. However, the uptake of EMI-Im was still found to be higher for the samples treated at 90°C than for those treated at 65°C. Following the soak of the samples in the ionic liquid / methanol mixture, they were placed between two cellulose filter papers and dried at 110°C under 70 torr vacuum for 3.5 hours in order to drive the methanol out of the membranes. The samples were then weighed again and stored in glass jars until testing. As with the unplated samples that were studied using SAXS, NMR, and FTIR, the uptake of the ionic liquids by the polymer was found to be dependent on the counterion. The smaller counterions have a higher affinity for methanol and therefore the uptake of ionic liquid is largest for the membranes exchanged with the smaller cations.

As before, the content of ionic liquid within the polymer is reported as the volume of ionic liquid as a percentage of the dry volume of the polymer. This is determined from the dry and swollen weights of the polymer and the density of the dry polymer and the ionic liquid using equation 2.1. The densities of the ionic liquids were obtained from the literature and are presented in Table 3.1. The dry densities of the platinum–plated Nafion^{TM} mem-

Table 5.1: Measured dry density of plated and unplated Nafion^{TM} polymer in five cation forms. All values are in g/cm^3

cation	unplated	plated
Li	1.97	2.50
K	2.11	2.60
Cs	2.14	2.69
EMI	1.81	2.45
TEA	1.72	2.31

branes were obtained from weight and volume measurements using the process described in Section 2.1. The densities of the platinum–plated membranes are presented in Table 5.1. The densities of the dry unplated membranes are also shown for reference. Clearly, the density of the polymer has not changed by the addition of the electrode, but by measuring the density of the plated membranes in this way, the additional weight of the platinum metal is accounted for. This allows comparisons to be made between plated and unplated samples at equivalent swelling levels. By subtracting the measured density of the unplated membranes from the measured density of the plated membranes, the loading of platinum metal per unit membrane volume was determined for each counterion form. These values were then averaged and multiplied by the nomimal thickness of the Nafion^{TM}-117 membrane (183 μm) to estimate the loading of platinum per unit membrane area to be approximately 10 mg/cm^2.

For the actuators described in Chapter 2, the gold surface layer was added to the membranes by electroplating prior to the introduction of the ionic liquid. This was found to result in cracking of the gold. Although the process was improved by adding ethanol to the plating solutions, thus increasing the size of the as–plated membranes, the cracking problem was never completely solved by this method. For this reason, the gold electrodes on the actuators studied in this chapter were applied after the swelling of the membranes with ionic liquid.

After the membranes were plated with platinum and swollen with ionic liquid, they were painted on both sides with a solution composed of a commercially–available Nafion^{TM} suspension (5% polyer, by weight) and isopropyl alcohol (91% by weight). The solution was allowed to dry under a heat lamp. This thin layer of Nafion^{TM} polymer on top of the platinum layer facilitates adhesion of the gold electrode to the transducer. The strips were arranged side-by-side, five at a time, on a sheet of waxed paper–backed gold leaf.

Another sheet of gold leaf was placed on top of the strips and they were pressed at 180°C and 5.6 MPa for 10 seconds. After pressing, the waxed paper backing sheets are peeled away. Finally, the edges of the samples were trimmed and their finished length, width, and thickness were measured. Because this layer of gold was applied after the membranes were swollen with ionic liquid, its integrity was not compromised by the swelling process.

5.3 Testing Protocol

In order to characterize the electromechanical transduction behavior of the ionic liquid–swollen Nafion^{TM} membranes, the free strain generated in response to a voltage input was measured. This testing was performed in the frequency domain using a random input signal and in the time domain with a step input. The experimental setup and methods used to perform these tests were discussed in Section 2.3.1 of this document.

A second experimental setup was used to measure the Young's modulus of the polymer transducers–see Figure 5.1. In this setup, the polymer sample is fixed between two gold foil electrodes in a spring-loaded clamp. In this case the clamp is linearly displaced by an electromagnetic shaker. The tip of the sample is in contact with the load application point of a 10-gm load cell and is constrained as such (a small prebend in the sample ensures that it remains in contact with the load cell.) A random voltage signal is used to drive the shaker; the motion of the clamp is measured with a linear potentiometer and the resulting reaction force at the tip of the sample is measured by the load cell. The displacement and force signals are collected by a Tektronics Fourier analyzer and a frequency response is computed. This frequency response is the bending stiffness of the sample, which asymptotically approaches a constant value at low frequency. This low-frequency stiffness can be used with the sample's geometry to compute the elastic modulus from

$$Y = \frac{8\frac{F}{\delta}L_f^3}{\pi^3(\frac{wt^3}{12})}. \tag{5.1}$$

Equation 5.1 was derived by Franklin (33) and is valid for the sliding–pinned beam geometry utilized for the modulus testing. In this equation Y is the elastic modulus, $\frac{F}{\delta}$ is the bending stiffness of the sample, w is the sample width, t is the thickness of the sample, and L_f is the free length of the sample. Several simplifying assumptions are made in order to determine the elastic modulus from the two–point bending test. First, the transducer

strips are assumed to obey Euler–Bernoulli beam theory, which is appropriate for small deformations. Second, viscoelastic effects are neglected in computing the elastic modulus. Again, this is valid because of the low frequency of the measurement. Finally, the beam is assumed to be homogeneous and isotropic, although the three–layer transducer strips are clearly not homogeneous and probably not isotropic. However, the modulus of the polymer dominates the stiffness of the strips (9) and the electrodes are the same for all of the samples. Also, the diffuse and particulate nature of the electrodes makes estimations of their stiffness very uncertain. The assumption of a homogenous beam allows comparisons of the measured modulus to be made between different samples.

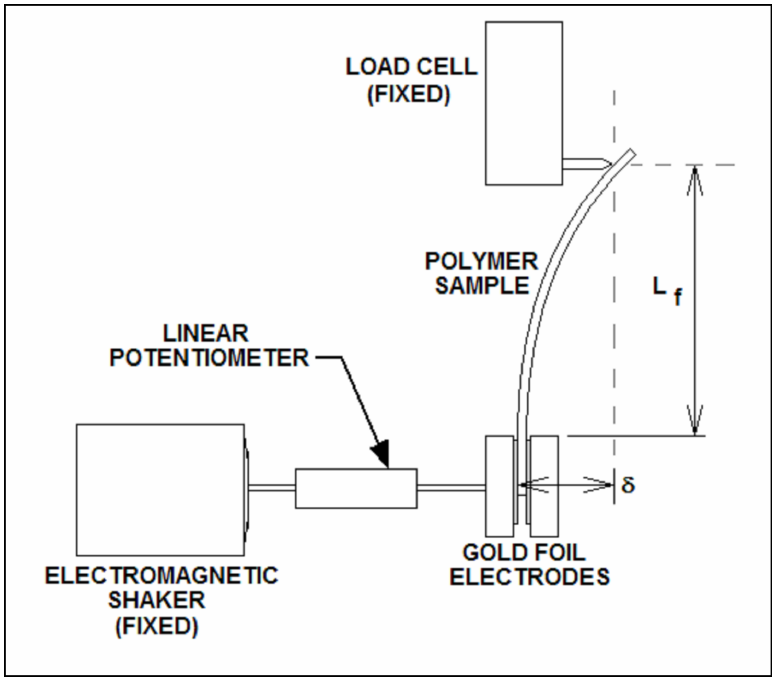

Figure 5.1: A schematic of the experimental setup used to measure the modulus of the transducer.

Nafion^{TM} transducers can also function as electromechanical sensors. In order to measure the sensing response of these materials, the setup shown in Figure 5.1 was used. As with the modulus test, the tip of the sample is constrained and the base of the sample is displaced by an electromagnetic shaker; the displacement is measured with a linear potentiometer. This situation generates an induced strain in the membrane that gives rise to a charge buildup at the electrodes. This charge can be measured using the circuit shown in Figure 5.2. This circuit behaves as a filter and its gain is therefore frequency dependent, but at frequencies sufficiently larger than the corner frequency its gain can be approximated

as $\frac{V}{q} = C_f^{-1}$, where V is voltage output of the circuit in Volts, q is the charge in Coulombs, and C_f is the value of the feedback capacitor in Farads. The output of this circuit and the displacement of the polymer clamp are measured by a Tektronics Fourier analyzer and a transfer function between charge and deflection is generated, $\frac{q}{\delta}$. This transfer function and the geometry of the sample can be used to compute the frequency response between charge and induced strain from

$$\frac{q}{\epsilon} = \frac{\frac{q}{\delta} L_f^2}{t}. \tag{5.2}$$

In this equation, $\frac{q}{\epsilon}$ is referred to as the strain sensitivity of the sample. The stress sensitivity can also be calculated by dividing the strain sensitivity by the elastic modulus of the sample.

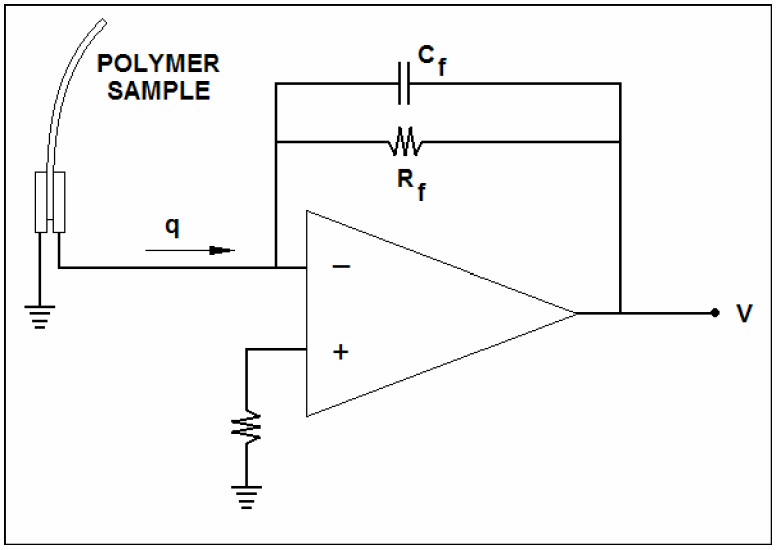

Figure 5.2: The circuit used to measure the charge output of a Nafion™ sensor.

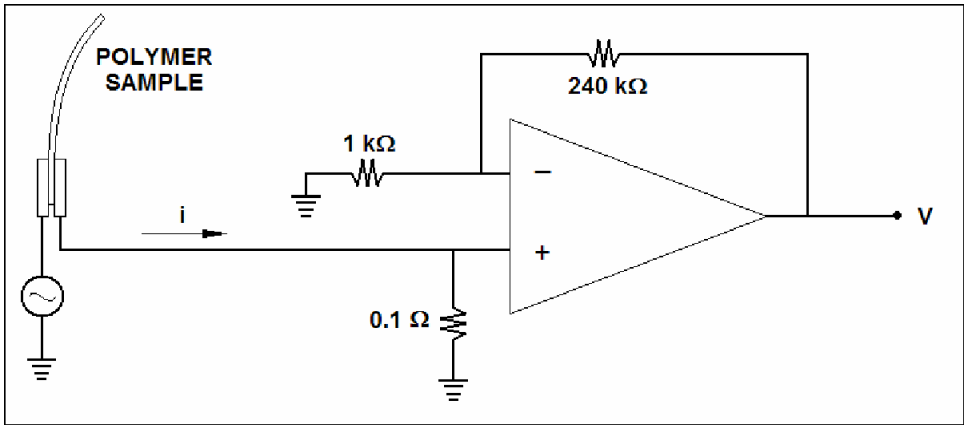

Figure 5.3: The circuit used to measure the current through a Nafion™ transducer when driven with a voltage input.

The impedance of these materials was also measured in the course of this work. In order to determine the electrical impedance, the current drawn by the membrane for a given voltage input was measured using the circuit shown in Figure 5.3. As can be seen, this circuit operates by amplifying the voltage drop across a 0.1 Ω resistor placed in series with the polymer sample; the gain of the circuit is $\frac{V}{i} = 41.5$ mA/V. The value of this resistor is chosen to be small enough that its effect on the current through the polymer can be neglected. The polymer is driven with a random voltage signal and the voltage and current are measured with a Tektronics Fourier analyzer. From this the voltage-to-current frequency response is generated, which is converted to the complex impedance of the polymer sample using the gain of the current measuring circuit.

5.4 Results

5.4.1 Actuation Response

The FTIR and NMR results presented in Chapter 4 demonstrated that the counterions of the Nafion^{TM} polymer are the primary charge carriers in an ionic liquid–swollen Nafion^{TM} membrane. The mobility of the cations was found to increase with increasing content of ionic liquid. Also, the EMI-Tf ionic liquid was found to be more effective at mobilizing the cations than the EMI-Im ionic liquid. This chapter will investigate the transduction behavior of these membranes. This investigation will lead to an understanding of the mechanisms of transduction in ionic liquid–swollen Nafion^{TM} membranes.

One of the principal experiments that was performed on the ionomeric polymer actuators involved the measurement of the generated free strain under excitation with a random voltage input. Representative strain-to-voltage frequency responses for potassium–exchanged actuators swollen with EMI-Tf ionic liquid are shown in Figure 5.4. As can be seen, the measured strain has been normalized by the input voltage. The peak located at around 20 Hz is the resonance associated with the first bending mode of the beam. As can be seen, this peaks shift towards lower frequency as the content of ionic liquid within the actuator is increased.

The position of the bending resonant frequency is related to the mechanics of the system. For a simple single degree of freedom undamped system, the resonant frequency is

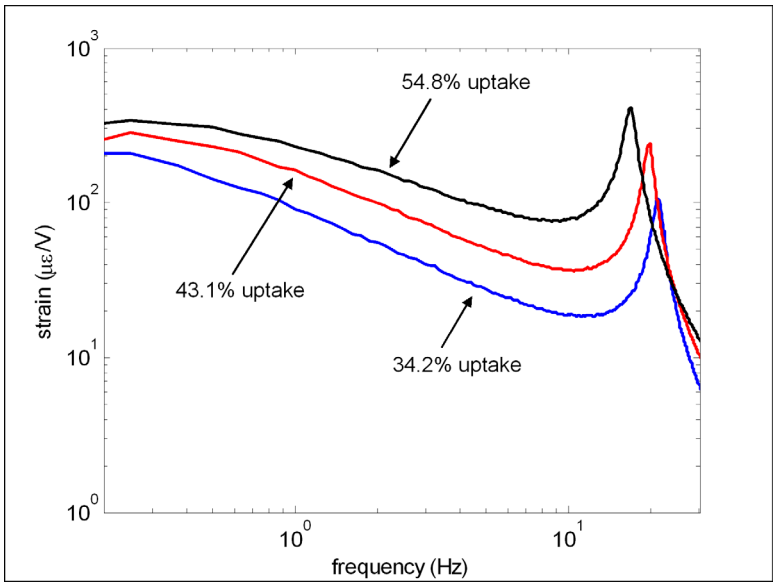

Figure 5.4: Generated strain per unit volt for K^+ form Nafion^{TM} actuators swollen to the indicated level with EMI-Tf ionic liquid.

related to the mass (m) and stiffness (k) by

$$\omega_n = \sqrt{\frac{k}{m}}, \tag{5.3}$$

where ω_n is the resonant frequency. As the content of ionic liquid within the membrane is increased, the mass is increased and the stiffness is decreased. The stiffness is decreased because the elastic modulus is decreased. The relationship between the stiffness of a beam is and its elastic modulus is illustrated in equation 5.1, where $\frac{F}{\delta}$ is stiffness and Y is modulus. The elastic modulus of the samples was determined using the two–point bending test described in Section 5.3. Figure 5.5 illustrates the effect of increasing the loading of ionic liquid on the measured modulus. Nemat-Nasser has performed a similar experiment on water–swollen Nafion^{TM} membranes over a range of hydration levels and has found that the modulus exhibits a -4/3 power relationship with the uptake of diluent (97). Considerable scatter is present in the data presented in Figure 5.5, and due to the small range of swelling level, it is not clear that the modulus exhibits a -4/3 power relationship with the uptake. However, the modulus of the transducers is seen to decrease as the content of ionic liquid within the membrane is increased.

Other aspects of the responses plotted in Figure 5.4 are related to the speed of the actuation response of the polymers. As can be seen, the slope of the curves in the frequency range below the first resonant peak decreases as the content of ionic liquid within

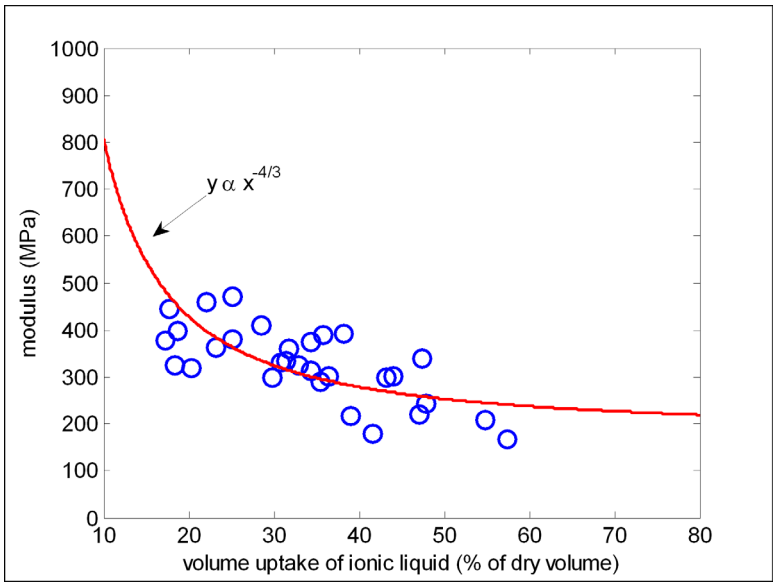

Figure 5.5: Measured elastic modulus versus uptake for the ionic liquid–swollen Nafion^{TM} transducers.

the material increases. Therefore, at low frequency, the strain response of the actuators is similar but as the frequency is increased, the difference between the three strain responses increases. This is because at low frequency the motion of the polymer is able to track the voltage input. However, as the speed of the input increases, the motion is decreased in magnitude and lags farther behind the input due to the limited mobility of the ions. This can be observed by plotting the phase of the strain output with respect the the input voltage—see Figure 5.6. As can be seen, at low frequency the output lags the input by 25-45 degrees. Due to the limited mobility of the ions in the polymer, *very* low frequency excitation is required in order for zero phase lag to be observed. As the input frequency is increased, the output lags more, until the phase reaches a value of about -80° just below the first resonance. Just as the slope of the strain-to-voltage frequency response is lower for the more swollen actuators, the phase lag is also lower for the more highly swollen actuators. Both of these factors are related to the increased speed of the actuation response as the content of ionic liquid within the polymer is increased.

A more accurate way to determine the speed of response of the actuators is by measuring their step response in the time domain. Shown in Figure 5.7a is the response of three potassium–exchanged Nafion^{TM} actuators swollen to different levels with EMI-Tf ionic liquid and excited with a 1.5V step input. Although the amplitudes of the responses

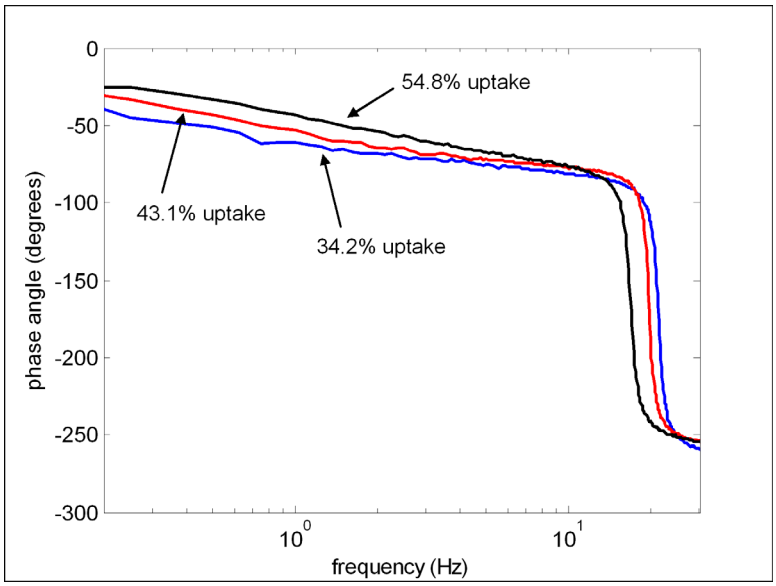

Figure 5.6: Phase angle between generated strain and input voltage for three potassium–form Nafion^{TM} actuators swollen with EMI-Tf.

are different, this could be caused by a number of factors, most notably inconsistencies in the position of the actuators within the clamp. However, of interest is the fact that the response speed of the actuators increases as the content of ionic liquid within the material increases. In this case the response speed is defined as the initial strain rate of the actuator immediately after the step is applied. It is interesting to note that the step responses shown in Figure 5.7a exhibit two time constants, a fast rise when the step is applied followed by a slower forward relaxation that persists for the duration of the two–minute test. A similar behavior was observed for the actuators swollen with the EMI-Im ionic liquid, except that the rate of the initial rise was much slower as compared to the actuators swollen with EMI-Tf—see Figure 5.7b. For both of the ionic liquids, the initial rise increased in speed as the content of ionic liquid within the actuators was increased.

To study this effect more fully, the initial strain rate of the actuators was determined from the step response and plotted versus the uptake of EMI-Tf ionic liquid—see Figure 5.8. This data was obtained by measuring the slope of the response with respect to time for the first 100 milliseconds immediately after the step was applied. As can be seen, the speed of the actuators increases with increasing uptake of ionic liquid and also with increasing size of the counterions. A similar trend relating the critical uptake of ionic liquid to the size of the counterions was observed in the FTIR and NMR results presented in Chapter 4.

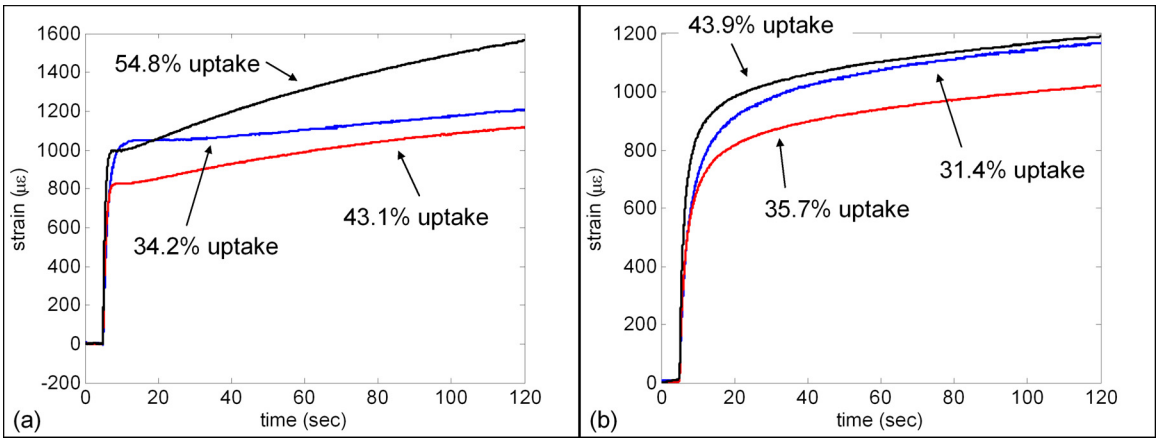

Figure 5.7: Response of three potassium–form Nafion^{TM} membrane actuators swollen with (a) EMI-Tf ionic liquid and (b) EMI-Im ionic liquid to a 1.5V step input.

In that case, the critical uptake was found to decrease for increasing counterion size. The trend was explained by the fact that the electrostatic force binding the counterions to the sulfonate exchange sites is decreased by increasing the size of the counterions, thus reducing the amount of ionic liquid required to displace the counterions. Therefore, the amount of excess ionic liquid beyond the critical uptake increases with increasing size of the counterions, for a given swelling level. From Figure 5.8, it is clear that this leads to an increase in the mobility of the counterions within the membrane. In the FTIR and NMR results, the critical uptake was observed as an inflection point in the data. However, by plotting the response speed versus the molar uptake of ionic liquid, it is apparent that the swelling level of EMI-Tf ionic liquid for all of the actuator samples falls above the critical uptake for each counterion—see Figure 5.9. Therefore, an inflection point in the actuation speed versus the swelling level is not observed.

As compared to the actators swollen with the EMI-Tf ionic liquid, the actuators swollen with the EMI-Im ionic liquid exhibited a slower response—see Figure 5.10. Again, this data was obtained by measuring the slope of the step response for the first 100 milliseconds just after the step was applied. As can be seen, the data follows the same trend of increasing speed with increasing content of ionic liquid and increasing ion size. Overall, the slower response of the EMI-Im–swollen actuators would seem to indicate that the ions within these actuators are less mobile than the ions within the EMI-Tf–swollen actuators. This is in agreement with the NMR results, in which the mobilities of Li^+, Na^+, and Cs^+

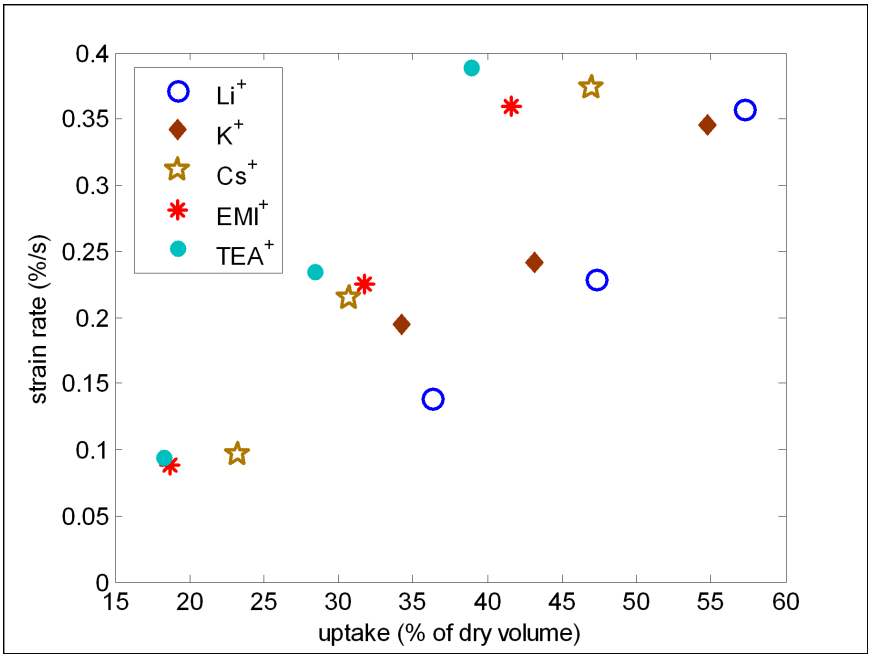

Figure 5.8: Initial strain rate (from the step response) versus the volumetric uptake of EMI-Tf ionic liquid for Nafion^{TM} actuators in five different counterion forms.

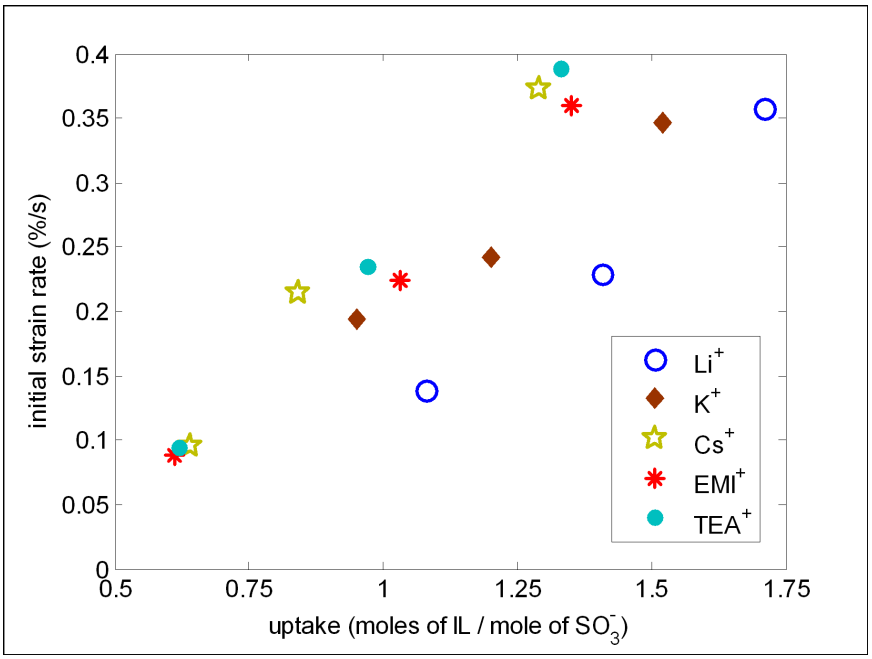

Figure 5.9: Initial strain rate (from the step response) versus the molar uptake of EMI-Tf ionic liquid for Nafion^{TM} actuators in five different counterion forms.

ions in Nafion^{TM} membranes were found to be higher for membranes swollen with EMI-Tf ionic liquid as compared to those swollen with EMI-Im ionic liquid. This is despite the fact that the viscosity of the EMI-Im ionic liquid is lower than that of the EMI-Tf ionic liquid. This can likely be explained by considering that the EMI-Im ionic liquid was found to disrupt the clustered morphology of the Nafion^{TM} polymer, whereas the EMI-Tf ionic liquid was found to preserve this morphology, as determined by SAXS analysis. The disruption of the morphology of the polymer apparently leads to an overall decrease in the ionic conductivity of the membrane.

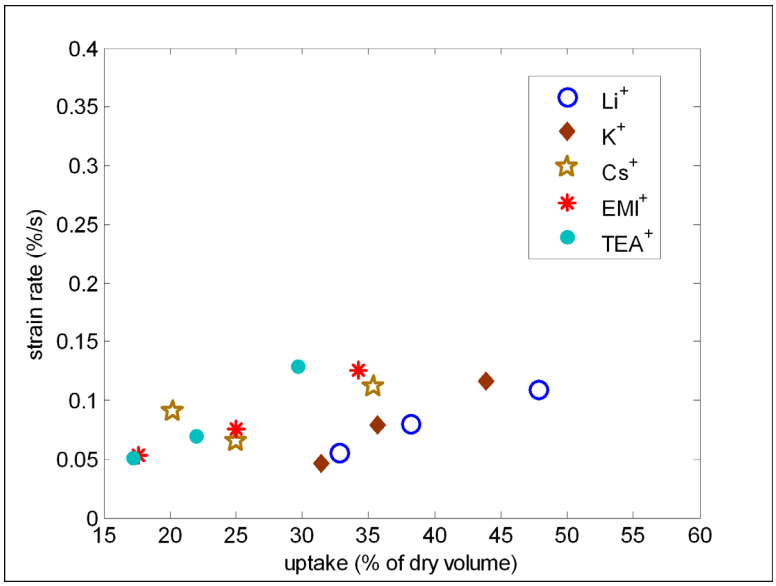

Figure 5.10: Initial strain rate (from the step response) versus uptake of EMI-Im ionic liquid for Nafion^{TM} actuators in five different counterion forms.

5.4.2 Impedance Analysis

Another way to investigate the ion mobility within ionomer membranes is to perform measurements of the complex impedance. This impedance is then used to compute the ionic conductivity of the material, which is a measure of the ability of the ions to move within the polymer. In this work the measurement of ionic conductivity was performed in two different ways. One technique for measuring the ionic conductivity used the method of Zawodzinski et al. (139). In this technique, the real and imaginary impedance of an unplated membrane sample is measured over a wide range of frequencies. A special fixture was constructed to perform these tests—see Figure 5.11a. This fixture consisted of a glass–filled Teflon block

embedded with two brass electrodes, 32 mm long and separated by a distance of 3.25 mm. The sample under test was placed on top of these electrodes and uniform contact to the electrodes was ensured by pressing on the top of the Nafion^{TM} film with a second glass–filled Teflon block and a weight. By the method of Zawodzinski et al., a Nyquist plot of the impedance is generated from the complex impedance, in which the real part of the impedance is plotted on the x–axis and the imaginary part on the y–axis—see Figure 5.12. The impedance that is used to compute the ionic conductivity is then the real part of the impedance when the magnitude of the imaginary part is at a minimum, as shown in the figure. The conductivity is determined from this impedance and the test geometry by

$$\sigma = \frac{l}{Rtw}, \tag{5.4}$$

where σ is the ionic conductivity, l is the distance between the electrodes (3.25 mm), R is the impedance, t is the thickness of the membrane, and w is the length of the electrodes (32 mm).

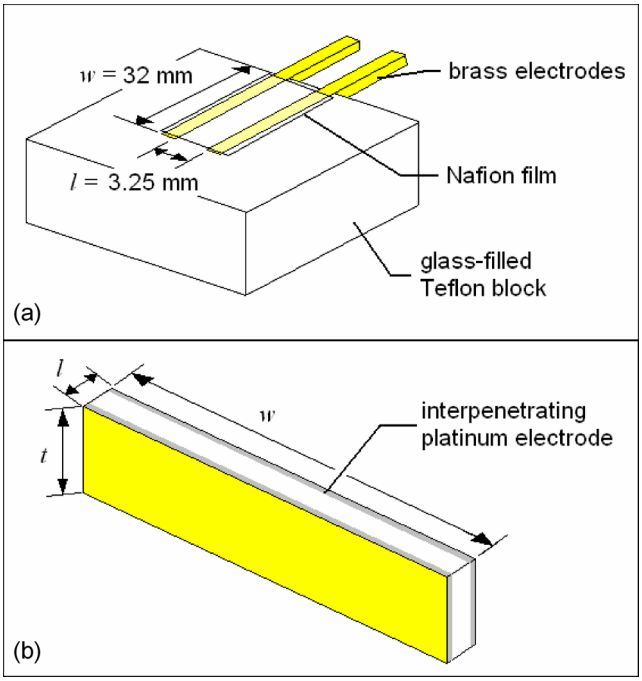

Figure 5.11: Geometrical parameters used to calculate the ionic conductivity for the (a) unplated membranes, (b) plated membranes.

This method was used to determine the ionic conductivity of some of the unplated ionic liquid–swollen membranes. However, this testing could only be performed for a small number of the samples due to the low conductivity of most of the membranes and the limited

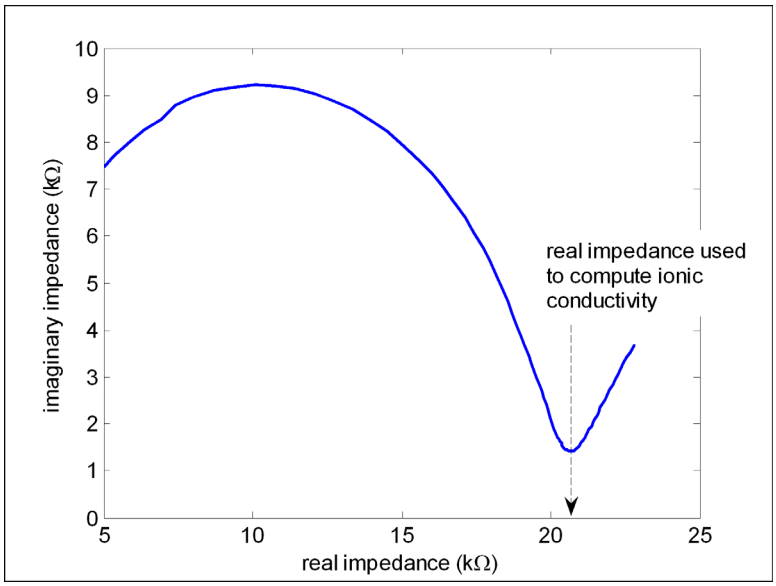

Figure 5.12: Nyquist plot of the impedance of an unplated, lithium form Nafion^{TM} membrane swollen with 45.5% by volume (1.35 mol/mol) of EMI-Tf ionic liquid. The ionic conductivity is computed from the real impedance measured when the imaginary impedance is at a minimum,

capabilities of the available equipment. Also, the ionic conductivity could not be measured by this technique for the plated samples due to the presence of the metal electrodes. For the metal plated membranes, a different method was used. The complex impedance of the plated strips was measured across their thickness during the frequency domain actuation testing using the circuit shown in Figure 5.3. The impedance that was used to compute the ionic conductivity was taken to be the magnitude of the impedance averaged over the frequency range 100-200 Hz. The ionic conductivity was then calculated using equation 5.4. The geometrical parameters that were used for this calculation are shown in Figure 5.11b. As can be seen, these parameters were unique for each strip and measured before each test.

Figure 5.13 shows a comparison of the ionic conductivity obtained using both methods. As can be seen, the ionic conductivity measured for the unplated membranes is larger than the ionic conductivity measured for the plated membranes. This can most likely be attributed to anisotropy in the Nafion^{TM} membranes that is introduced by extrusion of the films during the manufacturing process. Whereas the ionic conductivity for the unplated membranes was based on impedance measurements performed in the plane of the Nafion^{TM} films, the ionic conductivity for the plated membranes was measured through the thickness of the films. Evidence for this anisotropy is provided by the findings of Gebel et al., which

revealed the swelling process of Nafion^{TM} membranes with a diluent to be anisotropic (40). Also, Mueller has found the proton conductivity and diffusion coefficient of Nafion^{TM}-117 membranes to be higher in the planar direction than in the thickness direction (96). This is consistent with the results of the current study. Additional evidence is provided by Rollet el al. (112). They determined that the diffusion coefficient for sodium ions within a sulfonated polyimide membrane was higher in the planar direction than in the thickness direction. Both Mueller and Rollet et al. supported their conclusions with NMR and conductivity measurements and both attributed the difference in the observed conductivities to anisotropy of the films.

Based on these previous studies, the most likely explanation for the differences observed in the ionic conductivities measured by the two methods in the current work is anisotropy of the Nafion^{TM} films. However, as can be seen in Figure 5.13, the two methods predicted similar trends relating the ionic conductivity to the content of ionic liquid. Therefore, both methods produce reliable measurements of ionic conductivity and within a given data set, valid comparisons can be made. However, it should be noted that these results should only be compared to those of another researcher with caution and consideration to the geometry of the test and orientation of the films.

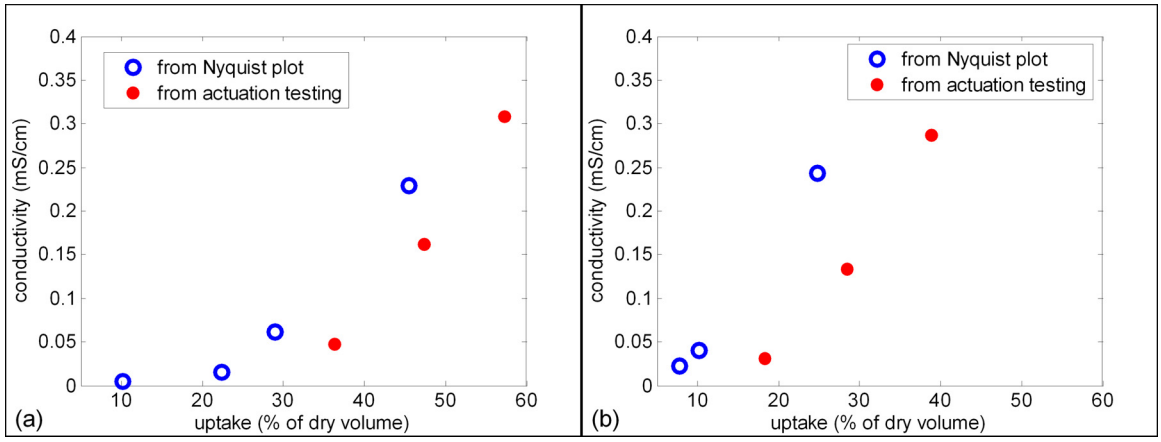

Figure 5.13: Ionic conductivity versus uptake of EMI-Tf ionic liquid using the method of Zawodzinski et al. (139) for the unplated membranes and as determined from the impedance measured during the actuation testing for the plated membranes. (a) Data for membranes in the Li^+ form, (b) data for membranes in the TEA^+ form.

Also of interest in Figure 5.13a is the fact that the ionic conductivity (determined from the Nyquist plot) of the lithium–exchanged membranes exhibits an inflection point at

an uptake of ionic liquid of about 0.67 mol/mol. This is consistent with the FTIR study, in which the critical loading of EMI-Tf ionic liquid was found to be 0.66 mol/mol, for lithium–exchanged membranes. This confirms the assertion, already presented by the spectroscopic investigations, that the behavior of the ionic liquid–swollen membranes undergoes a change as the content of ionic liquid passes through the critical uptake. The inflection point is not observed for the TEA form membranes because there are not enough data points on each side of the critical uptake, which from the FTIR study was determined to be 0.44 moles of EMI-Tf ionic liquid per mole of exchange sites. However, it is clear from the figure that the TEA–form membranes exhibit a much higher ionic conductivity than the lithium–form membranes, for equivalent levels of swelling with EMI-Tf ionic liquid.

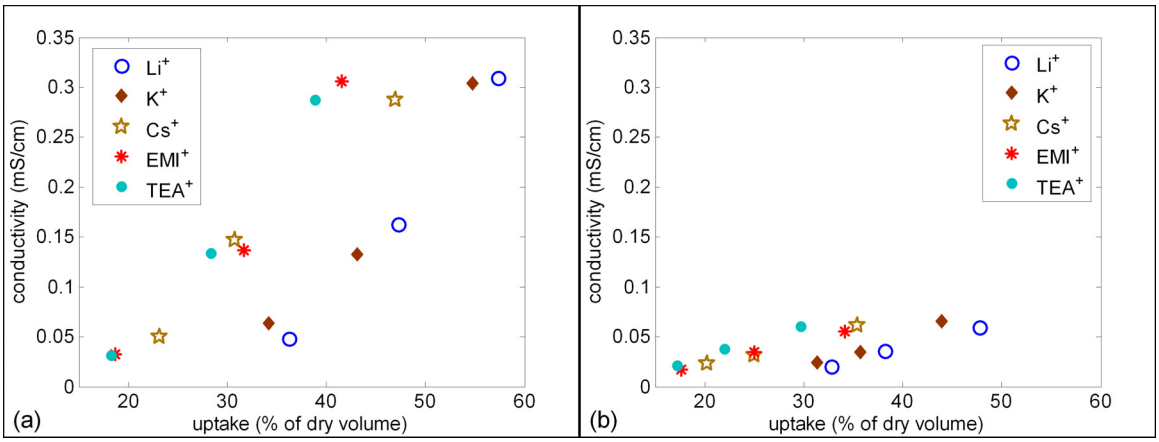

Figure 5.14: Ionic conductivity versus uptake of ionic liquid for platinum plated Nafion^{TM} membranes in five different counterion forms and swollen with (a) EMI-Tf ionic liquid, (b) EMI-Im ionic liquid.

Like the measured speed of the step response, the ionic conductivity of the polymers is found to increase when the content of ionic liquid within the membrane is increased—see Figure 5.14. From the figure, this increase seems to follow a linear trend with uptake, for each cation form of the membrane. Zawodzinski et al. have previously observed the ionic conductivity of a proton–form Nafion^{TM} membrane to increase linearly with increasing content of water (139). It is believed that the expected inflection points are not observed in the conductivity data because all of the data points are above the critical uptake of ionic liquid, which is specific to each counterion form of the membrane. Also, the conductivity shows a dependence on the cation radius and is higher for the membranes that were exchanged with the larger cations, for both ionic liquids. This is similar to the trend relating the critical

uptake to the counterion size, as discussed in Chapter 4. Also in concert with the actuation speed data, the conductivity is found to be higher for the EMI-Tf–swollen membranes than for the EMI-Im–swollen membranes.

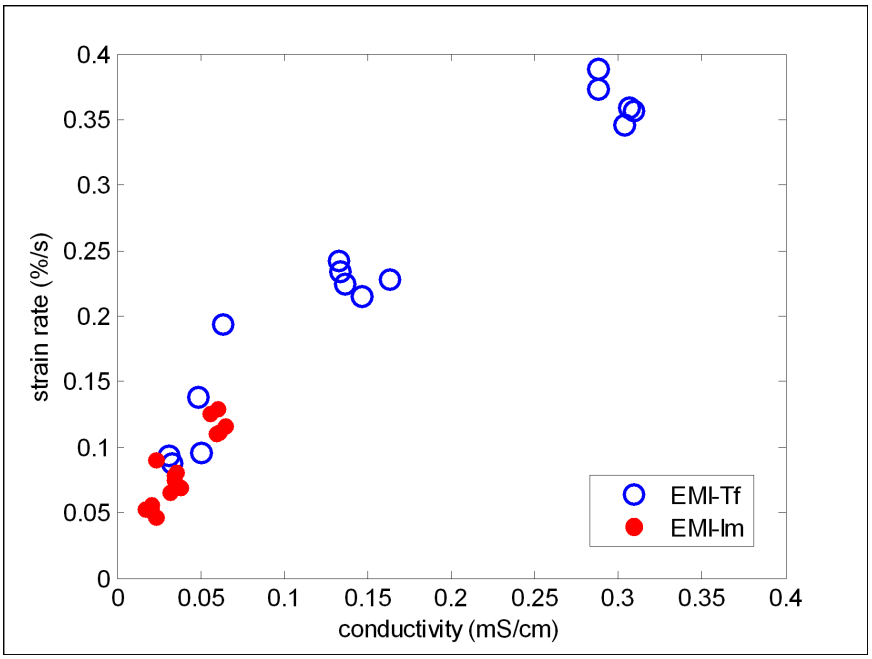

Figure 5.15: Initial strain rate (from the step response) versus ionic conductivity for platinum plated Nafion™ membranes in five different counterion forms and swollen with EMI-Tf and EMI-Im ionic liquid.

Both the actuation (step response) testing and the impedance testing revealed that the mobility of the ions within the Nafion™ membrane is increased when the size of the counterion is increased and when the content of ionic liquid within the membrane is increased. Also, the ions are more mobile for the membranes swollen with the EMI-Tf ionic liquid than for those swollen with the EMI-Im ionic liquid. The relationship between the conductivity and the speed of response can be seen in Figure 5.15. As can be seen, the response speed exhibits a linear dependence on the ionic conductivity, with a slope very close to 1. This trend does not show a dependence on the size of the ion or the structure of the ionic liquid. This is because both metrics are directly related to the mobility of the ions. Therefore, if the ion mobility decreases, then the actuation speed will decrease and the ionic conductivity will decrease, but the relationship between them will remain unchanged. As can be seen from Figure 5.15, although the relationship between actuation speed and conductivity is not dependent on the structure of the ionic liquid, the membranes swollen

with the EMI-Tf ionic liquid exhibited higher conductivities and actuation speeds than the membranes swollen with the EMI-Im ionic liquid.

5.4.3 Sensing Response

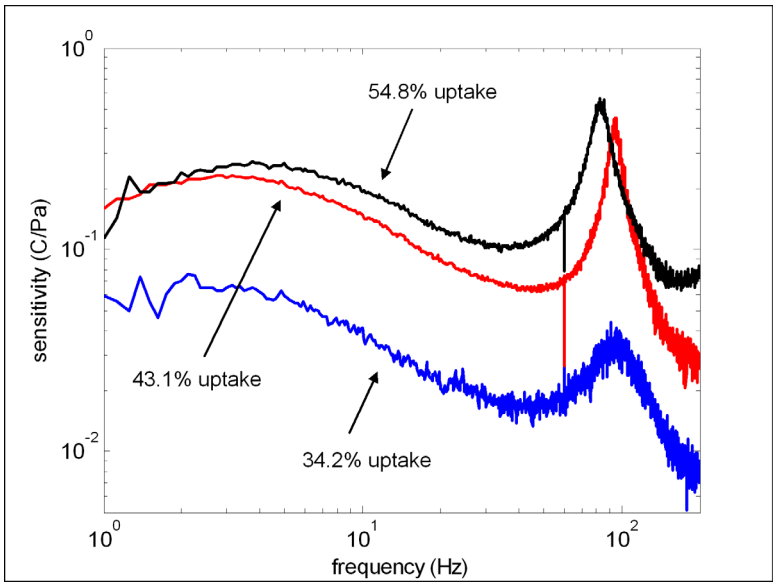

Figure 5.16: Stress sensitivity versus frequency for three potassium–form Nafion^{TM} membranes plated with platinum electrodes and swollen with EMI-Tf ionic liquid.

In addition to their behavior as electromechanical actuators, Nafion^{TM} membranes are also able to function as sensors. In this capacity a measureable charge is developed across the thickness of the membrane when a deformed by a mechanical input. The same platinum plated and ionic liquid–swollen membranes that were characterized as actuators were also tested as sensors using the methods and equipment described in Section 5.3. The sensing characterization was only performed in the frequency domain, with a random displacement input to the polymer strip. Step response testing was not performed. Shown in Figure 5.16 are three frequency responses between charge and stress for potassium–exchanged transducers swollen to various levels with EMI-Tf ionic liquid. This data was obtained by first computing the strain sensitivity using equation 5.3 from the measured charge output and imposed deflection. The strain sensitivity was then converted to a stress sensitivity using the measured elastic modulus of the sample. The stress sensitivity is generally a more useful metric because the charge redistribution that occurs within the material arises from the development of internal stresses upon deformation. Therefore, all other things being

equal, a polymer with a lower modulus will generate less charge than one with a higher modulus, for the same imposed strain. As can be seen in Figure 5.16, the charge output for a given stress input increases as the content of ionic liquid within the membrane increases. This increase is due to increased mobility of the ions in the polymer.

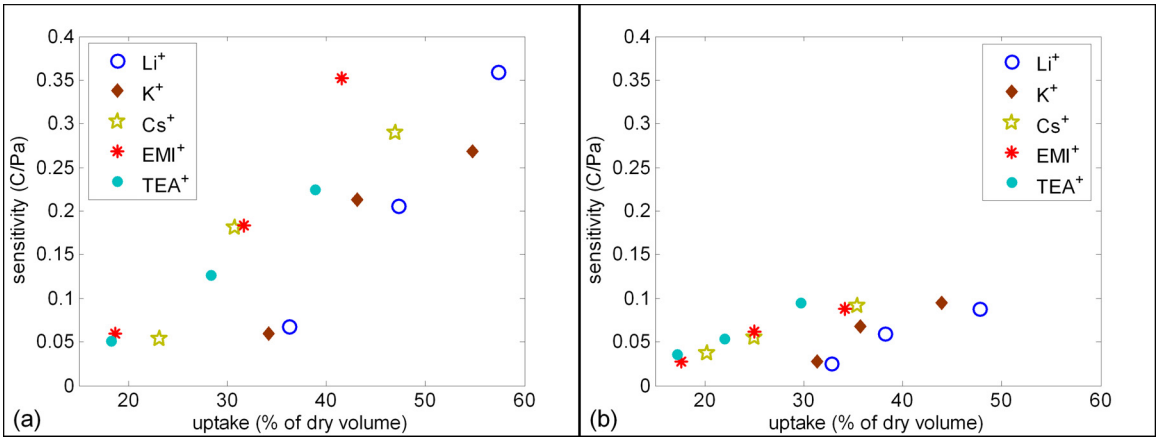

Figure 5.17: Stress sensitivity at 5 Hz for platinum plated Nafion™ transducers in five different counterion forms and swollen with (a) EMI-Tf ionic liquid, (b) EMI-Im ionic liquid.

This can be seen more clearly in Figure 5.17. Plotted in this figure is the stress sensitivity at 5 Hz versus uptake of ionic liquid for each counterion. As can be seen, the sensitivity of the transducers increases as the content of ionic liquid increases and also increases as the size of the counterion increases. Just as with the actuation speed and the conductivity measurements, this trend is due to an increase in the mobility of the ions within the polymer. From Figure 5.17, it is clear that the sensing results also support the conclusion that the ions are more mobile within the membranes swollen with EMI-Tf ionic liquid than within those swollen with EMI-Im ionic liquid.

The ion mobility that is reflected in the sensing results can also be interpreted by measuring the rolloff in the charge-to-stress frequency response. As can be seen from Figure 5.18, the sensing frequency response exhibits a decrease in magnitude as frequency is increased. A very similar phenomenon is observed in the actuation strain-to-voltage measurement—see Figure 5.4. This rolloff is indicative of limited mobility of the ions within the polymer and the slope of the rolloff can be used as a qualitative measurement of ion mobility. As shown in Figure 5.18, the slope of the rolloff decreases with increasing content of ionic liquid and also with increasing ion size. As with the previous results,

this demonstrates that the mobility of the ions within an ionic liquid–swollen Nafion^{TM} membrane increases with increasing uptake of ionic liquid and increasing counterion size. This result also indicates that the EMI-Tf–swollen transducers exhibited less rolloff in their sensing response than the EMI-Im–swollen transducers.

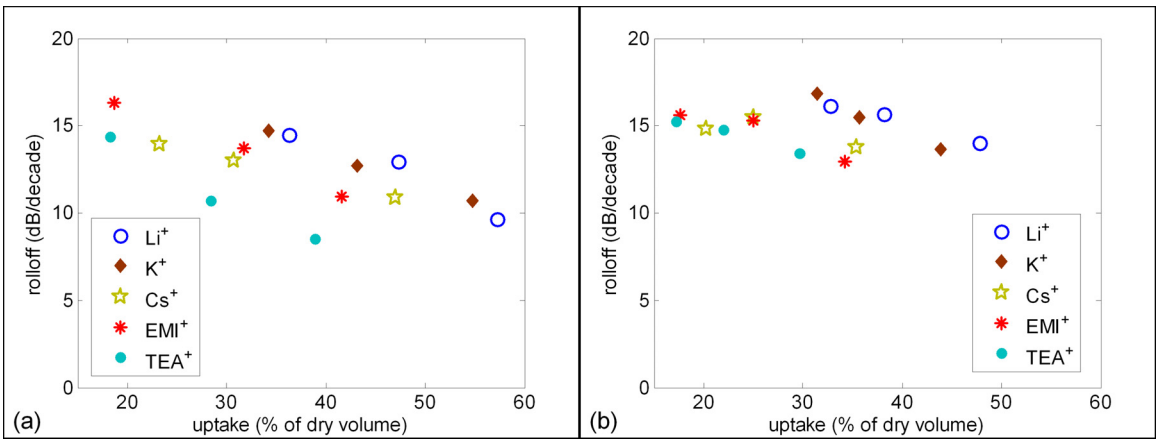

Figure 5.18: Rolloff in the stress sensitivity versus frequency response (between 5 and 20 Hz) for platinum plated Nafion^{TM} transducers in five different counterion forms and swollen with (a) EMI-Tf ionic liquid, (b) EMI-Im ionic liquid.

5.5 Summary and Conclusions

This chapter presented the results of an investigation into the transduction behavior of Nafion^{TM} membranes swollen with ionic liquids. The actuation behavior, ionic conductivity, and sensing performance were all evaluated for two different ionic liquids over a range of swelling levels in Nafion^{TM} membranes that were exchanged with five different cations. The results reveal that the actuation speed, ionic conductivity, and sensitivity are all increased by increasing the size of the counterion and by increasing the content of ionic liquid within the membrane. This is due to an increase in the mobility of the ions. Also, the EMI-Tf ionic liquid was found to result in superior performance than the EMI-Im ionic liquid. All of these findings are consistent with the results of the FTIR and NMR characterizations that were presented in Chapter 4.

The increase in ion mobility with increasing counterion size is consistent with the decrease in the critical uptake with increasing counterion size that was observed for the FTIR and NMR results. This indicates that the larger counterions are released from the exchange sites at a lower content of ionic liquid than the smaller counterions. Therefore, the

amount of excess, non–associated ionic liquid within the polymer increases with increasing counterion size, for a given swelling level. Also, the ionic conductivity for the unplated lithium–exchanged membranes exhibited an inflection point at and uptake of EMI-Tf ionic liquid of 0.67 mol/mol, which matches the critical uptake of EMI-Tf ionic liquid of 0.66 mol/mol that was determined from the FTIR testing. The ionic conductivity measurements obtained from the platinum plated membranes did not exhibit this inflection point because all of the samples were swollen with ionic liquid to levels above the critical uptake.

The EMI-Tf–swollen transducers were also found to exhibit higher ion mobility than those swollen with the EMI-Im ionic liquid. This was manifested in the actuation speed, ionic conductivity, and sensitivity. The limited mobility of the counterions in the EMI-Im–swollen membranes can be attributed to the disrpution of the clustered morphology of the Nafion^{TM} polymer by the EMI-Im ionic liquid. This was revealed by SAXS testing and was discussed in Chapter 3. This disruption has an inhibiting effect on the ion transport properties of the membrane and leads to decreased ion mobility.

Ionic liquids have been demonstrated to be viable diluents for electromechanical transducers based on Nafion^{TM} membranes. The next chapter will present a theoretical interpretation of the mechanisms of transduction based on the available data.

Chapter 6

Physical Interpretation of Transduction

Ionic liquid–swollen Nafion^{TM} membranes have been characterized using small angle X-ray scattering (SAXS), Fourier transform infrared spectroscopy (FTIR), and nuclear magnetic resonance spectroscopy (NMR). These membranes have also been plated with metal electrodes and characterized for their performance as electromechanical transducers. These results have offered insight into the internal structure of the membranes and the arrangement of the ions within. In this chapter, the results of these studies will be used to develop a theory of transduction. Specifically, this theory will be used to explain the mechanisms of charge motion in ionic liquid–swollen Nafion^{TM} membranes and the factors affecting these mechanisms.

6.1 Influence of Morphology on Transport Properties

In the course of this work, two different ionic liquids were studied: 1-ethyl-3-methylimidazolium trifluoromethanesulfonate (EMI-Tf) and 1-ethyl-3-methylimidazolium bis(trifluoromethanesulfonyl)imide (EMI-Im). Both of these ionic liquids possess a disubstituted imidazolium cation, but have different anions. These ionic liquids were chosen because many of their physical properties, including melting point, ionic conductivity, electrochemical stability window, and viscosity. However, whereas the EMI-Tf ionic liquid is water miscible, the EMI-Im ionic liquid is not. This difference was found to have a profound effect on the behavior of the membranes swollen with the ionic liquids.

The differences in the behavior of the two ionic liquids as diluents in Nafion^{TM} membranes can be explained by considering the way in which the ionic liquids affect the morphology of the membranes. It is well–known that the unique ion transport properties of Nafion^{TM} are due in part to the morphology of the polymer (46; 60; 89; 137; 138; 136). Nafion^{TM} polymers are believed to possess a quasi–phase separated morphology. The ionic groups (sulfonate exchange sites and counterions) and any diluent present in the polymer is thought to aggregate into clusters that are embedded in an inert fluorocarbon matrix phase (43; 44; 60; 46; 62; 27). The clusters are then interconnected by short, narrow channels that form conductive pathways within the membrane. It is this network of ionic clusters within the fluorocarbon polymer that allows ion transport to occur.

In Chapter 3, the results of a small angle X-ray scattering (SAXS) study on ionic liquid–swollen Nafion^{TM} membranes were presented. SAXS is a useful tool for probing the morphology of ionomers and has been used extensively to investigate the morphology of water–swollen Nafion^{TM} (44; 62; 27; 111). A typical SAXS result for a Nafion^{TM} membrane, exhibits an ionomer peak, a small–angle upturn, and a crystalline shoulder. The ionomer peak is associated with the average spacing between the ionic clusters (44; 62; 27), the small–angle upturn is attributed it to the presence of large–scale heterogenieties in the distribution of the clusters (62; 27; 89), and the crystalline shoulder is attributed to the presence of some crystallinity in the fluorocarbon backbone phase of the Nafion^{TM} polymer (89; 34; 86).

Therefore, of the three prominent features of the SAXS result for Nafion^{TM} two of them (the ionomer peak and the small–angle upturn) are related to the presence of the ionic clusters. For the membranes swollen with the EMI-Tf ionic liquid, both of these features were present in the SAXS results. This is illustrated in Figure 6.1, in whic the SAXS results for two Nafion^{TM} membranes in the potassium ion form are shown, one swollen with EMI-Tf ionic liquid and one swollen with EMI-Im ionic liquid. The absolute intensity is arbitrary and the curves have been shifted vertically for clarity. As can be seen, the membrane swollen with the EMI-Tf ionic liquid exhibits the classical ionomer peak and small angle upturn that are associated with the presence of the ionic clusters. However, for the membranes swollen with the EMI-Im ionic liquid, the features were not present.

The absence of the ionomer peak and low angle upturn in the SAXS results for the membranes swollen with EMI-Im ionic liquid indicates that the introduction of EMI-Im

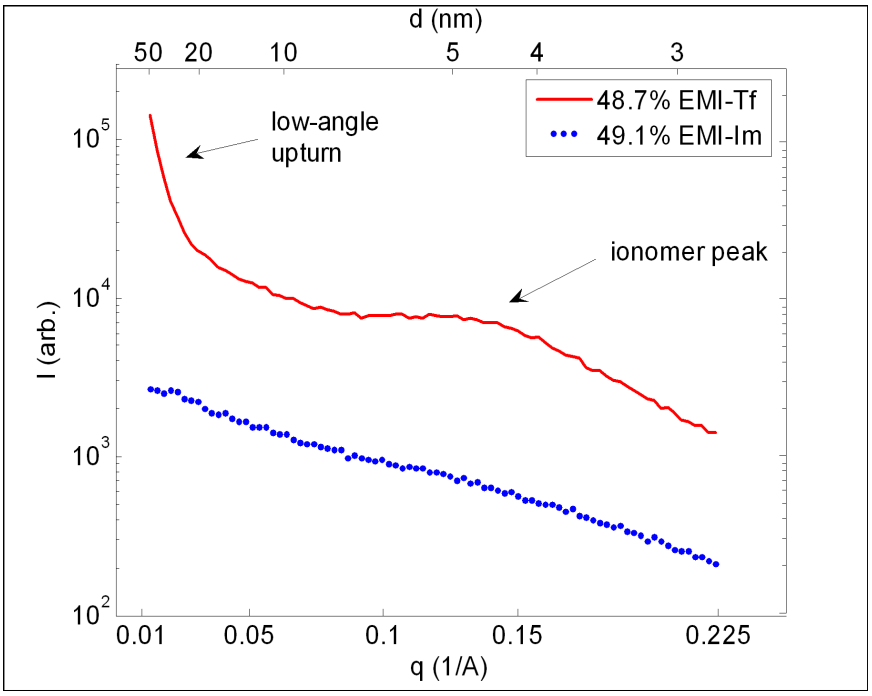

Figure 6.1: SAXS results for Nafion^{TM} membranes in the potassium ion form swollen with EMI-Tf ionic liquid and EMI-Im ionic liquid.

ionic liquid into the Nafion^{TM} membrane disrupts the clustered morphology of the polymer. By contrast, the SAXS results seem to indicate that the clustered morphology is preserved in the membranes swollen with EMI-Tf ionic liquid. This can be rationalized by considering the difference in the hydrophobicity of the two ionic liquids. The EMI-Tf ionic liquid is water miscible, and is therefore able to diffuse into the quasi–phase separated ionic regions of the membrane and not into the fluorocarbon regions. In effect, the EMI-Tf ionic liquid behaves similarly to water in this regard.

However, the EMI-Im ionic liquid is hydrophobic and therefore is not readily miscible with the hydrophilic ionic clusters. From the SAXS results it seems that this results in a fundamental change to the morphology of the polymer. The disruption of the clustered morphology by the EMI-Im ionic liquid most likely involves the partial incorporation of the ionic liquid into the fluorocarbon matrix phase of the membranes. The EMI-Im ionic liquid is hydrophobic and its anion is highly fluorinated. Therefore, it should be miscible with the fluorocarbon phase of the polymer. If the EMI-Im ionic liquid is at least partially absorbed into the fluorocarbon phase, then the mobility of the backbone chains of the Nafion^{TM} would be increased. This could lead to some of the fluorocarbon polymer diffusing into

the clusters, decreasing in the contrast between the two phases of the polymer. Based on the SAXS results, it seems that this is the case. The EMI-Im ionic liquid is incorporated into both phases of the membrane and results in partial homogenization of the polymer. With the distinction between the hydrophilic ionic phase and the hydrophobic fluorocarbon phase blurred, the conductive network of clusters is disrupted. The connectivity of the ionic domains is disturbed and the ion transport properties of the membranes are diminished.

This serves to explain the reason for the differences observed in the ionic conductivity between the membranes swollen with EMI-Tf ionic liquid and EMI-Im ionic liquid. However, the SAXS results also reveal useful information relating the size of the counterion and the uptake of ionic liquid to the arrangement of the counterions. The position of the ionomer peak in the SAXS result is related to the average spacing between the clusters. The SAXS test does not give any information relating to the actual size or shape of the clusters. However, by making some simplifying assumptions, conclusions regarding trends can be drawn. First, for the EMI-Tf ionic liquid, the assumption will be made that the ionic liquid is only absorbed into the clusters. This is reasonable because the ionic liquid is water miscible and should not be compatible with the hydrophobic fluorocarbon matrix phase. Second, the fluorocarbon matrix phase will be assumed to be incompressible. Based on these assumptions, an increase in the average spacing between the clusters can arise due to an increase in the average diameter of the clusters or by agglomeration of the clusters, resulting in a reduction in their number density. In the current scenario, both of these situations will be associated with an increase in the average size of the clusters.

The results presented in Chapter 3 revealed that the average spacing between the clusters increased with increasing size of the counterions and also with increasing content of ionic liquid. From the arguments presented above, this is indicative of an increase in the average size of the clusters. By increasing the size of the clusters, the volume of the conductive regions within the polymer is increased. Therefore, by increasing the cation size or the uptake of ionic liquid within the membrane, the ionic conductivity of the membrane is enhanced.

6.2 Theory of Ion Arrangements

In Chapter 4, the results of an infrared spectroscopy investigation on ionic liquid–swollen Nafion^{TM} membranes was presented. This investigation focused on the symmetric stretching frequency of the sulfonate group of the polymer. For dry membranes, the symmetric sulfonate stretching frequency was found to increase with decreasing counterion size. This increase is related to an increased polarization of the S—O dipole (83; 29; 75; 12). As the cation size is decreased, the positive charge of the cation becomes closer to the sulfonate exchange site. This increases the electric field in the vicinity of the exchange site and results in increased polarization of the sulfonate. Several researchers have noted that the symmetric sulfonate stretching peak shifts in frequency when the membrane is swollen with water (83; 29; 75; 12). This shift is caused by the solvation of the cations by water, which generates separation between the exchange sites and the cations and shields the sulfonates from the electric field of the cations. For all counterion forms of the membrane, the symmetric sulfonate stretching peak is found at about 1058 cm^{-1} in the fully water–swollen polymers (83).

Lowry and Mauritz have performed infrared investigations of Nafion^{TM} membranes at a number of intermediate water contents and have observed that the symmetric stretching frequency of the sulfonate group does not change above a certain critical uptake of water (83). This indicates that above this uptake the cations are effectively shielded from the exchange sites and that additional water does not participate in this shielding. This suggests that below the critical uptake, water that is introduced into the polymer enters into the hydration shells of the cations and anions and that above the critical uptake the water simply occupies the interstitial spaces of the polymer but does not associate with the ions. Of great interest is that Lowry and Maurtiz found the critical uptake to decrease as the size of the cation was increased (83). This is because the larger cations are less tightly bound to the sulfonate exchange sites. Therefore, less water is required to shield the exchange sites from the influence of the cations.

A similar study has been performed in this work on Nafion^{TM} membranes exchanged into various counterion forms and swollen over a range with EMI-Tf ionic liquid. The results of this study were remarkably similar to the results presented by Lowry and Mauritz. The symmetric sulfonate stretching frequency was found to be higher for smaller cations and

was found to shift upon the introduction of EMI-Tf ionic liquid into the polymer. At high swelling levels, the symmetric sulfonate stretching peak is located at 1052 cm^{-1} for all of the counterion forms of the membrane. The magnitude of the peak shift from the dry state to the swollen state is larger for the smaller counterions and is the smallest for the EMI^+ ion. This suggests that in the ionic liquid–swollen membranes, the EMI^+ ion of the ionic liquid is associated with the sulfonate exchange sites. Therefore, the counterions of the membrane are displaced away from the exchange sites. The displacement of the cations away from the exchange sites by the EMI^+ ions of the ionic liquid causes them to become associated with the trifluoromethanesulfonate ("triflate") anions of the EMI-Tf ionic liquid. This idea is also supported by FTIR evidence that examined the symmetric sulfonate stretching frequency of the triflate anion.

As with the results of Lowry and Mauritz, the infrared study with ionic liquid–swollen membranes reveals that the symmetric sulfonate stretching peak becomes constant above a certain critical uptake of ionic liquid. Therefore, the critical uptake is manifested as an inflection point in the FTIR and NMR results. The critical uptake is defined as the minimum amount of ionic liquid required to cause complete dissociation of the counterions from the sulfonate exchange sites. The critical uptake is found to decrease with increasing size of the counterions. The same behavior was observed by Lowry and Mauritz for Nafion^{TM} membranes swollen with water (83). The reason for this trend is that the electrostatic forces binding the cations to the exchange sites are inversely related to the distance between the positive and negative charge. Therefore, the larger cations are less strongly bound to the sulfonate exchange sites and are more easily displaced. Thus, less ionic liquid is required to cause this displacement.

Nuclear magnetic resonance (NMR) investigations were also performed to support the FTIR studies. In this work, NMR was used to probe the mobility of the counterions of the polymer when swollen with an ionic liquid. As ionic liquid is added to the membrane, the NMR results reveal that the mobility of the counterions is increased. This is consistent with the displacement of the counterions from the sulfonate exchange sites by the ionic liquid. In the swollen membranes, the counterions are associated with the anions of the exchange sites. This results in an increase in the counterion mobility because the anions of the ionic liquid are not bound to the polymer backbone and are therefore are relatively more free to move than the fixed sulfonate sites. The NMR results indicate that the counterion mobility

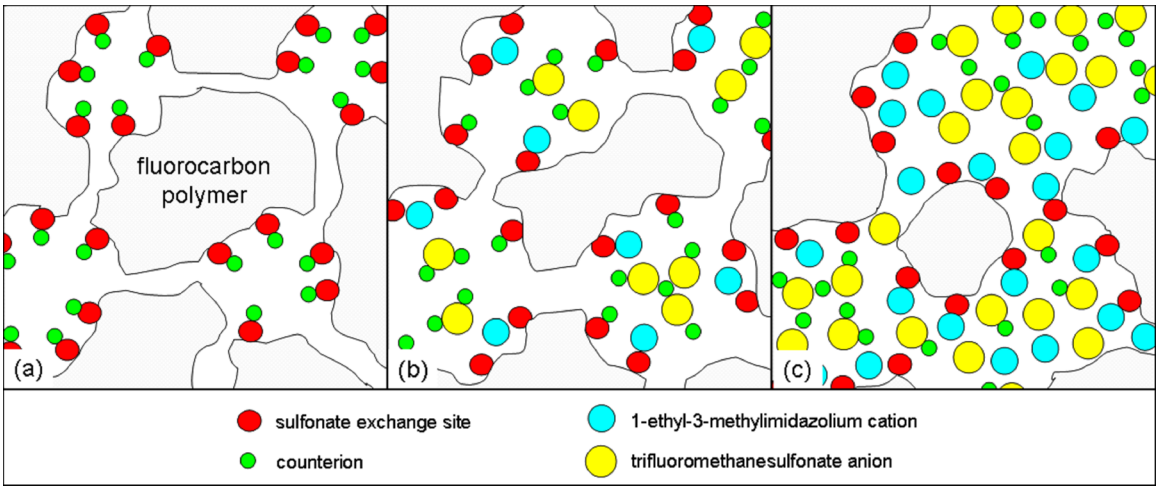

Figure 6.2: Theory of ion associations within a Nafion^{TM} membrane (a) dry, (b) swollen to below the critical uptake with EMI-Tf ionic liquid, (c) swollen above the critical uptake with EMI-Tf ionic liquid.

does not significantly increase above the critical uptake of ionic liquid. This is consistent with the notion that all of the counterions are displaced from the sulfonate exchange sites when the loading of ionic liquid has reached the critical uptake. The critical uptake that was determined from the NMR results was found to be in good agreement with the critical uptake that was determined from the FTIR results.

It is interesting to note that for all of the counterion forms of the membrane, the critical uptake was found to be less than 1.0 mole of ionic liquid per mole of exchange sites. This is surprising considering that the sulfonates, counterions, and EMI^+ and triflate ions of the ionic liquid are all univalent. Therefore, one counterion should be replaced by one EMI^+ ion when the membrane is swollen with ionic liquid. The results presented in Chapter 4 and summarized above suggest that each EMI^+ ion is able to effectively associate with more than one sulfonate exchange site. This suggests that each triflate anion also associates with more than one counterion. Above the critical uptake, additional ionic liquid that is added to the membrane does not participate in the dissociation of the counterions from the exchange sites. However, the additional ionic liquid does participate in the transport of the counterions within the membrane as will be described in the next section.

A graphical illustration of the evolution of the ion associations as EMI-Tf ionic liquid is added to an initially dry Nafion^{TM} membrane is shown in Figure 6.2. This illustration is based on conclusions drawn from the FTIR and NMR investigations. As can be seen, the

addition of the ionic liquid to the membrane displaces the counterions from the exchange sites. This is accomplished by association of the EMI^+ cations with the exchange sites and the triflate anions with the counterions. Above the critical uptake of ionic liquid, many of the ionic liquid molecules do not participate in these associations. The ionic liquid also serves to expand the ionic clusters and interconnecting channels within the membrane. This expansion increases the connectivity of the conductive pathways in the polymer, which in addition to the displacement of the counterions from the exchange sites, leads to increased ion mobility in the membranes.

6.3 Mechanism of Charge Transport

Electromechanical transduction in ionomer membranes is related directly to motion of charge within the membranes (117; 97; 2; 79). The amount of strain that can be generated by an ionomeric membrane actuator is proportional to the displaced charge (2; 79), and the speed of the actuation is proportional to the ionic conductivity (see Figure 5.15). Therefore, by understanding the charge transport mechanisms in ionic liquid–swollen Nafion^{TM} membranes, a physical interpretation of transduction can be gained.

Based on the results presented in this dissertation, several key concepts describing the interaction between the ionic liquid and the Nafion^{TM} polymer have been presented. First, the SAXS results demonstrated that the structure and particularly the hydrophobicity of the ionic liquid has a dramatic effect on the morphology of the polymer. NMR and ionic conductivity testing revealed that through its effect on the morphology, the ionic liquid can dramatically alter the mobility of the ions within the polymer. The FTIR and NMR testing also introduced the idea of a critical uptake of ionic liquid. This critical uptake is the minimum amount of ionic liquid that is required to release all of the counterions from the sulfonate exchange sites. Testing has revealed that this critical uptake exhibits a decreasing trend with increasing counterion size. The predominant reason for this trend is that the electrostatic binding energy between the counterions and the exchange sites is reduced as the size of the counterions is increased. However, the effect of the counterion radius on the size of the clusters within the polymer almost certainly plays a role as well. There is also likely a small contribution due to the decreased binding energy between the counterion and the triflate anion of the ionic liquid with increasing counterion size.

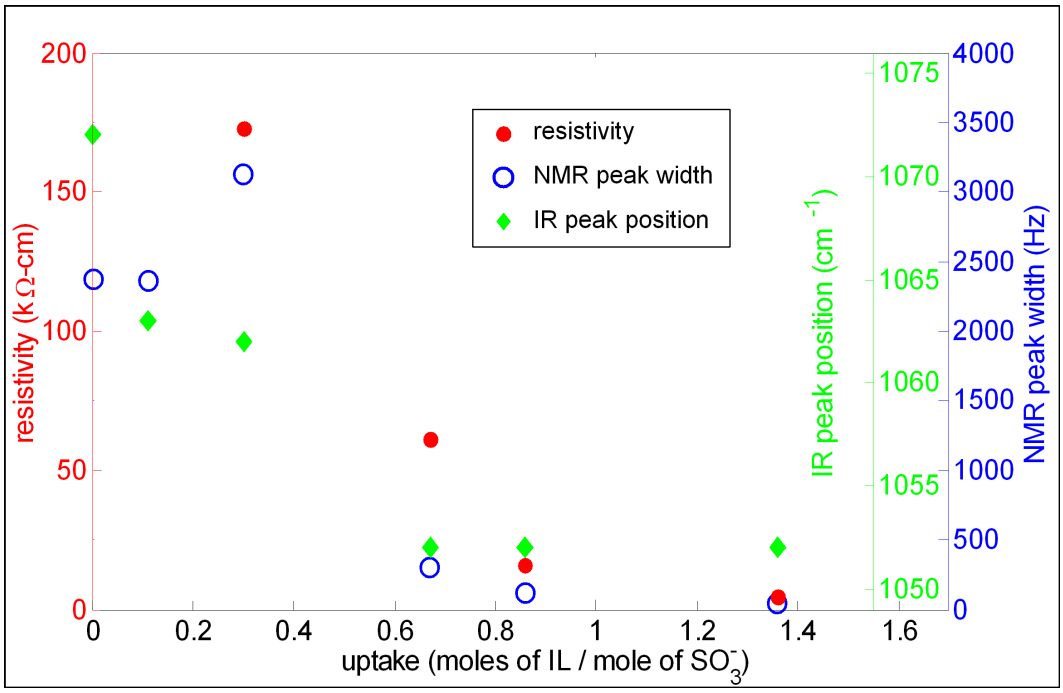

Figure 6.3: Resistivity, NMR peak width, and symmetric sulfonate stretching frequency versus uptake for Nafion^{TM} membranes in the lithium ion form and swollen with EMI-Tf ionic liquid.

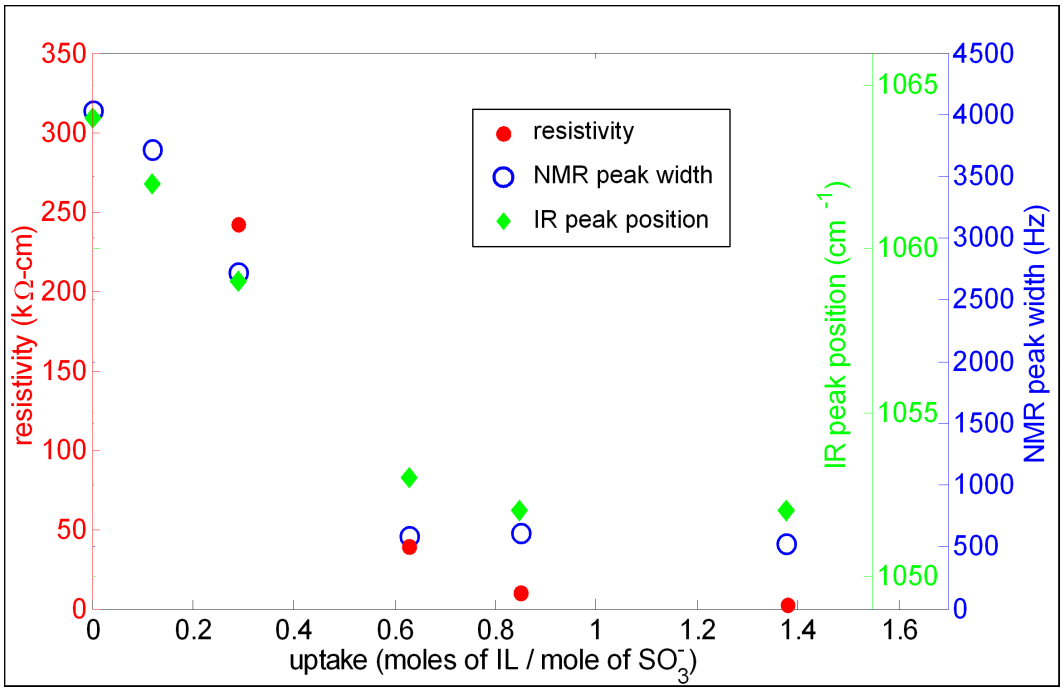

Figure 6.4: Resistivity, NMR peak width, and symmetric sulfonate stretching frequency versus uptake for Nafion^{TM} membranes in the sodium ion form and swollen with EMI-Tf ionic liquid.

It is this concept of the critical uptake that will be used to explain the mechanisms of charge transport within ionic liquid–swollen Nafion^{TM} membranes. Figures 6.3 and 6.4 show the FTIR results, NMR results, and ionic conductivity results for Nafion^{TM} membranes swollen with EMI-Tf ionic liquid and in the lithium and sodium forms, respectively. The resistivity in these plots is the inverse of the ionic conductivity and was obtained for the unplated membranes using the method of Zawodzinski et al. as described in Section 5.4.2. As can be seen, all three results exhibit an inflection point at the critical uptake (determine to be 0.66 mol/mol for lithium and 0.65 mol/mol for sodium). This indicates that the behavior and properties of the membranes undergo a fundamental change at this loading of EMI-Tf ionic liquid. As stated before, the critical uptake is the minimum loading of ionic liquid required to displace all of the counterions from the sulfonate exchange sites.

Below the critical uptake, the resistivity decreases substantially, indicating that the ability of the ions to move about within the polymer is greatly enhanced by their dissociation from the sulfonate sites by the ionic liquid. The FTIR results confirmed that the counterions are associated with the triflate anions of the ionic liquid in the swollen membranes. The NMR results revealed that the mobility of the counterions is higher in this state than when associated with the sulfonate exchange sites. This is expected considering that the sulfonate exchange sites are covalently bound to the side chains of the Nafion^{TM} polymer, whereas the triflate anions are not. This change of state also leads to a decrease in the measured resistivity of the material. However, at the critical uptake, the resistivity exhibits an inflection point. This indicates that the mechanism of charge motion is changed above the critical uptake. In fact, this is the case. Below the critical uptake of ionic liquid, all of the triflate anions of the ionic liquid are associated with at least one counterion. Therefore, apart from small–scale rotational motion and local cooperative motion with the triflate anion, the counterions cannot effectively move about within the polymer. This is because no adjacent unoccupied anionic sites exist for the counterion to move to. However, above the critical uptake, the additional ionic liquid that is introduced is not involved in the displacement of the counterions from the exchange sites. Therefore, the additional triflate anions are unoccupied and are available for association with a counterion. By "hopping" from one unoccupied site to the next, the counterions can transport through the membrane. As more ionic liquid is added to the membrane, more unoccupied sites are present, thus increasing the ionic conductivity of the polymer. Therefore, the figure of metrit is the loading of

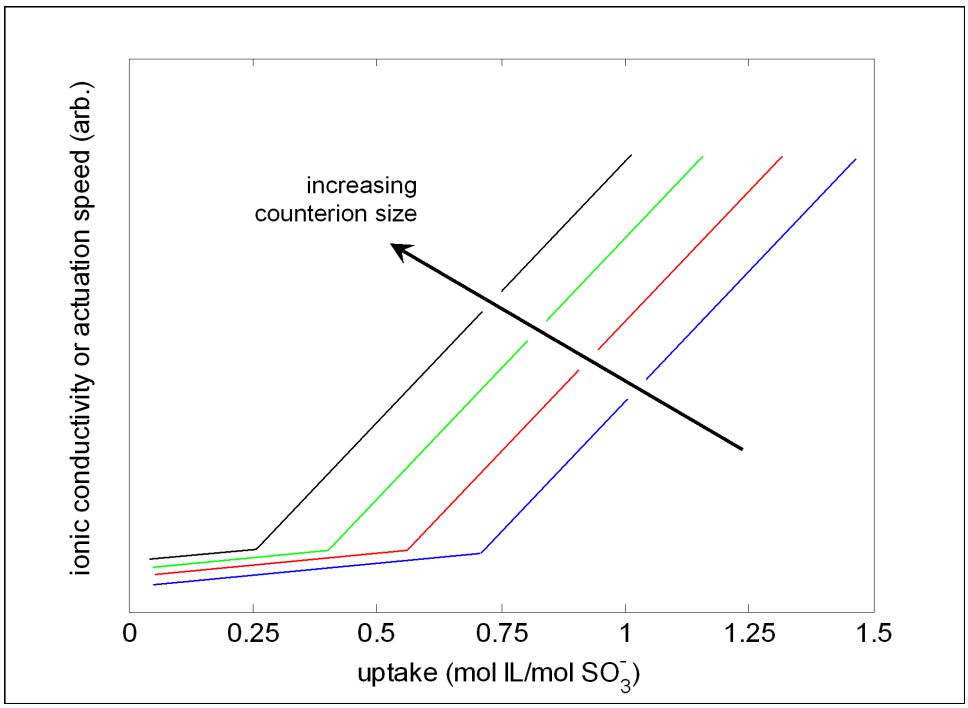

Figure 6.5: Predicted trend of ionic conductivity as a function of counterion size and loading of ionic liquid.

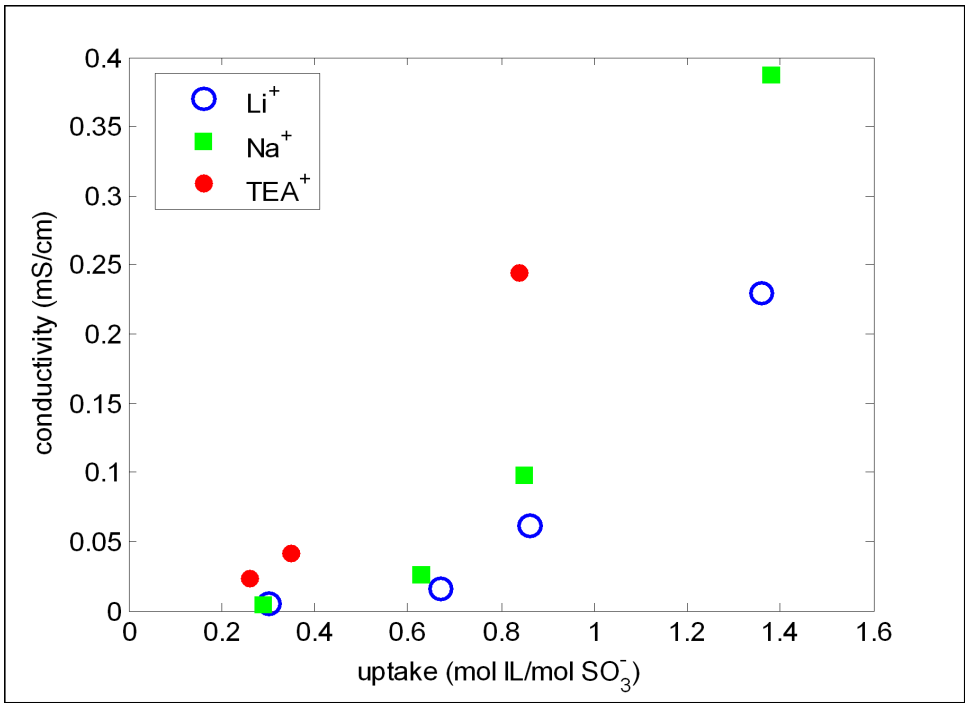

Figure 6.6: Measured ionic conductivity for Nafion^{TM} membranes in the Li^+, Na^+, and TEA^+ form swollen with EMI-Tf ionic liquid. The critical uptake can be seen as an inflection point in the curves.

ionic liquid *above* the critical uptake. This is because only the ionic liquid above the critical uptake able to significantly enhance the ionic conductivity by providing unoccupied anionic sites available for charge transport. Because the critical uptake decreases with increasing size of the counterions, this argument predicts that the ionic conductivity will be higher for membranes exchanged with larger counterions, for a given loading of ionic liquid. This is depicted in Figure 6.5.

In fact, experiment has revealed that this is the case—see Figure 6.6. This figure presents ionic conductivity versus uptake of ionic liquid for membranes swollen with EMI-Tf ionic liquid and in the lithium, sodium, and tetraethylammonium form. In this case the membranes were unplated and the ionic conductivity was measured using the method of Zawodzinski et al. As can be seen, the ionic conductivity increases with increasing content of ionic liquid. Also, for a given uptake of ionic liquid, the ionic conductivity increases with increasing counterion size. This is because the critical uptake of ionic liquid decreases with increasing size of the counterions. As the critical uptake of ionic liquid decreases, the amount of "free" ionic liquid within the membrane increases, for a given uptake. This free ionic liquid is responsible for the transport of the counterions within the membrane and the ionic conductivity increases as the amount of free ionic liquid increases.

The critical uptake can be seen as an inflection point in the ionic conductivity curve. For the lithium and sodium form samples, the inflection point closely matches with the critical uptake of 0.66 mol/mol for lithium and 0.65 mol/mol for sodium that was determined from the spectroscopic investigations. For the TEA form samples, the critical uptake was determined to be 0.44 mol/mol of EMI-Tf ionic liquid. The critical uptake for the TEA–exchanged membranes is not observed in Figure 6.6 due to the small number of data points. By the argument that has been presented, if the conductivity is plotted against the loading of ionic liquid normalized by the critical uptake, the data should reduce to a single curve—see Figure 6.7. The scale of the x–axis in this figure is the uptake of ionic liquid divided by the critical uptake (f_c) and is unitless. Where available, the critical uptake determined from the NMR analysis was used for this calculation. Otherwise, the critical uptake determined from the FTIR analysis was used. As can be seen from Figure 6.7, the discrepancies between the three curves are significantly reduced by this approach. This supports the argument that the observed effect of the counterion size on the ionic conductivity is related to the effect of the counterion size on the critical uptake.

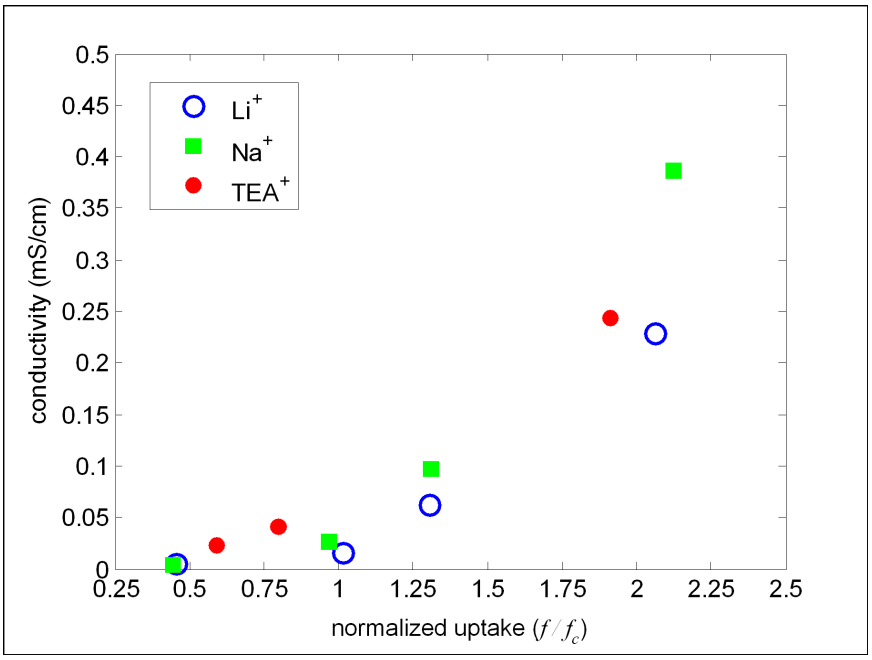

Figure 6.7: Ionic conductivity versus the uptake of EMI-Tf ionic liquid normalized by the critical uptake for Nafion^{TM} membranes in the lithium, sodium, and TEA ion forms.

A similar trend to the one shown in Figure 6.6 was also observed for the response speed of the plated EMI-Tf–swollen membranes. This result was presented in Section 5.4.1, Figure 5.8. For that data, all of the samples were swollen above the critical uptake with EMI-Tf ionic liquid and so an inflection point in the curves was not evident. Also, the actuation speed was observed to be strongly dependent on both the uptake of ionic liquid and the counterion size. Based on the theory of charge transport that has been presented, this dependence on the counterion size is due to the effect that the counterion size has on the critical uptake of ionic liquid. This is demonstrated in Figure 6.8. As can be seen, when the uptake of ionic liquid is normalized by the critical uptake, the actuation speed follows a single, universal trend for all of the counterion forms of the membrane. This result provides supporting evidence for the model for counterion transport within the EMI-Tf–swollen membranes by hopping between triflate anions.

The model suggests that the ionic liquid that is initially added to the membrane serves to displace the counterions from the exchange sites. The counterions then associate with the anions of the ionic liquid. Above the critical uptake, additional ionic liquid does not participate in this exchange. However, this "free" ionic liquid is critical to the charge

transport mechanism in that the counterions hop from one free anion to the next in conducting through the polymer. As the counterion size is increased, the critical uptake is decreased. Therefore, for a given swelling level, the percentage of the ionic liquid available for cation transport will increase with increasing size of the counterions. Thus, the figure of merit for ionic liquid–swollen Nafion^{TM} membranes is not the absolute loading of ionic liquid, but the loading above the critical uptake. This can be clearly seen in Figure 6.8 in which the actuation speed, when plotted versus the uptake normalized by the critical uptake, exhibits a single, universal curve, independent of the counterion size.

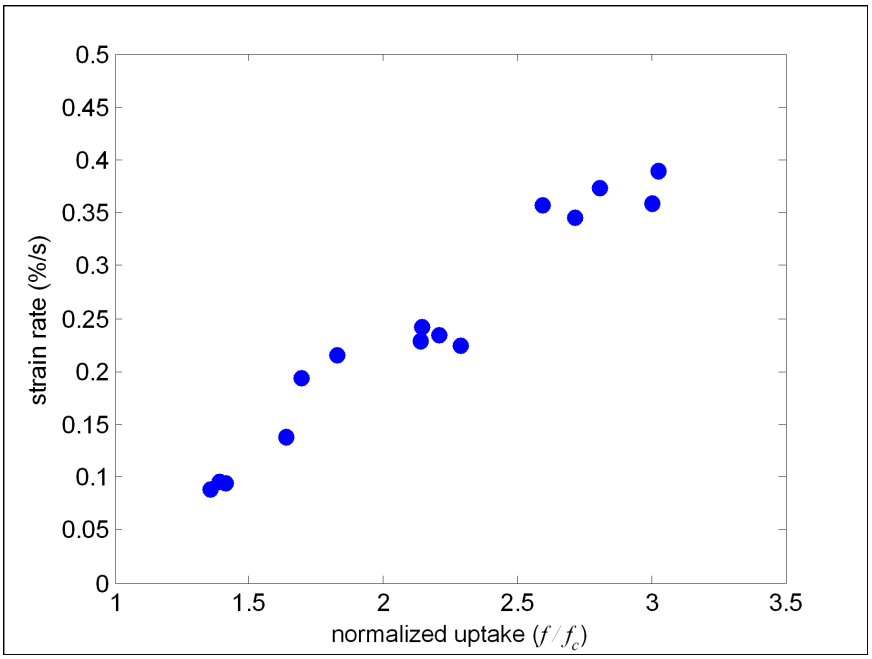

Figure 6.8: Actuation speed versus the normalized uptake of EMI-Tf for Nafion^{TM} membranes in five different counterion forms.

Chapter 7

Conclusions

The purpose of this research has been to demonstrate the use of ionic liquids as diluents for ionomeric polymer transducers based on Nafion^{TM} membranes. The role of the ionic liquid is to facilitate ion motion within the membrane and allow the electromechanical transduction to occur. Traditionally, water has been used in this capacity. However, the use of water imposes limits on the performance of the transducers, particularly in regard to their long–term stability in a non–aqueous environment. To overcome these limitations, methods have been developed to replace the water with an ionic liquid. The ionic liquid–swollen transducers have been studied by a variety of techniques in order to make determinations regarding the transduction mechanisms in these materials.

7.1 Summary and Conclusions

Ionic liquids have been shown to be viable diluents for ionomeric membrane transducers. In the current work, Nafion^{TM} membranes swollen with two ionic liquids were studied by small angle X-ray scattering (SAXS), Fourier transform infrared spectroscopy (FTIR), nuclear magnetic resonance spectroscopy (NMR), and by characterization of their transduction behavior.

As compared to water–swollen transducers, a Nafion^{TM} actuators swollen with ionic liquid exhibited a slower response. Also, the ionic liquid–swollen actuators were found to not exhibit the characteristic back–relaxation that has often been observed in water–swollen materials. Characterization of the long–term stability revealed that the strain generated by an ionic liquid–swollen actuator decreased by less than 30% after continuous operation for

over 250,000 cycles with a 1.5 V, 2 Hz sine input in air. By contrast, the strain generated by a water–swollen actuator driven with the same signal decreased by 96% after only 3600 cycles.

SAXS results revealed that the water miscible EMI-Tf ionic liquid preserves the quasi–phase separated morphology of the Nafion^{TM} membrane, in which the ionic groups and diluent aggregate into clusters that are embedded in an inert, semi–crystalline fluorocarbon matrix and form an interconnected network. However, SAXS revealed that the EMI-Im ionic liquid disrupts this morphology, lessening the constrast between the two phases and possibly leading to some mixing of the phases. This disruption interrupts the connectivity of the networked clusters and inhibits the ionic conductivity of the polymers swollen with the EMI-Im ionic liquid. The SAXS also reveals that the mean spacing between the ionic clusters is increased by increasing the uptake of ionic liquid and by increasing the size of the counterions. Based on theories of the mechanisms of cluster swelling, this increase in the mean intercluster spacing is thought to arise from an increase in the mean size of the clusters themselves. Therefore, the size of the clusters increases with increasing uptake of ionic liquid and increasing counterion size. This increase in cluster size enhances the ability of ions to transport within the conductive channels of the polymer.

FTIR and NMR investigations have also been performed on ionic liquid–swollen Nafion^{TM} in an effort to elucidate the predominant ion associations within the membranes. These results reveal that the cations of the ionic liquid displace the counterions of the polymer away from the sulfonate exchange sites. The counterions then associate with the anions of the ionic liquid. The mobility of the counterions is increased by this exchange due to the increased mobility of the ionic liquid anions as compared to the relatively fixed sulfonate exchange sites. From the FTIR and NMR results, the concept of a critical uptake of ionic liquid was introduced. The critical uptake is the minimum amount of ionic liquid that is required for all of the counterions to be displaced from the sulfonate exchange sites. From the spectroscopic investigations, it has been shown that the critical uptake decreases with increasing size of the counterions. This is because the electrostatic binding energy between the counterions and the exchange sites decreases with increasing counterion size. Therefore, as the counterion size is increased, less ionic liquid is required to displace the counterions. Above the critical uptake, additional ionic liquid does not associate with the counterions or the exchange sites.

Characterization of the electromechanical transduction behavior of the membranes revealed that the speed of the actuation response and the ionic conductivity were increased by increasing the size of the counterions and by increasing the uptake of ionic liquid within the membrane. The actuation speed was observed to be linearly proportional to the ionic conductivity, with a constant of proportionality very close to 1.0. Ionic conductivity measurements of some of the membranes revealed an inflection point very near the critical uptake of ionic liquid, as determined from the spectroscopic investigations. This suggests that the charge transport mechanism undergoes a change at the critical uptake.

Above the critical uptake, the transport of counterions within the polymer is suggested to rely on the presence of ionic liquid molecules that are not associated with the counterions or the exchange sites. The "free" ionic liquid molecules represent available anionic sites for the counterions to occupy. By "hopping" between adjacent sites, the counterions are able to conduct through the polymer. As more available sites are introduced into the polymer, the freedom of movement of the counterions increases. The figure of merit for ionic liquid–swollen Nafion^{TM} membranes is the loading of ionic liquid *above* the critical uptake. Therefore, for a given loading of ionic liquid, the ionic conductivity will increase as the critical uptake is reduced. This is because as the critical uptake is reduced, more of the ionic liquid will be able to participate in the transport of the counterions. Because the critical uptake decreases with increasing counterion size, this leads to increasing ionic conductivity (and actuation speed) with increasing counterion size. This model of charge transport is able to connect the results of the spectroscopic investigations to the results of the electromechanical characterizations. The model is supported by calculations that demonstrate that the effects of the counterion size and the uptake of ionic liquid on the electromechanical response are accounted for by considering the critical uptake as the relevant parameter of the model.

Ionic liquids are effective diluents for ionomeric polymer transducers. The function of the ionic liquid is to enhance the ionic conductivity of the polymer. The ionic liquid mobilizes the counterions of the membrane by displacing them from the sulfonate exchange sites. The ionic liquid also swells the conductive phase of the polymer, enhancing the connectivity of the ionic cluster network. At a certain critical uptake of ionic liquid, all of the counterions have been released from the exchange sites. Above this critical uptake, the counterions are able to transport through the expanded conductive network by hopping

along the anions of the ionic liquid. The ionic conductivity of the membranes is enhanced by increasing the uptake of ionic liquid because more anionic sites are available to participate in this hopping mechanism.

7.2 Significant Contributions

This research has demonstrated the use of ionic liquids as diluents for ionomeric polymer transducers. A significant contribution of this work was the development of methods to incorporate ionic liquids into Nafion^{TM} membranes and to apply metal electrodes to ionic liquid–swollen Nafion^{TM} membranes. Characterization of the actuation response of these materials reveals that they possess much greater stability when operated in air than their water–swollen counterparts. The low–frequency response is also enhanced by the use of an ionic liquid.

Additionally, the membranes have been investigated over a range of experimental parameters, including the structure of the ionic liquid, the counterion within the membrane, and the loading of ionic liquid within the membrane. This investigation elucidated effect of these experimental parameters on the morphology of the membranes and the ion associations within the membranes. Independently, the electromechanical transduction behavior of the membranes was investigated over the same range of experimental parameters. Based on these investigations, a model was formulated to explain the charge transport mechanisms within the ionic liquid–swollen Nafion^{TM} membranes. This model is able to account for the effect of the counterion size and loading of ionic liquid on the transduction behavior.

This work has represented the first demonstration of the use of an ionic liquid as a diluent for Nafion^{TM} membrane transducers. In addition to demonstrating improved performance over the current state-of-the-art, this research has yeilded a model that can be used to guide future improvements to these transducers through tailoring of the ionic liquids and ionomer membrane.

7.3 Recommendations for Future Work

This work has contributed to the development of improved ionomeric transducers by demonstrating the use of ionic liquids to replace water as the diluent in these devices. Also, an understanding of the transduction mechanisms in the ionic liquid–swollen ionomers has been

gained. Some possible areas of continued research include:

- Although Nafion^{TM} membranes are the most commonly used for ionomeric polymer transducers, this is more by neccessity than by design. An important area of research is the development of new ionomer materials that offer improved transduction performance due to their molecular structure. The development of improved ionomers should seek to enhance the interactions that lead to favorable performance, based on the revelations presented in this work.

- In addition to the design of new ionomers, research to discover new ionic liquids is also possible. An important aspect of the ionic liquid is its viscosity. If lower viscosity ionic liquids could be developed then the actuation speed of ionomeric transducers could be increased. The desired structure of the ionic liquid may be predicted based on the understanding of the charge transport mechanisms presented in this research. For example, in order to ensure favorable interactions with the hydrophilic ionic groups of the ionomer, the ionic liquid should be water miscible.

- A key aspect of the proposed model of charge transport in ionic liquid–swollen Nafion^{TM} membranes is the critical uptake. However, due to the large range of swelling levels of ionic liquid that were investigated, the critical uptake was difficult to resolve for some counterion forms of the membranes. In order to investigate this phenomenon in more detail, additional data near the critical uptake should be collected.

- One of the obstacles that hindered progress in the initial stages of this research was the problem of electrode cracking when the Nafion^{TM} membranes were swollen with ionic liquid. Although this was overcome by the application of gold leaf to the membranes after the swelling process, the gold leaf is highly fragile and subject to damage. An important contribution would be the development of an improved electroding process that yeilds a more robust transducer.

Bibliography

[1] B. J. Akle, M. D. Bennett, and D. J. Leo. High–strain ionomeric–ionic liquid electroactive actuators. *Sensors and Actuators A: Physical*, 2005. in press.

[2] B. J. Akle, D. J. Leo, M. A. Hickner, and J. E. McGrath. Correlation of capacitance and actuation in ionomeric polymer transducers. *Journal of Materials Science*, 40:1–10, 2005.

[3] P. Aldebert, M. Guglielmi, and M. Pineri. Ionic conductivity of bulk, gels, and solutions of perfluorinated ionomer membranes. *Polymer Journal*, 23:399–406, 1991.

[4] K. Asaka and K. Oguro. Bending of polyelectrolyte platinum composites by electric stimuli part II. response kinetics. *Journal of Electroanalytical Chemistry*, 480:186–198, 2000.

[5] Y. Bar-Cohen and S. Leary. Electro-active polymer (EAP) characterization methods. In *EAP Actuators and Devices*, volume 3987, pages 12–16. SPIE, 2000.

[6] Y. Bar-Cohen, S. Leary, M. Shahinpoor, J. Harrison, and J. Smith. Flexible low-mass devices and mechanisms actuated by electroactive polymers. In *EAP Actuators and Devices*, volume 3669, pages 51–56. SPIE, 1999.

[7] Y. Bar-Cohen, S. Leary, M. Shahinpoor, J. O. Harrison, and J. Smith. Electro-active polymer (EAP) actuators for planetary applications. In *EAP Actuators and Devices*, volume 3669, pages 57–63. SPIE, 1999.

[8] M. Bennett and D. Leo. Ionic liquids as stable solvents for ionic polymer transducers. *Sensors and Actuators A: Physical*, 115:79–90, 2004.

[9] M. D. Bennett and D. J. Leo. Manufacture and characterization of ionic polymer transducers employing non-precious metal electrodes. *Smart Materials and Structures*, 12:424–436, 2003.

[10] P. Bonhôte, A. Paula Dias, N. Papageorgiou, K. Kalyanasundaram, and M. Grätzel. Hydrophobic, highly conductive ambient-temperature molten salts. *Inorganic Chemistry*, 35:1168–1178, 1996.

[11] C. Brevard. *NMR of Newly Accesible Nuclei, volume 1*, chapter 1, pages 3–19. Academic Press, 1983.

[12] K. M. Cable, K. A. Mauritz, and R. E. Moore. Effects of hydrophilic and hydrophobic counterions on the coloumbic interactions in perfluorosulfonate ionomers. *Journal of Polymer Science: Part B: Polymer Physics*, 33:1065–1072, 1995.

[13] J. Ceynowa. Electron microscopy investigation of ion exchange membranes. *Polymer*, 19:73–76, 1977.

[14] M. Chomakova-Haefke, R. Nyffenegger, and E. Schmidt. Structure reorganization in polymer films of nafion due to swelling studied by scanning force microscopy. *Applied Physics A: Solids and Surfaces*, 59:151–153, 1994.

[15] E. I. Cooper and E. J. O'Sullivan. New,stable, ambient-temperature molten salts. In *Proceedings of the Eighth Interational Symposium on Molten Salts*, pages 386–396. The Electrochemical Society, 1992.

[16] P. de Gennes, K. Okumura, M. Shahinpoor, and K. J. Kim. Mechanoelectric effects in ionic polymer gels. *Europhsics Letters*, 50:513–518, 2000.

[17] A. E. Derome. *Modern NMR Techniques for Chemistry Research*. Pergamon Press, 1987.

[18] J. Ding, D. Zhou, G. Spinks, G. Wallace, S. Forsyth, M. Forsyth, and D. MacFarlane. Use of ionic liquids as electrolytes in electromechanical actuator systems based on inherently conducting polymers. *Chemistry of Materials*, 15:2392–2398, 2003.

[19] M. Doyle, S. Choi, and G. Proulx. High-temperature proton conducting membranes

based on perfluorinated ionomer membrane–ionic liquid composites. *Journal of the Electrochemical Society*, 147:34–37, 2000.

[20] M. Doyle, M. Lewittes, M. Roelofs, and S. Perusich. Ionic conductivity of nonaquoues solvent–swollen ionomer membranes based on fluorosulfonate, fluorocarboxylate, and sulfonate fixed ion groups. *Journal of Physical Chemistry B*, 105:9387–9394, 2001.

[21] M. Doyle, M. Lewittes, M. Roelofs, S. Perusich, and R. Lowrey. Relationship between ionic conductivity of perfluorinated ionomeric membranes and nonaqueous solvent properties. *Journal of Membrane Science*, 184:257–273, 2001.

[22] DuPont. *Nafion Membranes NE-112, NE-1135, N-115, N-117*. Product Information.

[23] Eamex Corporation Website. http://www.eamex.co.jp/index_e.html, 2005.

[24] A. Eisenberg, B. Hird, and R. Moore. A new multiplet-cluster model for the morphology of random ionomers. *Macromolecules*, 23:4098–4107, 1990.

[25] A. Eisenberg and J.-S. Kim, editors. *Introduction to Ionomers*. Wiley, 1998.

[26] J. Elliott and S. Hanna. A model-independent maximum-entropy method for the inversion of small-angle x-ray diffration patterns. *Journal of Applied Crystallography*, 32:1069–1083, 1999.

[27] J. Elliott, S. Hanna, A. Elliott, and G. Cooley. Interpretation of the small angle x-ray scattering from swollen and oriented perfluorinated ionomer membranes. *Macromolecules*, 33:4161–4171, 2000.

[28] M. Falk. An infrared study of water in perfluorosulfonate (nafion) membranes. *Canadian Journal of Chemistry*, 58:1495–1501, 1980.

[29] M. Falk. *Perfluorinated Ionomer Membranes*, chapter 8, pages 139–170. American Chemical Society, 1982.

[30] K. Farinholt and D. J. Leo. Modeling of electromechanical charge sensing in ionic polymer transducers. *Mechanics of Materials*, 36:421–433, 2004.

[31] T. C. Farrar and E. D. Becker. *Pulse and Fourier Transform NMR, Introduction to Theory and Methods*. Academic Press, 1971.

[32] W. Ford and T. Hart. Viscosities and conductivities of the liquid salt triethyl-*n*-hexylammonium triethyl-*n*-hexylboride and its benzene solutions. *Journal of Physical Chemistry*, 80:1002–1004, 1976.

[33] J. W. Franklin. Electromechanical modeling of encapsulated ionic polymer transducers. Master's thesis, Virginia Tech, 2003.

[34] M. Fujimura, T. Hashimoto, and H. Kawai. Small-angle x-ray scattering study of perfluorinated ionomer membranes. 1. origin of two scattering maxima. *Macromolecules*, 14:1309–1315, 1981.

[35] M. Fujimura, T. Hashimoto, and H. Kawai. Small-angle x-ray scattering study of perfluorinated ionomer membranes. 2. models for ionic scattering maxima. *Macromolecules*, 15:136–144, 1982.

[36] J. Fuller, A. Breda, and R. Carlin. Ionic liquid–polymer gel electrolytes. *Journal of the Electrochemical Society*, 144:L67–L70, 1997.

[37] J. Fuller and R. Carlin. Facile preparation of tetrafluoroborate and trifluoromethanesulfonate room-temperature ionic liquids. In *Proceedings of the Eleventh International Symposium on Molten Salts*, pages 227–230. The Electrochemical Society, 1998.

[38] J. Fuller and R. Carlin. Ionic liquid–polymer impregnated nafion electrolytes. In *Proceedings of the Twelfth International Symposium on Molten Salts*, pages 27–31. The Electrochemical Society, 1999.

[39] A. Garton. *Infrared Spectroscopy of Polymer Blends, Composites, and Surfaces.* Hanser Publishers, 1992.

[40] G. Gebel, P. Aldebert, and M. Pineri. Swelling study of perfluorosulphonated ionomer membranes. *Polymer*, 34:333–339, 1993.

[41] G. Gebel and J. Lambard. Small-angle scattering study of water-swollen perfluorinated ionomer membranes. *Macromolecules*, 30:7914–7920, 1997.

[42] G. Gemmecker. Advanced NMR spectroscopy. course taught at the University of Wisconsin, Madison. Notes available online at www.spectroscopynow.com, 1999.

[43] T. Gierke. Ionic clustering in "nafion" perfluorosulfonic acid membranes and its relationship to hydroxyl rejection and chlor–alkali efficiency. In *presented at the 152nd Meeting, Atlanta, GA*, page 319C. The Electrochemical Society, 1977.

[44] T. Gierke, G. Munn, and F. Wilson. The morphology in nafion perfluorinated membrane products, as determined by wide- and small-angle x-ray studies. *Journal of Polymer Science, Polymer Physics Edition*, 19:1687–1704, 1981.

[45] T. Gierke, G. Munn, and F. Wilson. *Perfluorinated Ionomer Membranes*, chapter 10, pages 195–216. American Chemical Society, 1982.

[46] T. D. Gierke and W. Y. Hsu. *Perfluorinated Ionomer Membranes*, chapter 13, pages 283–307. American Chemical Society, 1982.

[47] A. J. Grodzinsky and J. R. Melcher. Electromechanics of deformable charged polyelectrolyte membranes. In *Proceedings of the 27th Annual Conference on Engineering in Medicine and Biology*, volume 16, page 485. Alliance for Engineering in Medicine and Biology, 1974. paper 53.2.

[48] A. J. Grodzinsky and J. R. Melcher. Electromechanical transduction with charged polyelectrolyte membranes. *IEEE Transactions on Biomedical Engineering*, BME-23(6):421–433, 1976.

[49] S. Guo, T. Fukuda, N. Kato, and K. Oguro. Development of underwater microrobot using ICPF actuator. In *International Conference on Robotics and Automation*, pages 1829–1834. IEEE, 1998.

[50] S. Guo, T. Fukuda, K. Kosuge, F. Arai, K. Oguro, and M. Negoro. Micro catheter system with active guide wire. In *International Conference on Robotics and Automation*, pages 79–84. IEEE, 1995.

[51] R. Hagiwara, T. Hirashige, T. Tsuda, and Y. Ito. Acidic 1-ethyl-3-methylimidazolium fluoride: A new room temperature ionic liquid. *Journal of Fluorine Chemistry*, 99:1–3, 1999.

[52] R. Hagiwara and Y. Ito. Room temperature ionic liquids of alkylimidazolium cations and fluoroanions. *Journal of Fluorine Chemistry*, 105:221–227, 2000.

[53] R. Hagiwara, K. Matsumoto, Y. Nakamori, T. Tsuda, Y. Ito, H. Matsumoto, and K. Momota. Physiochemical properties of 1,3-dialkylimidazolium fluorohydrogenate room-temperature molten salts. *Journal of the Electrochemical Society*, 150:D195–D199, 2003.

[54] R. H. Hamlen, C. E. Kent, and S. N. Shafer. Electrolytically activated contractile polymer. *Nature*, 206:1149–1150, 1965.

[55] T. Hashimoto, M. Fujimura, and H. Kawai. *Perfluorinated Ionomer Membranes*, chapter 11, pages 217–248. American Chemical Society, 1982.

[56] M. Havenith. *Infrared Spectroscopy of Molecular Clusters*. Springer–Verlag, 2002.

[57] C. Heitner-Wirguin. Infra-red spectra of perfluorinated cation-exchanged membranes. *Polymer*, 20:371–374, 1979.

[58] J. P. Hornak. The basics of NMR. ebook. Available online at www.cis.rit.edu/htbooks/nmr/bnmr.htm, 2002.

[59] W. Hsu, J. Barkley, and P. Meakin. Ion percolation and insulator-to-conductor transition in nafion perfluorosulfonic acid membranes. *Macromolecules*, 13:198–200, 1980.

[60] W. Hsu and T. Gierke. Ion transport and clustering in nafion perfluorinated membranes. *Journal of Membrane Science*, 13:307–326, 1983.

[61] F. Hurley and T. Weir. Electrodeposition of metals from fused quaternary ammonium salts. *Journal of the Electrochemical Society*, 98:203–206, 1951.

[62] P. James, J. Elliott, T. McMaster, J. Newton, A. Elliott, S. Hanna, and M. Miles. Hydration of nafion studied by afm and x-ray scattering. *Journal of Materials Science*, 35:5111–5119, 2000.

[63] P. James, T. McMaster, J. Newton, J. Newton, and M. Miles. In situ rehydration of perfluorosulphonate ion-exchange membrane studied by afm. *Polymer*, 41:4223–4231, 2000.

[64] J. Kao, W. Macknight, W. Taggart, and G. Cargill III. Structure of the cesium salt of an ethylene-methacrylic acid copolymer from its radial distribution function. *Macromolecules*, 7:95–100, 1974.

[65] A. Katchalsky. Rapid swelling and deswelling of reversible gels of polymeric acids by ionization. *Experientia*, 5:318–319, 1948.

[66] A. Keshavarzi, M. Shahinpoor, K. J. Kim, and J. Lantz. Blood pressure, pulse rate, and rhythm measurement using ionic polymer-metal composites sensors. In *EAP Actuators and Devices*, volume 3669, pages 369–376. SPIE, 1999.

[67] R. G. Kidd. *NMR of Newly Accesible Nuclei, volume 1*, chapter 5, pages 103–131. Academic Press, 1983.

[68] B. P. Kirkmeyer, R. C. Puetter, A. Yahil, and K. I. Winey. Deconvolution of scanning transmission electron microscopy images of ionomers. *Journal of Polymer Science Part B: Polymer Physics*, 41:319–326, 2003.

[69] V. Koch, C. Nanjundiah, and R. Carlin. Hydrophobic ionic liquids. U.S. Patent 5,827,602, 1998.

[70] R. Komoroski and K. Mauritz. A sodium-23 nucelar magnetic resonance study of ionic mobility and contact ion pairing in a perfluorosulfonate ionomer. *Journal of the American Chemical Society*, 100:7487–7489, 1978.

[71] R. Komoroski and K. Mauritz. *Perfluorinated Ionomer Membranes*, chapter 7, pages 113–138. American Chemical Society, 1982.

[72] C. S. Kothera and D. J. Leo. Bandwidth characterization in the micropositioning of ionic polymer actuators. *Journal of Intelligent Material Systems and Structures*, 16:3–13, 2005.

[73] W. Kuhn. Reversible dehung und kontraktion bei anderung der ionisation eines netzwerks polyvalenter fadenmolekulionen. *Experientia*, 5:318–319, 1948.

[74] W. Kuhn, B. Hargitay, A. Katchalsky, and H. Eisenberg. Reversible dialation and contraction by changing the state of high-polymer acid networks. *Nature*, 165:514–516, 1950.

[75] W. Kujawski, Q. T. Nguyen, and J. Neel. Infrared investigations of sulfonated ionomer membranes. i. water–alcohol compositions and counterions effects. *Journal of Applied Polymer Science*, 44:951–958, 1992.

[76] N. Lakshminarayanaiah. *Transport Phenomena in Membranes*, chapter 1, pages 1–9. Academic Press, 1969.

[77] J. H. Laurer and K. I. Winey. Direct imaging of ionic aggregates in Zn-neutralized poly(ethylene-co-methacrylic acid) copolymers. *Macromolecules*, 31:9106–9108, 1998.

[78] A. Lehmani, S. Durand-Vidal, and P. Turq. Surface morphology of nafion 117 membrane by tapping mode atomic force microscopy. *Journal of Applied Polymer Science*, 68:503–508, 1998.

[79] D. J. Leo, K. Farinholt, and T. Wallmersperger. Computational models of ionic transport and electromechanical transduction in ionomeric polymer transducers. In *EAP Actuators and Devices*. SPIE, 2005. paper 5759-24.

[80] Z. Liang, W. Chen, J. Liu, S. Wang, Z. Zhou, W. Li, G. Sun, and Q. Xin. Ft-ir study of the microstructure of nafion^{TM} membrane. *Journal of Membrane Science*, 233:39–44, 2004.

[81] M. Lopez, B. Kipling, and H. Yeager. Exchange rates and water content of a cation exchange membrane in aprotic solvents. *Analytical Chemistry*, 48:1120–1122, 1976.

[82] M. Lopez, B. Kipling, and H. Yeager. Ionic diffusion and selectivity of a cation exchange membrane in nonaqueous solvents. *Analytical Chemistry*, 49:629–632, 1977.

[83] S. Lowry and K. Mauritz. An investigation of ionic hydration effects in perfluorosulfonate ionomers by fourier transform infrared spectroscopy. *Journal of the American Chemical Society*, 102:4665–4667, 1980.

[84] W. Lu, A. G. Fadeev, B. Qi, E. Smela, B. R. Mattes, J. Ding, G. M. Spinks, J. Mazurkiewicz, D. Zhou, G. G. Wallace, D. R. MacFarlane, S. A. Forsyth, and M. Forsyth. Use of ionic liquids for π-conjugated polymer electrochemical devices. *Science*, 297:983–987, 2002.

[85] K. Mallavarapu and D. J. Leo. Feedback control of the bending response of ionic polymer actuators. *Journal of Intelligent Material Systems and Structures*, 12:143–155, 2001.

[86] D. Manley, D. Williamson, R. Noble, and C. Koval. Morphological changes and facilitated transport characteristics for nafion membranes of various equivalent weights. *Chemistry of Materials*, 8:2595–2600, 1996.

[87] C. L. Marx, D. F. Caulfiend, and S. L. Cooper. Morphology of ionomers. *Macromolecules*, 6:344–353, 1973.

[88] K. Mauritz and R. Mei Fu. Dielectric relaxation studies of ion motions in electrolyte–containing perfluorosulfonate ionomers. 1. NaOH and NaCl systems. *Macromolecules*, 21:1324–1333, 1988.

[89] K. A. Mauritz and R. E. Moore. State of understanding of nafion. *Chemical Reviews*, 104:4535–4585, 2004.

[90] J. Mazurkiewicz, P. Innis, G. Wallace, D. MacFarlane, and M. Forsyth. Conducting polymer electrochemistry in ionic liquids. *Synthetic Metals*, 135-136:31–32, 2003.

[91] R. S. McLean, M. Doyle, and B. B. Sauer. High-resolution imaging of ionic domains and crystal morphology in ionomers using afm techniques. *Macromolecules*, 33:6541–6550, 2000.

[92] P. Millet, F. Andolfatto, and R. Durand. Preparation of solid polymer electrolyte composites: Investigation of the ion-exchange process. *Journal of Applied Electrochemistry*, 25:227–232, 1995.

[93] P. Millet, F. Andolfatto, and R. Durand. Preparation of solid polymer electrolyte composites: Investigation of the precipitation process. *Journal of Applied Electrochemistry*, 25:233–239, 1995.

[94] P. Millet, R. Durand, E. Dartyge, G. Tourillon, and A. Fontaine. Precipitation of metallic platinum into nafion ionomer membranes. *Journal of the Electrochemical Society*, 140(5):1373–1379, 1993.

[95] M. Mojarrad and M. Shahinpoor. Ion-exchange-metal composite sensor films. In *Smart Materials and Structures*, volume 3042, pages 52–60. SPIE, 1997.

[96] J. M. Mueller. Complex impedance studies of electrosprayed and extruded nafion membranes. Trident Scholar project report, US Naval Academy, 2004. report no. 324.

[97] S. Nemat-Nasser. Micromechanics of actuation of ionic polymer-metal composites. *Journal of Applied Physics*, 92(5):2899–2915, 2002.

[98] S. Nemat-Nasser and S. Zamani. Experimental study of nafion- and flemion-based ionic polymer-metal composites (IPMCs) with ethylene glycol as solvent. In *EAP Actuators and Devices*. SPIE, 2003. paper no. 5051-26.

[99] K. Newbury. *Characterization, Modeling, and Control of Ionic Polymer Transducers*. PhD thesis, Virginia Tech, 2002.

[100] K. Newbury and D. J. Leo. Chemoelectric and electromechanical modeling of ionic polymer materials. In *12th International Conference on Adaptive Structures and Technologies*, 2001. 220-231.

[101] K. Newbury and D. J. Leo. Mechanical work and electromechanical coupling in ionic polymer bender actuators. In *Proceedings of the ASME International Mechanical Engineering Conference and Exposition*. ASME, 2001. paper AD-23705.

[102] K. Oguro. Actuator element. U.S. Patent 5,268,082, 1993.

[103] K. Oguro, Y. Kawami, and H. Takenaka. Bending of an ion-conducting polymer film-electrode composite by an electric stimulus at low volage. *Journal of Micromachine Society*, 5:27–30, 1992.

[104] L. Pauling. The sizes of ions and the structure of ionic crystals. *Journal of the American Chemical Society*, 49:765–790, 1927.

[105] J. Pernak, A. Czepukowicz, and R. Poźniak. New ionic liquids and their antielectrostatic properties. *Industrial and Engineering Chemistry Research*, 40:2379–2383, 2001.

[106] A. I. Popov. Alkali metal nmr and vibrational spectroscopic studies on solvates in non–aqueous solvents. *Pure and Applied Chemistry*, 41:275–289, 1975.

[107] Z. Porat, J. Fryer, M. Huxham, and I. Rubenstein. Electron microscopy investigation of the microstructure of nafion films. *Journal of Physical Chemistry*, 99:4667–4671, 1995.

[108] T. Rashid and M. Shahinpoor. Force optimization of ionic polymermic platinum composite artificial muscles by means of orthogonal array manufacturing method. In *EAP Actuators and Devices*, volume 3669, pages 289–298. SPIE, 1999.

[109] S. Reiberer and K. Norian. Analytical electron microscopy of nafion ion exchange membranes. *Ultramicroscopy*, 41:225–233, 1992.

[110] X. Ren and S. Gottesfeld. Electro-osmotic drag of water in poly(perfluorosulfonic acid) membranes. *Journal of the Electrochemical Society*, 148:A87–A93, 2001.

[111] E. Roche, M. Pineri, R. Duplessix, and A. Levelut. Small-angle scattering studies of nafion membranes. *Journal of Polymer Science: Polymer Physics Edition*, 19:1–11, 1981.

[112] A.-L. Rollet, O. Diat, and G. Gebel. Transport anisotropy of ions in sulfonated polyimide ionomer membranes. *Journal of Physical Chemistry B*, 108:1130–1136, 2004.

[113] K. Sadeghipour, R. Salomon, and S. Neogi. Development of a novel electrochemically active membrane and 'smart' material based vibration sensor/damper. *Smart Materials and Structures*, 1:172–179, 1992.

[114] D. J. Segalman, W. R. Witkowski, D. B. Adolf, and M. Shahinpoor. Theory and application of electrically controlled polymeric gels. *Smart Materials and Structures*, 1:95–100, 1992.

[115] M. Shahinpoor. Ionic polymer–conductor composites as biomimetic sensors, robotic actuators, and artificial muscles—a review. *Electrochimica Acta*, 48:2343–2353, 2003.

[116] M. Shahinpoor, Y. Bar-Cohen, J. Simpson, and J. Smith. Ionic polymer-metal composites (IPMCs) as biomimetic sensors, actuators and artificial muscles - a review. *Smart Materials and Structures*, 7(6):R15–R30, 1998.

[117] M. Shahinpoor and K. Kim. Ionic polymer-metal composites: III. modeling and simulation as biomimetic sensors, actuators, transducers, and artificial muscles. *Smart Materials and Structures*, 13:1362–1388, 2004.

[118] R. Shannon. Revised effective ionic radii and systematic studies of interatomic distances in halides and chalcogenides. *Acta Crystallographica*, A32:751–767, 1976.

[119] J. Sun, D. MacFarlane, and M. Forsyth. A new family of ionic liquids based on the 1-alkyl-2-methylpyrrolinium cation. *Electrochimica Acta*, 48:1707–1711, 2003.

[120] Y.-M. Sun, I. Favre, L. Schild, and E. Moczydlowski. On the structural basis for size–selective permeation of organic cations through the voltage–gated sodium channel. *Journal of General Physiology*, 110:693–715, 1997.

[121] T. E. Sutto, H. C. D. Long, and P. C. Trulove. Physical properties of substituted imidazolium based ionic liquids gel electrolytes. *Zeitschrift fur Naturforschung A: Journal of Physical Sciences*, 57a:839–846, 2002.

[122] S. Tadokoro, T. Murakami, S. Fuji, R. Kanno, M. Hattori, and T. Takamori. An elliptical friction drive element using an ICPF (ion conducting polymer gel film) actuator. In *International Conference on Robotics and Automation*, pages 205–212. IEEE, 1996.

[123] S. Tadokoro, S. Yamagami, T. Takamori, and K. Oguro. Modeling of nafion-pt composite actuators (icpf) by ionic motion. In *EAP Actuators and Devices*, pages 92–102. SPIE, 2000.

[124] R. Tannenbaum, M. Rajagopalan, and A. Eisenberg. Fourier transform infrared studies of ionic interactions in perfluorinated acid copolymer blends. *Journal of Polymer Science: Part B: Polymer Physics*, 41:1814–1823, 2003.

[125] M. Tant, K. Mauritz, and G. Wilkes, editors. *Ionomers: Synthesis, Structure, Properties and Applications*. Blackie, 1997.

[126] T. Tsuda, T. Nohira, Y. Nakamori, K. Matsumoto, R. Hagiwara, and Y. Ito. A highly conductive composite electrolyte consisting of polymer and room temperature molten fluorohydrogenates. *Solid State Ionics*, 149:295–298, 2002.

[127] M. W. Urban. *Attenuated Total Reflectance Spectroscopy of Polymers: Theory and Practice*. American Chemical Society, 1996.

[128] F. Vidal, C. Plesse, D. Teyssié, and C. Chevrot. Long-life air working conducting semi-ipn / ionic liquid based actuator. *Synthetic Metals*, 142:287–291, 2004.

[129] P. Walden. *Bulletin Scientifique de l'Académie Impériale des Sciences de Saint-Pétersbourg*, 1800:405–422, 1914. citen in W. Xu, E.I. Cooper, and C.A. Angell, *Journal of Physical Chemistry B*, 107:6170-6178, 2003.

[130] J. Wilkes, J. Levisky, and R. Wilson. Diakylimidazolium chloroaluminate melts: A new class of room-temperature ionic liquids for electrochemistry, spectroscopy, and synthesis. *Inorganic Chemistry*, 21:1263–1264, 1982.

[131] K. I. Winey, J. H. Laurer, and B. P. Kirkmeyer. Ionic aggregates in partially Zn-neutralized poly(ethylene-ran-methacrylic acid) ionomers: Shape, size, and size distribution. *Macromolecules*, 33:507–513, 2000.

[132] M. Winter, 2005. http://www.webelements.com.

[133] W. Xu, E. Cooper, and C. Angell. Ionic liquids: Ion mobilities, glass temperatures, and fragilities. *Journal of Physical Chemistry B*, 107:6170–6178, 2003.

[134] I. V. Yannas and A. J. Grodzinsky. Electromechanical energy conversion with collagen fibers in an aqueous medium. *Journal of Mechanochemistry and Cell Motility*, 2:113–125, 1973.

[135] C. L. Yaws, editor. *Chemical properties handbook : physical, thermodynamic, environmental, transport, safety, and health related properties for organic and inorganic chemicals*. McGraw–Hill, 1999.

[136] H. Yeager and B. Kipling. Ionic diffusion and ion clustering in a perfluorosulfonate ion–exchange membrane. *The Journal of Physical Chemistry*, 83:1836–1839, 1979.

[137] H. L. Yeager. *Perfluorinated Ionomer Membranes*, chapter 4, pages 40–63. American Chemical Society, 1982.

[138] H. L. Yeager and A. Steck. Cation and water diffusion in nafion ion exchange membranes: Influence of polymer structure. *Journal of the Electrochemical Society*, 128:1880–1884, 1981.

[139] T. A. Zawodzinski, M. Neeman, L. . Sillerud, and S. Cottesfeld. Determination of water diffusion coefficients in perfluorosulfonate ionomeric membranes. *Journal of Physical Chemistry*, 95:6040–6044, 1991.

[140] D. Zhou, G. Spinks, G. Wallace, C. Tiyapiboonchaiya, D. MacFarlane, M. Forsyth, and J. Sun. Solid state actuators based on polypyrrole and polymer-in-ionic liquid electrolytes. *Electrochimica Acta*, 48:2355–2359, 2003.

Appendix A

Initial SAXS Investigation Performed at Virginia Tech

An initial SAXS investigation was also performed at Virginia Tech, using a slit system. This setup, which is not shown, is fundamentally similar to the system shown in Figure 3.3, except that it does not contain the collimating pinholes. The initial study that was performed at Virginia Tech was used to motivate the more thorough investigation that was performed at the Army Research Laboratory. The interpretation of the results is the same for both experimental configurations.

For the initial investigation, the samples were in the proton form and prepared using the methods described in Chapter 2. A total of six samples were studied, one swollen with each of five ionic liquids and also a dry sample. The uptake of ionic liquid for each sample is provided in Table 2.2. The SAXS results obtained for these samples are presented in Figure A.1. Note that the scale of the y–axis is arbitrary and the curves have been shifted vertically for clarity. For the full name of each ionic liquid refer to Table 2.1. As can be seen from the figure, the ionomer peak and small–angle upturn are observed in these results. In general, the position of the ionomer peak shifts to smaller d values as the uptake of ionic liquid is increased. For the two BMPyr–cation ionic liquids (uptake 18.2% and 31.0%), the ionomer peak is just above 3 nm. For the EMI-Tf–swollen membrane (uptake 48.2%), the ionomer peak is located at $d \approx 5$ nm (q=0.13 Å). For the two $P(C_6)_3C_{14}$–cation ionic liquids (uptake 84.4% and 117.2% by volume), the ionomer peak is not clearly observed. The ionomer peak is most evident for the SAXS result of the membrane swollen with the water–miscible EMI-

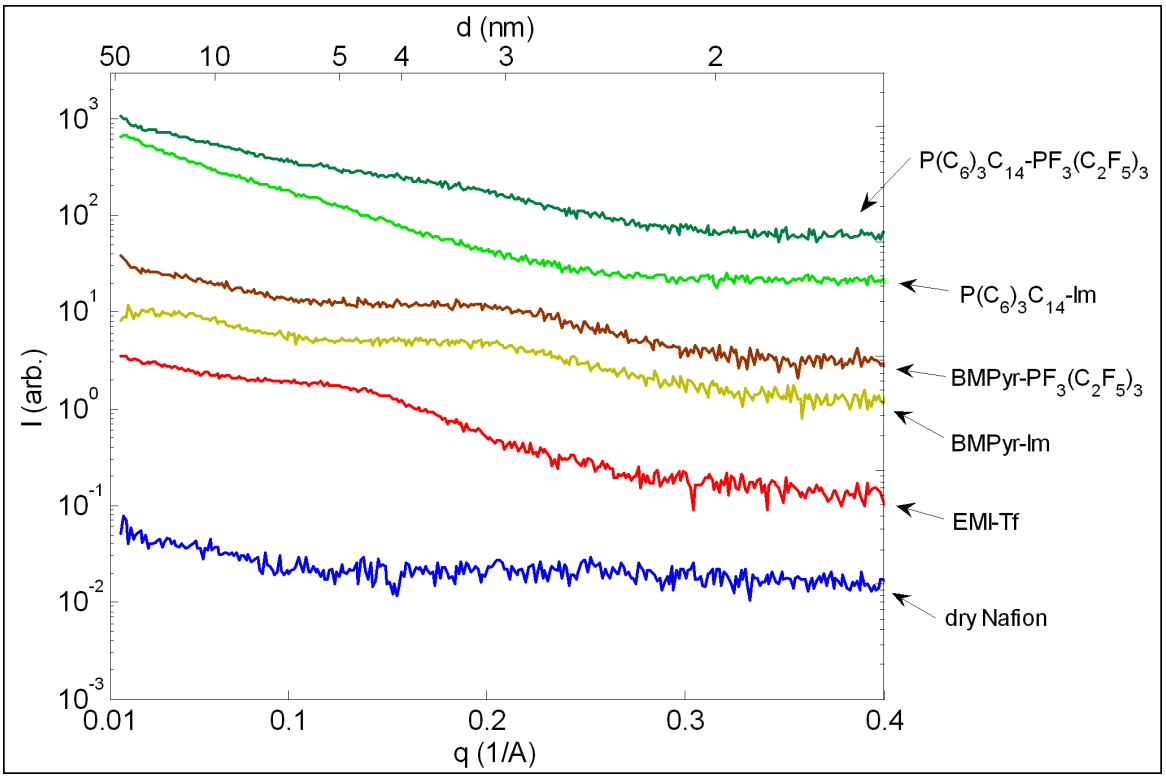

Figure A.1: Scattered intensity (arbitrary units) versus q for a dry Nafion^{TM} membrane and Nafion^{TM} membranes swollen with five ionic liquids. All samples were in the proton form.

Tf ionic liquid. This result likely indicates that the clustered morphology of the polymer is most strongly manifested in the membrane swollen with EMI-Tf ionic liquid as compared to those membranes swollen with the other hydrophobic ionic liquids. For the dry Nafion^{TM} polymer, the ionomer peak is not evident in the SAXS result.

The initial testing performed at Virginia Tech demonstrated the ability of SAXS to characterize the morphology of ionic liquid–swollen Nafion^{TM} membranes. This testing provided the foundation for the more structured investigation that was performed at the Army Research Laboratory.

Vita

The author, Matthew Damon Bennett was born on July 31, 1977 in Blacksburg, Virginia to Daniel Bennett and Cheryl Gill. He grew up in South Carolina with his mother and stepfather, Robert Gill. Matthew attended high school at Riverside High School in Greer, South Carolina and was always very interested in science and engineering. In the fall of 1995 Matthew left home to attend Virginia Tech, where he majored in mechanical engineering. During the summer after his sophomore year he assisted Dr. Jan Helge Bøhn in an undergraduate project to build an aircrew oxygen mask using rapid prototyping. In his senior year Matthew served as the propulsion design crew chief on Virginia Tech's Human Powered Submarine Team. That year the team won first place in five out of eight categories at the ASME-sponsored international competition and took second place in the other three categories. Following graduation with a B.S. degree in May of 2000, Matthew enrolled in the graduate school at Virginia Tech. In the first semester of his Master's work, Matthew was a graduate teaching assistant for Mechanical Engineering Lab II, a senior-level course in the mechanical engineering department. He performed his Master's research under the advisement of Dr. Donald Leo in the Center for Intelligent Material Systems and Structures. For his Master's work, Matthew investigated new methods of depositing the metal electrodes on water–swollen Nafion^{TM} polymer transducers, focusing specifically on the use of non–noble metals. Matthew completed his Master's degree in the fall of 2002 and began work on his PhD under the advisement of Dr. Donald Leo. During the first semester of his PhD work, he traveled to Wollongong, Australia to perform research under the advisement of Dr. Gordon Wallace and Dr. Geoff Spinks of the Intelligent Polymer Research Institute at the University of Wollongong. Although this work focused mainly on the combination of ionomeric and conducting polymer materials for novel actuators, it was also the genesis of the use of ionic liquids to replace water in ionomeric transducers. After completion of

his PhD, Matthew will move on to pursue a career as director of a small business aimed at finding commercial applications for ionomeric polymer transducers.